ISSN 0918-4597

NRIM

Research Activities

1996

National Research Institute for Metals

Japan

Sengen Site

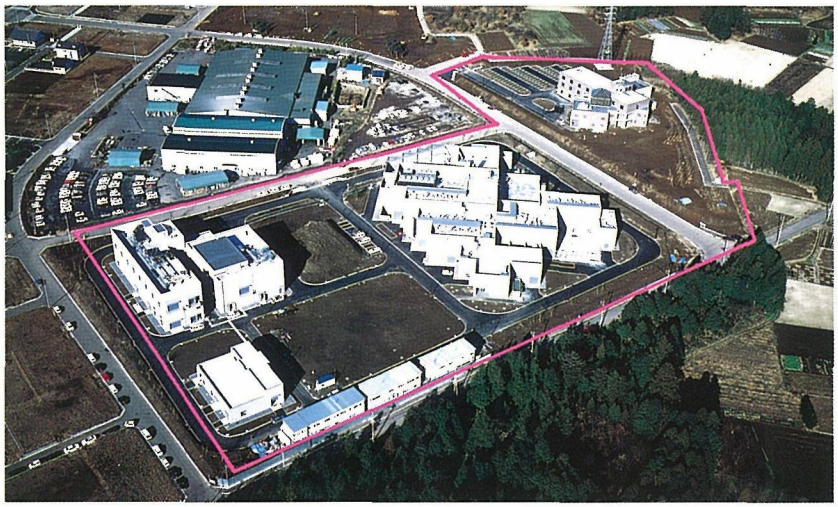

Sakura Site

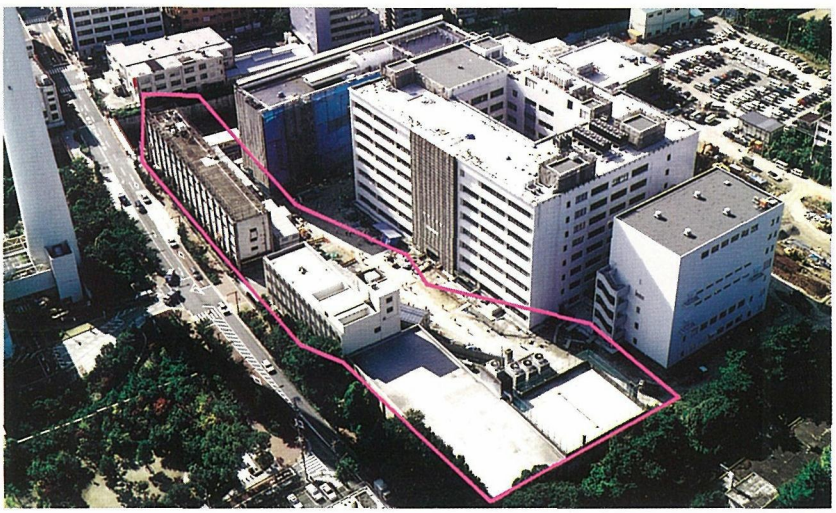

Meguro Site

Preface

I am pleased to present "NRIM Research Activities 1996." This report summarizes the annual activities of the National Research Institute for Metals (NRIM), focusing on our research programs and the progress we have made over the past year. NRIM is a research institution attached to the Science and Technology Agency of the government of Japan and was established in 1956. Since then, NRIM has played an essential role in the field of research and development of metals, alloys and other materials. An ongoing effort has been to improve the reliability of existing materials, which is documented in the "NRIM Creep and Fatigue Data Sheet" series of publications.

On July 1, 1995, NRIM moved its headquarters from Tokyo to Tsukuba Science City, where there are many world-class experimental facilities and various supercomputers. With the support and efforts of sponsors, staff, and the community, we have built a Center of Excellence for fundamental materials research in Tsukuba. Responding to the present social and economic needs of Japan, we are establishing a "Frontier Structural Materials Research Center" as part of the "New Century Structural Materials Project." We have already started an R&D program to create future "ultra steels" at the center, making full use of the excellent resources available at NRIM. In this way, NRIM continues to expand its activities for advanced materials research.

To all of you who have supported NRIM, we greatly appreciate your continued understanding and encouragement.

Masatoshi Okada

Dr. Masatoshi OKADA
Director-General

NRIM Research Activities
1996

Contents

Research Topics

Research Topics

❐ Advanced EPMA X-ray Image Analysis with a Phase Diagram

M. Fukamachi
Materials Physics Division

A new method of computer image analysis is proposed and applied to the characterization of the fine structure of superconducting oxide $YBa_2Cu_3O_{7-X}$. In this method, in order to characterize the structure of a material, the EPMA X-ray images are analysed with a pair of phase diagrams of ternary systems. Phase diagrams have been used in metallurgical study to show the relation between phases in the alloy system and the concentrations of constituent elements. EPMA is an instrument used to measure the chemical compositions in a local area of a solid specimen surface. The analysis of digital X-ray images of the EPMA with the phase diagram seems to be useful in characterizing the fine structures of materials. The proposed analytical method facilitates the identification of phases and the construction of maps to reveal the distribution of the identified phase on the specimen surface.

The EPMA X-ray images are analysed with a stand-alone personal-use small computer as well as the multiple-computer system used in this work. The original image size is 1000*640 pixels. The X-ray images of a whole or small part of an area of interest can be transferred to the computers with a LAN system or with floppy disks according to the demand of researchers. The application programs for data analysis are available in BASIC or C language.

In this report, an example is shown for the characterization of YBaCuO super-conducting oxide. The material YBaCuO superconducting oxide is produced with the method invented at NRIM. The powder of metals Y, Ba and Cu is added to the block of silver in a ratio of about 10 wt %. The materials are melted at high temperature. The melt is cooled to solidify into the structure of an alloy phase of Y-Ba-Cu precipitated along the grain boundary of silver. The material is heated again in the atmosphere to oxidize the Y-Ba-Cu alloy phase and to transform it into superconducting oxide. The material is cooled slowly to room temperature, and the material with the structure of superconducting oxide distributed along the boundary between the silver grains is produced. The transition temperature to the state of super-conduction depends on the concentration of oxygen. The phase with transition temperature higher than 90 K is the phase represented by $YBa_2Cu_3O_7$. The phase with the formula $YBa_2Cu_3O_{6.5}$, which satisfies the atomic valence relation among oxygen and the metal elements, has the transition temperature lower than 60 K. Thus, the quantitative analysis of oxygen concentration must be included in the characterization of YBaCuO superconducting oxide.

The superconducting oxide has four kinds of elements and is analysed with a pair of ternary phase diagrams. First, the concentrations of pixels are plotted on the ternary-phase diagram of Y-Ba-Cu. The pixels with the composition of YBa_2Cu_3 are selected. Next, these selected pixels are plotted on another ternary phase diagram of O-Ba-Cu, Y-

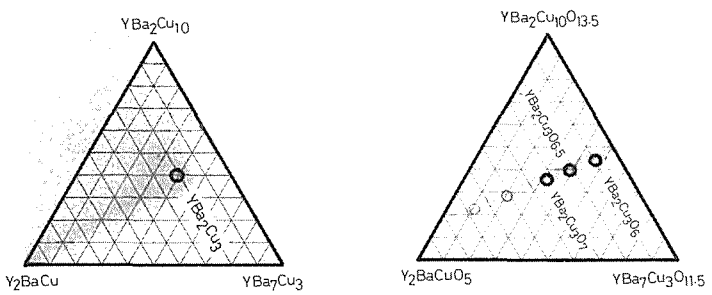

Fig. 1 Concentrations of pixels are analysed on a pair of ternary phase diagrams. First, pixels with composition YBa_2Cu_3 are selected on the Y-Ba-Cu phase diagram. Next, concentrations of selected pixels are analysed on the O-Ba-Cu ternary phase diagram to identify the pixels with superconducting phase $YBa_2Cu_3O_7$.

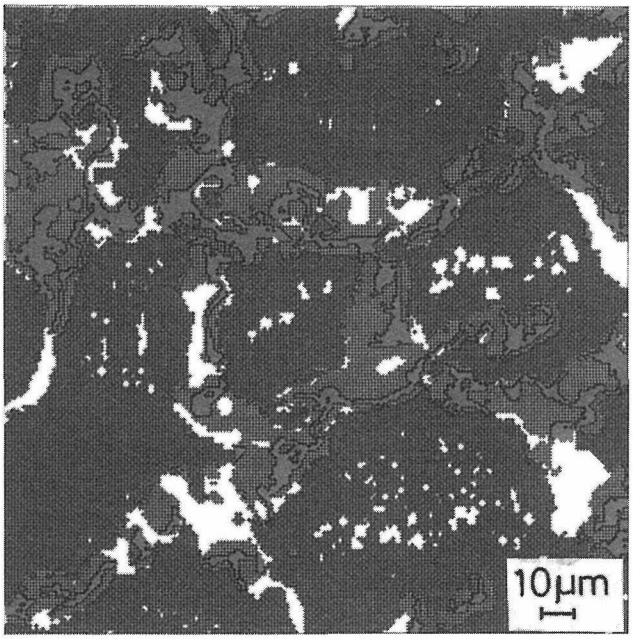

Fig. 2 Distribution of superconducting phase $YBa_2Cu_3O_7$ on specimen surface is shown as regions painted red.

O-Cu or Y-Ba-O. In Fig. 1, the concentrations are plotted on the ternary phase diagram of O-Ba-Cu. The pixels with composition $O_7Ba_2Cu_3$ are selected. In this way, the pixels with composition of superconducting phase $YBa_2Cu_3O_7$ are selected.

In Fig. 2, the pixels of superconducting phase $YBa_2Cu_3O_7$ are painted red. Fine strings or thin sheets of superconducting phases are observed along the boundary region of silver grains. The pixels painted green have the composition of YBa_2Cu_3 with the concentration of oxygen smaller or larger than $YBa_2Cu_3O_7$. The pixels painted purple are the grains of silver. The unpainted white region indicates that more phases other than those specified above are included in the specimen. Thus, structure can be examined in detail with this method. The results are used to improve the production process of superconducting oxide.

Keywords: EPMA X-ray image, computer image analysis, YBaCuO superconducting oxide

References

1. K.F.J. Heinrich and D.E. Newbury, "Electron Probe X-ray Microanalysis", *Metals Handbook, 9th Edition*, American Society for Metals, 10(1986): 516–535.
2. H. Baker, "Introduction to Alloy Phase Diagrams", *ASM Handbook*, American Society for Metals, 3(1992): 1–29.
3. G.F. Vander, "Image Analysis", *Metals Handbook, 9th Edition*, American Society for Metals , 10(1986): 309–322.

❒ High Pressure Apparatus for in situ X-ray Diffraction and Electrical Resistance Measurement at Low Temperature

J. Tang and T. Matsumoto
Materials Physics Division

The high pressure technique is one of the most effective tools for finding new behavior based on a decrease of a material's volume. For instance, the atomic arrangement in crystals may change, resulting in structural phase transformations, or the electronic structure may change, resulting in the insulator-metallic transition. At low temperature, drastic changes in property also occur frequently, among which superconductivity has been a well-known example. Thus it is very important to investigate the phenomena induced at high pressure and low temperature for materials science. Structural study is especially essential for understanding the origin of change in the electronic properties under such extreme conditions.

We have developed an apparatus that allows us to carry out *in situ* X-ray diffraction and electrical resistance measurement simultaneously under high pressure and at low temperature. The present apparatus indicated in Fig. 1(a) and (b) consists mainly of (1) a high pressure unit, (2) an X-ray diffraction unit and (3) a low temperature unit. Hydrostatic pressure is generated by the cubic-anvil type high pressure unit which uniformly compresses the cubic-shaped gasket (enclosing a sample inside) as pressure medium made from the mixture of amorphous boron and epoxy resin. The X-ray diffraction unit is composed of the tungsten rotor target and the energy dispersive detector. The optical alignment of X-ray is automatically regulated to compensate for the positional change of the sample, which is caused by an increase and/or a decrease in pressure and temperature.

Compared with X-ray experiments at ambient pressure, the sample size is usually much smaller in high pressure experiments, and thus it takes a longer time for high-precision data collection. Moreover, the heat capacities of the pressure generation unit are very large. Therefore, it is difficult for the temperature at any specific

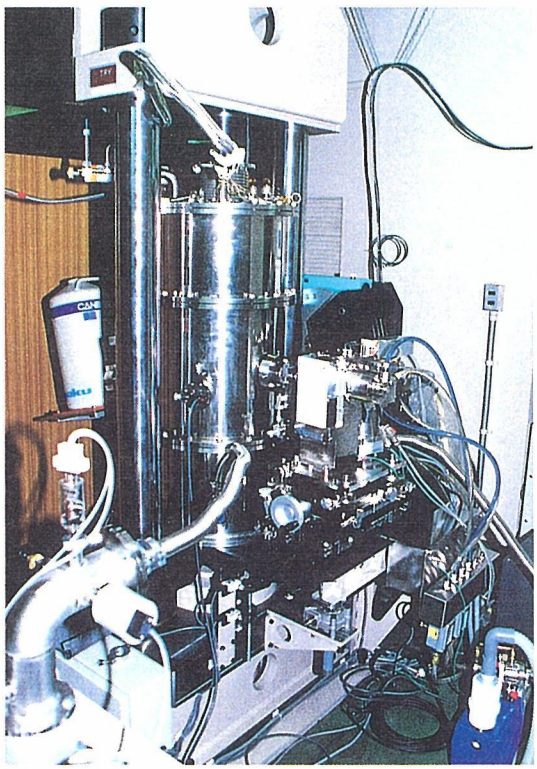

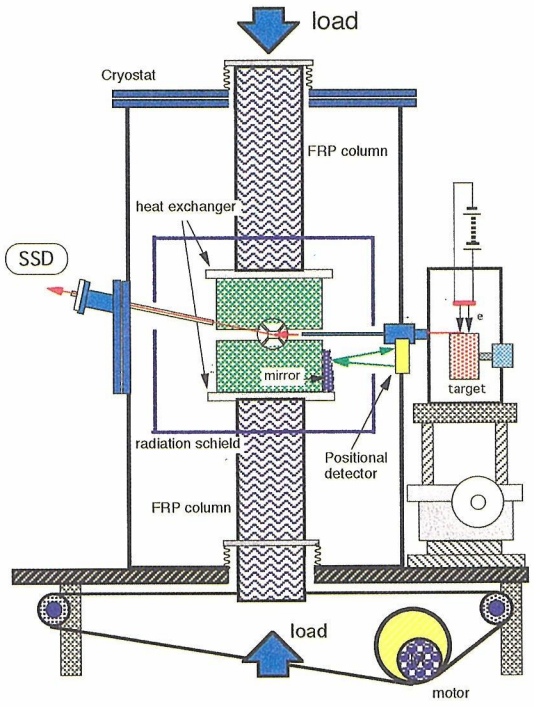

Fig. 1(a) Photography of the high pressure apparatus for in situ X-ray diffraction and (b) schematic of the apparatus.

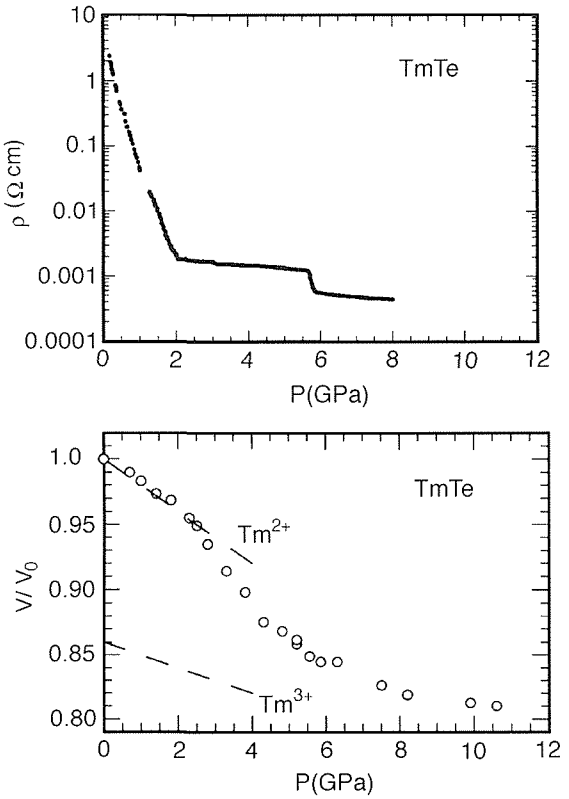

Fig. 2 Pressure dependence of electrical resistivity (upper panel) and the volume changes (lower panel) of TmTe.

position to be controlled and kept stable throughout the experiment at low temperature. To meet these challenges, the thermal conduction method has been introduced for controlling sample temperature. We newly developed the heat exchanger for flowing liquid gas, which was mounted directly on to the anvils. The high vacuum inside the cryostat must be kept for the adiabatic condition during operation at low temperature. This system has been successfully used to operate at pressures up to 9 GPa and temperatures down to 7 K.

In order to measure the electrical resistance during X-ray experiments, we divide the gasket into two parts. The bulk sample in the lower part is used for measurements of electrical resistivity. The powder sample in the upper part is used for X-ray diffraction.

As an example of the simultaneous measurements, Fig. 2 shows the results of electrical resistivity and the volume changes of TmTe as functions of pressure. TmTe has been known to be a material of mixed valence. In the upper panel of the figure, it can be clearly seen that the resistivity changed remarkably in the pressure range of 2 to 6 GPa. Correlating these changes with structural parameters, the lower panel gives the pressure dependence of the volume. Detailed analysis of this result has led us to conclude that the changes in electrical resistivity resulted in the change in valence of Tm ions.

We are now expanding the capabilities of this system to accommodate even higher pressures and lower temperatures, so that the pressure effect on the material properties other than electrical resistivity, such as magnetic properties, can also be investigated under extreme conditions of low temperature and high pressure.

Keywords: high pressure, low temperature in situ X-ray diffraction

❒ Mesoscopic Magnetic Arrays Fabricated by High-Resolution Electron-Beam Lithography

I. Nakatani
Physical Properties Division

Since around the end of the 1980s, new fields of research on magnetic quantum effects and magnetic quantum devices have been opened. They are the spin-dependent electron scattering effect, the spin-valve effect, the magnetic tunneling effect and so on, which are based on controlling the exchange interaction essential for ferromagnetism, and they sharply contrast with controlling the technical magnetization for ferromagnetism as done in the past. To conduct basic research on the magnetic quantum effects and to realize new concepts of magnetic quantum devices, the key technology is to fabricate the well-defined structure of the deep submicron or sub-100nm regime[1]. Electron-beam nanolithography has a potential application for developing such nanoscale fabrications of magnetic materials. One of the most critical issues in the nanolithography process for magnetic materials is the RIE (reactive-ion-etching) process. Magnetic materials, whose main constituent elements are transition elements, are inactive in an ordinarily used RIE.

In this study, a series of techniques for electron-beam nanolithography have been developed, including a novel RIE method useful for magnetic materials[2].

Fabrications of Nanostructures

The pattern generation was performed by a high-resolution electron-beam writing on a resist film of α methylstyren-α chloromethylstyren copolymer overlaid on amorphous carbon film that was sputtered on a glass substrate or on permalloy (80%Ni-4.5%Mo-Fe) thin film formed on a glass substrate. The amorphous carbon film can reduce the proximity effect, leading to high-resolution electron-beam writings. For pattern transfer to the permalloy films from the resist patterns defined by the electron-beam writing, two different methods have been studied. One is the lift-off method, which is for a negative transfer, and the other is the RIE method, which is for a positive transfer. By the lift-off method, the high estresolution of array structures of permalloy thin wires of 60nm width and of two dimensional lattice structures of permalloy small dots of 100nm were achieved, as shown in Photos 1(a) and (b).

The RIE method involves the rf plasma of a gas mixture of NH_3-CO aimed at the formation of volatile transition metal carbonyls[2]. A maximum etching rate of 35nm/min and a highly anisotropic etching for the permalloy was obtained at a composition of about 50mol%NH_3-CO at a pressure of 2.4×10^{-3} Torr. The etching selectivity ratios of permalloy to SiO_2 or Si were about 10 or 4, respectively. By this RIE method, arrays of permalloy thin wires 200nm wide and 300 spaced with clear-cut features were fabricated, as shown in Photo 2.

Ferromagnetic Resonances on Thin Wire Arrays of Permalloy

Ferromagnetic resonances were measured on the arrays of permalloy thin wires in the uniform rf field H_a at 9.224GHz in a TE_{011} cavity applying uniform dc magnetic fields. Multiple resonances were observed at the higher (or lower) field rather than at the field of main resonance of a uniform precessional mode. Figures 1(a), (b) and (c) show FMR spectra as a function of static magnetic fields H_a on the three principal axes of the array, parallel to the x-axis, y-axis and z-axis, respectively. When

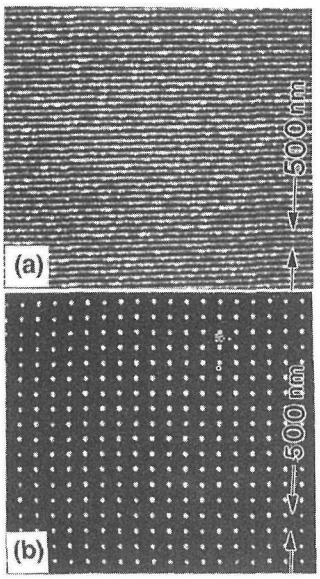

Photo 1 Permalloy nanostructures fabricated by using the lift-off method; (a) thin wire array, (b) square lattice of small dots.

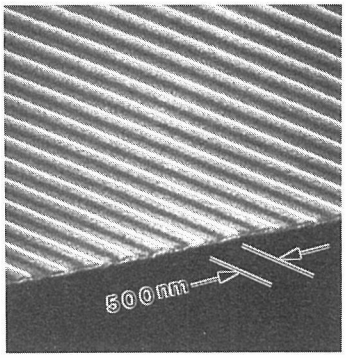

Photo 2 Permalloy thin wire array fabricated by using reactive ion etching.

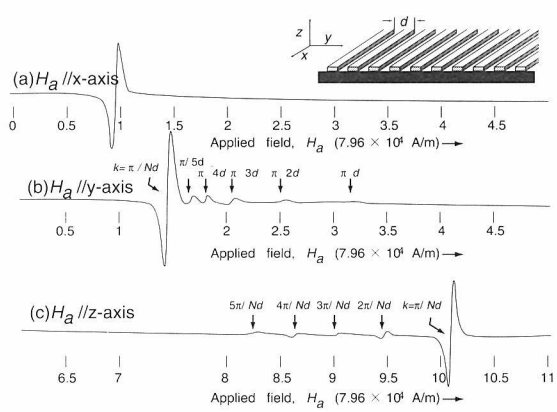

Fig. 1 FMR spectra of micro array of permalloy stripes; (a) static field H_a is parallel to the x-axis, (b) H_a parallel to the y-axis (Case I), (c) H_a parallel to the z-axis (Case II).

H_a was in the x-axis, i.e., parallel to stripes, a uniform precessional mode was observed. Case I: When H_a was in the y-axis, i.e., normal to stripes and parallel to array plane, multiple resonances were observed at the higher field rather than at the field of main resonance, as indicated by arrows in the figure. Case II: While H_a is in the z-axis, i.e., normal to stripes and normal to array plane, multiple resonances appeared in the lower field rather than in the field of main resonance. These types of multiple resonances can be observed for the other stripe arrays with 2μm or 3μm periods. These multiple resonances are unlike Kittel's spin wave excitation, because the thickness of the sample is not greater than the wavelength of the spin wave. Magnetostatic modes are excluded, because the samples used are metallic and were placed in a uniform r f field.

The magnetic moment of each stripe makes a precession motion around the DC magnetic field H_a with the frequency of microwave frequency, but each magnetic moment is bound to all other stripes in the array by the local field coming from dipole-dipole interaction between the stripes. By an analysis of equation of motion for the magnetic moment system, it was the stripes. By an analysis of equation of motion of the magnetic moment system, it was elucidated that the magnetic dipole standing waves are excited in the plane of the array, and that the standing waves have multiple modes with various waved lengths. The projections of the magnetic dipole standing waves of case I and case II are illustrated in Figs. 2(a) and 2(b), respectively. In both cases, the half wavelength of the standing wave and nNd, where N is the total number of stripes in the array, and n is an integer from 1 to N. The wave has a velocity of about one-hundredth part of the light velocity.

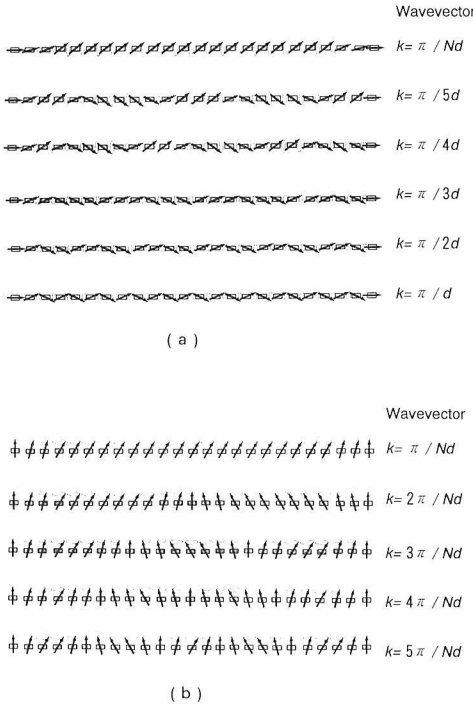

Fig. 2 Schematic views of cross-section of thin wire array in which main mode and higher order modes of standing wave are excited; (a) Case I (Transverse wave), (b) Case II(Longitudinal wave).

Keywords: magnetical material, electron-beam nanolithography, reactive-ion-etching, thin wire array, ferromagnetic resonance

References

1. I. Nakatani, "Ultramicro Fabrications of Magnetic Materials by Electron-Beam Lithography", *J. Magn. Soc. Jpn.* 19(1995): 831–839: in Japanese.
2. I. Nakatani, "Ultramicro Fabrications on Fe-Ni Alloys Using Electron-Beam Writing and Reactive-ion Etching", *IEEE Trans. Magn.* 32(1996): No. 9.

❒ Atomistic Investigation of Ni-Base Single Crystal Superalloys Using Monte Carlo Simulations and Atom-Probe Microanalyses

H. Murakami and H. Harada
Computational Materials Science Division

Introduction

Although nickel-base single crystal superalloys have already been developed extensively for turbine blade applications, there are continuing efforts to improve the mechanical properties of these alloys for next-generation aeroengines. These superalloys have $L1_2$ ordered γ' precipitates in γ matrices. Their mechanical properties are thus expected to be controlled by the microstructural parameters of the two phases, such as their inherent mechanical properties, and interaction between the two phases.

Monte Carlo Simulations (MCS)[1,2] have been employed to predict temporal and spatial evolution of the atomic arrangement, and the kinetics of ordering of nickel-base superalloys. An additional advantage of MCS is that, since the position of every single atom in the system is predicted, MCS enables three dimensional representation of the atomic configurations.

This article demonstrates the visualization of atomic configuration derived from MCS. Additionally, the chemistry at the γ/γ' interface simulated by MCS is compared with that obtained by Atom-probe Field Ion Microscopy (APFIM). The superalloy investigated is TMS-71[3] (Ni-12.7Al-6.9Cr-6.2Co-4.0Mo-2.8Ta- 0.8Re in at%), which has recently been proposed by our research group and was designed using a regression-analysis-based Alloy Design Program[4] by adding Co and Re to the base material TMS-63 to improve creep properties in all temperature ranges.

Procedure of Monte Carlo Simulations

Initial structure can be generated by assigning numbers which are distinct by atom species on random lattice sites according to the composition of the alloy. The kinetics of ordering can be controlled by the direct exchange of a randomly selected single atom with one of its neighboring atoms. To simplify the simulation, the Lenard-Jones pair potential was utilised for the calculation of atomic interaction. The values of the Lenard-Jones pair potential parameters were identical to those employed for the Cluster Variation Method calculation of fcc materials[5,6]. The simulations were performed on 16×16×16 or 32×32×32 fcc unit cells (16,384 or 131072 atoms, respectively), under periodic boundary conditions at 1323 K.

Visualization of Atomic configuration

Using MCS, the distribution of atoms in the system is described as shown in Fig. 1, where the 7th atomic layer of the system is highlighted. Fig. 2 shows the 2-dimensional arrangement of atoms, normal to the <100> direction. The atom species in TMS-71 may be identified by their size and brightness. Since pure Ni layers and Ni+Al mixed layers must appear in turn along <100> for pure fully-ordered Ni_3Al, it is possible to identify the ordered γ' phase from MCS as indicated by the arrows. Accordingly, the site occupancy of alloying elements in the γ' phase may also be understood.

Chemistry change at γ/γ' interfaces

The composition changes at γ/γ' interfaces may be determined by APFIM analysis, since the analysis is of atoms successively field-evaporated from the specimen surface and chemically identified. When the cumulative number of each solute atom is plotted against the total number of detected atoms in a 'ladder diagram', the horizontal axis includes depth information and the gradient corresponds to the local composition of that alloying element. Fig. 3 shows a typical ladder diagram of the composition change at a γ/γ' interface obtained by APFIM. Note the enrichment of Re in the γ phase in the vicinity of the interface.

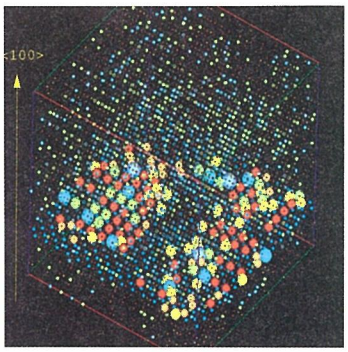

Fig. 1 The 3-dimensional representation of the atomic arrangement of TMS-71, derived from the Monte Carlo Simulations after 20000 Monte Carlo Steps

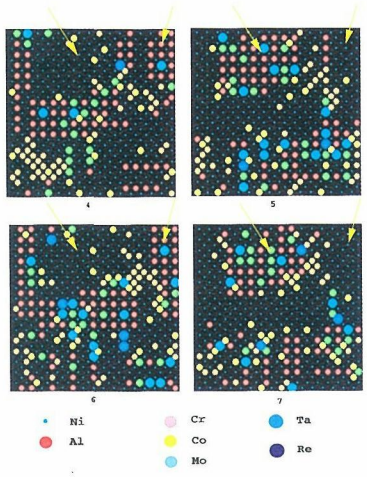

Fig. 2 The atomic arrangement from the 4th to the 7th layers normal to the <100> direction showing the ordered regions by the arrows.

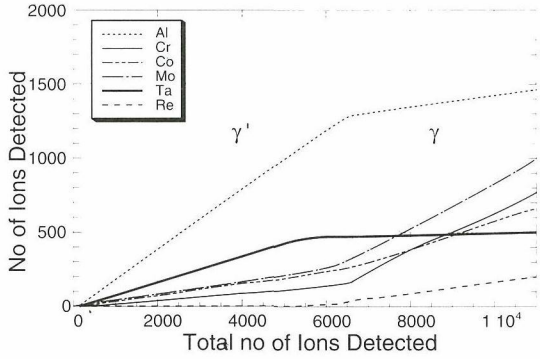

Fig. 3 The ladder diagram of TMS-71 obtained by APFIM.

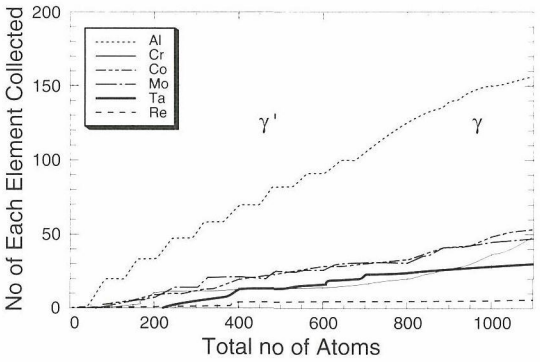

Fig. 4 The virtual ladder diagram of TMS-71 simulated by MCS.

This ladder diagram may be simulated using MCS by analysing a cylinder along the <100> direction (containing, for example, 40 atoms per atomic layer). Fig. 4 shows a so-called 'virtual ladder diagram' across a γ/γ' interface, similar to Fig. 3 except that the number of atoms 'detected' is smaller by a factor of 10. When Al atoms are plotted in a ladder diagram, Ni layers appear as horizontal lines whereas mixed layers appear as inclined lines in the ordered γ' region. It is thus clear that the left side in Fig. 4 represents the ordered γ' phase and the right represents the γ phase. The composition changes between the two phases may also be observed for Co, Cr and Ta. However, the composition changes are not as clear as those experimentally obtained by APFIM. It is suggested that further investigation will be of help in obtaining more detailed comparisons between the numerical simulations and the experimental results.

Acknowledgment

The authors are very grateful to Prof. Y.Saito at Waseda University and Dr. H.G.Read for many useful suggestions.

Keywords: Ni-base single crystal superalloys, Monte Carlo Simulations, Atom-Probe Field Ion Microscopy, γ/γ' two phase structure

References

1. H. Murakami, Y. Saito, M. Enomoto, and H. Harada, "Atomistic Investigation of Ni-Base Single Crystal Superalloys Using Cluster Variation Method, Monte Carlo Simulations and Atom-Probe Microanalyses" *proceedings of the Workshop 'Modelling and Simulation for Materials Design'*, held in NRIM, (1996): 256–261.
2. Y. Saito, H. Murakami, and H. Harada, "Modelling of Microstructure in Ni-Base Superalloys" *ibid*, (1996): 160–165.
3. H. Murakami, P.J. Warren, and H. Harada, "Atom-probe Microanalyses of Some Ni-base Single Crystal Superalloys", *Proceedings of the 3rd International Charles Parsons Turbine Conference "Materials Engineering in Turbines and Compressors"*, New Castle, U.K., (1995): 343–350.
4. H. Harada et al, "Computer Analysis on Microstructure and Property of Nickel-base Single Crystal Superalloys", *Proceedings of the 5th International Conference on Creep and Fracture of Engineering Materials and Structures*, Swansea, U.K., (1993): 255–264.
5. M. Enomoto and H. Harada, "Analysis of γ'/γ Equilibrium in Ni-Al-X Alloys by the Cluster Variation Method with the Lennard-Jones Potential", Metall. Trans., 20A(1989): 649-664.
6. M. Enomoto, H. Harada, and M. Yamazaki, "Calculation of γ'/γ Equilibrium Phase Compositions in Nickel-base Superalloys by Cluster Variation Method", CALPHAD, 15(1991):143–158.

❒ Development of Platinum Metals Base Refractory Superalloys

Y. Yamabe-Mitarai, Y. Koizumi, H. Murakami, Y. Ro, T. Maruko, and H. Harada
Computational Materials Division

Introduction

A new class of superalloys, namely "refractory superalloys," has been proposed. This new concept is defined as alloys with fcc and $L1_2$ coherent two phase structures similar to Ni-base superalloys which are known as turbine blade or vane materials in gas turbine, but with a considerably higher melting temperature. Platinum group metals are ideal base elements for these alloys because of their higher melting temperatures compared to Ni, whose melting temperature is 1453°C, and superior oxidation resistance to so-called refractory metals, i.e., Nb, Mo, Ta and W. Of the platinum group metals, Rh, Pd, Ir and Pt have the fcc structure like Ni, while Ru and Os have the hcp structure. Ir, with the highest melting temperature among the platinum group metals with the fcc structure (at 2443°C), was selected as the base metal for the refractory superalloys, and the fcc structure can be equilibrated with the $L1_2$ structure according to binary phase diagrams, e.g., in Ir-Nb and Ir-Ti systems. Also, the fcc/$L1_2$ coherent two-phase structure is expected to be formed in these Ir alloys since their lattice parameter misfit is around 1%. The strength at 1800 °C was investigated in Ir-Nb and Ir-Ti alloys.

Microstructure

The dark field image taken with a super-lattice reflection($g = 1\bar{1}0$) from the $L1_2$ phase of the Ir-15at%Nb alloy heated at 1200 °C for 1 week in the beam direction of [111] by TEM is shown in Fig. 1.

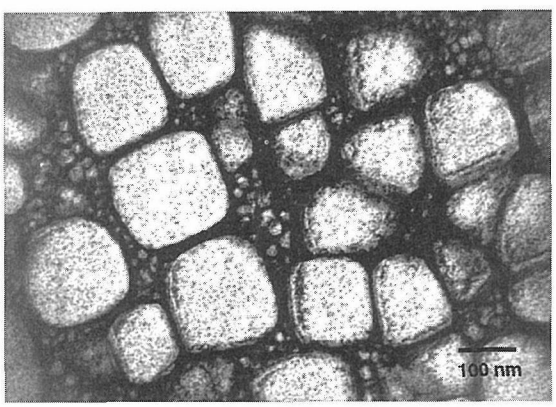

Fig. 1 Dark field image ($g = 1\bar{1}0$) of the Ir-15at%Nb alloy heat treated at 1200°C for 1 week.

The phase with bright contrast is the Ll_2 phase. The $L1_2$ precipitates of 100 to 250 nm in size are surrounded by finer Ll_2 precipitates of about 20–30 nm in size. This microstructure is similar to the typical coherent two-phase structure in Ni-base superalloys, except that the size of the precipitates (coarse ones) is about one-fifth the size in the Ni-base superalloys. The results of X-ray diffraction of Ir-15at%Ti and Ir-15at%Nb alloys show both the fcc and Ll_2 structures. These data show that the fcc/Ll_2 coherent two-phase structure is also formed in the Ir-Nb and Ir-Ti systems.

Compression test

The stress-strain curves obtained by the compression test at 1800°C are shown in Fig. 2. The 0.2% flow stress of pure Ir, which is 20.3 MPa, is drastically improved by Nb or Ti additions. The 0.2% flow stress of the Ir-15at%Nb and 15at%Ti alloys, which have the fcc/$L1_2$ coherent two-phase structures, are 212 and 222 MPa, respectively. For references, the compressive yield stress of a Nb alloy (Nb-18at%Al-4at%W) at 1800°C (1), the tensile yield stresses of a W-base HfC dispersion

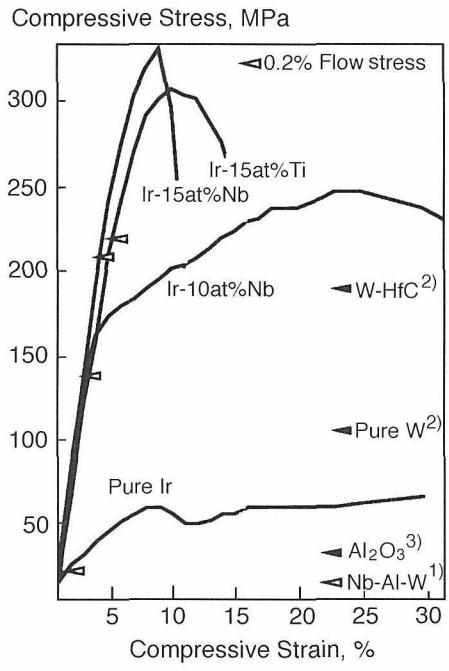

Fig. 2 Compressive stress-strain curve of the Ir-10, 15Nb, 15Ti alloys and pure Ir at 1800°C.

hardening alloy (W-0.35wt%Hf-0.025wt%C) (2) at 1650°C and Al_2O_3 (3) at 1800°C and the ultimate tensile stress of pure W at 1800°C are also shown in Fig. 2. Solid symbols are used for the tensile test results. The strength of Ir alloys is equivalent to the strengths of pure W (103 MPa) and W- HfC alloys (197 MPa), which are believed to be the strongest metallic materials available at this temperature and larger than those of the Nb alloy (12 MPa) and Al_2O_3 (28 MPa). The compressive ductilities of the Ir-15at%Nb and 15at%Ti alloys are not large. Macroscopic observation of the fractured samples revealed that grain boundary cracking caused the fracture. This may show that it is necessary to add grain boundary strengthening elements when used in a polycrystalline form, as in the case of Ni-base superalloys. Another solution may be to eliminate grain boundaries by forming single crystals.

It should also be noted in Fig. 2 that the Ir-10at%Nb alloy, which is expected to have the fcc single phase at 1800°C according to the phase diagram, has a high 0.2% flow stress (144 MPa) as well as a large compressive ductility. This suggests that Nb acts not only as a $L1_2$ precipitate former but also as a solid solution hardener in Ir. Further strengthening by adding 15at%Nb is attributed to the precipitation hardening of the Ll_2 phase. In any case, the data show that the balance of strength and ductility can be controlled by adjusting Nb content in the Ir-Nb binary system.

The Ir-10at%Nb, 15at%Nb and 15at%Ti alloys showed compressive ductilities at room temperature, which are 12.7, 8.1 and 8.6% (interrupted) in compressive strain, respectively.

Oxidation test

Oxidation resistance of the Ir-15at%Nb alloy and three reference alloys, pure W, Nb-20.4Al and Nb-4.2W-21.3Al (at%), were examined. The samples of these alloys were heated at 1800°C for 1 hour in air. Pure W and the Nb-base alloys were completely vaporized. Only the Ir-base alloy remained after the heating, with the metal loss being 0.03 mm from the surface. These simple screening tests show that the Ir-base refractory superalloys have good oxidation resistance as well as superior mechanical properties at such ultra-high temperatures.

Acknowledgment

We are grateful to Mr. S. Nishikawa of Furuya Metal CO., Ltd. for preparing Ir alloy ingots. We are also grateful to Mr. N. Sasaki and Mr. Y. Matsumoto of Japan Ultra-high Temperature Materials Research Center for carrying out the compression test at 1800°C. Part of this work was carried out under the auspices of the UK-Japan cooperative science program, organized by the Royal Society and the Japan Society of the Promotion of Science.

Keywords: fcc/Ll_2 two-phase coherent structure, high-temperature compressive strength, oxidation resistance

References

1. T. Yamagata, Proc. Fifth Symp. on High-Performance Materials for Severe Environments, (International Conference Hall, Dec. 5–6, 1994), 107.
2. W. F. Brown, Jr, H. Mindin and C. Y. Ho, eds., *Aerospace Structural Metals Handbook*, 5 (CINDAS/Purdue University, 1992): 5501–5502.
3. J. Wadsworth, J. Wittenauer and T. G. Nieh, "Proc. Critical Issues in the Development of High Temperature Structural Materials," eds. N. S. Stoloff, D. J. Duquette and A. F. Giamei, TMS, Hawaii 1993, 89.

❒ Transmission Electron Microscopic Study of Cr Precipitates in Cu-Cr in-situ Composite

Y. Jin, K. Adachi, *T. Takeuchi, and H. G. Suzuki
*Mechanical Properties Division, *High Magnet Division*

High-strength (>800MPa) and high-conductivity (>80%IACS) Cu material has a strong application potential in the electrical and electronic industries. In order to reach this goal, extensive studies[1-4] are now being carryed out on various Cu in-situ composites which have much higher concentrations of the secondary element than dilute Cu alloys. In these materials, aging treatment is crucial for obtaining good conductivity and further improving the strength. However, to the authors' knowledge, there is still no report concerning the aging characteristics of any Cu-Cr in-situ composite, although numerous results[5-6] have been published on dilute Cu-Cr alloys. In dilute Cu-Cr alloys, two precipitation problems remain unsolved: (a) Although significant aging effects are observed from 673K to 773K, microstructurally, no precipitates are seen until 748K. On the other hand, Kamijo et al.[7]. predicted by free energy calculation that homogeneous nucleation should happen due to the fluctuation of composition. (b) Different arguments exist concerning the crystal structure of the metastable precipitates up to peak-hardness. Some researchers believe the metastable precipitates to have an fcc or hcp structure while others suggest a bcc structure. In the present work, we have clarified the above two problems by investigating systematically the Cr precipitation in the Cu matrix of a Cu-15wt%Cr in-situ composite, by means of analytical transmission electron microscopy (TEM) and high resolution electron microscopy (HREM).

The material was prepared by melting high-purity Cu (99.99at%) and Cr (99.99at%) in a vacuum furnace at 1813K. The ingot was hot forged at 1173K and then cold rolled into sheets with a reduction of up to 99.9% in thickness. The samples were solution treated under vacuum at 1273K for 1hr, quenched in water, and then aged under vacuum for 1hr at temperatures ranging from 473K to 1173K.

Fig. 1(a) shows the TEM bright-field (BF) image of the Cu matrix in the studied composite aged at 473K for 1hr. Only the dislocations (A) introduced by water quenching can be seen. Fig. 1(b) is the BF image of the Cu matrix aged at 673K for 1hr. In contrast to the previous work on dilute Cu-Cr alloys, Cr-rich clusters (B) were observed although their size is too small to produce coherent strain contrast. Since the corresponding hardness testing and electrical conductivity measurements have displayed significant aging effect, some evidence of precipitation should be seen microstructurally. The existence of these Cr-rich clusters also confirms the theoretical prediction of Kamijo et al.[5]. Fig. 1(c) shows the BF image of the Cu matrix in the peak-hardened condition (773K/1hr). In contrast to the material in the under-aged condition, typical coffee-bean contrast (C) is observed, suggesting that these precipitates are fully coherent with the Cu matrix and possess the same fcc lattice, and thus should be Cr GP zones. Fig. 1(d) is the BF image of the Cu-matrix at the peak electrical conductivity condition (873K/1hr). Unlike the case for the peak-hardened condition, most of the precipitates (D) were found to be rod-like with an associated high strain field. The observed precipitates are similar to that observed for dilute

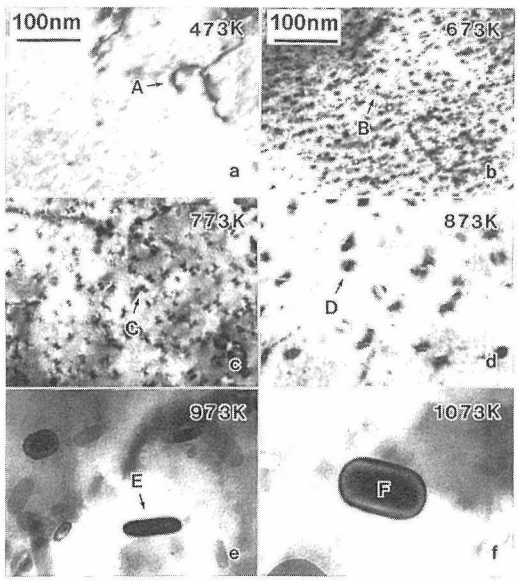

Fig. 1 TEM bright-field images of the Cu matrix aged at (a) 473K/1hr, (b) 673K/1hr, (c) 773K/1hr, (d) 873K/1hr, (e) 973K/1hr and (f) 103K/1hr. The orientation is close to <011>Cu.

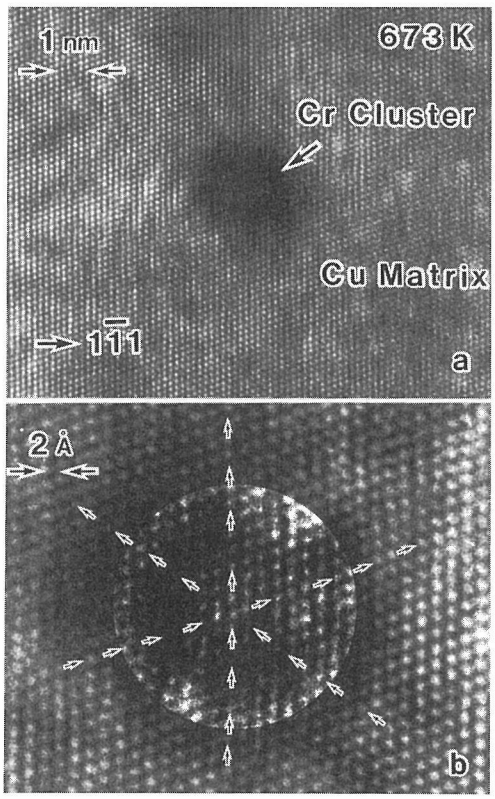

Fig. 2 (a) HREM image of the Cr-rich cluster in the Cu matrix in [011] orientation aged at 673K/1hr, and (b) Computer-processed image showing the coherency of the cluster.

Cu-Cr alloys at the same aging temperature, and have been identified to be the coherent Cr phase of bcc crystal structure. Fig. 1(e) is the BF image of the Cu matrix held at 973K for 1hr. Unlike the peak electrical conductivity condition, incoherent rod-shaped precipitates (E) were observed. The observed precipitates are also similar to that observed for dilute Cu-Cr alloys at the same aging temperature, and are generally believed to be the incoherent Cr phase of bcc crystal structure, possessing a K-S relationship with the Cu matrix. Fig. 1(f) shows the BF image of the Cu matrix at an even higher aging temperature (1073K/1hr). Only a small amount of bulk-like incoherent Cr bcc precipitate phase (F) can be observed. The existence of the Cr-rich cluster in the Cu matrix has also been verified with HREM techniques. Fig. 2(a) shows the HREM image of a Cr-rich cluster of around 3nm in size, in [011]Cu orientation at 673K/1hr aging condition. The Cr-rich cluster displays a darker contrast than the surrounding Cu matrix. More information can be obtained by improving the image of the cluster with computer image processing techniques, and the result is shown in Fig. 2(b). It can be seen that the Cr-rich cluster appears to be fully coherent with the surrounding Cu matrix and have the same fcc lattice although lattice distortion exists.

To summarize, the Cu-Cr in-situ composite has similar aging behavior as dilute Cu-Cr alloy. However, in contrast to dilute Cu-Cr alloy, nanoscale Cr-rich clusters were observed in the Cu matrix in the early-aged condition, which matches not only the corresponding results of hardness testing and electrical conductivity measurement but also the previous prediction from free energy theory. In addition, the precipitates in the Cu matrix at the peak-hardened condition are identified to be Cr GP zones.

Keywords: Cu in-situ composite, Cr precipitation, transmission electron microscopy

References

1. W.A. Spitzig, A.R. Pelton, and F.C. Laabs, "Characterization of the Strength and Microstructure of Heavily Cold Worked Cu-Nb Composites", *Acta Metall.*, 35 (1987): 2427–2442.
2. C. Biselli and D.G. Morris, "Microstructure and Strength of Cu-Fe In Situ Composites After Very High Drawing Strains", *Acta Mater.*, 44 (1996): 493–504.
3. Y. Sakai, K. Inoue, and H. Maeda, "New High-strength, High-conductivity Cu-Ag Alloy Sheets", *Acta Metall. Mater.*, 43 (1995): 1517–1522.
4. Y. Jin, K. Adachi, T. Takeuchi, and H. G. Suzuki, "Microstructural Evolution of a Heavily Cold-rolled Cu-Cr In-situ Metal Matrix Composite", *Mater. Sci. Eng. A*, 212 (1996): 149–156.
5. R.W. Knights and P. Wilkes, "Precipitation of Chromium in Copper and Copper-Nickel Base Alloys", *Metall. Trans.*, 4 (1973): 2389–2393.
6. P. Humble and D. Borland, "Precipitation in a Cu-0.55wt%Cr Alloy, G.C. Weatherly", *Acta Metall. Mater.*, 27 (1979): 1815–1828.
7. T. Furukawa, M. Watanabe, and T. Kamijo, "Homogeneous Nucleation of Coherent Precipitation in Copper-Chromium Alloys", *Acta Metall. Mater.*, 36 (1988): 1763–1769.

❒ Making New Metal-Organic Compounds with Unusual Electronic Structures- Chemical, Electrochemical, and Spectroscopic Properties of Phthalocyanines of Group 15 Elements-

H. Isago and Y. Kagaya
Chemical Processing Division

Fabrication of molecular devices, where one molecule functions as one device, is one of the most challenging projects in current and future science. In a number of biological systems, such as enzymes, which can be considered as well-designed molecular devices, unusual electronic structures have often been observed in their reaction centers where some metal ions play an important role. In recent years, phthalocyanines and their metal compounds (MPcs), which are industrially important organic dyes, have attracted much attention in the field of electronics, nonlinear optics, and photosensitization in electron-transfer reaction. They are also of interest from the viewpoint of the similarity in their molecular and electronic structures to those of reaction centers of enzymes. For example, lanthanoid compounds ligating two phthalocyanines are known to have structures similar to those of the reaction center of photosynthetic bacteria. Originally, this work was intended to make bismuth- and antimony-phthalocyanines similar to the lanthanoid-phthalocyanines because both of the group-15 elements are stable in the trivalent oxidation state and have ionic radii close to those of lanthanoids(III). Although the obtained compounds ligate only one phthalocyanine (Fig. 1), they are much more interesting than what we wanted. In this review, we wish to figure out the unusual properties of the bismuth- and antimony-phthalocyanines.

Compositions, Chemical Properties, and Solubility Characteristics

The bismuth-[(1)] and antimony-phthalocyanines[(2)] were synthesized for the first time in our laboratory with conventional procedures that were modified a bit. The former has the composition, [Bi(pc)X], where pc^{2-} and X^- denote phthalocyanine dianion, $C_{32}H_{16}N_8^{2-}$, and monoanion (Cl^- and Br^-), respectively[(1)]. Although it is unknown whether the compounds should be presented as [Bi(pc)X] or as $[Bi(pc)]^+X^-$, electrochemistry of [Bi(pc)Br][(3)] has supported the latter formula, at least in solutions. [Bi(pc)X]s are relatively soluble in polar solvents, but insoluble in nonpolar solvents normally used for the known MPcs. In solutions, [Bi(pc)X]s were unstable against water, acids, and bases; the bismuth ion is quite labile and readily expelled from the pc macrocycle. On the contrary, the antimony compound has been isolated as $[Sb(pc)Cl_2]^+X^-$ (X^- = monoanion, such as hexachloroantimonate, perchlorate, and so on)[(2)]. This is surprising because the central antimony ion is pentavalent although trivalent antimony ($SbCl_3$) was used as the starting material. $[Sb(pc)Cl_2]^+$ is more soluble than [Bi(pc)X]s in solvents normally used for the known MPcs. This is stable against water and acids (even in concentrated H_2SO_4) but readily reduced even by weak reducing agents such as organic amines. Such ionic MPcs were unknown until this work.

Electrochemistry

Figure 2 shows cyclic voltammograms of [Bi(pc)X]s and $[Sb(pc)Cl_2]^+$. The first oxidation (Ox), the first and second reduction waves (Red1 and Red2) in that of [Bi(pc)Cl] (Fig. 2a) are all pc-macrocycle-centered. The voltammetric feature (including the redox potentials) is typical of the known MPcs with electrochemically-inactive central metal ions. That of [Bi(pc)Br] (Fig. 2b) was essentially the same

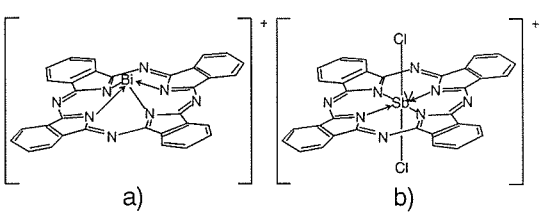

Fig. 1 Proposed molecular structures of a) $[Bi(pc)]^+$ and b) $[Sb(pc)Cl_2]^+$.

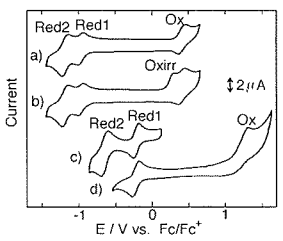

Fig. 2 Typical cyclic voltammograms of a) [Bi(pc)Cl], b) [Bi(pc)Br] (in dimethyl formamide), c) negative scan and d) positive scan of $[Sb(pc)Cl_2]^+$ (in dichloromethane).

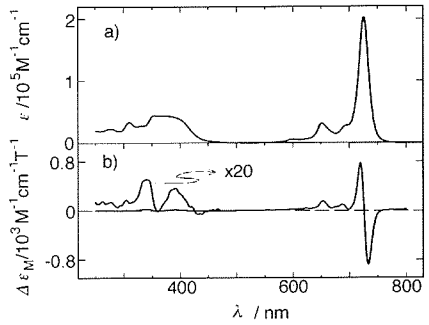

Fig. 3 The a) UV and b) MCD spectra of $[Sb(pc)Cl_2]^+$ (in dichloromethane).

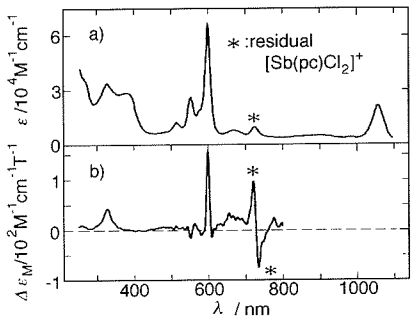

Fig. 4 The a) UV and b) MCD spectra of one-electron-reduced species of $[Sb(pc)Cl_2]^+$ (in dichloromethane).

except for the appearance of an additional oxidation wave (Oxirr), indicating that [Bi(pc)Br] dissociated into $[Bi(pc)]^+$ and Br^- in solutions. Although the voltammogram of $[Sb(pc)Cl_2]^+$ is similar in its shape to that of the [Bi(pc)Cl], surprisingly the redox potentials are significantly anodically shifted by ca. 1 V (Fig. 2c and 2d); its first reduction potential is the smallest of those of the known MPcs. The facile reduction of $[Sb(pc)Cl_2]^+$ might be useful in the field of electronics, photosensitization in solar cell, and for a new electron acceptor for synthetic metals or superconductors, and molecular magnets.

Spectroscopy

Figure 3 shows the electronic absorption (UV) and magnetic circular dichroism (MCD) spectra of $[Sb(pc)Cl_2]^+$. Although MPcs are known to show an intense absorption band generally in the visible region (650–680 nm), which is assigned as an electronic transition from their HOMO to LUMO and is called as a Q-band, $[Sb(pc)Cl_2]^+$ shows the most bathochromically shifted Q-band at 726 nm of the known MPcs. Likewise, [Bi(pc)X]s show a red-shifted Q-band at 716 nm. All of the [Bi(pc)X]s and $[Sb(pc)Cl_2]^+$ show a distinctive Faraday A-term in their MCD spectra (the derivative-shape line under the Q-band in Fig. 3b), indicating that they have high symmetry (as shown in Fig. 1). Their intense Q-bands in the near-infra-red region might be useful in the field of optoelectronics, nonlinear optics, and for the other optical devices where semiconductor-lasers play important roles.

Quite recently, we have reported UV and MCD spectra of electrochemically-generated one-electron-reduced species of $[Sb(pc)Cl_2]^+$ (its smallest reduction potential allowed us to obtain such species)[4]. As shown in Fig. 4, both the UV and MCD spectra showed a single intense band at 599 nm. On the basis of these spectra, we concluded that the transitions observed were orbitally degenerate in their ground state and that their symmetry was reserved even upon reduction. This is quite surprising because one-electron-reduced MPcs were believed to be distorted in symmetry due to significant Jahn-Teller effect until we reported these spectra. The facile reduction and the retention of high symmetry of $[Sb(pc)Cl_2]^+$ even upon reduction could be useful in the fabrication of new types of molecular magnets.

Concluding Remarks

We have briefly referred to the unusual properties of new phthalocyanines of group-15 elements. In particular, the antimony-phthalocyanine might be promising in some fields. However, the causes of such anomalies are still unknown. We have offered some hypotheses but most of them are under investigation[1-4]. The answers would be given by further study, especially with the aid of theoretical work such as molecular orbital calculations. Further synthetic works on new compounds are also in progress.

Keywords: phthalocyanine, antimony, bismuth, electrochemistry, spectroscopy

References

1. H. Isago and Y. Kagaya, "Syntheses and Characterization of Bromo- and Chloro (phthalocyaninato)bismuth(III) Complexes", *Bull. Chem. Soc. Jpn.*, 67 (1994): 383–389.
2. Y. Kagaya and H. Isago, "Facile Reduction of Dichloro(phthalocyaninato)antimony(V) Cation", *Chem. Lett.*, (1994): 1957–1960.
3. H. Isago and Y. Kagaya, "Redox Potentials of Bromo- and Chloro(phthalocyaninato) bismuth(III) Complexes", *Bull. Chem. Soc. Jpn.*, 67 (1994): 3212–3215.
4. H. Isago and Y. Kagaya, "Spectroscopic Properties of One-Electron-Reduced Species of Dichloro(phthalocyaninato)antimony(V) Cation", *Bull. Chem. Soc. Jpn.*, 69 (1996): 1281–1288.

❒ Formation of Stably Induced Laser Plasma and Its Characteristics

S. Tsukamoto, K. Hiraoka, Y. Asai, and H. Irie*
*Advanced Materials Processing Division, *Environment Performance Division*

Introduction

CO_2 laser has been widely used as an energy source for material processings such as welding, cladding, alloying, cutting, drilling, PVD and so on. One of main problems of the processing is that the interaction between the laser beam, metal vapour and gases produces a laser-induced plasma. Once the plasma forms, it absorbs or scatters the laser beam and leads to a reduction in heat input or power density. Some interesting research works have been done to analyse the characteristics of the plasma and to discuss the laser-plasma interaction[1), (2)]. It is very difficult, however, to measure the distributions of the electron density and the temperature of the plasma, because they fluctuate very rapidly during the laser processing.

Recently, we have developed a new method for producing a laser plasma which is large and stable enough to analyse the characteristics[3)]. In the present topics, we introduce the method and the characteristics of the plasma.

Formation of Large and Stable Laser Plasma

A stably induced laser plasma can be obtained by a good combination of an arc and a laser beam as shown in Fig. 1. A focused laser beam was irradiated onto an arc plasma generated in a horizontal direction. An assist gas of Ar, N_2, He or a mixed gas thereof was flowed through a coaxial nozzle of 5 mm in diameter. A local part of the arc plasma which was heated by laser irradiation was separated from the arc and went upward due to its buoyancy when the laser power exceeded 1.2 kW.

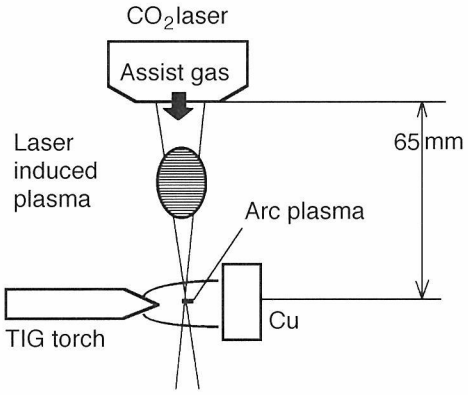

Fig. 1 Formation method of stably induced laser plasma.

With an adequate coupling of the laser power and the flow rate of the assist gas, the laser plasma stood still in space between the nozzle and the arc as shown in Fig. 2 (a). Once the plasma formed, it continued to exist by absorbing laser power even if the arc was shut off. The size of the plasma increased with increasing the laser power and the flow rate of the assist gas. This plasma is large and stable enough for its characteristics to be analysed.

Characteristics of Laser Induced Plasma

The stably induced Ar plasma was characterised by the following methods. The incident laser power I_0 and the laser power passed through the plasma (I_1) were measured using a power probe with an absolute accuracy of 5%. Average absorption coefficient α is obtained by

$I_1 = I_0 \exp(-\alpha x)$

where x is the plasma length. The radial distribution of the electron density was evaluated by measuring the infrared radiation from the plasma on the basis of the Abel inversion. In the infrared range, Bremsstrahlung is expected to be dominant and the spectral radiance is in proportion to the square of the electron density[4)]. The electron temperature distribution was calculated numerically from the value of the electron density on an assumption that the plasma was in local thermodynamic equilibrium. Figures 2 (b) and (c) show a typical example of the electron

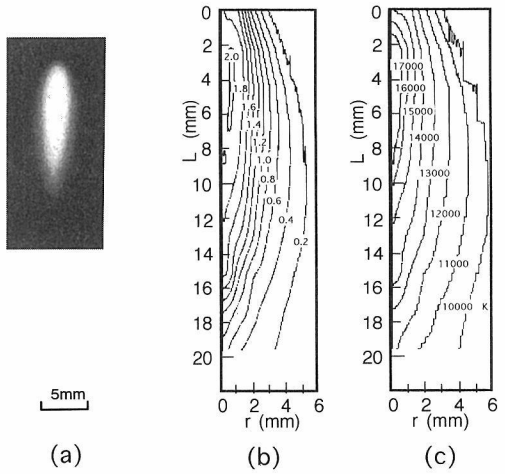

Fig. 2 Typical example of (a) stably induced laser plasma, (b) electron density and (c) electron temperature profiles of the plasma.(Laser power : 3.8 kW, Assist gas : Ar, 15 L/min)

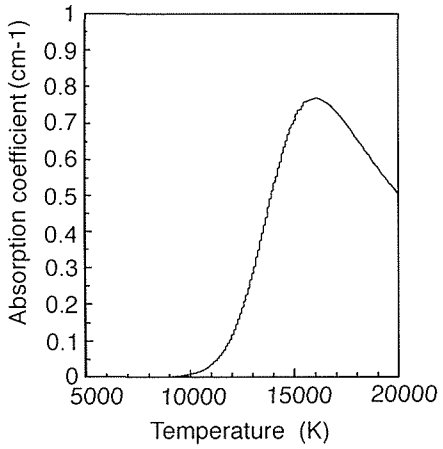

Fig. 3 Calculated absorption coefficient of pure Ar.

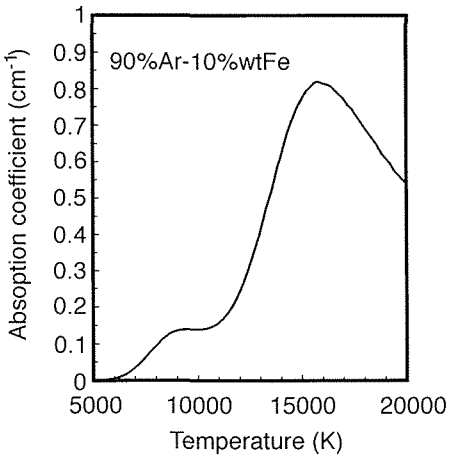

Fig. 4 Calculated absorption coefficient of Ar-10wt%Fe.

density and temperature profiles.

The laser energy absorbed in the plasma increased with increasing the laser power, whereas the average absorption coefficient of the plasma had an approximately constant value of 0.6 cm^{-1} independent of the laser power. This suggests the state of the plasma is not affected by the laser power. In fact, maximum values of the electron density and the electron temperature of the plasma showed 2.0×10^{17} cm^{-3} and 18000-19000 K in all ranges of the laser power, respectively. Only the plasma size was affected by the laser power. The temperature profile was spread with increasing the power.

The absorption coefficient was calculated numerically from the experimental data of the electron density and temperature on the basis of inverse Bremsstrahlung theory[5]. The results agreed well with those obtained by the experiment, indicating that the absorption of the laser energy is caused by inverse Bremsstrahlung. The calculation of the absorption coefficient for Ar plasma revealed that the absorption was most remarkable at 16200 K and it decreased above the temperature as shown in Fig. 3. This is the reason why the plasma temperature was saturated at 18000 to 19000 K.

In the laser processing, metallic elements vaporised from the substrate may affect the absorption property, because their ionisation energy is normally less than that of gases. Then, the absorption coefficient of Ar-10wt%Fe was calculated and shown in Fig. 4. The ionisation of Fe causes a plateau at 9000–10000 K, but a large peak can be seen at 16000 K due to ionising Ar. This indicates that the metallic elements do not exert a great influence on the absorption property if the plasma does not include a large amount of metallic elements. On the other hand, the laser processing phenomenon such as weld penetration is significantly affected by the composition of the assist gas. Our experimental data of the absorption coefficient also indicated the effect of the gas composition. Ar-N_2 mixed gas slightly reduced the absorption coefficient due to a large thermal conductivity. The addition of He to Ar assist gas significantly decreased the absorption coefficient because of the large ionisation energy of He.

The stably induced laser plasma which we developed is quite unique. It can be generated in space without electrodes. We are planning to develop this method to a new materials processing.

Keywords: CO_2 laser, laser processing, laser induced plasma, absorption, electron density, thermal plasma

References

1. W. Sokolowski, G. Herziger, and E. Beyer, "Spectral Plasma Diagnostics in Welding with CO_2 Lasers", *Proc. 1st European Congress on Optics*, SPIE 1020 (1988): 96–102.
2. "I. Miyamoto, and H. Maruo, Spacial and Temporal Characteristics of Laser-Induced Plasma in CO_2 Laser Welding", *Proc. LAMP'92*, (1992): 311–316.
3. S. Tsukamoto, K. Hiraoka, Y. Asai, H. Irie, M. Yoshino, and T. Shida, "Characteristics of Stably Induced Laser Plasma", *Proc. ICALEO'96*, (1996).
4. T. Ohji, T. Shiwaku, Y. Hirata, and K. Hiraoka, "Measurement of Arc Plasma by the IR Plasma Diagnostic Method", *IIW Document*, Doc. 212-881-95: (1995).
5. T.P. Hughes, "Plasmas and Laser Light, The Institute of Physics", (1975): 39–54.

❒ Application of AFM Technique on Bacteria Corrosion

N. Washizu and H. Masuda
Failure Physics Division

Microbiologically influenced corrosion (MIC) is corrosion caused by microorganisms. It is difficult to work out a countermeasure for MIC because it is almost impossible to predict the corrosion rate, which changes in compliance with the amount and the activity of microorganisms. Therefore, MIC is a serious problem.

In many cases, iron oxidizing bacteria (IOB) play important roles in MIC. Figure 1 shows metabolism of IOB. IOB live on Fe^{2+} and oxidize it in acid water. Fe^{3+}, which is product of IOB, is an oxidant and corrodes metals. When Fe^{3+} oxidizes metals, it is reduced to Fe^{2+} on which IOB live. With this cyclic reaction of Fe^{2+} and Fe^{3+}, multiplication of IOB increases corrosion rate, and corrosion accelerates multiplication of IOB.

In this research, we have examined what happened to metallic surfaces and cells of IOB in the initial stage of the corrosion. To observe cells of IOB, we applied an atomic force microscope (AFM) with which it is possible to observe the shapes on a nm scale in the atmosphere.

Initial corrosion induced by IOB

Figure 2 shows an AFM image of a cell of IOB and a hollow around the cell on the surface of SUS 304 steel, which is a typical stainless steel. The size of this cell was approximately 1mm X 0.5mm. The hollow had the same shape as the cell. According to this fact, if IOB adsorb on the surface of SUS 304 steel, the part of the surface near the cell of IOB is corroded selectively. It seems that the hollow around the cell formed by this selective corrosion grows into a visible pit, which is the characteristic of MIC of stainless steel.

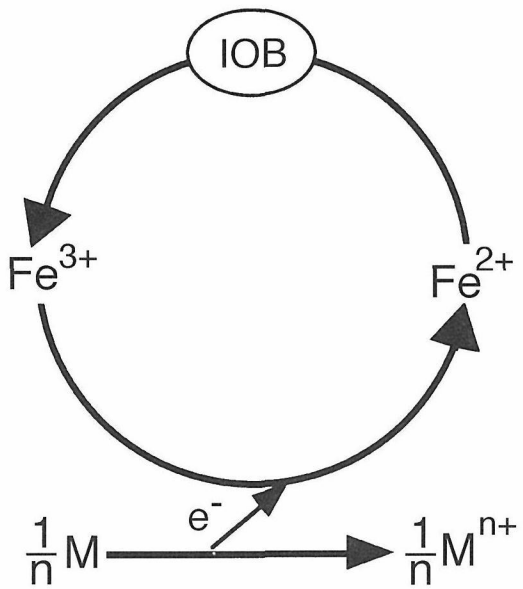

Fig. 1 Metabolism of IOB and corrosion induced by IOB.

Corrosion and activity of IOB

Figure 3 shows an AFM image of a surface of SUS 304 steel on which corrosion was induced along grain boundaries. A cell of IOB adsorbed on the surface near the grain boundaries. This bacterium was bigger than ordinary ones and had a narrow part in the center of the cell, which means that the cell was segmenting and active. The reason for this activation of IOB seems to be that Fe^{2+} was produced in the corrosion site by the reduction of Fe^{3+} and by the corrosion of solid iron which is the principal element of stainless steel.

Figure 4 shows an AFM image of a surface of SUS 304 steel with a pit of approximately 800 nm. It was also observed that a cell of IOB which crept into the pit was segmenting. The reason for the creep of the cell of IOB seems to be that the cell was seeking Fe^{2+} and that Fe^{2+} was produced in the pit by corrosion. It seems that IOB which crept into the pit got Fe^{2+}, became active and segmented.

Figure 5 shows an AFM image of a surface of SUS 304 steel on which 2 cells of IOB were

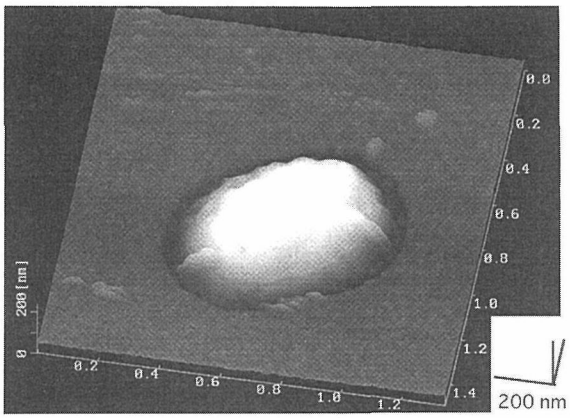

Fig. 2 AFM image of a cell of IOB and corrosion induced by the cell on a surface of SUS 304 steel.

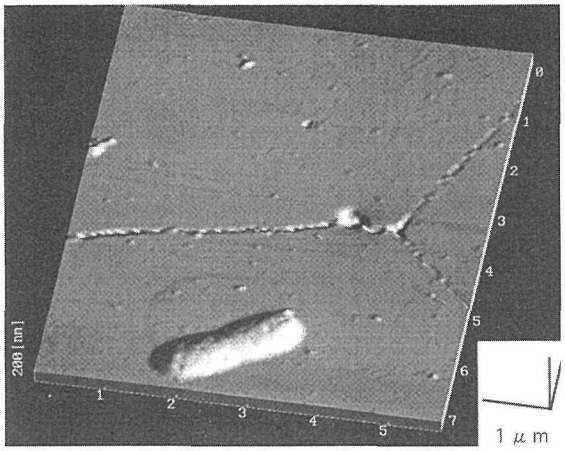

Fig. 3 AFM image of IOB which segmented and corrosion along grain boundaries on a surface of SUS 304 steel.

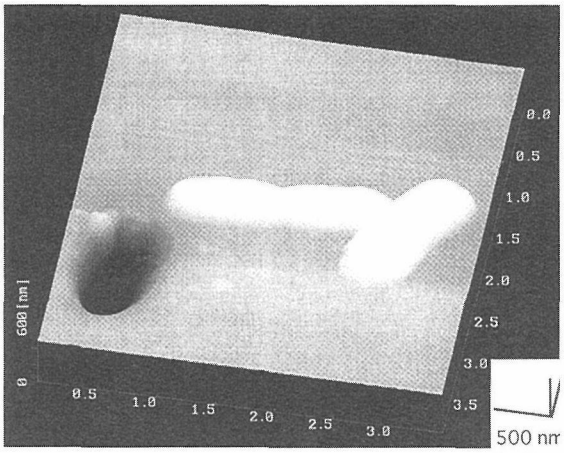

Fig. 5 AFM image of two cells of IOB near a pit on a surface of SUS 303 steel.

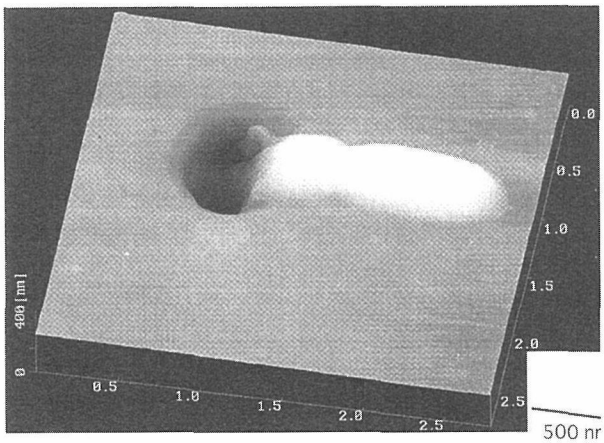

Fig. 4 AFM image of IOB which crept into a pit on a surface of SUS 304 steel.

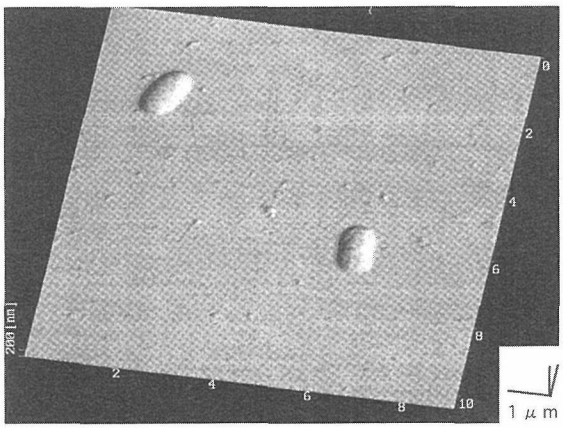

Fig. 6 AFM image of two cells of IOB on a surface of SUS 304 steel where corrosion was not induced.

observed near a pit. One of these IOB which was closer to the pit was active and segmented. The distance between this bacterium and the pit was approximately 500 nm. The other was located at a distance of 2 μm from the pit and did not segment. This result means that the difference in activity of IOB depends upon whether a bacterium is close or not to a pit on a μm scale.

Figure 6 shows an AFM image of a surface of SUS 304 steel which was not corroded. Two cells of IOB observed on the surface did not segment. This bacterium was not active because Fe^{2+} was not supplied by corrosion.

Conclusion

In this research, we examined initial corrosion induced by IOB from the point of view of single cells. The results are as follows:

1. IOB induce corrosion on a surface of stainless steel where IOB adhere.
2. IOB which adhere to a corrosion site become active.

Keywords: microbiologically influenced corrosion, iron oxidizing bacteria, Fe^{2+}, Fe^{3+}, atomic force microscope

❒ Creep Rates of Austenitic Steels during Carbide Precipitation

F. Abe
Environmental Performance Division

Many microstructural changes take place in heat-resisting steels and alloys at high temperature and affect their creep deformation behavior. In the present research, the effect of carbide precipitation on creep rate has been investigated for 10Cr-30Mn austenitic steels containing 0.003, 0.11, 0.26 and 0.55% carbon. After solution-annealing, the creep test was carried out at 873 K for up to about 10^4 h. These steels are proper for an investigation on the effect of carbide precipitation, because the carbon addition of up to 0.5 wt% causes only one kind of carbide, $M_{23}C_6$. This simplifies the interpretation of the results. High-Mn austenitic steels are promising as a replacement for conventional Fe-Ni-Cr stainless steels suitable for fusion reactor structures as regards a reduced radioactivation property.

Creep rates in transient creep region

The creep curves consisted of a primary or transient creep region, where the creep rate decreased with time, and of a tertiary or accelerated creep region, where the creep rate increased with time after reaching a minimum creep rate. In the neighborhood of the minimum creep rate, the change in creep rate with time was very small, suggesting that this area corresponds to the steady-state creep region. In the high-carbon steels, 0.26C and 0.55C, the extensive precipitation of $M_{23}C_6$ occurred during creep, causing a significant decrease in creep rate. The effect of the $M_{23}C_6$ precipitation on the creep rate curves was analysed using the general equation for diffusion-controlled growth of precipitates from supersaturated solid solution. The creep rate curves in the transient creep region were described as [1-2]

$$\log \dot{\varepsilon} = A - (1/3)\log t - \alpha y \quad (1)$$

$$y = y_0\left\{1 - \exp\left[-(Kt)^{2/3}\right]\right\}, \quad (2)$$

where A is a constant depending on stress and carbon concentration, α proportional constant, y the amount of precipitated solute atoms at the time t, y_0 the total amount of available precipitate atoms in solution and K is the rate constant. The calculated curves shown in Fig. 1 provide a reasonable approximation for the experimental results over most of the transient region. The last term, α y, on the right side of Eq.[1] represents the decrease in creep rate by the $M_{23}C_6$ precipitation during creep and was negligibly small for the low carbon 0.003C and 0.11C steels. The time exponent 2/3 in Eq.[2] is related to the stress-induced

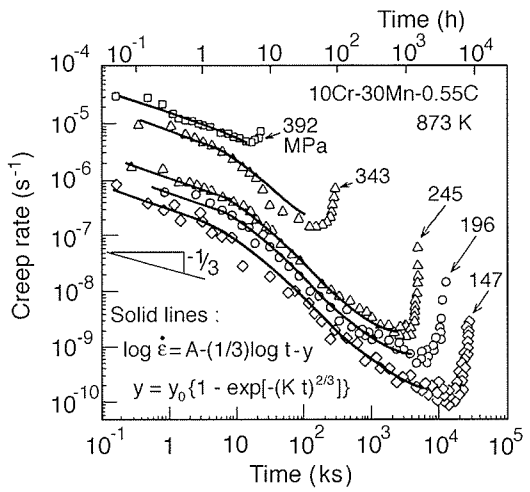

Fig. 1 Calculated creep rate curves for the 10Cr-30Mn-0.55C steel using Eq.[1], compared with the experimental results.

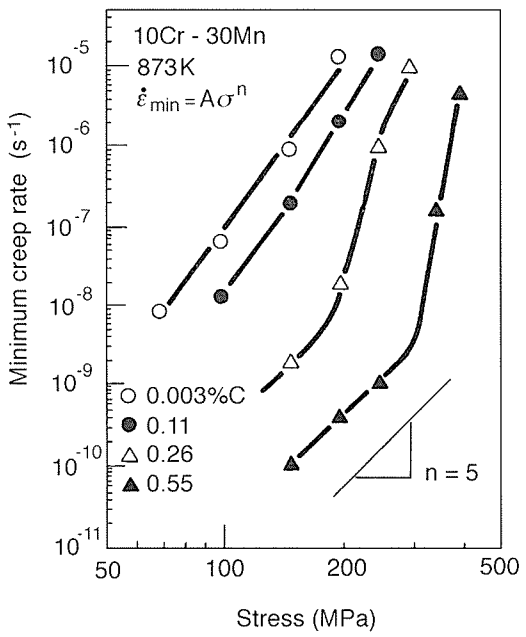

Fig. 2 Stress dependence of minimum creep rate.

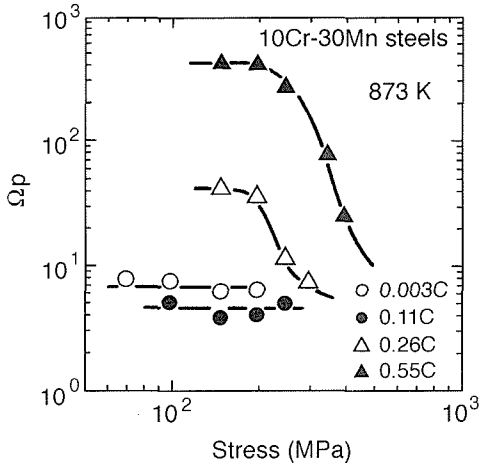

Fig. 3 Change in Ωp with stress. The Ωp is given by $d\ln\dot{\varepsilon}/d\varepsilon$, after reaching a minimum creep rate.

precipitation of $M_{23}C_6$ on dislocation lines which were produced by creep deformation.

Minimum creep rate

In the high carbon 0.26C and 0.55C steels, the stress exponent n of the minimum creep rate ($\dot{\varepsilon}\min = B\sigma^n$) changed from very high values above 20 at high stresses to a low value of about 5 at low stresses (Fig. 2). Taking into account Eqs.[1] and [2], the effect of the $M_{23}C_6$ precipitation on the stress dependence of the minimum creep rate was described as

$$\dot{\varepsilon}_{\min} = B\sigma^n \exp(-\alpha y'), \tag{3}$$

where y' is the y at the time at which the creep rate exhibits a minimum value. The term exp(-αy') decreases with increasing the $M_{23}C_6$ precipitation. This indicates that the stress dependence of the minimum creep rate during carbide precipitation results from not only the stress exponent *n* but also the term exp(-αy'). After completion of the $M_{23}C_6$ precipitation, the exp(-αy') is regarded as constant and the stress dependence at low stresses and long times is the same as that of the low carbon steels.

Acceleration of creep rate

After reaching a minimum creep rate, the logarithm of creep rate increased linearly with strain but not linearly with time. Therefore, the acceleration of creep rate was evaluated by $\Omega p = d\ln\dot{\varepsilon}/d\varepsilon$, which is the same as the creep damage parameter defined by Prager. In the low carbon 0.003C and 0.11C steels, the Ωp was as low as 6 and was interpreted as the acceleration of creep rate by an apparent increase in stress caused by a decrease in cross section with strain. In the high carbon 0.26C and 0.55C steels, the Ωp increased from the low value similar to the low carbon steels at high stresses and short times to the high values up to about 40 and 400 for the 0.26C and 0.55C steels, respectively, and then saturated after completion of the $M_{23}C_6$ precipitation (Fig. 3)[2-3]. The precipitation and agglomeration of the $M_{23}C_6$ precipitates along grain boundaries promoted the formation of creep-cavities and grain boundary fracture, causing an increase in Ωp.

Creep rupture life

The time to rupture t_R was expressed as[2-3]

$$t_R = 1.45/(\dot{\varepsilon}_{\min}\Omega p) \tag{4}$$

for all the specimens with different stress levels and different carbon levels. This indicates that the t_R is determined by the product of the $\dot{\varepsilon}_{\min}$ by Ωp but not by the $\dot{\varepsilon}_{\min}$ alone.

Keywords: creep rate, austenitic steel, carbide, precipitation

References

1. F. Abe, "Creep and Creep Rate Curves of a 10Cr-30Mn Austenitic Steel during Carbide Precipitation", *Metall. Trans.* 26A (1995): 2237–2246.
2. F. Abe, K. Kimura, E. Baba, O. Kanemaru and K. Yagi, "Creep Curve Analysis and Creep Life Evaluation of 10Cr-30Mn Austenitic Steels", *Proc. Intern. Symp. on Materials Aging and Component Life Extension* (1995): 1075–1084.
3. E. Baba, O. Kanemaru, F. Abe and K. Yagi, "Effect of Cold-rolling on Creep Behavior of a 10Cr-30Mn Austenitic Steel", *Tetsu-to-Hagane* 81 (1995): 845–850: in Japanese.

❒ Large Single Crystal Growth of New Borocarbide Superconductors

H. Takeya
1st Research Group

Since the discovery of a new family of borocarbide intermetallic superconductors $RETM_2B_2C$(RE=rare earths, TM=Ni, Pd, Pt), a great number of studies on the crystal structure and the various physical properties have been performed[1,2]. So far, most of physical measurements on YNi_2B_2C have been performed on the arc-melted polycrystal samples, which contain a lot of micro-cracks formed due to thermal stress during cooling. In addition, they commonly contain a small amount of the second phases. According to our preliminary study, YNi_2B_2C is likely to melt incongruently and decompose to YB_2C_2 and a liquid phase at a sufficiently high temperature. This makes it difficult to grow single crystals from the stoichiometric melt. In such a case, a promising method is the flux method. Xu et al.[3] have reported that the platy single crystals of $RENi_2B_2C$ can be obtained by the flux method using Ni_2B flux. However, it is very difficult to grow larger single crystals with sufficiently high quality by the flux method because the process of the growth is rather uncontrollable.

In this study, we have succeeded in growing single crystals of YNi_2B_2C with cm-dimensions by a floating zone (FZ) method. The arc-melted polycrystalline YNi_2B_2C was made from the stoichiometric composition of the starting materials, yttrium blocks(99.9%), nickel balls(99.99%), boron flakes(99.8%) and graphite sheets(99.995%). Several polycrystalline buttons were re-melted together and cast into a cylindrical form as a feed rod with dimensions of about 8 mm in diameter and 120 mm in length. The apparatus for the crystal growth was an infrared heating furnace with double ellipsoidal mirrors (ASGAL Co.) as well as two 2.0 kW halogen lamps as the heat source. Purified argon gas was introduced in the furnace and was flowing through the oxygen trap to prevent oxidation of the sample rods. The flowing rate was set at a rate between 1.5 l/min and 0.5 l/min. The feed and the seed shafts were rotated oppositely at the rate of 15 rpm and 12 rpm, respectively. The growth speed was set between 1.0 mm/h and 2.3 mm/h. Observation of the metallurgical structure and composition analyses were performed by an electron microscope JEOL JSM-840F with an energy dispersive X-ray analyser (EDX). The superconductivity of the grown crystals was measured using a Quantum Design SQUID magnetometer.

In Fig.1, an example of the as-grown boule is shown. The growth rate in this case is 2.3mm/h. No solvent was used in the single crystal growth experiments. The crystal has two well developed habits of the {001} plane along the growth direction, which was determined by the X-ray Laue method.

All diffraction peaks of the X-ray powder diffraction pattern using the crushed powder of YNi_2B_2C single crystal can be assigned by the tetragonal YNi_2B_2C phase and no impurity phase is identified. From this data the lattice parameters for the a and c axes are determined to be a=3.5265(1) and c=10.5415(3), respectively. These values are in good agreement with the ones obtained from the arc-melted polycrystals.

Figure 2(a) shows the back-scattered electron micrograph of the grown crystal along the growth

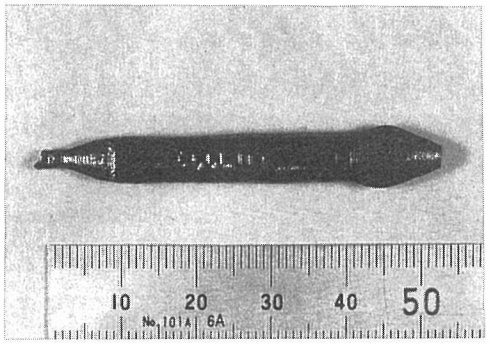

Fig. 1 A photograph of the as-grown boule of YNi2B2C by the floating zone method.

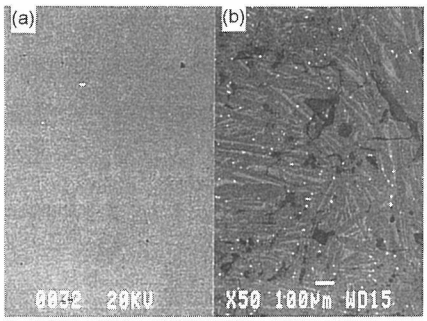

Fig. 2 Back-scattered electron micrographs of (a) the grown crystal along the growth direction and (b) the arc-melted polycrystal.

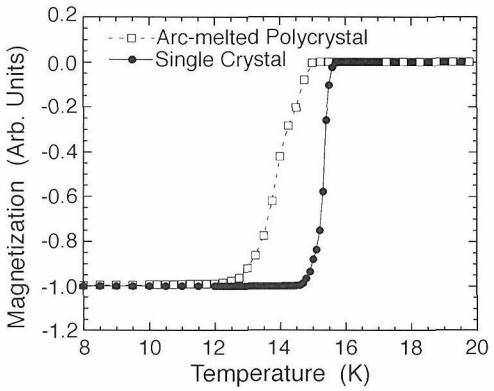

Fig. 3 Superconducting transitions of the arc-melted polycrystal and the grown single crystal.

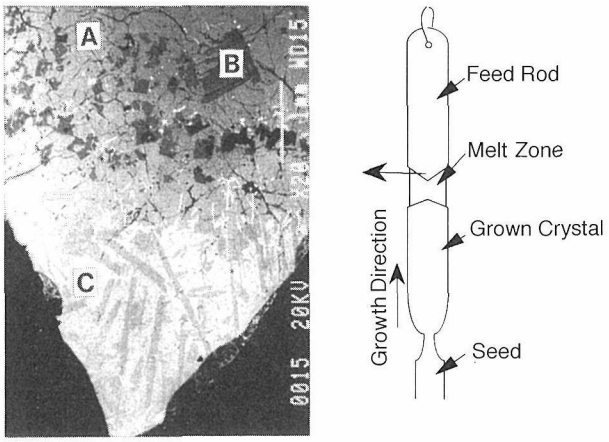

Fig. 4 Back-scattered electron micrograph of the tip of the feed rod.

direction, compared with that of arc-melted buttons (Fig. 2(b)). The arc-melted buttons contain many cracks and a trace of the second phase. On the contrary, no second phase can be seen in the FZ grown single crystal. The number of cracks are remarkably reduced in the FZ single crystal.

In Fig. 3, the superconducting transition of the FZ single crystal sample measured by magnetization in 0.5mT is compared with the polycrystal. The superconducting transition with T_C=14.8K and ΔT_C=2.3K for the arc-melted polycrystal is improved in the grown crystal with T_C=15.6K and ΔT_C=0.7K. Although our preliminary metallurgical study suggested that YNi_2B_2C was an incongruent melting material, the single crystals of YNi_2B_2C have been successfully grown without using any solvent. In order to understand the growth mechanism of this compound, the molten zone was slowly separated with cooling and the microstructure was analysed in detail. Figure 4 is a back-scattered electron micrograph at the tip of the feed rod. According to the analyses by EDX and X-ray diffraction, regions **A** and **B** are identified to be YNi_2B_2C and YB_2C_2, respectively. Region **C** is speculated to be the composition of $YNi_4(B,C)_x$. A considerable amount of YB_2C_2 is seen just above the molten zone compared with the trace amount in the feed rod, and the molten zone is rich in Ni. This suggests that YNi_2B_2C decomposes to YB_2C_2 and the Ni-rich solution at the tip of the feed rod. The Ni-rich solution forms the molten zone and the single crystal of YNi_2B_2C seems to be precipitated from the Ni-rich solution, though no solvent is prepared at the beginning. It seems that the appropriate solvent is naturally and self-consistently formed in the process of the growth.

Keywords: single-crystal growth, anisotropic superconductor, magnetization

References

1. R. Nagarajan, C. Mazumder, Z. Hossain, S. K. Dhar, K.V. Gopalakrishnan, L.C. Gupta. C. Godart, B.D. Padalia, and R. Vijayaraghavan, *Phys. Rev. Lett.*, 72(1994): 274.
2. R.J. Cava, H. Takagi, B. Batlogg, H.W. Zandbergen, J.J. Krajewski, W.F. Peck, Jr., R.B. van Dover, R.J. Felder, T. Siegrist, K. Mizuhashi, J.O. Lee, H. Eisaki, S.A. Carter and S. Uchida, *Nature* 367(1994): 146.
3. M. Xu, P.C. Canfield, J.E. Ostenson, D.K. Finnemore, B.K. Cho, Z.R. Wang and D.C. Johnston, *Physica* C, 227(1994): 321.

❒ Quantitative Analyses of Oxygen Content in $YBa_2Cu_3O_{7-d}$ Thin Films

J. Ye* and K. Nakamura
*1st Research Group,*Material physics division*

$YBa_2Cu_3O_{7-\delta}$ (YBCO) superconducting thin films have been the subject of considerable interest since shortly after the discovery of bulk superconducting materials. Extensive efforts have been made in preparing thin films with better superconducting properties and better crystallinity. Because thin films are not prepared in a thermodynamically equilibrium state, various defects such as cation disordering, stacking faults, oxygen deficiency and others are inevitably generated during the growth process. Among these defects, oxygen deficiency (content) is the most prominent factor controlling superconducting properties of as-grown YBCO films. For bulk YBCO, the subject has been widely investigated both in superconducting transition temperature and structure change including c-lattice parameter, and correlation between c-lattice parameter and oxygen content has been established. In thin films, however, the c-lattice parameter depends not only on oxygen content but also on the growth conditions, such as substrate material, substrate temperature and pressure during deposition. Therefore, oxygen content in thin films cannot be simply determined from c-lattice parameter, as usually done in powder samples. Here, we report an effective method for determining oxygen content from X-ray intensity change which is caused by the structural change accompanied by oxygen deficiency[1-3].

The oxygen deficiency of YBCO thin films was controlled by equilibrating the oxygen potential of the films with that of the bulk YBCO of known oxygen deficiency, as described in detail in the previous paper[1]. Fig. 1 shows the c-lattice parameter of YBCO films equilibrated with the bulk YBCO samples. From the figure, a smooth variation of the c-lattice parameter with the increasing oxygen deficiency can be seen, indicating the accuracy of the oxygen controlling experiments. It is also interesting that although the c-lattice parameter of fully oxygenated as-grown YBCO films is different from the bulk sample, the c-lattice parameter of the oxygen-controlled thin films changes with d with the gradient parallel to that of the bulk sample.

Another interesting phenomenon observed from the X-ray diffraction is the dramatic change in the intensities of 00*l* reflections. Fig. 2 shows the change of 00*l* reflection of YBCO film with various controlled δ values. For a clear view, the I(00*l*)/(005) are multiplied by 1.4, 2.13, 1.45, 32, 1, 0.95 for 001 to 007 reflections, respectively. It is

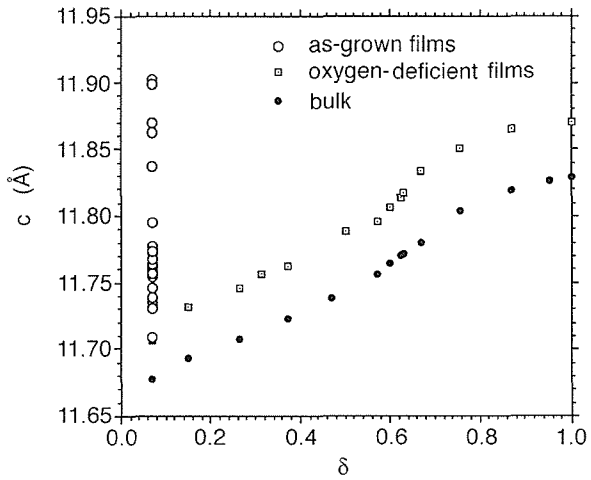

Fig. 1 Dependency of c-lattice parameters with oxygen deficiency δ in bulk YBCO samples (solid circles) and thin films (squares and triangles are for those prepared by MBE and RF sputterring methods, named as N6112 and N2228b, respectively). For bulk samples, error bars are smaller than the symbols [2].

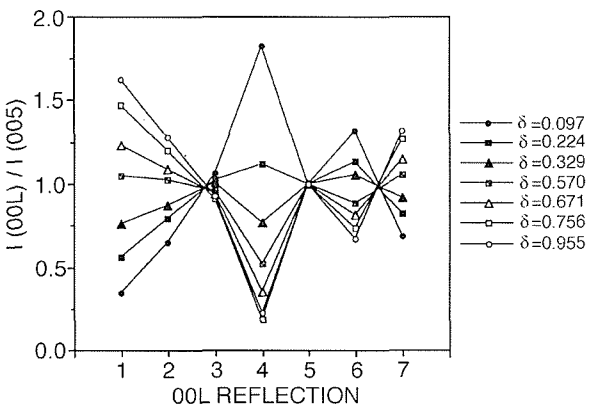

Fig. 2 Relative changes in integrated intensity of 00l reflections of $YBa_2Cu_3O_{7-\delta}$ thin films to their 005 reflections. For a clear view, the I(00l)/I(005) values were multiplied by 1.40, 2.13, 1.45, 32, 1, 0.95 and 3.85 for 001 to 007 reflections, respectively. Symbols represent films of different oxygen contents (δ values shown with numerals[2]).

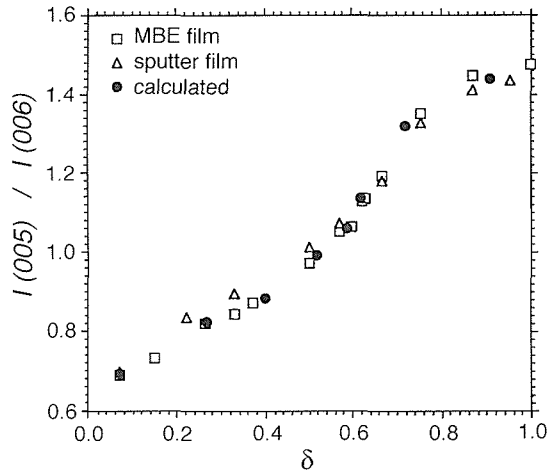

Fig. 3 Dependency of observed and calculated I(005)/I(006) values with oxygen deficiency δ[2]. Squares are for MBE prepared thin films (N6112), triangles for sputterring prepared films (N2228b), and solid circles for those calculated based on the models built by Jorgensen et al. [4]

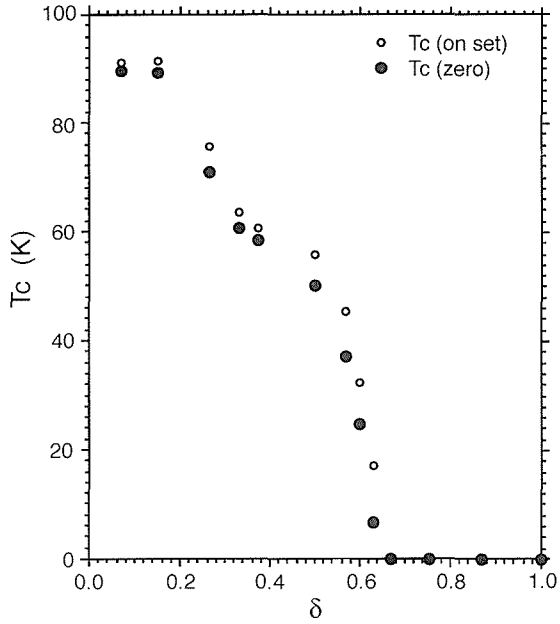

Fig. 4 Superconducting transition temperatures Tc (on set in small open circles and zero point in large solid circles) vs. oxygen deficiency δ in YBCO thin films.

shown that the two strongest reflections 005 and 006 behave in a totally opposite sense with δ values, and they are both diffracted at relatively high 2θ angles. This make the measuring of their accurate intensities. We chose these two reflections as the calibrating parameter of the oxygen deficiency. Fig. 3 is a plot showing the δ dependency of the I(005)/I(006) of the two thin films, along with that which was calculated on the basis of models established by Jorgensen et al.[(4)]. A good agreement between the observed and calculated values is recognized. It should be emphasized that the I(005)/I(006) value is a function of the δ value if other defects such as cation disorder are absent. If cation disorder (Y substituted by Ba) is generated during the growth process, the I(005)/I(006) ratio changes to the reverse direction with increasing disorder[(3)]. In this case, post annealing at 850°C for 30 min is necessary to get an ordered cation arrangement.

Fig. 4 shows the relation between Tc and the δ value. It is obvious that the Tc vs. δ value relation in thin YBCO films is almost the same as that in bulk material, indicating that the oxygen potential control and determination applied in the present study is very accurate. It is concluded that quantitative analyses using the measured 00l integrated intensity data of the oxygen-deficient thin films confirmed that the structural properties of oxyge-deficient thin films are basically identical to those reported in bulk samples. It is also concluded that a relationship between the measured I(005)/I(006) value and the oxygen deficiency could be used as a good calibrating factor of oxygen deficiency in thin films.

Keywords: YBCO thin film, oxygen deficiency, MBE, sputtering, oxide superconductors, X-ray diffraction

References

1. K. Nakamura, J. Ye and A. Ishii, "Oxygen Potential Control in $YBa_2Cu_3O_{7-\delta}$ Thin Films", *Physica*, C213(1993): 1–13.
2. J. Ye and K. Nakamura, "Quantitative Structure Analysis of $YBa_2Cu_3O_{7-\delta}$ Thin Films: Determination of Oxygen Content from X-ray Diffraction Patterns", *Phys. Rev.*, B 48(1993): 7554–7564.
3. J. Ye and K. Nakamura, "Systematic Study on the Growth Temperature Dependence of Structural Disorder in $YBa_2Cu_3O_{7-\delta}$ Thin Films", *Phys. Rev.*, B 50(1994): 7099–7160.
4. J.D. Jorgensen, B.W. Veal, A.P. Paulikas, L.J. Nowicki, G.V. Crabtree, H. Claus, and W.K. Kwok, "Structural Properties of Oxygen-deficient $YBa_2Cu_3O_7$-d", *Phys. Rev.*, B 41(1990): 1863.

❒ An Analysis of Effect of Bubble Morphology and Workhardening Exponent on Helium Embrittlement by Finite Element Method

H. Shiraishi
2nd Research Group

Helium embrittlement is analysed by applying the two-dimensional elastic-plastic finite element method based on continuum mechanics. This program was written by the present author and can treat large-scale plastic deformation. In this program, triangular mesh elements are used assuming plane stress condition. Mises yield criterion, J2 flow theory, and the type of n-th power workhardening law are assumed. The morphology of grain boundary helium bubbles is approximated by repeated boundary condition of corresponding displacements. The effect of workhardenability and bubble morphology is surveyed.

Figure 1 shows an example of calculated conventional stress/strain curves and Figure 2 shows a summary of the effect of bubble size and density under constant workhardening exponent on deformation mode and total elongation. The deformation mode is divided into two categories: (1) localization of strain in near grain boundary region and (2) unloading and cessation of deformation in near grain boundary region. In the former case, the reduction of total elongation results in which is interpreted as helium bubble embrittlement. In the latter case, the deformation proceeds in the grain interior region beyond the so-called plastic instability point, and no embrittlement occurs.

The loss of elongation has been considered to be controlled by the bubble areal fraction on grain boundary[(1)]. This is partly true along boundary AB in the figure. The increase of bubble density can recover the total elongation, as illustrated by the border BC. This is inferred due to change of stress and strain distribution near grain boundary. Within the parameter region where helium embrittlement occurs, the elongation decreases monotonously with increase of bubble size and bubble density, as expected.

The reduction of the workhardening exponent is revealed to cause severe helium embrittlement in the case of strain localization mode near grain boundary.

In view of preventing helium embrittlement, the high workhardening exponent is essential. The high helium bubble density is also effective, but bubble coalescence due to temperature excursion

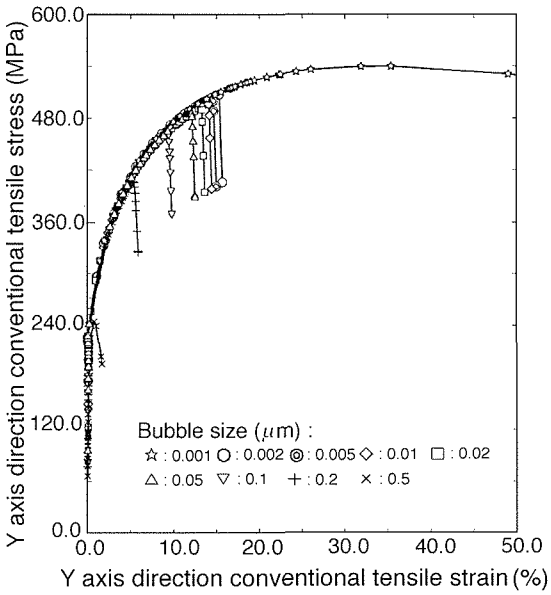

Fig. 1 Effect of helium bubble size on stress/strain curves. Workhardening exponent: 0.3, Bubble density: 1.0/μm, Grain size: 20.0μm

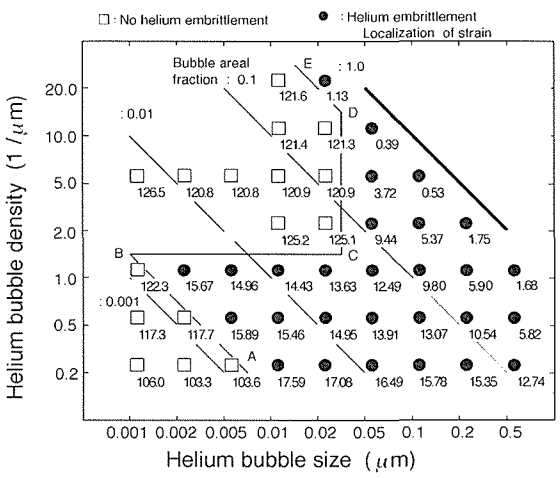

Fig. 2 Effect of bubble morphology at grain boundary on helium embrittlement in case of workhardening exponent: 0.3.

must be monitored.

Keywords: helium embrittlement, finite element method, bubble morphology, workhardenability

Reference

1. J. I. Bennetch and W. A. Jesser, *J. Nutl. Muter.*, 103 & 104(1981): 809.

❒ Microstructure Control of γ -TiAl Base Alloys by Heat Treatment

T. Kumagai, E. Abe, M. Nakamura, T. Kimura*, and M. Isoda*
*3rd Research Group, *Materials Characterization Division*

Intermetallic compound γ -TiAl base alloys are candidate materials for high-temperature structural applications because of their attractive properties, such as high specific strength, high melting temperature and reasonable oxidation resistance. However, improvement of room-temperature ductility and high-temperature strength is required in order for these γ-base alloys to be used as engineering materials. Recent study has shown that the ternary element (Sb) addition is effective in improving high-temperature strength due to the combination of solution-hardening and particle (Sb-rich D8m phase)-reinforcement[1]. On the other hand, extensive studies have revealed that the room-temperature ductility of γ-TiAl alloys containing a small amount of α_2-Ti_3Al, so-called Ti-rich TiAl alloys, is superior to that of γ single-phase alloys, and that the refinement of microstructure is effective in improving the ductility.

In general, an as-cast Ti-rich TiAl alloy shows a coarse α_2/γ lamellar grain structure. This lamellar grain structure is thermally stable, so isothermal forging and/or the hot extrusion are needed for refinement of the microstructure. However, we succeeded in producing a fine $\gamma + \alpha_2$ two-phase microstructure only by heat treatment, which is the combination of quenching from the high-temperature α phase field and subsequent aging in the $\gamma + \alpha$ (or α_2) two-phase field[2, 3]. Fig. 1(a) shows a fine γ grain structure of Ti-48at.%Al heat treated at 1683K for 30min, followed by ice water quenching (IWQ). Figs. 1(b) and (c) show fine $\gamma + \alpha_2$ two-phase structures of the IWQ samples subsequently aged at lower-temperature (1473K) for 24hr and higher-temperature (1573K) for 1hr, respectively.

The single-phase γ grain structure as shown in Fig. 1(a) is formed metastably due to the $\alpha \rightarrow \gamma$ massive transformation, since there is not the equilibrium γ single-phase field in a Ti-48at.% Al alloy. Thus, the fine $\gamma + \alpha_2$ two-phase structure is easily obtained by the subsequent aging treatment, as shown in Figs. 1(b) and (c). A number of fine α_2 plates, which lie on the four equivalent $\{111\}_\gamma$ planes, in the γ grain interiors together with fine α_2 particles at the γ grain boundaries are observed in these microstructures. In addition, the long-time aging treatment at lower-temperature (1473K) causes discontinuous precipitation and coarse α_2 plates formation, as shown in Fig. 1(b) (marked by arrow). However, this discontinuous precipitation is suppressed in the samples aged at higher-temperature (1573K), and the fine $\gamma + \alpha_2$ two-phase structure remains stable.

The tensile properties of the fine $\gamma + \alpha_2$ two-phase structure of Ti-48at.%Al are being investigated. However, we observed the effect of the α_2 phase on the tensile properties utilizing isothermally forged and homogenized Ti-49 and

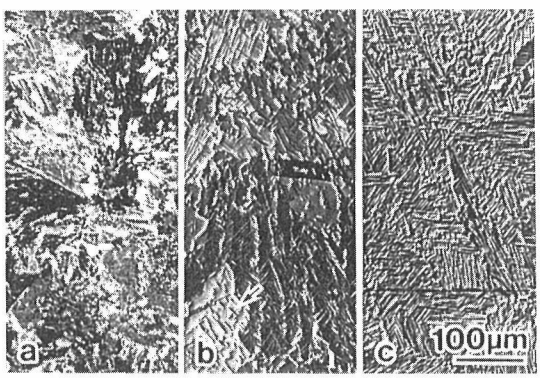

Fig. 1 Optical microstructures of (a) massively transformed Ti-48at.%Al sample and subsequently aged samples at (b) lower-temperature (1473K for 24hr) and (c) higher-temperature (1573K for 1hr).

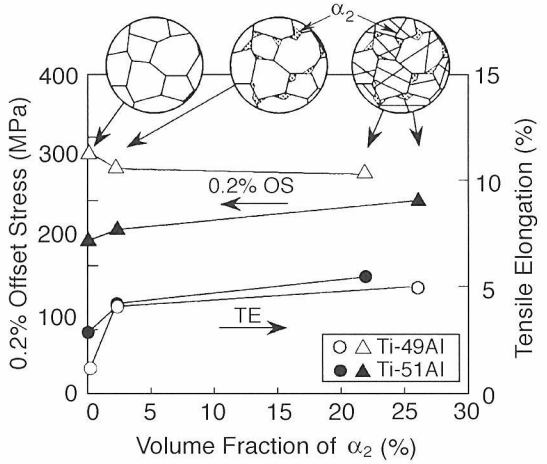

Fig. 2 Room-temperature tensile properties of Ti-49 and 51at.%Al as a function of the α_2 laths, together with the microstructure morphology.

51at.%Al alloys as received materials[4]. Three types of microstructures obtained by the heat treatments are as follows : type (I) equiaxed γ grain structure, type (II) γ grain structure with the α_2 laths at the γ grain boundaries and type (III) γ grain structure with the α_2 laths both in the γ grain interiors and at the γ grain boundaries. In addition, the matrix γ grain size in the three types of microstructures is about 100μm. Fig. 2 shows the tensile properties at a nominal strain rate of $10^{-4}s^{-1}$ in a chamber evacuated to 10^{-3}Pa. This result indicates that the α_2 phase improves the tensile elongation without decreasing the tensile strength in both Ti-49 and 51at.%Al alloys. Based on this result, the tensile properties of the fine $\gamma + \alpha_2$ two-phase structure, as shown in Fig. 1, are expected to be better still.

In this paper, only the results of the microstructural control of the Ti-Al binary alloy by the heat treatments were reported. However, this control method utilizing the $\alpha \leftrightarrow \gamma$ phase transformation can be applicable not only to the Ti-Al binary alloy but also the Ti-Al-X ternary alloys[2], and further advancement is expected for the future.

Keywords: intermetallic compounds, TiAl, phase transformation, microstructure, tensile properties

References

1. K. Hashimoto, M. Nobuki, H. Doi, E. Abe, and M. Nakamura, "High Temperature Strength and Room Temperature Ductility of TiAl Base Alloys with Antimony", *Proc. 124th TMS Int. Symp. on Gamma Titanium Aluminides*, (1995): 761–770.
2. M. Takeyama, T. Kumagai, M. Nakamura, and M. Kikuchi, "Cooling Rate Dependence of the α/γ Phase Transformation in Titanium Aluminide and Its Application to Alloy Development", *in Structural Intermetallics*, eds. R. Darolia et al., (1993): 167–176.
3. T. Kumagai, E. Abe, M. Takeyama, and M. Nakamura, "Reaction Process of ag Massive Trans-formation in Ti-rich TiAl Alloy", *MRS Symp. Proc.*, 364 (1995): 181–186.
4. T. Kumagai and M. Nakamura, "Effects of Aluminum Content and Microstructure on Tensile Properties of TiAl Alloys", *Scripta Mater.*, 34 (1996): 1147–1154.

❐ Magnetization Measurement Using the Hybrid Magnet at NRIM

H. Kitazawa, S. Nimori, and G. Kido
4th Research Group

Recently, a hybrid magnet system was constructed at the National Research Institute for Metals (NRIM)[1] and the maximum field of up to 36.5 T became possible to generate for 30 mm bore and that of 32.2 T for 50 mm bore. The magnetization measurement is one of the most crucial experimental methods for investigating the magnetic properties of various substances (magnetic materials, superconducting materials, etc.) in a high-magnetic field. Very recently, a reliable and efficient magnetometer was developed by means of the sample-extraction method for the hybrid magnet[2]. A magnetization process for various magnetic substances has been measured up to 30 T so far. In this report, we introduce our homemade magnetometer and recent results obtained by using it[2, 3].

When a magnetic sample is passed through a coil, the coil induces a voltage proportional to the change of magnetic flux across the coil. Basically, the magnetization can be derived by the time-integration of the induction voltage. Two coils with the same structure are connected in the opposite direction to cancel out the voltage induced by the change of magnetic field. To save the machine time, magnetization data of up to four samples are measured with two pairs of the compensated coils, as shown in Fig. 1. Each sample is successively inserted and drawn out by computer-controlled air pistons during the sweep of the field. The induction voltage is A/D converted and is integrated in the same computer.

The hexagonal intermetallic compound RPd$_2$Al$_3$ (R = light rare earth element) has the PrNi$_2$Al$_3$-type structure which consists of R-Pd layers and pure-Al layers alternating along the c-axis. The magnetic properties in these systems hold interest in relation to the heavy fermion superconductor UPd$_2$Al$_3$ (Tc = 2 K)[4], which shows planar anti-ferromagnetic ordering below 14 K. Polycrystalline CePd$_2$Al$_3$[5, 6] is an antiferromagnetically ordered (T_N = 2.8 K, k = [0, 0, 1/2]) heavy fermion compound (γ_0 = 380 mJ / mol K^2). Neutron diffraction experiments revealed that the ordered Ce moments of 0.47 μ_B at saturation lie in the basal plane. PrPd$_2$Al$_3$ remains paramagnetic down to 1.5 K. The anti-ferromagnetic structure of NdPd$_2$Al$_3$[7] below T_N = 7.7 K corresponds to a propagation vector k = [1/2, 0, 0] and the ordered Nd moments of 2.3 μ_B at saturation lie in the basal plane. For RPd$_2$Al$_3$ compounds, polycrystalline and single crystalline samples often show different magnetic behavior. We mention the absence of long-range magnetic ordering in single crystalline CePd$_2$Al$_3$ down to 0.5 K[8, 9]. The reason for the latter may be caused by site disorder and/or vacancies of Pd and Al atoms, but the effect has never been completely understood. A systematic study of magnetic properties should lead to the understanding of the fundamental interactions of RPd$_2$Al$_3$ compounds including the heavy fermion superconductor UPd$_2$Al$_3$.

Single crystals of RPd$_2$Al$_3$ (R = Ce, Pr and Nd) were grown with the Czochralsky pulling method using a tetra-arc furnace in pure Ar atmosphere. Isothermal magnetizations $M(H)$ at 4.2 K are shown in Fig. 2 for the single crystals. To qualitatively analyse the observed magnetic anisotropy, we consider CEF effects by including information from inelastic neutron scattering (INS)

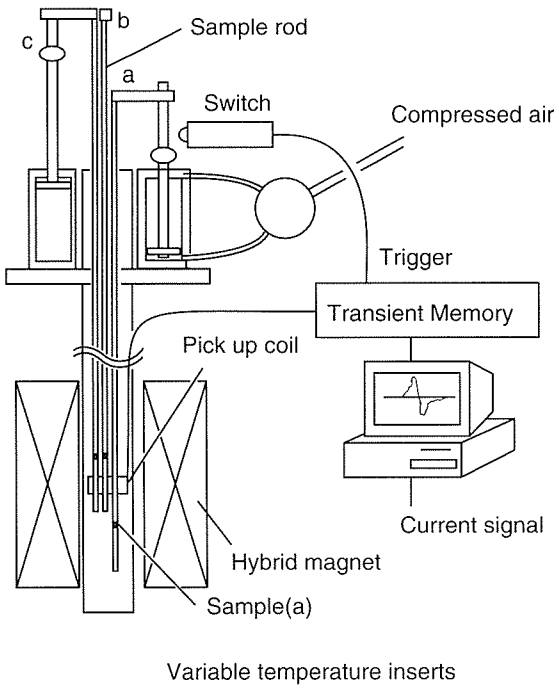

Fig. 1 Block diagram of the NRIM sample extract magnetometer.

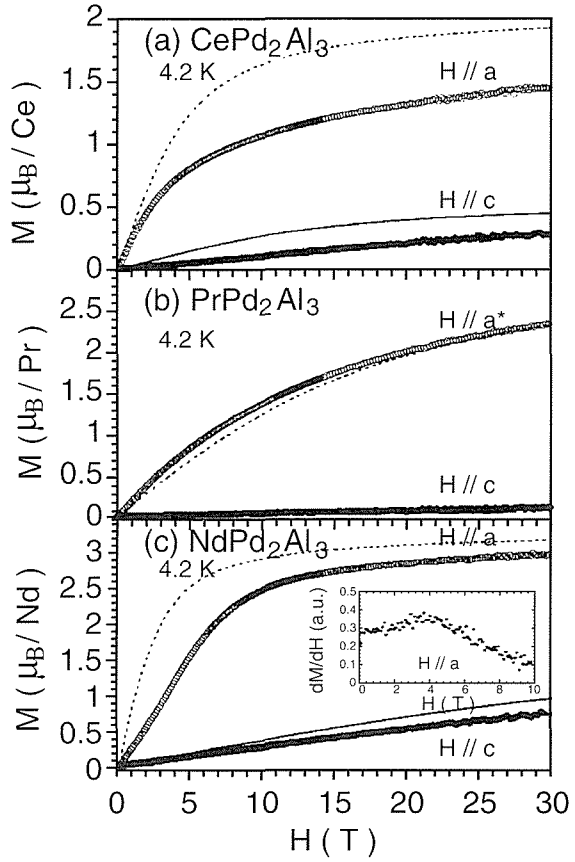

Fig. 2 Magnetization curves M(H) for RPd_2Al_3 (R = Ce, Pr, Nd) single crystals at 4.2 K.

experiments as far as known[10, 11]. For simplicity, magnetic exchange interactions are neglected. The Hamiltonian for CEF interactions of hexagonal symmetry is given by

$$H_{CEF} = B_2^0 O_2^0 + B_4^0 O_4^0 + B_6^0 O_6^0 + B_6^6 O_6^6 \qquad (1)$$

where the B_n^m denote CEF parameters and the O_n^m are operator equivalents. The solid and dashed curves in Fig. 2 and CEF parameters in Table 1 were derived by least-square fitting of $M(H)$ curves and temperature dependence of magnetic susceptibility with the CEF excitation energies fixed to the values determined by the INS experiments. In $PrPd_2Al_3$ the magnetization curves are well reproduced by the calculated ones. The excited CEF doublet state Γ_5 is located at about 65 K above the singlet CEF ground state Γ_1. On the other hand, for $CePd_2Al_3$ and $NdPd_2Al_3$ the amplitudes of the magnetization are smaller than calculated ones. These differences are caused by

Table 1: CEF parameters for RPd_2Al_3 compounds.

RPd_2Al_3	B_2^0 (K)	B_4^0(K)	B_6^0 (K)	B_6^6 (K)
$CePd_2Al_3$	47	0.83	-	-
$PrPd_2Al_3$	7.0	-0.13	-1.0E-3	-5.0E-2
$NdPd_2Al_3$	4.4	5.5E-3	-1.3E-4	-1.7E-3

the Kondo effect ($CePd_2Al_3$) and by antiferromagnetic exchange interactions ($NdPd_2Al_3$). For a quantitatively more precise description, effects of magnetic interactions must be included in the calculation.

Keywords: hybrid magnet, high field magnetization, rare earth compounds

References

1. K. Inoue, T. Takeuchi, T. Kiyoshi, T. Asano, Y. Sakai, K. Itoh, G. Kido, and H. Maeda, *Physica,* B 211 (1995): 17.
2. G. Kido, K. Takehana, S. Uji, T. Terashima, S. Nimori, S. Ikeda, H. Kitazawa, M. Oshikiri, and H. Aoki, *J. Magn. Magn. Mater.*, 157/158 (1996): 550.
3. H. Kitazawa, J. Tang, S. Nimori, F. Iga, A. Dönni, T. Matsumoto, and G. Kido: to be published.
4. C. Geibel, C. Schank, S. Thies, H. Kitazawa, C.D. Bredl, A. Böhm, M. Rau, A. Grauel, R. Caspary, R. Helfrich, U. Ahlheim, G. Weber, and F. Steglich, *Z. Phys.*, B 84 (1991): 1.
5. H. Kitazawa, C. Schank, S. Thies, B. Seidel, C. Geibel, and F. Steglich, *J. Phys. Soc. Jpn.*, 61 (1992): 1461.
6. A. Dönni, P. Fischer, B. Roessli, and H. Kitazawa, *Z. Phys.*, B 93 (1994): 449.
7. A. Dönni, H. Kitazawa, P. Fischer, T. Vogt, A. Matsushita, Y. Iimura, and M. Zolliker, *J. Solid State Chem.*, 127 (1996): 169 .
8. H. Kitazawa, A. Mori, S. Takano, T. Yamadaya, A. Matsushita, T. Matsumoto, N. Sato, T. Komatsubara, C. Schank, C. Geibel, and F. Steglich, *Physica,* B 186–188 (1993): 612.
9. S.A.M. Mentink, G.J. Nieuwenhuys, A.A. Menovsky, J.A. Mydosh, H. Tou, and Y. Kitaoka, *Phys. Rev.*, B 49 (1994): 15759.
10. S.A.M. Mentink, G.J. Nieuwenhuys, A.A. Menovsky, J.A. Mydosh, A. Drost, E. Frikkee, Y. Bando, T. Takabatake, P. Böni, P. Fischer, A. Furrer, A. Amato, and A. Schenck, *Physica,* B 199–200 (1994): 143.
11. A. Dönni, A. Furrer, M. Zolliker, and H. Kitazawa, *PSI annual report,* (1995).

❒ Fermi Surface Study in YNi_2B_2C Superconductor

T. Terashima
4th Research Group

The de Haas - van Alphen (dHvA) effect, quantum oscillations of magnetization periodic in the inverse of the magnetic field, is the most direct and powerful tool for probing the Fermi surface and related properties of metals. Recently, a new field to be studied with the dHvA effect has opened up: the dHvA effect in the mixed state of type-II superconductors. The first observation was reported by Grabner and Robbins for $NbSe_2$ in 1976[1]. Recent experiments carried out on type-II superconductors such as V_3Si, Nb_3Sn, κ-$(ET)_2Cu(NCS)_2$, and YNi_2B_2C have confirmed that the dHvA oscillation can be observed deep in the mixed state and showed that the superconductivity brings about an extra damping to the dHvA oscillation amplitude but no change in the dHvA frequency[2,3]. While theoretical controversy about the mechanism of the dHvA effect in the mixed state is not yet settled, at least it is widely accepted that the extra damping can be related to the magnitude of the superconducting gap. Since the dHvA effect can probe each piece of the Fermi surface separately, an exciting possibility emerges that the superconducting gap and its anisotropy may be determined for each piece of the Fermi surface.

The boro-carbide superconductor YNi_2B_2C, having a high superconducting critical temperature T_c of 15.6 K, is a feasible compound for detailed study of the dHvA effect in the mixed state. The moderate upper critical field H_{c2} of about 8.8 T is accessible by a commercial superconducting magnet, and hence a direct comparison between the dHvA oscillations in the mixed and normal states can be made by using the same experimental setup. In the present study, the dHvA oscillation coming from a small ellipsoidal electron pocket, α, has been observed in a wide magnetic field range from the normal state down to 2 T in the mixed state without interruption[4].

High-quality single crystals of YNi_2B_2C were grown by a floating zone method by Takeya (1st Research Group) et al.[5]. The dHvA effect measurements at temperatures down to 0.05 K and magnetic fields up to 16 T were performed with a superconducting magnet integrated with a dilution refrigerator. Using the low-frequency field modulation technique, the dHvA oscillation was detected at the second harmonic of the modulation frequency.

Figures 1(a) and (b) show the dHvA oscillations of the α Fermi surface in the mixed state. In most of the previous studies, the observation of the dHvA oscillation immediately below H_{c2} was hindered by the peak effect[2]. However, we could observe the dHvA oscillation in the peak effect region [Figure 1(a)]. While the oscillations are somewhat unclear in the raw data because of the large background due to the peak effect, the oscillations clearly manifest themselves after subtraction of the background, and it is found that the oscillation amplitude exhibits a node in the region. The α oscillation persists down to surprisingly low fields, i.e., 2 T [Figure 1 (b)].

The magnetic field dependence of the reduced oscillation amplitude is summarized in Fig. 2. In the normal state, the logarithm of the reduced amplitude varies linearly with the inverse of the magnetic field as is usually expected. The amplitude is strongly suppressed immediately below Hc_2. However, it recovers at lower fields and remains as large as about 30 % of the linear extrapolation of the normal state data. The prominent damping of the amplitude in the peak effect region can be explained by the enhanced pinning in this region. The pinning causes a macroscopic spatial variation of the magnetic field inside a sample and also screens the applied modulation field. Both suppress the dHvA oscillation amplitude. At lower fields below the peak effect region, the pinning becomes considerably small, and hence the main cause of the observed damping is the superconducting gap. Therefore, we will compare the low field data and theoretical predictions of the extra damping of the dHvA oscillation amplitude in the mixed state.

Maki and Stephen examined the dHvA effect in

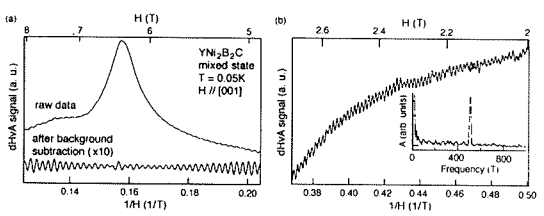

Fig. 1 dHvA oscillations in the superconducting mixed state of YNi_2B_2C.

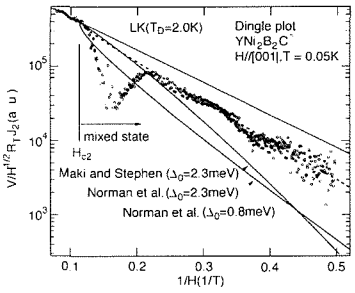

Fig. 2 The field dependence of the dHvA oscillation amplitude in the normal and mixed states of YNi_2B_2C.

the mixed state neglecting the detailed structure of the vortex lattice and based on an approximate quasiparticle Green's function in the mixed state[6]. On the other hand, recently, Dukan and Tešanović, and Norman et al. have derived the quasiparticle band structure by treating the vortex lattice explicitly[7]. Both approaches lead to a conclusion that the superconductivity brings about the extra damping of the dHvA oscillation amplitude without modifying the dHvA frequency. The damping factor may be expressed as $\exp(-2\pi\Gamma/\hbar\omega_c)$. Here Γ is a measure of the Landau level broadening due to the superconducting energy gap and is given by

$$\Gamma = \frac{\sqrt{\pi}}{2}\frac{\Delta^2}{\sqrt{\varepsilon_F \hbar\omega_c}} \quad \text{(Maki and Stephen) or}$$

$$\Gamma = 0.6\Delta\left(\frac{\varepsilon_F}{\hbar\omega_c}\right)^{-1/4} \quad \text{(Norman et al.).}$$

where Δ is the average superconducting energy gap in a magnetic field and can be calculated from the zero-field superconducting gap Δ_0 using a standard BCS formula. By using Δ_0 of 2.3 meV estimated from tunneling measurements[8], we have evaluated the theoretical damping factors, and the resultant field dependences of the oscillation amplitude are shown in Fig. 2. Apparently, the observed amplitude is much larger than the theoretical predictions or the extra damping is much smaller than that theoretically expected from Δ_0 of 2.3 meV. The discrepancy seems to indicate that this particular Fermi surface, the α surface, is much less gapped than the others. An intuitive argument for this is as follows. The cyclotron energy or the spacing between the Landau levels at 2 T is calculated to be 0.64 meV. On the other hand, if we assume that Δ_0 of the α surface is 2.3 meV, the average energy gap Δ at 2 T is estimated to be 2.0 meV. An observation of the dHvA effect at fields where the superconducting energy gap overwhelms the Landau level spacing seems very unlikely. Therefore, we suppose the gap of the α surface is much smaller than the average gap of 2.3 meV. A trial fit to the data is made for the theory of Norman et al. with Δ_0 as a free parameter and gives Δ_0 of about 0.8 meV (Fig. 2).

In conclusion, we have carried out the Fermi surface study of the boro-carbide superconductor YNi_2B_2C. The dHvA oscillation of the α Fermi surface has been observed down to 2 T in the superconducting mixed state. The oscillation amplitude at the lowest fields is much larger than predicted by the theories. We suppose that the α Fermi surface is much less gapped than the other Fermi surfaces.

Keywords: de Haas - van Alphen effect, Fermi surface, mixed state

References

1. J.E. Graebner and M. Robbins, "Fermi-Surface Measurements in Normal and Superconducting 2H-$NbSe_2$", *Phys. Rev. Lett.*, 36 (1976): 422–425.
2. R. Corcoran et al., "De Haas - van Alphen Effect in the Superconducting State", *Physica*, B 206 & 207 (1995): 534–541.
3. T. Terashima et al., "De Haas - van Alphen Oscillations in the Normal and Superconducting States of the Boro-carbide Superconductor YNi_2B_2C", *Solid State Commun.*, 96 (1995): 459–463.
4. T. Terashima et al., "Small Superconducting Gap on Part of the Fermi Surface of YNi_2B_2C from de Haas-van Alphen Effect", *Phys. Rev. B.*
5. H. Takeya et al., "Single Crystal Growth of Quaternary Superconductor YNi_2B_2C by a Floating Zone Method", *Physica*, C 256 (1996): 220–226.
6. K. Maki, "Quantum Oscillation in Vortex States of Type-II Superconductors", *Phys. Rev. B*, 44 (1991): 2861–2862. "Superconductors in Strong Magnetic Fields: de Haas - van Alphen Effect, M.J. Stephen", *Phys. Rev., B* 45 (1992): 5481–5485.
7. S. Dukan and Z. Tešanović, "De Haas - van Alphen Oscillations in a Superconducting State at High Magnetic Fields", *Phys. Rev. Lett.*, 74 (1995): 2311–2314. "Magnetic Oscillations and Quasiparticle Band Structure in the Mixed State of Type-II Superconductors", M.R. Norman et al., *Phys. Rev., B* 51 (1995): 5927–5942.
8. T. Ekino et al., "Superconducting Energy Gap in YNi_2B_2C", *Physica*, C 235–240 (1994): 2529–2530.

❒ The Highest Steady Field Magnet in the World Has Come into Operation

K. Inoue, T. Kiyoshi, M. Kosuge, A. Sato, F. Matsumoto, H. Nagai, and H. Maeda
High Magnetic Field Research Station

We succeeded in generation of the highest steady magnetic field in the world by using a 40 T class hybrid magnet system, which we have been developing since 1989. We have begun to use the magnetic field for several kinds of experiments. A magnetic field is one of the fundamental physical parameters and has remarkable influences on the many physical properties. Therefore, the high field experiments of several kinds of materials, such as superconductors, magnetic materials, semiconductors, organic materials, macromolecules, etc., are very effective for finding out their essential characteristics. There are many problems expected to be solved by using the high-magnetic field.

A hybrid magnet, composed of an outer superconducting magnet and an inner water-cooled magnet, is the most economical system for generating extremely high, steady magnetic fields. A superconducting magnet, consuming no electric power with theoretical upper limit of generation field, is used for an outer magnet. A water-cooled magnet, consuming a huge amount of electric power without theoretical upper limit of generation field, is used for an inner magnet. Hybrid magnets, generating fields above 30 T, are now in operation at two laboratories in Europe, one laboratory in the USA, and two laboratories in Japan (NRIM and Tohoku University). The National High Magnetic Field Laboratory, opened recently in the USA, is developing a 45 T class hybrid magnet system.

The outer superconducting magnet of our hybrid magnet is designed to generate background fields of up to 15 T in a room-temperature bore of 400 mm. The high designed field of the superconducting magnet was determined in consideration of the expensive power rate in Japan and the superior technology of high-field superconductors in Japan. The outer superconducting magnet consists of 58 double pancake windings with a 470 mm inner diameter; each pancake is wound with four kinds of superconductors (G1, G2, G3, and G4), where the grading depends on the experienced field distribution. The G3 and the G4 conductors are Nb-Ti monolith superconductors with a different Cu ratio, while the G1 and the G2 conductors are $(Nb,Ti)_3Sn$ Cu-housing conductors with a different Cu ratio. We adopted a new structure for the $(Nb,Ti)_3Sn$ Cu-housing conductor. We made a clearance between $(Nb,Ti)_3Sn$ monolith and Cu-housing in the high-field superconductor, which reduces the harmful compressive strain induced in the $(Nb,Ti)_3Sn$ monolith with high-field generation.

The outer superconducting magnet is cooled by soaking in a liquid helium bath of 4.2 K and has

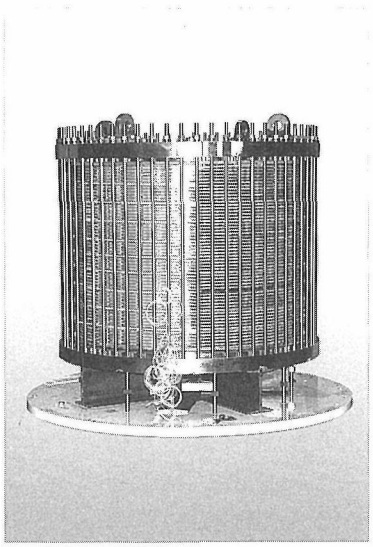

Fig. 1 Outer view of superconducting magnet for 40 T class hybrid magnet.

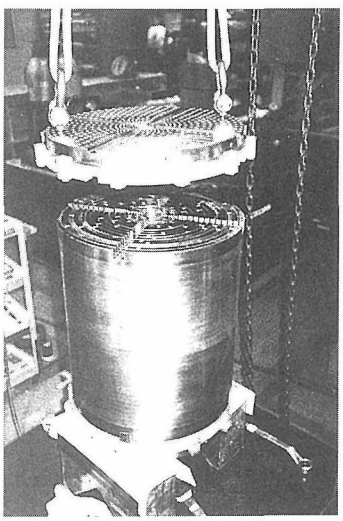

Fig. 2 Outer view of Insert A for 40 T class hybrid magnet.

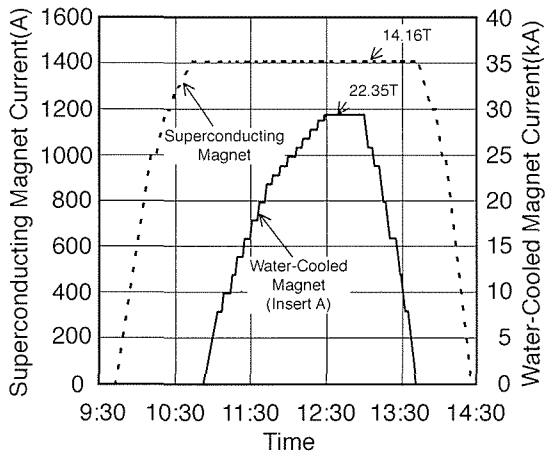

Fig. 3 Test operation curves of up to 36.5 T using Insert A in hybrid mode.

helium-cooling channels not only between the pancakes but also between the winding layers. All the superconductors have enough Ic margin in full operation and large Cu ratios. Therefore, the outer superconducting magnet is designed to be cryogenically stabilized when excited up to 15 T. The inductance, the maximum operation current, and the maximum stored energy are 58.17 H, 1476.1 A, and 63.37 MJ, respectively. An outer view of the superconducting magnet is shown in Fig. 1.

We have fabricated two types of water-cooled polyhelix magnets, Inserts A and Insert B, for our hybrid magnet system. The main conductor material of both water-cooled magnets is Cu-Al_2O_3 alloy, having a promising combination of high mechanical strength (0.2 % yield strength of 420 MPa) and high conductivity (89 % IACS). Some helical coils of Insert B are made of Cu-Cr alloy (0.2 % yield strength of 380 MPa and conductivity of 91 % IACS).

Insert A is composed of 18 coaxial helical coils and designed to generate incremental fields of up to 25 T (total fields of up to 40 T) in a clear bore of 30 mm under a background field of 15 T with electric power consumption of up to 13.3 MW (400 V × 33.3 kA). The designed flow rate of cooling water is 646 m^3/h. The maximum hoop stress, induced in the helical coils of Insert A, is designed as 337 MPa in full operation. Fig. 2 shows the outer view of Insert A. On the other hand, Insert B is composed of 15 coaxial helical coils and designed to generate incremental fields of up to 20 T (total fields of up to 35 T) in a clear bore of 50 mm under a background field of 15 T with electric power consumption up to 10.8 MW (341 V × 31.7 kA). The designed flow rate of cooling water is 700 m^3/h. The maximum hoop stress, induced in the helical coils of Insert B, is designed as 291 MPa in full operation.

The outer superconducting magnet has been tested many times and could generate central fields of up to 14.2 T without any experience of quench. In addition, the superconducting magnet has experienced forced current dumping eight times from about 1400 A (about 14 T) to 0 A with decay time of about 55 sec through an external dump resister. We did not observe the generation of normal zone during every forced current dumping, which proved that the superconducting magnet is stabilized well up to 14 T. Insert A and Insert B have also been tested separately and could generate central fields of up to 20 T and 25 T, respectively. To date, we have succeeded in generating steady fields of 36.5 T and 32.3 T in clear bores of 30 mm and 50 mm using Insert A and Insert B, respectively, in hybrid mode. Both of these values are new world records for a steady magnetic field, considering their clear bores. Fig. 3 shows the test operation curves up to 36.5 T using Insert A in hybrid mode.

We will gradually increase the generated fields up to the designed values after detailed investigations on the system and the parts. We already opened utilization of the magnet to inner users. In the near future, we will open utilization to outer users, when we have enough experience in operating the hybrid magnet system and have enough time to operate it for many measurements.

Keywords: hybrid magnet, steady high field, superconducting magnet, water-cooled magnet

References

1. K. Inoue, T. Kiyoshi, M. Kosuge, K. Itoh, H. Maeda, S. Hanai, M. Tezuka, T. Kojo, S. Murase, Y. Dozono, and K. Matsutani, "40 T Class Hybrid Magnet, K. Inoue", *Physica B*, 216 (1996): 181–185.
2. S. Murase, S. Nakayama, Y. Wachi, T. Fujioka, S. Hanai, N. Aoki, M. Ichihara, M. Hakamata, K. Noguchi, N. Shiga, K. Inoue, T. Takeuchi, K. Itoh, T. Kiyoshi, and H. Maeda, "Development of $(Nb,Ti)_3Sn$ and Nb-Ti Conductors for 15 T Superconducting Magnet of 40 T Class Hybrid Magnet", *Physica B*, 216, (1996): 233–235.
3. K. Inoue, T. Kiyoshi, M. Kosuge, T. Takeuchi, F. Matsumoto, H. Maeda, S. Hanai, M. Tezuka, and K. Matsutani, "First Test Operation of 40 Tesla Class Hybrid Magnet System": to be published in *IEEE Trans. on Magn.*

❒ Development of 1 GHz NMR Spectrometer: Preliminary Design and Fabrication of Test Conductors and Coils

T. Kiyoshi, K. Itoh, A. Sato, K. Inoue, and H. Wada
High Magnetic Field Research Station

Introduction

We have initiated the development of a 1 GHz superconducting NMR spectrometer that is based on the construction of a 23.5 T superconducting magnet; at the moment, this level of magnetic field is attainable only when an HTS (high *Tc* oxide superconductor) coil is used in combination with LTS (low *Tc* metallic superconductor) coils. In fiscal year 1995, preliminary design work of the NMR system was done, and high performance metallic superconductors and small HTS coils to be used for the NMR magnet in the system were prepared and tested.

Preliminary Design of NMR System

A schematic sectional view of the 1 GHz NMR magnet is shown in Fig. 1. In this design the LTS coils are operated in persistent mode at a field of 21.1 T in a 150 mm diameter cold bore. They are to be wound with NbTi and Nb_3 Sn conductors. The HTS coil is expected to generate an additional field of 2.4 T in a 54 mm room temperature bore. The cryostat shall be composed of two vessels, which enables parallel development of the LTS and the HTS coils. The LTS coils in the outer vessel are cooled with atmospheric superfluid helium at 1.8 K, while the inner HTS coil vessel is filled with liquid helium.

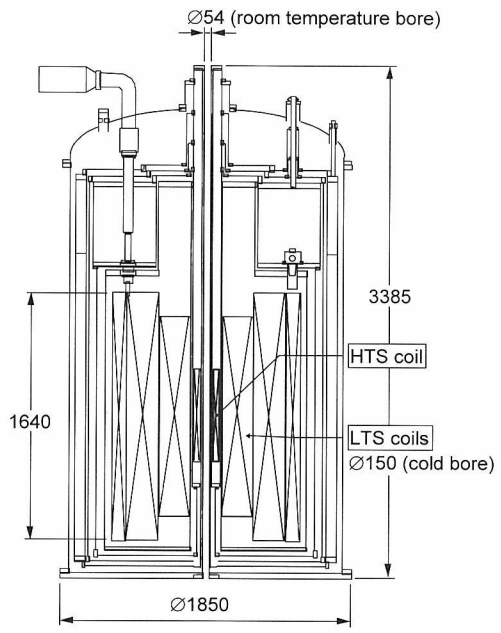

Fig. 1 A cross sectional view of a cryostat for a 1GHz NMR spectrometer.

Development of High Performance NbTi and Nb_3 Sn Conductors

Development of high performance metallic superconductors is one of the key issues in this project. LTS coil conductors are required to have high yield strength as well as high critical current density in order to make coil windings sufficiently

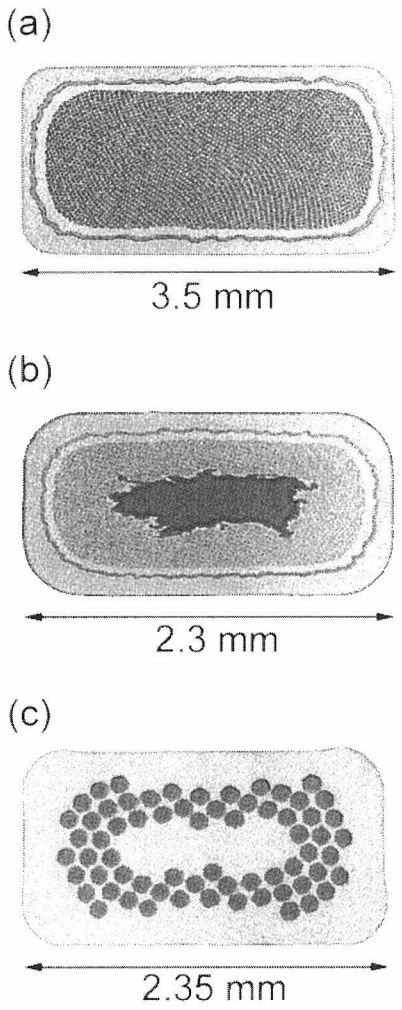

Fig. 2 Cross sectional photographs of newly developed metallic conductors. (a) HJC-Nb_3Sn, (b) HYS-Nb_3Sn, (c) HYS-NbTi

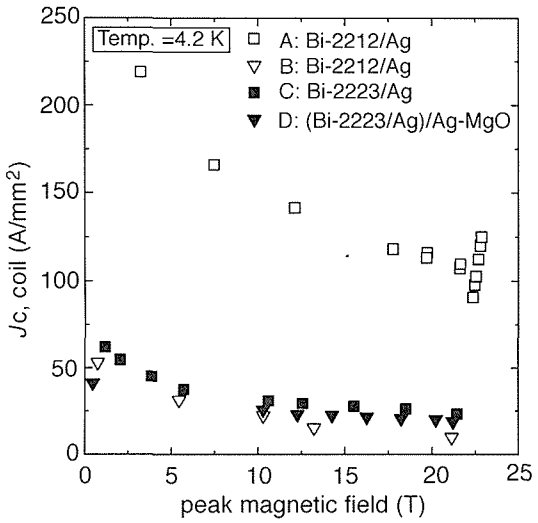

Fig. 3 Magnetic field dependence of critical coil current densities of the double-pancake HTS coils.

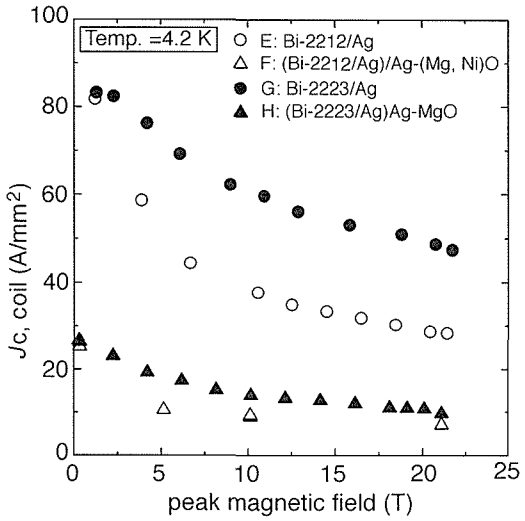

Fig. 4 Magnetic field dependence of critical coil current densities of the layer wound HTS coils.

compact. We developed three kinds of metallic test conductors; two Nb_3Sn conductors and one NbTi conductor. Cross sections of these conductors are shown in Fig. 2. One Nb_3Sn (HJC-Nb_3Sn) conductor was fabricated using a composite of Nb-7wt%Ta filaments in a Cu-14wt%Sn-0.3wt%Ti matrix, and had an overall-*Jc* of 33 A/mm^2 at 21 T and at 4.2 K with sufficiently large n values and low RRR. The other Nb_3Sn (HYS-Nb_3Sn) conductor contained Ta reinforcement and had a 0.2 % yield strength of 358 MPa at 4.2 K. This is the highest value ever reported for reinforced monolithic Nb_3Sn conductors. A high yield strength NbTi conductor (HYS-NbTi) was also newly developed. Its 0.2 % yield strength was improved by an additional rolling process after insulation coating. The value of 402 MPa at 4.2 K was achieved without spoiling the dielectric breakdown voltage of the insulator.

R&D Studies on Small HTS Coils

HTS coil development presents a lot of technological challenges. For the first step of the challenge, we have performed R&D studies on small HTS coils. The HTS coils were fabricated under common dimensional conditions: inner diameter more than 13 mm; outer diameter less than 49 mm; coil length less than 110 mm. Operation current was also restricted to be less than 300 A. According to the preliminary design of the HTS coil to be used in the 1 GHz NMR magnet, a critical coil current density (*Jc*,coil) of 70.5 A/mm^2 is required to generate a field of 2.4 T. We measured critical currents of the fabricated HTS coils up to 21 T.

Field dependence of *Jc*,coil of the double-pancake coils is compiled in Fig. 3. The critical current of Coil A made of a Bi-2212 conductor was measured six times at 21 T, as the critical current was changed and improved each time. The highest *Jc*,coil measured at 21 T was 125 A/mm^2. This value well exceeds the requirement of 70.5 A/mm^2. A central field of 22.8 T obtained with Coil A was the world magnetic field record on a fully superconducting coil system.

Figure 4 indicates field dependence of *Jc*,coil of the layer wound coils. Coil G made of a Bi-2223 conductor showed the best performance among the four, although even its *Jc*,coil could not exceed the required value of 70.5 A/mm^2 at 21 T. Lack of uniformity in a long conductor was the cause of this deterioration. Establishment of the fabrication process for long and uniform conductors is indispensable for obtaining a high performance layer wound HTS coil which is operated in a persistent mode.

Keywords: NMR spectrometer, high field magnet, metallic superconductor, oxide superconductor

❒ The NRIM Super XAFS - Development of High Power X-ray Generator for X-ray Absorption Fine Structure Experiments

K. Sakurai
High Resolution Beam Research Station

X-ray absorption fine structure (XAFS) provides information on the atomic-scale structure around a specific atom and has become an essential analytical tool in materials science. While the availability of a synchrotron source has facilitated the application of XAFS, instruments for carrying out measurements in an ordinary laboratory have been continuously improved since the middle of the 1970s. A lot of work has been devoted to developing a spectrometer to produce monochromatic X-rays efficiently from a continuum spectrum generated in a tube. Further important improvement has come with a special X-ray generator that is suitable for XAFS experiments, since most conventional X-ray sources for industrial use have so far been designed for either diffraction or fluorescence experiments. The NRIM super XAFS is the first powerful X-ray generator specially developed for XAFS.

The problems of laboratory XAFS are summarized as follows: (1) the low intensity of incident X-ray flux at the sample position, resulting in insufficient count statistics of the signal, because XAFS uses monochromatic X-rays from a weak Bremsstrahlung component, (2) the degradation of the spectrum caused by the 2nd or 3rd order harmonic reflections from a crystal monochromator, which is also significant at synchrotron sources and (3) the effect of a non-smooth spectral distribution mainly due to the characteristic lines of tungsten, which is a conventional filament material and which evaporates onto the anode. One should note that all of these problems are due to the characteristics of the conventional X-ray source. The author considers the design of the X-ray generator to be important in solving these problems. The essential specifications for a XAFS X-ray generator are as follows: (i) an extremely high tube-current (e.g. greater than 1000 mA), (ii) a narrow line focus (e.g. less than 0.1 mm at 6 deg. take off), (iii) low tube-voltage operation (e.g. 10~30 kV), and (iv) a filament free of emission lines which contaminate the useful part of the spectrum and/or with little evaporation (e.g. LaB_6).

Figures 1 and 2 show a photograph and a schematic drawing of the NRIM super XAFS. The present generator employs a LaB_6 cathode with a molybdenum anode. The diameter of an anode is 100 mm, and it rotates at 6,000 rpm for cooling purposes by means of a motor installed inside the cup. LaB_6 is a promising electron emitter because of its small work function, but it is not always easy to get a good filament for an X-ray tube. Because LaB_6 is ceramic it is therefore difficult to be formed into a coil heater. In the present study, a filament is prepared by slicing a LaB_6 rod (1 inch diameter)

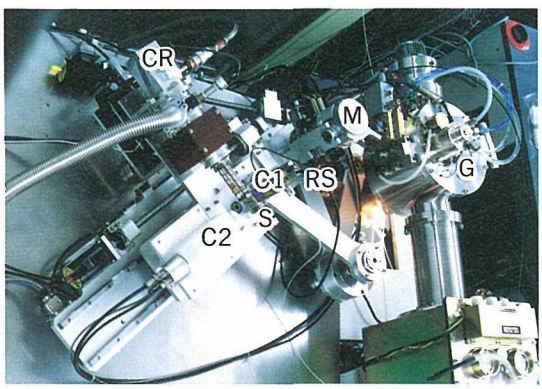

The X-ray generator and spectrometer. *G*: X-ray generator, *M*: crystal monochromator, *Rs*: receiving slit, C_1: proportional couter for measuring incident X-ray intensity, *S*: sample, *Cr*: cryorefirgerator, *C2*: scinitillation detector for measuring transmitted X-ray intensity.

Fig. 1 The NRIM super XAFS.

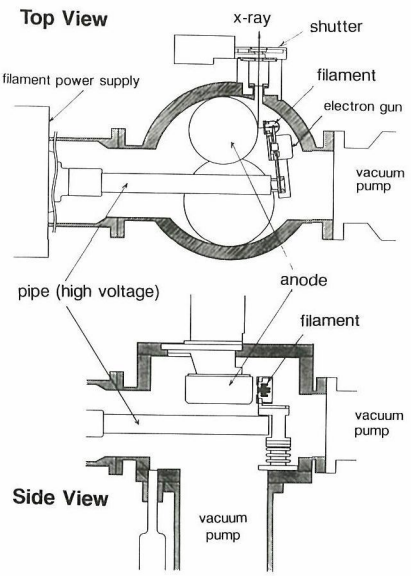

Fig. 2 Structure of the X-ray generator for XAFS (top and side views).

and cutting with an electro-discharging wire. It works at much lower temperatures (1750 ~ 2050 K) than a conventional tungsten filament, but almost double the current was needed for heating because of its small resistivity. The size of the electron emitter plane is 11 mm × 1.3 mm, and the shape of the filament has been optimized to get uniform heat distribution and to avoid the effect of thermal expansion. The cathode structure has been specially designed for low tube-voltage operation, which is necessary to avoid generating high energy X-rays that cause higher order harmonics at the monochromator. For example, since the energy range for Cu-K XAFS measurements is usually 8.8–9.5 keV, when the tube-voltage is set at 17.5 kV, one can avoid the effect of the 2nd order reflection. As yet, a conventional electron gun has not been designed for operation at less than 20 kV, and it is difficult to get a high tube-current in these circumstances. The new design realizes both a high tube-current and a narrow focus at low tube-voltages. Furthermore, the tube is equipped with two turbo molecular pumps for improving the vacuum to prolong the life of a LaB_6 filament, since it is very short under the condition for ordinary X-ray generation. The shape of the tube is also carefully designed to this end. The system pressure is around 1×10^{-7} Torr when operated at full power.

The NRIM super XAFS provides the maximum tube-current of 1,100 mA at low tube-voltage (14.5 ~ 18.0 kV) with a narrow line focus (0.1 mm × 10 mm at 6 deg. take off). When combined with a bent crystal spectrometer, intense monochromatic X-ray flux is available at the sample position. We observed 5×10^6 counts/(sec.mm^2) around the Cu K edge (8.99 keV) when the generator was operated at 17.5 kV, 1,100 mA and Ge(220) (Rowland radius 350 mm, Johansson) was used as a monochromator with 1 deg. divergence and 0.1 mm receiving slits. Further increase in intensity beyond 10^7 counts/(sec.mm^2) is expected by evacuating X-ray paths and slightly widening slits. The 2nd order harmonic (~18 keV) was not observed because it is not generated in an X-ray tube. Such a capability to control the spectral distribution of an X-ray source is an important feature which even a synchrotron does not possess. Because of the LaB_6 cathode, the equipment is also free from tungsten characteristic X-rays, which affect the measurement of many important absorption edges between 7 and 12 keV. The present X-ray source gives a very smooth continuum spectrum in the energy region between 6.5 and 30 keV except for the anode (molybdenum) characteristic lines. Since the evaporation rate of a LaB_6 filament is extremely low, lanthanum emission lines (4 ~ 6.3 keV) in the spectrum were weak enough. The measuring time for a sample of between 2 and 4 μt thickness is estimated to be usually around 30 min and, at most, 2 h for a difficult sample, when the accumulation count of transmitted X-rays and the point number of the spectrum are set as 10^6 and 300, respectively, and incident detector absorbs 20% of incident X-rays. Actually, the author obtained the absorption spectra of practical non-equilibrium materials in only 40 min, and the results were in good agreement with synchrotron experiments.

Thus, almost all of the problems in laboratory XAFS have been fixed by the NRIM super XAFS. As for a transmission technique, it is now possible to measure a spectrum to the same degree of quality as that obtained from a synchrotron in a reasonably short time, typically 30 min ~ 2 h. Synchrotron radiation is still an attractive X-ray source, even if most XAFS experiments become achievable in an ordinary laboratory. Undoubtedly, it is a very strong tool for especially difficult experiments in X-ray spectroscopy. The author expects that laboratory equipment and synchrotrons will both play a role in spectroscopic studies in the future, and is hopeful about further development of the XAFS field. The author would like to thank Mr. N. Osaka and H. Sakurai of the Rigaku for their technical cooperation in the present work.

Keywords: X-ray absorption fine structure, LaB_6 cathode, lanthanum hexaboride, laboratory XAFS, X-ray generator, rotating anode

References

1. K. Sakurai, "High-intensity x-ray line focal spot for laboratory extended x-ray absorption fine structure experiments", *Rev. Sci. Instrum.*, 64 (1993): 267.
2. K. Sakurai, "EXAFS experiments with high-power rotating anode", *Jpn. J. Appl. Phys. Suppl.*, 32-2(1993): 261.
3. K. Sakurai and H. Sakurai, "High-intensity low tube-voltage x-ray source for laboratory extended x-ray absorption fine structure measurements", *Rev. Sci. Instrum.*, 64(1993):2702, 65(1994): 2417.
4. K. Sakurai and H. Sakurai, "High power X-ray generator for XAFS experiments", *Rigaku Journal*, 2(1995): 41.
5. K. Sakurai, N. Osaka, H. Sakurai, and H. Izawa, "New rotating anode X-ray generator for XAFS experiments", *Adv. in X-Ray Anal.* 39(1996): in press.

❒ Development of a New System to Measure Shearing Cell Adhesive Force to Materials

A. Yamamoto, N. Maruyama, and M. Sumita
Biomaterials Research Team

Materials' Affinity for cells

Affinity for cells is one of the key properties for biomaterials, since they are always used adjacent to living tissue. Their required affinity for cells depends upon their applications in a human body. Materials for artificial bones, tooth roots, stems of hip joints and so on are required to adhere to cells quickly and firmly, while materials for artificial blood vessels or blood dialysis membranes are required to not adhere to cells or proteins to prevent the formation of blood clots. For the development of new biomaterials with superior biocompatibility, an evaluation of their affinity for cells is necessary.

For an implanted materials, evaluation of the shearing cell adhesive strength is important because a lateral load is applied to the cell adhered onto such implants as an artificial hip joint whose accompanies movement every walking step. Then, a shearing stress acts on the interface between the cell and the material, which induces the cell detached from the material's surface. However, no method or datum has been reported to directly measure the shearing cell adhesive force to materials.

In our research team, a new system to directly measure the shearing cell adhesive force was developed by means of a microcantilever.

Principle measuring shearing cell adhesive force to a material

A principle for the measurement of shearing cell adhesive force to a material is shown in Fig. 1. A cell adhered to a material at an XY-stage is moved (at the speed of $10\mu m \cdot s^{-1}$) to the tip attached to a cantilever(Fig. 1(a)). The distance between the pointed head of the tip and the material's surface is ca. 0.2μm. The cell touches the tip and a lateral load is applied to the cell (Fig. 1(b)). The cantilever is deflected corresponding to the cell adhesive strength. The cell is detached from the surface of the material (Fig. 1(c)). The cantilever deflection was measured by a sensor with a focusing-error-detection optical head.

In this system, no special treatment such as fixation or staining of cells is necessary prior to measurement. During measurement, the condition of the cells is observed by an optical microscope and possibly recorded on a videotape through a CCD camera.

A stainless steel cantilever (whose force constant is $3.1 Nm^{-1}$) with a pyramidal tip of silicon was used. The load P applied to the cell is given by the equation(1);

$$P = k \cdot \delta \qquad (1)$$

where k is the force constant of the cantilever and δ is the cantilever deflection. Shearing cell adhesive force is defined as the critical force which has the same magnitude as the applied load to the cell when the cantilever deflection becomes maximum.

Shearing cell adhesive force to glass

Shearing cell adhesive force to a glass surface was reproducibly measured. L929 cells were seeded and incubated for 2 days on the glass dish before measurement. A result of the measurement of the shearing cell adhesive force to glass is shown in Fig. 2 as a deflection curve, which is a relationship between the cantilever deflection and the displacement of the XY-stage.

Point A in Fig. 2 is the first point where the tip of the cantilever is attached to the cell. The cell starts to be transformed, because the bottom of the cell is adhered to the glass surface. The cantilever deflection increases in accompaniment to the

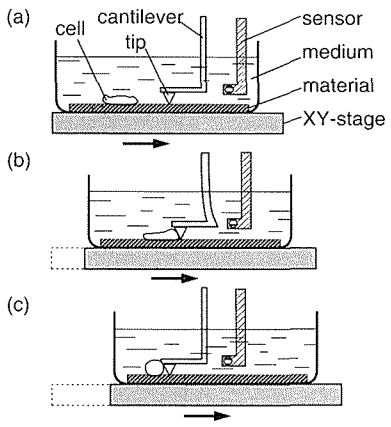

Fig. 1 Principle for measurement of shearing cell adhesive force to a material.

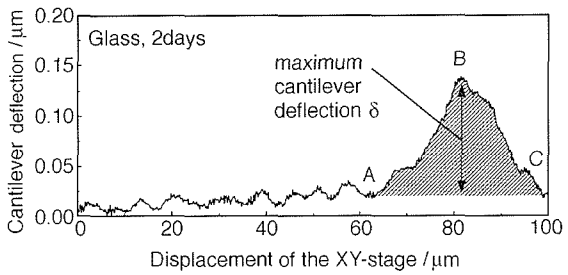

Fig. 2 A deflection curve of L929 cells to glass.

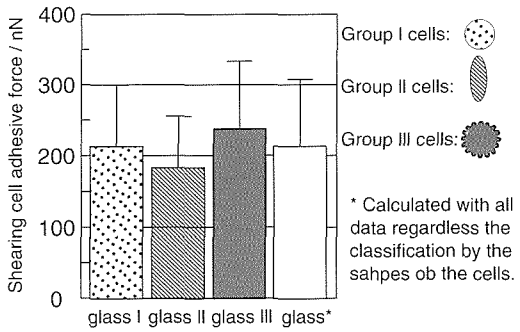

Fig. 3 shearing cell adhesive forces of L929 cells to glass.

movement of the XY-stage. The tendency of curve A-B seems to reflect the stiffness of the cell.

Point B in Fig. 2 is considered to be the point where the detachment of the cell starts. In curve B-C, the cantilever deflection decreases corresponding to the progress of the detachment of the cell. Finally, the cell is completely detached, and the cantilever deflection keeps a constant value. The cell adhesive force is the force that the maximum cantilever deflection gives. Area A-B-C-A is supposed to reflect the total energy necessary to remove the cell from the material's surface.

According to the deflection curves obtained, the shearing cell adhesive forces to glass surfaces are calculated by equation (1) and shown in Fig. 3. The data obtained were classified into three groups according to the shapes of the cells before measurement; round cells belong to group I, spindle-shaped cells belong to group II, and thin and spreading cells belong to group III. No significant difference in the shearing cell adhesive forces was observed among these groups. Irrespective of the groups, the total average of the cell adhesive force to glass was 217±93nN, where the sample number n was 37.

Shearing cell adhesive force to titanium, silver and aluminum

Shearing cell adhesive forces of L929 cells to titanium, silver and aluminum were measured and the results are shown in Fig. 4. Each of titanium,

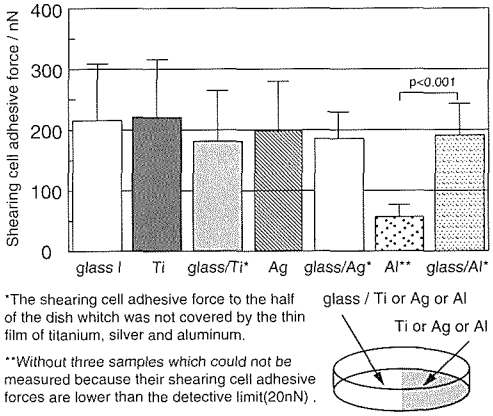

Fig. 4 Shearing cell adhesive forces of L929 cells to glass, titanium, silver and aluminum.

silver or aluminum was physically deposited on half of the glass dish and sterilized. L929 cells were seeded and incubated for 2 days before measurement. The shearing cell adhesive forces of L929 cells to titanium and silver were 221±96nN(n=25) and 200±83nN(n=8) on average, respectively. On the other hand, L929 cells' shearing cell adhesive force to aluminum was 61±19nN(n=6) excluding 3 samples lower than the detective limit(20nN), which was significantly smaller than those to other materials.

According to the result of the quantitative analysis, aluminum at 0.2ppm was detected in the medium recovered from the dish with aluminum film. However, aluminum ions dissolved into the medium are not considered to inhibit cell adhesion because the shearing cell adhesive force to the glass part of the dish with aluminum film is almost equivalent to that to the glass dish without any metal film.

In future works, the morphological dependence of cell adhesive force could possibly be examined based upon the adhesive area or the shapes of the cells by associating this system with an image analyzing system. Furthermore, it is expected to offer useful information to elucidate the mechanism of cell adhesion to materials by investigating the time-, cell kind- or material-dependence of cell adhesive force using this system.

Keywords: biomaterials, biocompatibility, cell adhesion, cantilever

Reference

1. A. Yamamoto, S. Mishima, Y. Ue, N. Maruyama, and M. Sumita, "Development of a new system to measure shearing cell adhesive force to materials", *J. Jpn. Soc. Biomater.*, 14(1996): 121–125: in Japanese.

Research in Progress 1995-1996

❐ List of Research Subjects

Numbers with circle indicate subjects newly started from April 1995.

Numbers with suquare indicate subjects ended by March 1995.

Characterization/Properties

Electronic and nuclear properties

(1) Study on Pressure Induced Electronic States of Correlated Electron Systems

(2) Self-Organized Criticality in Magnetic and Superconducting Systems

(3) Basic Research for the Control of Chemical Reactions by High Magnetic Field

4 Fabrication of Intrinsic Josephson Junctions and Evaluation of Their Physical Properties

5 Research on Low Dimensional System in High Magnetic Field

6 Studies on the Highly Correlated Electron Systems Under Multiple Extreme Conditions

7 Characterization and Control of the Optoelectric Properties of Small Crystalline Materials with Electron Probe Analysis

8 Materials with Atomic Scale Structures (COE Project)

[9] Pressure Effects on Physical Properties of Magnetic Materials

[10] Development of a High Pressure Apparatus for High Precision Electrical Resistivity Measurement and Its Application to Anomalous Pressure Effects in $PrBa_2Cu_4O_8$

[11] Structure and Electronic Properties of Silicides

[12] First-Order Phase Transitions in Magnetic and Superconducting Materials at Low Temperatures

[13] Fundamental Studies of Electromagnetic Materials with Strong Electron Correlations

[14] Research on Effective Masses of Wide Gap Semiconductors in High Magnetic Fields

[15] Electronic Properties in the Quantum Limit

Atomistic arrangement

16 Infrared and Raman Spectroscopy of Metal Oxides

17 Study on Atomic Scale Engineering of High Performance Films

[18] Quantification Study on High Resolution Transmission Electron Microscopy

[19] Determination of Order Parameters in Alloys from Electron Diffraction Intensities Using CCD Camera System and Its Application to Examination of Ordering Process

Phase transformation and micro structures

(20) Effect of High Magnetic Field on Phase Transformations and Its Possible Application to Transformation Texture Control

(21) Atom Probe Microanalysis of Advanced Metallic Materials

22 A Molecular-Dynamics Study of the Initial Prcess of Fracture

23 Atom Probe Microanalysis and Its Use in Materials Design

24 Synthesis of Superconducting and Supermagnetic Ultrathin Films by Use of Ion Implantation

[25] Effects of High Magnetic Field on Martensitic and Bainitic Transformations in Fe-Based Alloys

Sureface and interface properties

(26) Solid State Interfacial Reactions and Surface Analysis of Thin Solid Films

(27) Evaluation of Atomic Level Damage on Material

(28) Evaluation of Durability of Coatings for Structural Materials

29 Two Dimensional Photoelectron Spectroscopic Studies on Surface Structures and Properties

30 Research on Electrode Reaction between Metallic Ions and Carbonaceous Materials/Research on Electrochemical Characteristics of TiAl Alloy

31 Surface Analysis Database

32 Self-Control of Surface Composition of Thin Film and Its Application to Field Emitter

33 Fabrication of Nanometer-Scale Structures on the Extremely High Vacuum Surface

34 Fabrication and Characterization of Compound Semiconductor Nanometer Structures (Nanospace Laboratory Project)

35 Fabrication of Quantum Well Box Systems by Droplet Epitaxy for Advanced Optoelectronic Devices

36 Basic Study on Reaction between Materials and Bacteria

37 Electrochemistry and Modeling of Corrosion of Metals under Thin Water Layer

38 A Study on the Degradation of Materials by Ultraviolet-Light Irradiation

39 Evaluation of High-Performance Triazinedithiols As a Corrosion Inhibitor

Mechanical properties

(40) Effect of Cryogenic Temperature and Gas-Environment on Deformation and Fracture Behavior

(41) Remaining Life Prediction of Weldment for FBR by Creep Damage Evaluation

(42) Effect of the Interfacial Damage on Mechanical Properties for Ti-Based Matrix Composite

(43) NRIM Creep Data Sheets Project-V

(44) Ductile versus Brittle Behavior of Structural Steels

(45) Improvements of High Temperature Properties in Materials for High/Ultra-High Temperature Use

(46) Stability of Tetragonal Phase and Mechanical Properties of Transformation-Toughened Zirconia at High Temperature

47 Cyclic Deformation in a Corrosive Environment

48 Generalized Rule and Guide for Use of Fatigue Data

49 Long-Term Creep-Fatigue Properties of 316FR Stainless Steel for Fast Breeder Reactor

50 Study on Transient Behaviour of Deformation and Fracture at the Elevated Temperature

51 Characterization of Creep-Damaged Micro-structure of Stainless Steels by Computer Aided Quantitative Metallography

52 Relationship between Fatigue Crack Propagation and Cyclic Deformation of Small Specimens

53 Fatigue Strength Evaluation of Welded Joints in Synthetic Sea Water by $\sigma_{max} = \sigma_y$ Test

54 Fatigue Behavior of Brittle Materials at Elevated Temperatures

55 Study on Deformation and Fracture of Structural Materials at Cryogenic Temperatures

56 Assessment of Strength and Structural Materials Databases for Weldment in FBR (Fast Breeder Reactor) Components

57 NRIM Creep Data Sheet Project-IV

58 Toughness Improvement of Ceramics and Brittle Steels by Control of Precipitation and Phase Transformation

Mesurement and Evaluation

(59) Applicability of Photoaccoustic Spectroscopy Technique for Measurement of Thermal Diffusivity of Thermoelectric Materials

(60) Monitoring and Control of Thermal Plasma

(61) Application of in-situ Strain Measurement by the Laser Speckle Method

(62) Development of Fundamental Technologies for Excited Neutral Beams

63 Study on Flat and Mirror-finishing by Glow Discharge Plasma Using Rare Gas

64 Improvement of Resolution in EPMA X-Ray Image

65 Fundamental Study on Advanced Techniques of Physical Characterization of Metallic Materials and Their Application

66 Research on the Development of Chemical Analysis and Characterization Techniques for Metallic Materials

67 Modeling and Evaluation of Advanced Materials—A Coordinated Interlaboratory Research

68 Fundamental Study for Electromagnetic Evaluation of Materials

69 Nanoscopic Materials Damage Evaluation

70 Chemical Analysis of Organotin in Marine Environmental Samples

71 Understanding of the Mechanism of High Temperature Superconductivity

72 Study on the Vortex Pinning Mechanism in High Temperature Superconductors

73 In-situ TEM Observation and Structural Analysis of High Tc Superconductors for Fusion Reactors at Low Temperatures

74 Study on Deformation and Fracture of Materials under Irradiation

75 Fundamental Research on Flexible Structure and Machine Systems Using Advanced Materials

76 Development of Analytical Techniques for Characterization of Nuclear Materials Using New Generation Synchrotron X-Rays

77 Development for Unification System of Materials Scientific Database for Materials Properties Prediction

78 Study on Detection and Evaluation of Radiation Damages in Extreme Particle Fields

[79] Thermal and Electrical Properties of II-IV and V-VI Thermoelectric Semiconductors

[80] Energy Conversion Materials Fabricated with Functionally Graded Structure

[81] Self-Organizing Information-Base System Used for Creative Research and Development

[82] A Comparative Study of Nanostructure Characterization Techniques

[83] Correlation between Plasma Parameters and Evaporation in Free-Burning Arcs

[84] In-situ Measurement of Local Strain in High Temperature Range of Material and Detection of Defects by the Laser Speckle Method

[85] Research on Quantitative and Intelligent Nondestructive Evalution Techniques for Materials and Structures of High Reliability, Stage II

[86] Application of Rutherford Backscattering and Particle Induced X-Ray Emission Analyses to Material Science

Simulation and Theory

87 Development of Knowglede Database for High-Tc Superconducting Materials

88 Establishment of Multidimensional Evaluation of Human Senses for Materials Design

89 Theory of Thermal Reaction on Solid Surfaces

90 Thermodynamic Analysis of Transition Process from Metastable to Stable Phases

91 Computational Analysis of Mechanical Property and Structural Design of Materials Taking Microstructures into Account for Atomic Power Plants

92 Development of Virtual Experimental Technologies for Material Design

Materials

Ferrous Materials

(93) A Study of the Deformation and Fracture Mechanism of the High Strength Metal Matrix Composites

94 Fundamental Research for Intelligent Materials (Formation Process and Recovering Method of Creep Damage)

Non-ferrous Materials

95 Relationships between Fatigue Softening/ Hardening Behavior and TEM Structure of Titanium Alloys

Intermetallic compounds

(96) Fundamental Research on New Wear Resistance Materials of TiAl Based Composites

(97) Mesoscopic Structure Control and Properties of Intermetallic Compounds

98 Diffusion in Ordered Alloys and Prepara tion of Composition Gradiented Materials

99 Hydrogen Behaviors at Interfaces in Alloys

100 Improvement of Mechanical Properties of Intermetallic Compounds by Crystal Growth Control

101 High Performance Materials for Severe Environments-I (Microstructure and Properties of Intermetallic Compounds with High Specific Strength)

[102] Fundamental Study on the Search for Advanced Materials

[103] Basic Research on Intermetallic Compounds for Structural Applications

Composites

104 Development of High Strength Metal Base Composites with Excellent Physical Properties by the Advanced Bronze Method

105 High Temperature Strength and Fracture of Reinforced Oxide- and Nitride-Base Ceramics

106 Thermal Stability of Intermetallic Compound Matrix Composites Reinforced with Fibers

107 Development of Porous Ceramics Impregnated with Ionic Conductive Materials

Materials for mechanical application

108 High Temperature Mechanical Properties of Particulate Reinforced Titanium-Based Metal Matrix Composites

109 Design of Refractory Superalloys

[110] Effect of Particulate Distribution on the Mechanical Properties of Ti-Based Particulates Composites

[111] Intelligent Structural Materials

Materials for electronics application

112 Structure Control and Electromagnetic Properties of High Temperature Superconductors

113 Effect of High Energy Ion Irradiation on $Bi_2Sr_2CaCu_2O_x$ and $YBa_2Cu_3O_y$

114 Development of Superconducting Magnet for Magnetic Separation

115 Characterization and Application of Superconducting Thin Films Synthesized by Atomic Layer-by-Layer and Epitaxial Growth Methods

116 Stabilities of Superconducting Materials

117 Development of 1 GH_Z NMR Spectrometer

118 Development of High Strength/High Conductivity Materials for High Field Magnets

119 Microstructure and Electromagnetic-Characteristics Studies on V_3Si Multifilamentary Superconductors

120 Fabrication of High Strength Oxide Superconducting Wires for High Magnetic Field Applications

121 Evaluation of Long Oxide Superconductor Wires

[122] Study on the New Intermetallic Compound Superconductor

[123] Application of Cu-Ag Alloy Plates to Extremely High-Field Magnets

[124] Development of High-Jc Bi-Oxide Superconducting Wires

Magnetic materials

(125) Research on Quantum Magnetic Properties and Spinic Functions of Mesoscopic Magnetic Materials

126 Basic Research for Development of Intelligent Materials Aimed at Interactions between Atoms or Molecules

127 Fabrications and Spinic Functions of Mesoscopic Magnetic Materials

Opto-materials

(128) Single Crystal Growth of New Nonlinear Optical Materials by Means of Controlling Crystal Symmetry

(129) Energy Conversion Materials Fabricated with Composite Structures

(130) Effect of Aging Degradation on Localized Corrosion of Structural Materials for Light Water Reactors

(131) Influence of Nuclear Transmutations on Low Activation Structural Materials for Fusion Reactor Application

132 Research on Fundamental Science of Frontier Ceramics

133 Fundamental Study of Microstructures and Properties to Develop High Performance Materials for Severe Environment (II-High Temperature Intermetallic Compounds)

134 Development of Third Generation Nickel-Base Single Crystal Superalloys

135 Real-Time Investigation on Surface Reactions and Defect Growth Processes under Irradiation

136 Research on Utilization Technique of "Data-Free-Way" System for Nuclear Materials

[137] Material Synthesis to Control of Magneto-Thermal Properties by Changing Distance between Magnetic Ions

[138] Effect of Crevice on Low Cycle Fatigue Behavior of Pressure Vessel Steel in High Temperature Pressurized Water

[139] Environmental Degradation of Structural Materials for Light Water Reactors

Materials for envioromental performance

(140) Fundamental Study on the Processing for Ecomaterials

[141] Study on Design and Assessment Technology for Ecomaterials

142 Fundamental Study on Creation of Micro Stereom Fabrics by Powder Technology

Bio-materials, etc.

143 Fabrication and Fundamental Studies on the Materials with Nano-Mesoscopic and Nonperiodic Structures

144 Spectroscopic and Electrochemical Investigation of the Metal Complexes with an Unusual Electronic Structure

145 Fundamental Study on Biocompatibility of Materials

Processing

Sparation and systhesis

146 New Continuous Steelmaking Process

147 Processing and Development of Isotopically Controlled Materials(ICM)

Gaseous process

148 Development of Advanced Shape Memory Thin Films by Sputtering

149 Development of Shape Memory Thin Films Formed by PVD Method

Liquid state process

150 Manufacture Processing of Recyclable Simple-System Alloys

151 Basic Study on Refining of Molten Metal and Controlling of Solidification by Electromagnetic Force

152 Solidification in the Strong Magnetic Field

153 Investigation on Nucleation and Crystal Growth Mechanism under Heterogeneous Ambient Phase

154 Basic Technology Development of Materials Processing in a Short-Duration Microgravity Environment

155 Solidification Processing for Particle Dispersed Unidirectionally Grown Composites

156 Metastable Phase Solidification from Undercooled Liquid by Inducing External Nucleation Seed

Solid state process

157 Study on Combustion Synthesis

158 Heterogeneous Structure Design for High Plasticity and Wide Applicability of Simple System Alloys

159 Metallurgical Analysis of Micro-Machining Region

Powder processing

160 Oxidation Behavior of TiAl Intermetallic Compounds Produced by Powder Metallurgical Techniques

161 Characterization of Photocatalytic Properties of Ultrafine Particles Synthesized by Plasma Processing

162 Synthesis and Utilization of Mesoporous Materials

163 Coatings Formation by Powder Deposition Processes

164 Development of Particles Assembly Technology for Integration of Functions

165 Study on Solid State Chemical Reaction, Its Propagation and Meterials Syntyesis

166 Sintering of TiAl Intermetallic Compounds

167 Characterization of Composite Ultrafine Particles

168 Synthesis and Characterization of Advanced Materials Utilizing Colloidal Dispersed Systems

Joinig

169 Diffusion Bonding of Stainless Steel and Metals of Group IV–VI

170 Brazing Experiment under Micro-gravitation Using Parabolic Orbital Rocket

171 Influence of Surface Composition on Joining of Materials

172 Fundamental Research on Brazing and Electron Beam Welding in Space Environment

173 Corrosion of Dissimilar Metals Joints in Reactor Fuel Reprocessing Plants

Composite process

174 Micro Structure Control with Plastic Deformation under Mashy State

175 Forced Infiltration Process for Making Composite Structures

Process with aid of beam technolgy

176 Study on the Efficiency of Resonance Photoionization Process

177 Annealing of α'-Martensite Under Magnetic Field for Synthesis of $Fe_{16}N_2$

178 Analysis/Evaluation of Atomic Scale Compositional Change in Materials Due to the Radiation Damage

179 Study on Evaporation Process by High Energy Density Beams

180 Joint Research on the Structure and State Analysis of Metastable Liquid and/or Solid Gas Atom Clusters

Processing in special envioronment

(181) Fundermental Studies on Microbial Reactions with Inorganic Compounds

182 Study of Regenerator for Ultra-Low Temperatures

183 Development of Magnetic Separation Control System

❐ Research Programme

Characterization/Properties

Electronic and unclear properties

① Study on Pressure Induced Electronic States of Correlated Electron Systems

T. Matsumoto, Materials Physics Division
[April 1996 to March 1999]

There are numerous reports on correlated electron systems whose typical subjects are heavy fermion, the Kondo effect, valence fluctuation, metal-insulator transition, exotic superconductors and so forth. In spite of intensive efforts on these problems, we do not have a consensus on their mechanism completely. Thus, the purpose of this project is to quantitatively evaluate their thermal, electric, magnetic and structural properties at high pressure, and then to establish the unified picture and the unique character among them to clarify their mechanism. However, there are several barriers which prevent to promote the research in this field: First, the number of materials regarded as the correlated electron system is limited. The reason is due to the fact that they are mostly identified in artificial compounds containing the localized d- and f-electrons. Second, it is frequently difficult to get the compounds with high quality in the intrinsic items, for example, residual strains, purity, composition and crystallographic completeness. Finally, there is no obvious policy for the development of new material at present, because it seems to take a long time for the completion of systematic analyses on synthesis of compounds which have an interesting properties resulting from the strongly correlated electrons.

In addition to the evaluation of physical properties at high pressure, the following problems are concerned in this project: (1) New materials development containing the Yb element, in which the interesting behavior is expected from their electronic state. However, the reported number of Yb compounds is not so many, because it is very difficult to synthesize the compound due to high vapor pressure of Yb. In this work we expect to suppress this difficulty by using the new equipment for the synthesis. (2) Synthesis of single crystal with the highest quality which is already confirmed as the correlated electron system. (3) The structural refinements at ambient and high pressure. For understanding the physical properties at high pressure, it is necessary to get the correct information on crystal structure. So we will establish a technique of structural analysis at high pressure by using the diamond anvil cell.

Keywords: correlated electron system, pressure effect, materials development Yb compounds, structure refinement

② Self-Organized Criticality in Magnetic and Superconducting Systems

M. Uehara, Materials Physics Division
[April 1996 to March 1998]

Some 10 years ago it was noted that the thermal activation mechanism responsible for the diffusion of magnetic domain walls in the disordered alloy $SmCo_{3.5}Cu_{1.5}$ shows a strong anomaly below a temperature of 50K. This effect, initially attributed to quantum fluctuations, has been studied in detail. In particular it was shown that the evolution of the magnetic relaxation at low temperature fits a simple model where an effective temperature T*~10K accounts for tunneling of small portions of domain walls. At low temperatures below 2K, the magnetization reversal of $SmCo_{3.5}Cu_{1.5}$ takes place through successive magnetization jumps of nearly the same amplitude. Such a staircase behavior strongly suggests the existence of simultaneous wall motion on the scale of the sample, due to a thermal "avalanche effect" associated with dissipation, and initiated by wall tunneling events on a microscopic scale. It is expected that such behavior of the decay of metastable state is also observed in type II superconductors. Hysteresis loops of superconductors often show at low temperature large irreversible magnetization jump resulting from avalanche process. These avalanches result from a transfer of potential energy of vortices or domain walls to quasi-particles (conduction electrons, plasmons, phonons or spin wave). Such a dissipation effects leads to self heating of the sample. Many questions remain to be answered: physical reasons for jump events, relations with self-organized criticality. We propose measuring avalanche effects as well as switching field distributions in single crystals of magnetic and superconducting systems in more adiabatic conditions. This should allow us to make

a connection between this phenomenon and self-organized criticality.

Keywords: first-order phase transition, dissipation effects, avalanche process, self-organized criticality

Related Papers

1. M. Uehara, "Domain behavior in $SmCo_{3.5}Cu_{1.5}$ single crystals", *J. Appl. Phys.* 48 (1977): 5197–5200.
2. M. Uehara and B. Barbara, "Noncoherent quantum effects in the magnetization reversal of a chemically disordered magnet", *J. Physique*, 47(1986): 235–238.
3. M. Uehara and B. Barbara, B. Dieny, and P. C. E. Stamp, "Staircase behaviour in the magnetization reversal of a chemically disordered magnet at low temperature", *Physics Letters*, 114A (1986): 23–26.

3 Basic Research for the Control of Chemical Reactions by High Magnetic Field

H. Abe, 4th Research Group (present : High Magnetic Field Research Station)

[April 1996 to]

With the aim of producing new materials in the high magnetic fields more than 10T, we have started to investigate the possibility of controlling chemical reactions by the high magnetic fields. Taking advantage of the availability of high magnetic fields in Tsukuba Magnet Laboratories, we are to develop a methodology to measure magnetic field effects on each elementary process in chemical reactions. Such studies hitherto have been performed in the fields up to 2T and have given a clear ground for the interpretations of many aspects of the magnetic field effects on the photochemical reactions in solutions and on the dynamic behavior of electronically excited molecules in the gas phase. The aim of this project is not an extension of such studies to high fields, but the exploitation of the new research field, "the dynamics of excited molecules in high magnetic fields", which may be a basic research for the magnetic field control of chemical reactions.

Two pieces of apparatus are now under construction for the following experiments.

(1) Mechanism of photochemical reactions in solutions under 40T class pulsed magnetic field. The reaction is initiated by the excitation of the target molecules to the electronically excited state by the third harmonic of a pulsed YAG laser (355nm, 15ns). The creation and annihilation of the resultant reaction intermediate such as triplet state, radical pair, and bi-radical are observed by their transient absorption. The monitor light source is a Xe flash lamp. Trigger timing of the laser and the flash lamp is controlled to synchronize with the maximum field strength of the pulsed magnet.

(2) Dynamic behavior of electronically excited molecules in the gas phase under high magnetic fields up to 10T.

The target molecules are excited to a specific energy level located around its predissociation threshold by a tunable pulsed laser. Another tunable pulsed laser is used to detect a resultant dissociation fragment by observing a laser induced fluorescence. Changing the time interval between the firing of the lasers, time evolution of the creation and annihilation of the fragment is measured under magnetic fields up to 10T, which is applied by a liq. He free superconducting magnet. Magnetic field effects on the elementary processes of combustion reaction and photo-ionization will also be investigated.

Keywords: high magnetic field, chemical reaction, photo-dissociation, reaction intermediate

4 Fabrication of Intrinsic Josephson Junctions and Evaluation of Their Physical Properties

K. Hirata, 1st Research Group

[April 1995 to March 2000]

High temperature oxide-superconductors have been known to show a large anisotropy in magnetic and electronic properties in contrast with the conventional metal or intermetallic superconductors. This anisotropy comes from their structures, which are composed of superconducting CuO_2 layers, sandwiched with the insulating layers or less-conductive layers. The electrons are confined in two-dimensional system, and the coherence length perpendicular to the layers becomes very short (~1Å or less for $Bi_2Sr_2CaCu_2O_{8+\delta}$). This structural anisotropy causes much more interesting phenomena. It is quite reasonable that the Josephson effect may happen between the superconducting layers through the insulating or less-conductive layers. The Josephson effect has been actually observed in the voltage-current characteristics, and the dc-Josephson effect has recently been observed, too. High temperature superconductors have the Josephson effect as their own properties. The layerness of these materials leads also to the

peculiar characteristics in magnetic and electronic properties; magnetic phase diagram, the Josephson plasma resonance, second peak effect(fish tail), and so on.

This research program is planned to utilize the intrinsic properties of high temperature superconductors for the application such as the Josephson effect, and to find a new characteristic feature in these materials under various circumstances. For these purposes, it always becomes a key to grow a large single crystal with high quality. We will develop our technology to grow single crystals of high temperature superconductors by traveling solvent floating zone method, flux method and Czokralski method. Simultaneously, the evaluation of the single crystals will be performed to find a new function in the magnetic and electronic properties. Based on these results, the intrinsic properties will be analyzed theoretically for the application, and a new device will be tested.

Keywords: high temperature superconductors, intrinsic Josephson junction, Josephson devices

5 Research on Low Dimensional System in High Magnetic Fields

G. Kido, 4-th Research Group

[April 1995 to March 1996]

The quantum effect is one of the most interesting phenomena in the solid state physics and known to be remarkable in low dimensional systems. The spin-Peierls transition occurs in the one-dimensional S = 1/2 spin system with Heisenberg antiferro interaction, which follows a lattice distortion due to the dimerization of spin sites. This phase transition has been found in several organic conductors (TTF-CuBDT, $MEM(TCNQ)_2$ etc.) and inorganic materials $CuGeO_3$. The high magnetic field is quite effective to investigate these magnetic systems since it controls the degree of quantum effect. Another phase transition into the magnetic phase takes place under high magnetic field around 13 T for $CuGeO_3$ and 20 T for $MEM(TCNQ)_2$. The 40 T hybrid magnet and the 80 T pulsed magnet will be employed in the measurement. We are constructing apparatuses to measure the AC and DC susceptibility, magneto optical spectra in the wide region from far infrared up to ultra violet and magnetostriction at high magnetic fields.

The quantum hall effect is observed on the two-dimensional electron system which is realized at the interface in semiconductor. The accurate transport measurements at very low temperature in the high magnetic field are necessary to investigate it. A change of its optical property such as an energy shift of the luminescence is observed in connection with this phenomena. The precise measurements in very low temperature are also necessary in order to investigate it.

Keywords: low dimensional, spin Peierls, high magnetic field

6 Studies on the Highly Correlated Electron Systems under Multiple Extreme Conditions

H. Aoki, 4th Research Group and Tsukuba Magnet Laboratories

[April 1995 to March 2000]

We have developed several types of high field magnets, such as a hybrid magnet, in the preceding project. The capabilities of the developed magnets are proved to be of the highest class in the world. The purpose of this project is to develop several types of high precision detection systems under low temperatures and high pressures for the high field magnets and is to apply them to the study of the highly correlated electron systems.

Developments

(a) We have developed a detection system of the de Haas - van Alphen(dHvA) effect for a 50T pulsed magnet. dHvA frequencies ranging from 10T to 10000T have been successfully observed.

(b) We have developed a detection system of the filed modulation technique under high pressure for a 16T SCM/dilution refrigerator system. The dHvA signals are clearly observed under the multiple extreme conditions of 200mK, 7kbar and 16T.

Measurements

(a) We have successfully observed the dHvA signals both in the normal state and superconducting states of the new borocarbide superconductor YNi_2B_2C. The angular dependence of the dHvA frequencies and the effective masses in the high symmetry directions have been studied to reveal the Fermi surface properties. The field dependence of the signal amplitude in the superconducting state is studied and is compared with the predictions of the theories.

(b) We have carefully studied the wave form and the amplitude of the dHvA oscillations in the field region above the metamagnetic transition. The remarkable change of the f electron nature

from itinerant to localized across the transition have been confirmed. It is also found that the dHvA signals above the transition is difficult to understand in the framework of the conventional theory of the dHvA effect.

(c) New frequency branches in the heavy fermion compound UPt_3 have been revealed for the first time around the C axis.

Keywords: high magnetic field, low temperature, high pressure, highly correlated electron system

7 Characterization and Control of the Optoelectric Properties of Small Crystalline Materials with Electron Probe Analysis

K. Furuya, Y. Fukuda, M. Tanaka, and T. Saito, High Resolution Beam Research Station

[April 1995 to March 2000]

It is important to characterize and control the specific optoelectric properties of very small crystalline materials which are enclosed by other kind of materials, and which terminate the conducting electrons inside themselves. These types of small structures are feasible by burying nanometer-sized crystals into materials, and covering the surface of one material with other materials. In this study, the fabrication of those small "heterostructures" is carried out, and the correlation between atomic structure and photoluminescence properties are investigated.

Porous silicon is chosen for one example of non-equilibrium nanocrystals embedded in the bulk matrix. A highly porous silicon (PS) made by anodization is known as a material with the efficient visible photoluminescence (PL) at room temperature. Various models based on quantum size effects, quantum size/oxide defects, oxide defects, etc. have been proposed to explain the efficiency and spectrum of PL. Recently, the role of oxide in PS has proved to be important in the luminescence phenomena. However, the PL mechanism is not yet clear. PS is oxidized also in air at room temperature. Aging phenomena of PS is important from the view points of luminescence mechanism and application. Up to now, however, aging phenomena for only several minutes have been reported. In this study, the aging phenomena during 2 months have been investigated to clarify the relation between light-emitting properties and nanostructure or chemical composition. In addition, hydrogen irradiation was performed to clarify the importance of crystallinity for the PL efficiency.

The p-type Si wafers were used to fabricate light-emitting layers. Al was deposited on the back surface to ensure a uniform anodic current distribution. The PS layers were formed by anodization in HF - ethanol solutions. As an excitation source, a nitrogen laser with a wavelength of 337 nm, pulse width of 0.3 ns was used for PL measurements. The results indicated that PL peak positions were located at 600 - 650 nm and PL intensity increased with aging time. In all case, PL decay was not single exponential, but consisted of two components which decay exponentially with different lifetimes. This commonly appears in luminescence decays related to the presence of disordered state, and is not contradictory to the results of TEM observation which will be described later. The lifetimes ranged from one to several tens μs, and increased with aging time. Fourier transform infrared absorption measurements revealed that Si-O bonds in PS increased and Si-H bonds decreased with aging time. Hydrogen irradiation after the anodization caused the degradation of PL efficiency. High resolution TEM showed small Si crystals surrounded by the amorphous near the surface. The behavior of these crystals less than 10 nm in size seems to be correlated with the aging and hydrogen irradiation effects. The data suggest that the visible PL is attributed to the combined effects of nanostructure and oxide defects.

Keywords: small crystalline materials, surface terminated or buried particles, porous silicon(PS), photoluminescence(PL)

8 Materials with Atomic Scale Structures (COE Project)

M. Okada, Director-General

[April 1995 to March 2000]

Under its 5-year plan implemented in 1995, National Research Institute for Metals (NRIM) is conducting researches on the creation of advanced materials with atomic-scale structures exhibiting quantum phenomena. This research is promoted as one of the Center of Excellence Development Program (COE Project) of the Japanese Government, and is financed with the special coordination fund from the Science and Technology Agency (STA).

Main part of the COE Project is progressed at the Center of Advanced Physical Fields (CAPF) of NRIM, equipped with some extreme experimental environments such as high magnetic fields, high resolution beams and extreme high vacuum. The project is in fact designed to make use of the advantages of these extreme fields in researches

on advanced materials.

One year has passed since the project started in October 1995. During this period, NRIM invited as COE fellows 10 and 9 scientists from abroad and within Japan, respectively, to give more opportunities of discussions to NRIM staffs. Besides more than 40 seminars, an international symposium was organized, with similar intentions, in March 1996 on the Application of Nanometer Scale Technologies to Materials Science, with 90 scientists including 20 invited speakers. An Evaluation Committee, chaired by Prof. Tsukada from the University of Tokyo, verified the feasibility of the project plan.

Researches directly aiming at the development of atomic-scale materials are of the "top" importance in the project. This part includes either of investigating quantum phenomena in atomic-scale materials and developing technologies to fabricate and evaluate those materials. Research sub programs in this field receive the special funds from STA. COE project also includes researches with individual specific, originally proposed independently of the COE project. We incorporated them in the project, as they are particularly contributing to develop (1) techniques related to the advanced physical field, (2) analytical techniques for nanometer scale materials, and (3) materials exhibiting quantum phenomena. We call these researches "COE 'supporting'" researches.

Keywords: advanced physical fields, atomic scale structures, quantum phenomena

9 Pressure Effects on Physical Properties of Magnetic Materials

T. Matsumoto, Materials Physics Division

[April 1993 to march 1996]

Pressure is one of the most important parameters in the fields of materials science and also an effective tool to control the degree of hybridization between the 4f and conduction electrons which causes various interesting phenomena in rare earth intermetallics, such as heavy fermion, intermediate valence state, the Kondo effect and the RKKY interaction. Especially, we are very interested in their thermal and magnetic properties as a function of pressure to confirm the electronic state. High pressure techniques for the measurements of specific heat and magnetic susceptibility have been developed to proceed the research in this field. Using these techniques, we have investigated the origin of magnetic interaction in the $CePd_2Al_3$ and CePdAl systems. The pressure dependence of their Néel temperatures both of which were suppressed with pressure was explained by the competition between the Kondo effect and the RKKY interaction. Also, the strength of Kondo coupling was analyzed to be mainly due to the f-p hybridization by using the pressure dependence of their lattice constants.

We have also studied the pressure effect on Tc of the oxide superconductor, $Y_{2-x}Pr_xBa_4Cu_7O_{15}$ whose structure is regarded as an intergrowth of $YBa_2Cu_3O_7$ and $YBa_2Cu_4O_8$. As the result, the pressure coefficient of Tc was found to change from positive to negative with increasing Pr content. The change in the pressure dependence was interpreted by the magnetic breakdown of the Cooper pair caused by the magnetic moment of Pr atom.

Keywords: thermal and magnetic properties, Kondo effect, pressure effect, rare earth intermetallics

Related Papers

1. J. Tang, A. Matsushita, H. Kitazawa, and T. Matsumoto, "High pressure effect on the magnetic transition in heavy fermion systems $CePd_2Al_3$ and CePdAl", *Physica* B, 217(1996): 97–101.
2. J. Tang, A. Matsushita, H. Kitazawa, and T. Matsumoto, "Pressure dependence of magnetic ordering in Ce-Pd-Al intermetallic compounds," *Proc. of Intnat'l Conf. of AIRAPT '95*: in press.
3. A. Matsushita, Y. Yamada, N. Yamada, S. Horii, and T. Matsumoto, "Effects of pressure of the electrical resistivities of $PrBa_2Cu_4O_8$ and $Pr_2Ba_4Cu_7O_{15}$," *Physica* C, 242(1995): 381–384.

10 Development of a High Pressure Apparatus for High Precision Electrical Resistivity Measurement and Its Application to the Anomalous Pressure Effects in $PrBa_2Cu_4O_8$

A. Matsushita, Materials Physics Division

[April 1995 to March 1996]

The substitution of Y by Pr dramatically suppresses the superconductivity in Y-Ba-Cu-O high-Tc superconductors while the substitution by other rare-earth elements scarcely affects the superconductivity. Recently $Pr_1Ba_2Cu_4O_8$ (Pr124) was synthesized and the electrical resistivity of Pr124 was found to exhibit a broad peak around 190K. Below 190K the temperature coefficient of the electrical resistivity is positive. This metallic behavior provides an interesting

contrast to that of $Pr_1Ba_2Cu_3O_7$ (Pr123) which is semiconducting below room temperature. The semiconducting behavior of Pr123 has been a major evidence suggesting that the suppression of superconductivity in Pr123 is due to so-called hole filling. Therefore, the metallic behavior of Pr124 is interesting. Neither magnetic transition nor structural one have been found around the peak so far. Recently we found that the resistivity below the peak is insensitive to pressure while that above that increases with increasing pressure. This difference of pressure effect is a key to the understanding of the metallic behavior in Pr124.

In this project we developed a high pressure apparatus for high precision electrical resistivity measurement and investigated this anomalous behavior in detail. We proposed a possible explanation that the electrical conduction of Pr124 can be divided into two parts; one is the conduction through the CuO_2 planes and the other is that through the CuO double chains and attributed the metallic behavior to the conduction through the double chains. In this explanation any phase transition is not supposed. This model is consistent with the experimental results so far.

Keywords: high pressure, electrical resistivity, Pr substitution effect

11 Structure and Electronic Properties of Silicides

T. Hirano, Chemical Processing Division

[April 1993 to March 1996]

The purpose of the study is to investigate structure and electronic properties of metal disilicides. The disilicides concerned are $CoSi_2$/Si eutectic and high-pressure phases of $BaSi_2$.

$CoSi_2$/Si eutectic is selected because it forms Schottky barrier and the height is sensitive to the structure of the interface. The flat interface was formed at the low growth rate below 0.2 mm/h from the eutectic alloy by a floating zone method. Some interfaces with different misorientation were obtained. The Schottky barrier height of these interfaces is under measurement.

$BaSi_2$ has three different polymorphs, orthorhombic, cubic, and tetragonal phases. The first one is normal phase. The latter two are considered to be high-pressure phases, but it is not clear yet. Their physical properties are not known. We first confirmed this pressure-induced structural phase transition with *in situ* X-ray diffraction measurements. Interestingly, it became clear that both phases are quenched to ambient conditions without structural changes. We found that cubic phase is an n-type semiconductor while trigonal phase is a hole metal. In addition, the trigonal phase shows a superconducting with onset temperature of 6.8K. It is rarely known that high-pressure metallic phases are quenched. We are going to construct P-T phase diagram of $BaSi_2$ and discuss the transformation sequence under high pressure.

Keywords: silicides, interface, high-pressure

Related Papers

1. M. Imai and T. Hirano, "Electrical resistivity of metastable phases of $BaSi_2$ synthesized under high pressure and high temperature", *J. Alloys and Compounds*, 224 (1995): 111–116.
2. M. Imai, K. Hirata, and T. Hirano, "Superconductivity of trigonal $BaSi_2$", *Physica C*, 245 (1995): 12–14.
3. M. Imai and T. Hirano, "Electrical resistivity of three polymorphs of $BaSi_2$ and p-T phase diagram", *Mat. Res. Soc. Symp. Proc.*, 402 (1996): 567–572.

12 First-Order Phase Transitions in Magnetic and Superconducting Materials at Low Temperatures

M. Uehara, Materials Physics Division

[April 1993 to March 1996]

Recently much attention has been given to the dynamical nature in magnetic and superconducting systems due to the first-order phase transition in which the fluctuations of system of either thermal or quantum mechanical origin play an essential role and in a macroscopic system the metastable state undergoes transitions to a lower state. In disordered magnetic systems like $SmCo_{3.5}Cu_{1.5}$ magnetic domain walls move between pinning centers provided by the disorder. At high temperature this is known to occur via thermal activation: at low temperature we have shown previously that there is a crossover to quantum tunneling. It is expected that such behavior of the decay of metastable state is also observed in type II superconductors. We have shown that the concept of mean activation energy leads to coherent results on the mixed state nature in several high-Tc superconductors (HTSCs). We have found that the decay of the zero field cooled diamagnetic magnetization of HTSCs and several conventional superconductors such as $Ti_{50}V_{50}$ and A15 compound V_3Si single crystals can be explained in terms of a mean activation energy E which is found to be proportional to the reciprocal

magnetic field. The temperature variation of the penetration and exclusion rate of vortices obeys an Arrhenius type equation with an effective temperature $T^*=(\theta/2)\coth(\theta/2T)$. Here, θ is a characteristic temperature closely related to the crossover from thermal process to quantum tunneling of vortices. This study has been partly carried out within a cooperative scientific research program between STA(Japan) and CNRS (France); Laboratoire de Magnéisme Louis Néel.

Keywords: first-order phase transition, metastable state, quantum tunneling, magnetic relaxation

Related Papers

1. M. Uehara and B. Barbara,"Noncoherent Quantum Effects in the Magnetization Reversal of a Chemically Disordered Magnet", *J. Physique*, 47(1986): 235–238.
2. M. Uehara and B. Barbara, "Field and temperature dependence of the mean penetration rate of fluxons in the mixed state of high Tc superconductors", *J. Phys.*, I France 3 (1993): 863–870.
3. M. Uehara, T. Numazawa, T. Hirano, and B. Barbara, "Decay of Metastable States of High-Tc and Conventional "Low Tc" Superconductors", *Physica* C, 235 (1994): 2905–2906.

13 Fundamental Studies of Electromagnetic Materials with Strong Electron Correlations

K. Kadowaki, 1st Research Group

[April 1993 to March 1996]

Strong electron correlation effects have been known to give rise to unusual physical properties in metals and intermetallic compounds with rare earth and actinide elements. The ground state of these materials at low temperatures could be superconducting, magnetic ordering, normal Fermi liquid with highly renormalized effective masses or insulating, depending upon the systems, and cannot be predicted by the properties at high temperatures, even at the best of our present knowledge. In order to better understand the fundamental driving mechanism of these ground states, a broad spectrum of materials has been investigated: heavy fermion compounds such as $CeRu_2Si_2$, $CeCu_6$, URu_2Si_2,UPt_3 etc., a new class of magnetic superconductors such as RET_2B_2C (RE=Rare earth elements, T=Ni, Pd, Pt) and Kondo insulators such as FeSi, $Ce_3Bi_4Pt_3$, $Ce_3Sb_4Pt_3$, etc. For the study of physical properties of these materials it is essential to grow high quality single crystals. We have set up two multi-purpose single crystal growing furnaces: one is the four-arc furnace to grow single crystals with low vapor pressures and the other is an induction furnace with vertical and horizontal zone refining functions and with bridgeman as well as Czochralski method. We have succeeded in preparing large single crystals of mixed valent compound $CeRu_2$, magnetic superconductors such as $(Y,Ho,Er)Ni_2B_2C$, etc. Specific heat, resistivity, magnetoresistance, magnetization in the mixed state, de Haas van Alphen effect, Shuvnikov-de Haas Oscillation, etc. have been measured using high quality single crystals in order to understand the formation mechanism of highly correlated electronic state in these compounds.

Keywords: strong-electron correlations, heavy fermions, kondo effect, high quality single crystal growth

14 Research on Effective Masses of Wide Gap Semiconductors in High Magnetic Fields

M. Oshikiri, 4th Research Group

[April 1995 to March 1996]

The wide gap semiconductors have been shown to possess the potential for application in potentially attractive devices such as ultra violet lasers, high temperature operation devices, transparent electrode for solar energy devices and so on. This study aims to clarify the band structure near band edge of wide gap semiconductors using far infrared cyclotron resonances and to further develop the appropriate measurement systems.

Before now, cyclotron resonance experiments on n-GaP and n-ZnO have been carried out using a far infrared laser and a gunn oscillator as a radiation source, mainly in pulsed magnetic fields. Since the n-GaP has a double minima feature in the conduction band around the X point, the cyclotron resonance is complex and it is hoped that the resonances will be observed over a wide far range of the far infrared region so that the structure of the conduction band bottom can be determined. In our study, cyclotron resonances in the wide far infrared region (119, 215, 433, 690, 1500 μm) up to a magnetic field of 30 T have been observed. By fitting the cyclotron resonance data to the Landau level energy structure based on the double minima model, the band parameters of transverse effective mass m_t, longitudinal effective mass m_l, and the camel's back height ΔE have been determined to be 0.25 m_0, 0.90 m_0 and 2.7 meV, respectively. On the other hand, the effective

electron masses of n-ZnO reported previously were scattered over a wide range and no clear cyclotron resonance curve has been observed as far as we know. The effective mass estimated by us is approximately 0.3 m_0 with the magnetic field perpendicular to $(10\bar{1}0)$ surface at the resonant wavelength of 394 μm.

We are now planning to set up a water cooled Bitter pulsed magnet to make it easier to carry out the cyclotron resonance experiments and investigate other kinds of wide gap materials.

Keywords: cyclotron resonance, far-infrared, n-Gap, n-ZnO, effective mass determination

Related Papers

1. M. Oshikiri, K. Takehana, T. Asano, and G. Kido, "Far-infrared cyclotron resonance of wide-gap-semiconductors using pulsed high magnetic fields", *Physica* B, 216 (1996): 351–353.
2. M. Oshikiri, K. Takehana, T. Asano, and G. Kido, "Cyclotron Resonance of n-GaP in a Wide Far Infrared Region", J. Phys. Soc. Japan, 65 (1996): 2936–2939.

15 Electronic Properties in the Quantum Limit.

H.Aoki, 4th Research Group and Tsukuba Magnet Laboratories

[April 1995 to March 1996]

The high field magnets of National Research Institute for Metals (NRIM) are now become available for researches of various purposes. The purpose of the present project is to develop low temperature detection systems suitable for the high field magnets together with Grenoble High Field Magnet Laboratory (GHFML), which has profound experience in this field, and is to apply them to the studies of electronic properties in high magnetic fields.

a) We have developed a ^{3}He low temperature system for the hybrid magnet in NRIM. The system uses a sorption pump instead of an ordinary rotary pump, which is suitable to reach lower temperatures. We have also developed a reliable capacitance thermometer to control the sample temperature.

b) CeP has the NaCl structure and exhibits a complex phase diagram as functions of temperature and magnetic field. Date et al in Osaka university has found a successive step-wise increase of magnetization above 20T. It was found from the collaboration study with GHFML last year that the step wise increase coincides with the dHvA oscillation in the frequency and angular dependence which arises from a Fermi surface at the X point.

It is important to confirm that the step wise increase corresponds to a real magnetic phase transition. We have measured high field magneto-resistance by using the hybrid magnet which can detect the electronic structure change by the phase transition. Obvious changes of the magneto-resistance can be successfully observed. The field strength where the changes are observed and the hysteresis coincide with those of the step wise increase of magnetization. Theoretical studies are necessary to reveal the mechanism of this unusual magnetic behavior and its relation to the Fermi surface.

c) κ-$(ET)_2Cu(NCS)_2$ is an organic super-conductor whose Tc is about 10K. We have studied the combination frequencies of α and its magnetic breakdown orbit β by a torque method. It is found that the amplitudes and their temperature dependence can not be explained by conventional theories of the magnetic breakdown and the magnetic interaction effect. Further careful studies with other methods are necessary to investigate the origin.

Keywords: high magnetic field, hybrid magnet, magnetic transition, low carrier

Atomistic arrangement

16 Infrared and Raman Spectroscopy of Metal Oxides

T. Hirata, Materials Physics Division

[April 1995 to March 1998]

It is well known that phonons play a crucial role in many phenomena in solid state physics. By infrared and Raman spectroscopy, we are concerned with the following studies from the view-point of phonons. 1. The compositional effect on phonons in mixed oxides, where other metal cations with different ion radius and/or valence are substituted for the constituent cations; the mode behavior of substitutional solid solutions provides information concerning lattice distortions or force constants. 2. Interstitial solid solutions incorporated with ions, in reference to optical phonons of disordered system. 3. Phase transitions in solids; the normal-superconducting transition in high-T_c superconductors is an

example, paying attention to the electron-phonon coupling to understand the mechanism of superconductivity.

Keywords: phonons, infrared/Raman spectroscopy, metal oxides, phase transitions

17 Study on Atomic Scale Engineering of High Performance Films

T. Hatano, 1st Research Group
[April 1994 to March 1997]

The atomic scale engineering has been developed in the semiconductor field. The high performance materials are designed based on the prediction of quantum mechanics which rules the properties of materials in this dimension. The aim of this study is to extend this technique to the other materials such as high T_c superconducting oxides and molecular crystals. However, in these materials, the crystal structure is much more complicated and especially the molecules show a quite different characteristics in course of the film synthesis. The molecular beam epitaxy technique under ultra high vacuum and the electron diffraction technique are not the most suitable technique for these materials. To solve these problems, synthesis technique having higher selectivity and reactivity is necessary and other probe should be installed instead of the electron beam. As a new fabrication technique for these materials, we introduce a reactive deposition technique equipped with x-ray analysis system in the total reflection region.

The total reflection x-ray analysis technique was applied to the artificially layered $Bi_2Sr_2Ca_{n-1}Cu_nO_{2n+4}$ films prepared by sequential sputter deposition. In the $\theta/2\theta$ diffraction spectrum at the grazing incidence, the oscillatory pattern can be observed which is due to the interference of the reflected x-ray from the surface and interface of the film. Such patterns are also observed between the neighboring (00*l*) Bragg peaks. The number of oscillation exactly correspond to the number of units in the film. The thickness of the films can be analyzed in the scale of one atomic layer by this analysis. The atomically layer-by-layer synthesis can be established by this analysis. The superstructure of $Bi_2Sr_2Ca_{n-1}Cu_nO_{2n+4}$ system was successfully synthesized by applying these results to the deposition conditions. The total reflection x-ray analysis technique can be extended in another two ways. One is the *in-plane* x-ray diffraction which reveals the surface structure and the texture of the films. The other is the fluorescent x-ray analysis of the surface. The composition of the film surface can be analyzed. It is planned to apply these techniques for the *in-situ* analysis during the synthesis of high T_c superconducting oxide films.

Keywords: thin films, atomic scale characterization, x-ray total reflection

Related Papers

1. T. Hatano, A. Ishii and K. Nakamura, "Enhancement of T_c in $(Bi_2Sr_2Ca_3Cu_4O_{12+\delta})_1$ $(Bi_2Sr_2CaCu_2O_{8+\delta})_1$ superlattice film by charge transfer", *J. Appl. Phys.*, 79 (1996): 2566–2573.
2. T. Hatano and K. Nakamura, "Structure and properties of $Bi_2Sr_2Ca_{n-1}Cu_nO_{2n+4}$ films prepared by sequential sputter deposition", in "Bismuth based High Temperature Superconductors", ed. H. Maeda and K. Togano, Marcel Dekker, New York, (1996).

18 Quantification Study on High Resolution Transmission Electron Microscopy

S. Ikeda, Surface and Interface Division
[April 1993 to March 1996]

In the present study, we have tried to quantify the intensity of the high resolution electron microscopic image and electron diffraction intensities, with the aid of CCD cameras, and to obtain much more information than the conventional method with using photographic films. A slow scan CCD camera-image processor with a dynamic range of 10^4 is attached to the high resolution electron microscope, JEM-4000EX, with a point to point resolution of 0.17nm.

We identified the structure of recently discovered superconducting compound YPd_2B_2C. We identified the three dimensional structure of the reciprocal lattice. We compared the high resolution images with the computed ones using MacTempas software and found that the structure of this compound is basically the same as that of $LuNi_2B_2C$.

Another attempt is performed for the structure analysis of the newly synthesized material, SrV_2S_5. We found this material has the trigonal layered structure with a=0.33nm and c=3.5nm; The unit cell is composed of three blocks of subcells, which are stacked to c-direction having a shift in the c-plane. The position of Sr and V atoms are speculated by high resolution images and Patterson maps.

A trial was made whether distances and directions of the diffraction spots can be measured using an industrial low price CCD camera set on the view window of an electron microscope. It was

found the measurement is possible for the bright condition of the spots. The distortion was successfully corrected by varying the aspect ratio from 3:4 for the CCD camera to 1:1 for the printer.

Keywords: HRTEM, structure image, superconductor, YPd_2B_2C, SrV_2S_5, slow scan CCD camera

Related Papers

1. S. Ikeda, H. Fujii, T. Kimura, K. Kumakura, K. Kadowaki, and K. Togano, "High Resolution Transmission Electron Microscopic Studies on a Superconductor YPd_2B_2C compound", *Jpn. J. Appl. Phys.*, 33 (1994): 3896–3899.
2. S. Ikeda, "Setting of a Low Price CCD Camera on the View Window of TEM for Printing Out Electron Diffraction Patterns", *J. Electron Microscopy* 44 (1995): 485–487.

19 Determination of Order Parameters in Alloys from Electron Diffraction Intensities Using CCD Camera System and Its Application to Examination of Ordering Process

T. Kimoto, 1st Research Group
[April 1993 to March 1995]

The first objective of our research is to develop the system for determination of a long-range order (LRO) parameter in an alloy from the ratio of superlattice and fundamental reflection intensities in electro diffraction pattern, which are precisely and quickly measured by a cooled CCD camera of highest dynamic range of 64,000. The second objective is to apply the developed system to the examination of ordering process and the understanding of the physical properties related to ordering by measuring LRO parameter in a microscopic region. In 1993 and 1994, the development of the system was successfully performed by developing a new method to measure specimen thickness and a computer program to calculate a LRO parameter from electron diffraction intensities with the multi-slice method. It was verified that the LRO parameters of Cu_3Au determined by our developed system is in good agreement with the data by X-ray diffraction.

In 1995, we measured the LRO parameters near grain boundary in Cu_3Au and B-doped Ni_3Al with the developed system. It was found that LRO parameter decreased with approaching grain boundaries in Cu_3Au which was annealed for ordering after rapid quenching from high temperature of 850°C or 930°C. On the contrary, the LRO parameter increased with approaching grain boundary in Cu_3Au which was slowly cooled in a electric furnace from high temperature. These interesting phenomena were successfully explained on the assumption that excess vacancies introduced during annealing at high temperature of 850°C or 930°C promote ordering. In B-doped Ni_3Al, discernible difference of LRO parameter was not detected between the area near grain boundary and matrix. This may deny the previously proposed mechanism that the decrease of LRO parameter near grain boundary causes the ductility improvement in Ni_3Al by B-doping.

In 1995, we also developed a new method to measure experimentally the electron absorption coefficient for the first time in order to achieve much higher accuracy in the calculation of LRO parameter by considering the absorption effects. Consideration of the absorption effects in the calculation of LRO parameter allowed us to apply our developed system to the materials whose crystal structure is much more complicated than that of binary alloys.

Keywords: long-range order parameter, multi-slicemethod, cooled CCD camera, grain boundary, absorption effect

Phase transformation and microstructures

20 Effect of High Magnetic Field on Phase Transformations and Its Possible Application to Transformation Texture Control

S. Kajiwara, Physical properties division
[April 1995 to March 1998]

It is expected that magnetic field will affect transformation behavior, especially martensitic transformation, although much work has not been performed on this subject. There may be some effect of magnetic field on transformation temperature (Ms), transformation kinetics and transformation texture. In the present work, these effects are studied extensively on both types of athermal and isothermal transformations by using Fe-Ni-C, Fe-Ni-Co-Ti, Fe-Cr-C (athermal type) and Fe-Ni-Mn, Fe-Ni-Mn-C (isothermal type) alloys. The aim of the study is to clarify the basic process of the transformation mechanism and explore possibilities of texture control by applying magnetic field. In order to know the effects more explicitly, super high magnetic

fields, both pulse and stationary, have been employed. In the first fiscal year of this project, effect of Ms temperature in Fe-Ni-Mn and Fe-Ni-Mn-C alloys has been examined. Nominal chemical composition of the alloys used is shown in Table 1. These alloys are isothermally transformed below room tem-perature and exhibit C-curve in the TTT diagram. The nose temperature in the TTT diagram at which the most rapid reaction occurs is also listed as Tm in this table. Most of the alloys used are completely austenitic at room temperature except alloys No.1 and 2. In these two alloys, some amount (10-20%) of martensite is formed on cooling to room temperature from the austenitizing temperature. Specimens 0.5 mm thick were austenitized at 1370 K for 30 min and cooled to room temperature. The grain size of austenite was in the range of 50-80 μm. Pulse magnetic fields of 8-28 T with about 40 ms duration were stepwisely applied to these austenitized specimens at room temperature, starting from 8 T. The amount of martensite induced, f_p, is increased with increasing level of magnetic field; for alloy No.1 f_p started to increase as early as when 8 T was applied, for alloys No.2 ,3 and 7 f_p started to increase at 17 T. After some period of a constant increase with a low gradient, f_p began to rapidly increase at 16 T for alloy No.1, and at 25 T for alloys 2, 3 and 7. The values of f_p at the application of 28 T were listed in Table 1. While the above mentioned martensitic transformation induced by pulse magnetic field is considered as athermal transformation, it was found that the isothermal martensitic transformation occurs at room temperature by applying constant high magnetic field for a certain period of time. The amounts of martensite, f_s, formed isothermally at room temperature by applying a constant magnetic field of 22 T for 2 h are listed in the last column of Table 1. It should be noted here that alloys No.3, 4 and 7 are isothermally transformed as much as 60-80 % at room temperature although practically no martensitic transformation is induced for these alloys by application of pulse magnetic fields up to 25 T. We are now considering the factors which are responsible for such striking effect of magnetic field on the martensitic transformation.

Table 1 Alloy composition, nose-temperature, T_m, martenisite volume fraction, f_p and f_s, induced by pulse and stationary magnetic fields.

Alloy No.	mass %(Fe, bal)			T_m(K)	f_p(%)	f_s(%)
	Ni	Mn	C			
1	23	3.0	0	---	45	85
2	23	3.3	0	210	10	84
3	23	3.6	0	170	1	78
4	23	3.8	0	150	0	66
5	23	4.0	0	<77	0	3
6	23	4.2	0	<77	0	3
7	22	3.6	0.1	110	1	59

This research was performed in close collaboration of members of High Magnetic Field Research Station in Center of Materials Science under Extreme Environments of NRIM.

Keywords: isothermal martensitic transformation, super high magnetic field (pulse and stationary), transformation temperature

(21) Atom Probe Microanalysis of Advanced Metallic Materials

K. Hono, 3rd Research Group
[April 1996 to March 2001]

Properties of metallic materials are controlled by microstructures. Recent findings of nano-crystalline materials which arises various unconventional mechanical and magnetic properties stimulated researches in nanocrystalline microstructure control. Conventional structural materials such as steels, aluminum alloys, intermetallics and superalloys are all strengthen by controlling microstructures by making use of solid->solid phase transformations. The scale of the microstructures of these materials are becoming smaller and smaller, and many microstructures are in a subnanometer scale. Thus, microstructural characterizations of metallic materials in less than a nanometer scale resolution is essential for understanding the mechanisms of desirable properties. This study aims to obtain general understandings to materials properties by characterizing microstructures of some selected advanced materials. For this purpose, we employ the atom probe field ion microscope (APFIM) technique which is capable of analyzing local chemical compositions of alloying elements in less than a nanometer scale resolution. An advantage of using APFIM is that it can detect all elements including light atoms such as Li, Be, B, C, N and O which often make key roles in controlling materials properties. An appearance of a new atom probe developed for this project is shown in Fig. 1. This is a combination of a reflectron based energy compensated atom probe and a tomographic atom probe (TAP). The latter is a parallel type three dimensional atom probe, which is capable of mapping positions of individual atoms in a three dimensional space. For complementary micro-

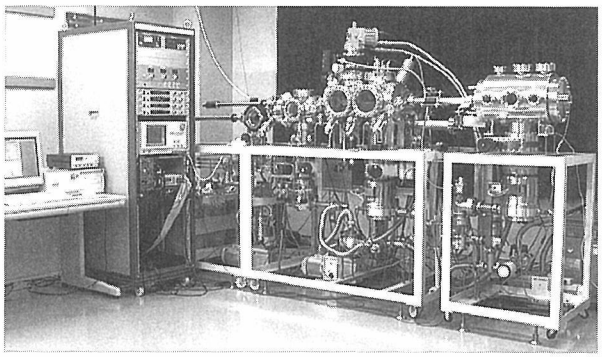

Fig. 1 Appearance of the NRIM atom probe.

structural characterization, conventional transmission electron microscopy (TEM) and high resolution electron microscopy (HREM) techniques are also employed. Our research interests include nanocrystalline magnetic materials, magnetic thin films, nanocomposite aluminum alloys, amorphous alloys, and phase transformations in steels and other alloys.

Part of this research is performed in collaboration with Institute for Materials Research (IMR), Tohoku University.

The most up-to-date reports of this project can be found in the following WWW site:

http://inaba.nrim.go.jp/apfim

Keywords: atom probe, APFIM, nanostructure, microstructure, phase transformations

22 A Molecular-Dynamics Study of the Initial Prcess of Fracture

K. Kusunoki, Computational Materials Science Division

[April 1994 to March 1997]

Using molecular-dynamics simulations, the present study aims to elucidate how the microscopic forces and displacements of atoms develop into the macroscopic ones. It also aims at an atomistic description of the macroscopic concepts such as crack, stress and strain.

We developed a simulator by which we can make both tensile and compression test of single crystals. A preliminary study, which used this simulator for both pure and solid solution of fcc crystals with modified Lennard-Jones type interatomic potentials, revealed that perfect crystals as well as crystals containing one vacancy cannot be fractured by crack initiation but by plastic deformation. This year, we newly developed two types of simulation programs, one for fcc-Cu crystals constructed with an embedded-atom-model (EAM) potential, and the other for bcc-α-Fe crystals with the Johnson's potential. It was demonstrated that, as far as we made tensile tests of fcc crystals under non-periodical boundary conditions, brittle fracture by nucleation and growth of cracks cannot take place even for crystals with a large amount of vacancy clusters and for mode-I systems. In this case, we observed the generation of the Schockley's partial dislocations at some stage of plastic deformation. It was also demonstrated that, in case of tensile tests for mode-I system of α-Fe crystal, brittle fracture take place at low temperatures and ductile fracture at high temperatures. These results are consistent with the general tendency for real materials with fcc and bcc structures.

We are now investigating into mechanisms which cause the above results from both an atomistic and crystallographical points of view.

Table 1 Alloy composition, nose temperature, Tm, of c-curve TTT diagram, amounts of martensite, fp and fs, induced by pulse and stationary high magnetic fields, respectively.

Alloy No.	Compositon (mass%, Fe:bal.)			T_m(K)	f_p(%)	f_a(%)
	Ni	Mn	C			
1	23	3.0	0	-	45	85
2	23	3.3	0	210	10	84
3	23	3.6	0	170	1	78
4	23	3.8	0	150	0	66
5	23	4.0	0	<77	0	3
6	23	4.2	0	<77	0	3
7	22	3.6	0.1	110	1	59

Keywords: molecular dynamics, fracture, atomistic models, crack

23 Atom Probe Microanalysis and Its Use in Materials Design

H. Harada, Computational Materials Design Division

[April 1994 to March 1997]

Microstructures of third generation Ni-base single crystal (SC) superalloys developed in NRIM are being analysed by an Atom Probe Field Iron Microscope (APFIM) equipped with a Three Dimensional Atom Probe (3D-AP). The state of γ/γ' phase equilibrium, including atomic configuration in the γ' phase, has been determined in the alloys. The results have been compared with estimations by computer modelling using Cluster Variation Method (CVM) and a very good

agreement has already been shown between them. CVM is now being applied to the development of Ni-base SC superalloys with further superior temperature capabilities.

A series of Al-containing NiTi-base intermetallic alloys newly developed in NRIM for possible applications as gas turbine discs have also been investigated. The precipitation behaviour of Ni_2TiAl phase which is coherent with NiTi matrix is thought to be the key to understanding the very high strength of the alloys. The APFIM/3D-AP has been again used to analyse the precipitates in terms of size, distribution and chemical composition. It has been possible to detect a very early stage of the Ni_2TiAl precipitation. Also 3D-mapping of the chemical composition clearly showed an evolution of the cuboidal precipitates during aging. Partitioning behaviour of some quaternary elements, such as Mo, Cr, are being investigated.

Keywords: Ni-base superalloy, NiTi-base alloy, Ni_2TiAl precipitate, phase equilibrium, atomic configuration, computer modelling

Related Papers

1. H. Murakami, H. Harada, and H.K.D.H. Bhadeshia, "The Location of Atoms in Re- and V-containing Multicomponent Nickel-base Single-crystal Superalloys", *Applied Surface Science*, 76/77(1994): 177–183.
2. Y. Koizumi, H. Murakami, and H. Harada, "Phase Decomposition in NiTi-Ni_2TiAl Alloy System, P.J.Warren", *Proc. 3rd International Charles Parsons Turbine Conference*, 25–27 April (1995), Newcastle upon Tyne, UK.
3. Y. Koizumi, Y. Ro, and H. Harada, "NiTi-base Intermetallic Alloys Strengthened by Al Substitutions", *Materials Science and Engineering A*, May, 1997: in press.

24 Synthesis of Superconducting and Supermagnetic Ultrathin Films by Use of Ion Implantation

K. Saito, Surface and Interface Division

[April 1994 to March 1996]

Superconducting Bi-Sr-Ca-Cu-O ultrathin films with the thicknesses of 30, 15, 7, 4 and 2 nm were synthesized by means of r.f. magnetron sputtering and were modified by irradiation of 100 keV Ar ions to a dose of about 10^{12} ions cm^{-2} at low temperatures, 10-20 K. For the film thickness of 30 nm to 7 nm,the obtained values of zero-resistance transition temperature,$T_{c,o}$, exceeded 100 K. For 4 nm or 2 nm thick ultrathin films, $T_{c,o}$ reached 88 K or 84 K, which is the highest value so far reported for the nearly one-unit or half-unit cell dimension. The film thickness and the interface structure have been identified by cross-sectional high-resolution electron microscopy (XHREM). The role of 100 keV range Ar ions in the thin film modification was interpreted in terms of a selective creation of "unit cell" scales of the low energy collision cascades in imperfect crystalline region and ion channeling through good crystalline region in ultrathin films.

In order to examine the film thickness dependence of $Fe_{16}N_2$ nitride formation, 50 nm thick Fe ultrathin films were implanted with nitrogen ions at room temperature. Unlike the case of 250 nm thick films, no $Fe_{16}N_2$ phase was produced in the as-implanted state, but α'-martensite phase was formed and its volume fraction exceeded 90 %. When the implanted film was coated with Au or Cu films to avoid nitrogen escape from the specimen surface and annealed at 473 K, the volume fraction of $Fe_{16}N_2$ phase was markedly improved to about 36%.

Keywords: superconductivity, giant magnetization, ultrathin films, BiSrCaCuO, $Fe_{16}N_2$, ion implantation

Related Papers

1. M. Kaise and K. Saito, "Synthesis and Ion Beam Modification of the Bi System Superconducting Ultrathin Films", *Surface & Coatings Technology*, 3(1996): 777–782.
2. H. Shinno and K. Saito, "Synthesis of $Fe_{16}N_2$ Iron Nitride by Means of Nitrogen Ion Implantation into Iron Thin Films", *Japan J.Inst.Metals*, (1996): 757–764.

25 Effects of High Magnetic Field on Martensitic and Bainitic Transformations in Fe-Based Alloys

H. Ohtsuka, Physical Properties Division

[April 1995 to March 1996]

Effects of high magnetic field on martensitic transformation behavior and microstructure at 4.2K have been studied in Fe-27Ni-0.8C(wt%) shape memory alloys. Effects of tensile stress and the combined effects of high magnetic field and tensile stress on martensitic transformation have been investigated as well in order to make clear the difference of the effects of magnetic field and tensile stress on the nucleation of martensite plates. The transformation temperatures under

magnetic field or tensile stress were measured. The extra driving forces necessary for martensitic transformation under magnetic field or tensile stress were calculated thermodynamically using experimental data. They are in good agreement with each other. In order to make clear the difference of the effects of magnetic field and tensile stress on martensitic transformation, two types of experiments were conducted, that is, the sequence of the application of magnetic field of 10T and the tensile stress of 220Mpa was changed. The amount of martensite formed by increasing the magnetic field under constant stress is larger than that formed by increasing the stress in the constant magnetic field, which shows that the effect of tensile stress on the number density of martensite is larger than that of magnetic field in this experimental condition.

Keywords: nucleation, tensile stress, Fe-Ni-C alloys

Related Paper

1. H. Ohtsuka, K. Nagai, S. Kajiwara, H. Kitaguchi, and M. Uehara, "Effects of High Magnetic Field and Tensile Stress on Martensitic Transformation Behavior and Microstructure at 4.2K in Fe-Ni-C Alloys", *Materials Trans. JIM*, 37(1996): 1044.

Surface and interface properties

(26) Solid State Interfacial Reactions and Surface Analysis of Thin Solid Films

S. Hofmann, Director of Special Research
[January 1996 to December 1998]

The purpose of this research is to obtain optimum growth conditions and properties of nitride thin films (e. g. CrN and TiN). This will be achieved by (a) controlled deposition and annealing (b) controlled solid state interfacial reactions which will be monitored by AES/XPS in combination with sputter depth profiling and (c) optimized inert interlayer and capping layers for thin film protection and stabilization.

To ensure high purity and performance, the films will be prepared in extreme high vacuum with combined evaporation and ion beam techniques for Cr, Ti and N, respectively. After fabrication, the thin films will be thoroughly characterized by AES/EPS depth profiling and, by TEM and by hardness, friction and wear measurements.

Ideal growth conditions will be searched by using nitrogen ion bombardment from a special ion source providing energies between 10 and 1000 eV. Solid state reactions at substrate/film and at metal/nitride interfaces will be studies mainly by high resolution depth profiling. In later experimental stages, multilayer structures will be fabricated and tested with respect to optimized properties.

Keywords: Surfaces, Interfaces, Thin Films, Nitrides, Coatings

(27) Evaluation of Atomic Level Damage on Material

H. Masuda, Failure Physics
[April 1996 to March 1999]

From this year we start the project to study the nanometer range of damage caused by corrosion. We study on four subjects: 1. development of surface potential and surface hardness measurement techniques by SPM. 2. mechanism of bacterium corrosion by in-situ SPM observation. 3. high temperature corrosion property of metals by both photo-electron emission measurement and SPM observation. 4. surface film property by STM processing. In this project we study the various corrosion mechanism, those are, initiation of atmospheric corrosion, the nucleation of oxide nodule, formation of pit by bacteria and growth of oxide films, by the nanoscopic level of SPM observation.

Keywords: SPM, Corrosion, High temperature, Bacteria

(28) Evaluation of Durability of Coatings for Structural Materials

T. Kodama, Environmental Performance Division
[April 1996 to March 1999]

With increasing maturity and longevity of Japanese society, there is an increasing demand for the prolonged use of infrastructures. Organic coating is the most widely used method of the protection of steel structures, and is the sole method of the protection of steel structures exposed in atmosphere. We will conduct exposure tests of polymer coatings in cooperation with external agencies at two sites in Japan and two sites in Thailand. Thailand was selected because of its tropical climate and strong sun light and because

of our long history of cooperation in this field. In the field work of atmospheric exposure, we will evaluate environmental factors affecting materials degradation, which will contribute to the construction of global database of materials durability. In parallel with the field tests, we will conduct laboratory experiments from basic viewpoints of polymer and metallurgical science. Laboratory researches include the chemical analyses of bonding and adhesion between metal and organic polymers, mechanism of polymer degradation particularly after irradiation by UV light and detection of under-film metallic corrosion. Also we will continue working on the electrochemical measurements of corrosion system under very thin water film, where a non-contact sensor, Kelvin probe will be used. It is possible to measure electrode potential without touching water layer. Both field and laboratory works described above will be effective in the clarification of mechanism of materials degradation and will contribute to the materials protection of infrastructures.

Keywords: atmospheric corrosion, photo-degradation of polymers, organic coatings, steel structures

29 Two Dimensional Photoelectron Spectroscopic Studies on Surface Structures and Properties

M. Shimoda, Materials Physics Division
[April 1995 to March 1997]

Sulfur (S)-terminated GaAs(001) surface is considered as a hopeful foundation of "droplet epitaxy", a useful method of fabricating quantum dot structures. RHEED and STM studies have revealed that a (2×6) reconstruction is dominant for this surface. The STM images show that the adsorbed S atoms form S-S dimers and that every one of six dimers is missing. In order to confirm these findings and to investigate the reconstruction of the surface S layer as well as the substrate layers, we performed photoelectron and Auger electron diffraction measurements. The observed diffraction patterns were compared with theoretically calculated ones by a single scattering cluster model with the spherical wave approximation. The model cluster contains only two parameters, the S-S interatomic distance of the dimer and the interlayer distance between the S and Ga layer. The missing dimer, the buckling of dimers and any modulation in the 2nd layer are not considered in our calculations. In spite of our simple model, we reached the conclusion that the S-S interatomic distance is about 0.24 nm and the interlayer distance between S and Ga layer is about 0.12 nm, in excellent agreement with the results from STM image analyses. Simulations with more realistic model are under way.

Keywords: photoelectron diffraction, Auger electron diffraction, GaAs, 2x6 reconstruction, sulfur-termination

30 Research on Electrode Reaction between Metallic Ions and Carbonaceous Materials/Research on Electrochemical Characteristics of TiAl alloy

I. Tomizuka, Physical Properties Division
[April 1994 to March 1997]

a) Various carbon fibers (CFs) were soaked in sulfuric acid and electrochemical impedance spectra (EIS) was observed at a cathodic potential and an anodic potential. The CFs prepared at higher temperature showed electro-capacity highly depending on angle velocity of applied potential and electro-resistance hardly depending on it, while the CFs prepared at lower temperature did the reverse.

b) Similar study was performed for two fibers which were prepared at different temperatures from an identical precursor containing sodium. The fiber prepared at the lower temperature behaved in an anomalous way: the capacity in the lower frequency range was smaller approximately by one digit and the resistance was larger by a considerable amount as compared with those of the other fibers of comparative crystallinity.

c) When an activated carbon fiber was soaked in a solution of sulfuric acid containing copper under various cathodic potentials, the rate of the decrease in residual concentration of the ion was proportional to the residual concentration. The concentration decreased by a considerable amount immediately after the soaking and did so at a lower rate common to all fibers in the following period. The initial decrease was relatively small for the ACF.

d) It has been implied by x-ray diffractometry that two types of metal hydride are present in the TiAl alloy, when it is kept in a sulfuric acid under a cathodic potential for a long period (Specimen A) or when it is kept in the same condition for a short period and then the Al atoms are dissolved preferentially under an anodic potential (Specimen B). An experiment was performed this year to check the presence of the two by a thermo-analysis procedure. The result on Specimen A revealed evolution of gas at two different temperatures.

Mass-spectrometry carried out simultaneously identified the gas being hydrogen. Thus their presence was well established for Specimen A. Similar work is in progress on Specimen B.

Keywords: electrode reaction, metallic ion, carbonaceous material, TiAl-based alloy

31 Surface Analysis Database

K. Yoshihara, Extrem High Vacuum Station
[April 1995 to March 1998]

In 1994 the Science and Technology Agency (STA) of Japanese Government launched a project to interconnect networks under various ministries and agencies. The project is called Inter-Ministry Computer Network System (IMNet). Every site joining to IMNet would have a connection with 600M bps to one of NOCs (Network Operation Centers) located in Tsukuba - Tokyo - Osaka. As a site of IMNet we are implementing a network-oriented database for surface chemical analysis such as AES and XPS spectra.

A workstation was installed in National Research Institute for Metals to collect the spectral data with VAMAS format from different analysis machines via computer networks and modem lines. Collected spectra are stored in the database. The surface analysis database can be retrieved via the Internet. If a personal computer is connected to the Internet, one can access the home page of the Surface Analysis Society of Japan(SASJ), whose address is "sekimori. nrim. go. jp". To cooperate this project, SASJ was established in 1995 and has the responsibility to provide the spectral data, and controls its quality. When the home page of SASJ is opened, one can select the database menu and retrieve a spectrum from the selection menu. The retrieved spectrum will be displayed on a screen as a "GIF" image. If the personal computer has already the Common Data Processing System in its memory, a retrieved spectrum can be downloaded by using the programs in it. The member of SASJ will be provided with the Common Data Processing System.

In future we hope all computers of the surface analysis machines can be connected to the system so that every surface analyst worldwide can share the spectral data and the common data processing software to identify the surface chemistry of new materials.

This research was performed in collaboration with the Surface Analysis Society of Japan and NTT cooperation.

Keywords: AES, XPS, Common Data Processing System, Internet, Database

Related Paper

1. K. Yoshihara and M. Yoshitake, "Construction of the Surface Analysis Network Database", *J. Surf. Anal.*, 1(1995): 369–374.

32 Self-Control of Surface Composition of Thin Film and Its Application to Field Emitter

K. Yoshihara, Extreme High Vacuum Station
[April 1995 to March 2000]

When a metal film deposited on substrate was heated in a vacuum, it was observed that the substrate element diffused to the surface of the film. The surface concentration of the segregant was always constant. Even if the segregated layer was removed by argon ion sputtering, the segregated layer of the saturated concentration was formed again by re-heating. Therefore, the surface composition of the segregated layer on the metal film is expected to have a self-controlling property.

It is well known that the surface adsorption of metal changes the work function of a solid surface. Therefore, it is expected to change the work function by the surface segregation. If the work function of materials can be lowered, we can produce a field emitter of high performance. Fowler-Nordheim relation shows that a half eV decrease in work function brings approximately 10 times increase in field emission current. The work function varies with a coverage of adsorbed materials. However, if we use the self-controlling property of segregation behavior on the metal film, then the stable work function on the surface, i.e., stable field emission current can be expected.

In this study, the stability of surface composition will be quantitatively analyzed in the wide range of temperature, and the change of work function by segregation will be measured. In 1995, the recovering rate of the surface composition during Ar ion sputtering in the case of Ti segregation on a Nb thin film, which is useful as an intelligent getter film was measured. The relation between the amount of adsorbed contaminant and the segregation behavior was also examined in case of Cu segregation on a Ti film.

Keywords: surface segregation, saturated surface composition, self-composition control, work function, field emitter

Related Papers

1. M. Yoshitake and K. Yoshihara, "Electric States of Segregated Metal Atom on Metal Surfaces and potential Use for Field Emitter", *J.Vac.Sci.Technol.*, A13(1995): 2407–2411.
2. M. Yoshitake and K. Yoshihara, "The Effect of the Gas Adsorption on the Segregation Behavior of Substrate Metal on Thin Film, *Appl.Surf.Sci.*, (1996): in print.

33 Fabrication of Nanometer-Scale Structures on the Extremely High Vacuum Surface

H. Nejo, Extremely high vacuum station

[April 1995 to March 1996]

1-1. So far, we have succeeded to fabricate nanometer-scale structures connected to macroscopic electric pads. Some methods of fabrication have been tried; ①Cluster extraction from STM tips by field in both UHV and ambient conditions ②Extraction of metal from macroscopic electrical pads using electromigration ③Extraction of clusters from Liquid-metal-ion source (LMIS) by heating up. Also, various attempts have been made to evaporate macroscopic electric pads on substrates; As for a mask ①Mechanically made thought-hole mask ②Mechanically made and farther electrochemical etched through-hole mask ③Through-hole is made using focused-ion-beam ④Just putting metal or carbon wire on a substrate ⑤Gap is fabricated using conventional e-beam lightingraphy followed by Ar ion sputtering for removing organic residue in UHV. As for a substrate ①Si substrate with native oxide on it ② Clean Si substrate gotten by flashing in UHV.

1-2. The electron standing wave on an Au(111) surface was observed at 30K using STM (Figure). The extension of the standing wave is 70 nm and this length is more than several ten times longer than that obtained by conventional observation done by Eiglen's group and Avouris' group. Another finding is that due to this long extension the direction of this standing wave is driven by the direction of the so-called herring-bone structure of an Au (111) surface.

For observing standing wave for a long distance, it is required that the phase of electronic wave is conserved. For fulfilling this requisite, two conditions should be satisfied; ① The temperature of the sample should be low enough so that a traveling electron is not scattered by a phonon. ②Only one component of k-vectors should be chosen so that various k-vectors do not cancel out each other. We cooled the sample to

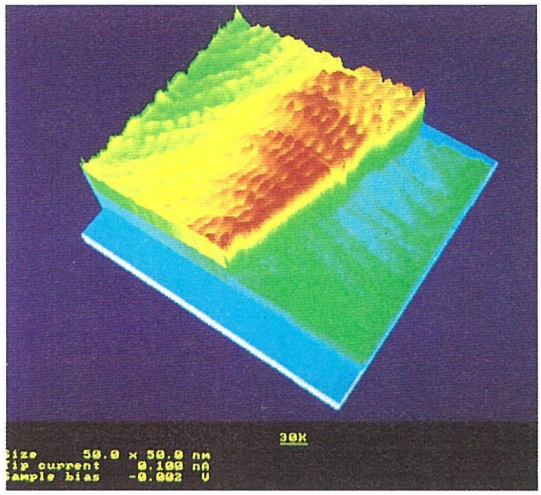

Fig. 1

30K for satisfying the condition 1. Also, the bias voltage between the scanning tunneling microscope tip and the sample was set to 3mV for satisfying the condition

2. This long extension of standing wave may open the way to realize the atomic scale quantum interference device.

Keywords: cluster extraction, nanometer-gap, electromigration, standing wave, scanning tunneling microscope

Related Papers

1. H. Nejo, V.A. Tkachenko, M. Tsukada and M. Aono "Suppression of electron tunneling through liquid crystal molecules due to infrared irradiation".
2. M.E. Welland and J.K. Gimzewski, "Ultimate Limits of Fabrication and Measurement", (1995): 171–179.
3. M.E. Welland and J.K. Gimzewskieds. "Ultimate Limits of Fabrication and Measurement": (Kluwer Academic Publishers, Dordrecht 1995): 115–120 .

34 Fabrication and Characterization of Compound Semiconductor Nanometer Structures (Nanospace Laboratory Project)

N. Koguchi, Center for Materials Science under Extreme Environments

[April 1994 to March 1997]

With the continuous reduction in the dimension of electronic devices, quantization effects become dominant and may disturb the function of the

device. Nanometer research, however, makes constructive use of quantum effects. Tunneling, single-electron transfer and wave interference can be used as a basis for novel devices. In 1994, Science and Technology Agency has organized several institutes and universities for a new research project, named `Nanospace Laboratory Project'. The target of this project is to fabricate and characterize the material structures with dimensions down to a few nanometers. In this project, we are now researching the fabrication and characterization of compound semiconductor nanometer structures. In order to fabricate these structures, we are researching three methods; self-organized formation by using adsorption phenomena, microfabrication using metal fine particles deposited on semiconductor quantum wells and Droplet Epitaxy combined with lithography by scanning tunneling microscopy(STM).

We have designed and introduced a new system suitable for the self-organized formation of nanometer structures. This system is composed of molecular beam epitaxy equipment combined with STM and reflectance difference spectroscopy instruments. We can perform in-situ observation of a surface during formation of nanometer structures using this new system.

It is necessary to investigate the S-terminated GaAs (001) to fabricate nanometer structures by Droplet Epitaxy combined with STM lithography. We have observed the S-terminated GaAs (001) with (2x6) surface reconstruction by STM and found out this reconstruction originating from the cell which contains five S-S adatom dimer and one missing dimer for the first time. Also we have estimated the structural stability of this (2x6) reconstruction by the first principles pseudo-potential calculation and confirmed the phenomena of electron transfer from S-S dimer to missing dimer.

InAs epitaxial microcrystals are useful for etching masks on GaAs/GaAlAs quantum wells to fabricate vertically combined GaAs/GaAlAs quantum dots.

Keywords: nanometer structure, molecular beam epitaxy, GaAs, scanning tunneling microscopy

Related Papers

1. N. Koguchi, S. Takahashi, and T. Chikyow, "New MBE Growth Method for InSb Quantum Well Boxes", *J.Crystal Growth*, 111(1991): 688–692.
2. N. Koguchi and K. Ishige, "Growth of GaAs Epitaxial Microcrystals on an S-terminated GaAs Substrate by Successive Irradiation of Ga and As Molecular Beams", *Jpn. J. Appl. Phys.* 32(1993): 2052–2058.
3. N. Koguchi, K. Ishige, and S. Takahashi, "New Selective MBE Growth Method for Direct Formation of GaAs Quantum Dots", *J. Vac. Sci. Technol.*, B 11(1993): 787–790.

35 Fabrication of Quantum Well Box Systems by Droplet Epitaxy for Advanced Optoelectronic Devices

N. Koguchi, Center for Materials Science under Extreme Environments

[April 1991 to March 1996]

Predictions of enhanced electron mobility device and advanced semiconductor laser with highly-monochromized and low threshold current density have been made in the quantum well box structure. Although the molecular beam epitaxy (MBE) method is known to be successful in growing finely layered structures and quantum well wires, it has not yet been successful to obtain the quantum well box structure.

We have proposed a new MBE growth method named as Droplet Epitaxy for the fabrication of some III-V compound semiconductor quantum well box structures. This method is based on incorporating V-column elements with III-column elements in the periodic table droplets which were deposited on an inert surface of the substrate by monolayer adsorption of the III and V-column elements. Some III-V compound semiconductor surfaces terminated with a VI-column element like S, Se or Te have been reported to provide an inert surface with appropriate dangling bonds suitable for supporting the adhesion of foreign atoms. Such surfaces are thought to be suitable for the growth of epitaxial microcrystals by the Droplet Epitaxy method.

We have demonstrated three dimensional growth of GaAs epitaxial microcrystals on an S-terminated GaAlAs substrate by Droplet Epitaxy. At the end of the process of Droplet Epitaxy the GaAs microcrystals are covered by an MEE(migration enhanced epitaxy) grown GaAlAs layers. By this technique a number of epitaxial microcrystals with a pyramidal shape were successfully obtained on the S-terminated substrate. The base size of each epitaxial microcrystals was about 10 nm × 10 nm with standard deviation of about 5% and the average distance between each microcrystals was about 10 nm in the case of substrate temperature of 50 C and the Ga molecular beam intensity of 3.3×10^{14}

cm^{-2} s^{-1}. The size and distribution of microcrystals correspond to those of Ga droplets. The measurements of the Ga droplet saturation density as functions of Ga molecular beam intensity and substrate temperature revealed the nucleation mechanism of Ga droplets on the S-terminated GaAs. The size of the smallest stable nucleus is one Ga-Ga pair on the substrate. It is necessary to fabricate nucleation sites for Ga droplets to arrange the site of each GaAs microcrystal. The selective deposition using finely focused Ga ion beam is also a promising method to arrange the site of each microcrystal. Finely focused Ga ion beam with an accelalation voltage of 30 eV makes an array of Ga droplets with an diameter of 200 nm without radiation damage.

Keywords: quantum well boxes, molecular beam epitaxy, GaAs, scanning tunneling microscopy

Related Papers

1. N. Koguchi, S. Takahashi, and T. Chikyow, "New MBE Growth Method for InSb Quantum Well Boxes", *J.Crystal Growth,* 111(1991): 688–692.
2. T. Chikyow and N. Koguchi, "Microcrystal Growth on a Se-terminated GaAlAs Surface for the Quantum Well Box Structure by Sequential Supplies of Ga and As Molecular Beams", *Appl.Phys. Lett.*, 61(1992): 2431–2433.
3. N. Koguchi and K. Ishige, "Growth of GaAs Epitaxial Microcrystals on an S-terminated GaAs Substrate by Successive Irradiation of Ga and As Molecular Beams", *Jpn. J. Appl. Phys.* 32(1993): 2052–2058.
4. N. Koguchi, "Fabrication of GaAs Quantum Dots by Droplet Epitaxy (Review).", *Oyo-Butsuri,* 65(1996): 926: in Japanese.

36 Basic Study on Reaction between Materials and Bacteria

H. Masuda, Failure Physics Division

[April 1993 to March 1995]

It is well known that some bacteria have special ability to oxidize Fe^{2+} to Fe^{3+}. This ability of oxidizing Fe^{2+} caused corrosion of metal. This year we studied the bacterium (Thiobacillus ferroxidans) corrosion on SUS304 stainless steel by an atomic force microscope (AFM). Figure shows the example of bacterium corrosion on SUS304 stainless steel. Bacterium corrosion usually starts by attaching bacteria to metal. The crevice corrosion starts under the bacteria and a pit whose size is equal to that of the bacterium is formed. Bacteria live by eating Fe^{2+} produced by pitting corrosion. The size of the pit produced by bacteria is very important to predict the crack initiation under loading condition.

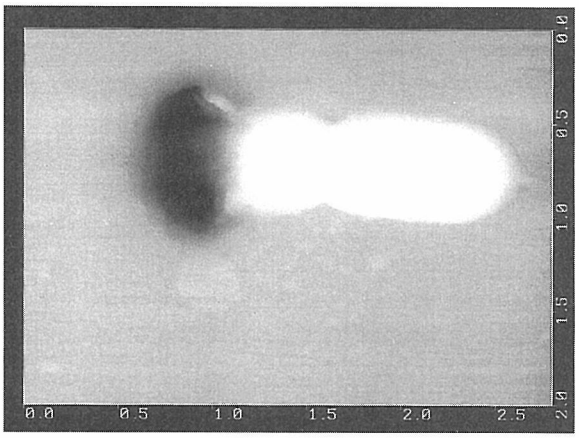

Fig. 1

Keywords: Bacteria, AFM

37 Electrochemistry and Modeling of Corrosion of Metals under Thin Water Layer

T. Kodama, Environmental Performance Division

[April 1993 to March 1996]

Several types of corrosion reaction occur through thin layer of water on metal surfaces in such cases as atmospheric corrosion and indoor corrosion. Electrochemical reactions occur in those cases at the boundary between thin water film and metal surface. The reaction rate is higher than that in bulk solution because of more active mass transfer and accelerated diffusion. Yet little information has been available on the mass-transfer and current distribution of local electrochemical reactions in the water layer because of experimental difficulties in the measurements in thin surface layer.

To measure the distribution of local electrode potential of metal, we prepared non-contact electrodes (Kelvin probe) of gold wires of 0.5 mm diameter. The probe was allowed to oscillate sinusoidally using an actuator. Electrode potential is converted from electric current flowing through the probe and sample electrode. The potential is equivalent to the contact potential difference between sample and gold electrodes. For the correlation of this potential to conventional electrochemical potential measured with reference to a well-established reference electrode (Ag/AgCl electrode), we prepared some

metal samples such as silver, copper and zinc. For example, in a 5% NaCl solution, the following chemical reaction occurs on a chlorinated silver surface.

$$Ag + Cl^- = AgCl + e^- \quad ; E = 0.227V \text{ vs. NHE}$$

We measured the electrode potentials of such reactions on metals as is expected to exhibit electrochemical equilibrium potentials using both the Kelvin probe (non-contact) and silver/silver chloride(contact). We obtained the following relationship between potentials measured with different reference electrodes.

$$E_{Ag/AgCl} = 0.044 + 0.980\ E_{Au}$$

The potential referred to the Kelvin probe (E_{Au}) is related linearly to electrochemical potential referred to the conventional electrode ($E_{Ag/AgCl}$) with a slope almost equal to unity: Kelvin probe potential gives values equivalent to electrochemical potential only with an offset. It is thus concluded that using a Kelvin electrode we can measure electrochemical potentials occurring in thin water film without perturbation to the system.

Keywords: thin water film, Kelvin probe, potential distribution, atmospheric corrosion

38 A Study on the Degradation of Materials by Ultraviolet-Light Irradiation

T. Kodama, Environmental Performance Division
[April 1995 to March 1996]

In the same line as the case of ISO exposure tests we have conducted exposure tests in cooperation with ASEAN countries for the period of five years beginning from 1988. The test has revealed that the corrosion rate of bare metals in Southeast Asia was of the same level as that of world average. Metallic corrosion was affected more by air pollutants. The degradation of polymer coatings, on the contrary, was much higher in these countries than in Japan. The climate and high level of ultraviolet light (UV) in the tropics accelerate the polymer degradation.

In this conjunction we started new exposure tests at two sites in Japan and two sites in Thailand. Counterpart agencies in the present study are Thailand Institute of Scientific and Technological Research (TISTR) and Chiang Mai University. Tested coating samples are alkyd, epoxy, polyurethane, and fluoride resin. For each type of resin three different colored samples were prepared with different pigments; clear, white and red. Exposure tests are carries out at two sites both in Japan and Thailand. For the monitoring of polymer degradation monthly measurement of an optical method (gloss retention) is to be carried out. Exposed samples are to be collected periodically and will be subjected to the Fourier transform infrared (FTIR) spectroscopy and gel permeation chromatography (GPC).

A laboratory simulation of UV degradation has been carried out using simulated paint films and artificial UV light source. Four types of resins were selected for degradation analyses; alkyd, epoxy, chlorinated rubber and polyurethane. Paints thus prepared were coated on glass substrate of a size 5 x 15 cm using a bar coater to the thickness of 50 micro meters. Paint samples were then placed in xenon-lamp weather meter for UV irradiation up to 410 hrs. The structure change was detected using Fourier transform infrared (FTIR) spectroscopy.

As an indicator of polymer degradation carbonyl band of 1724 cm^{-1} was used for epoxy and 2926 cm^{-1} for alkyd. The carbonyl production kinetics obeyed the following equation: $I = I_0\ (1\text{-}\exp(-kt))$. The equation is the same as first order rate of chemical kinetics indicating that chain scission is determined by random process. White pigment containing rutile retarded the deterioration process. For chlorinated rubber and polyurethane samples no structural change was detected at the present level of UV irradiation.

Keywords: UV-degradation, paint films, carbonyl formation, atmospheric corrosion

39 Evaluation of High-Performance Triazinedithiols As a Corrosion Inhibitor

H. Baba, Environmental Performance Division
[April 1993 to March 1996]

This project on surfactants of triazinedithiols (RTDT) has started in cooperation with universities, governmental research institutes and industry under the auspices of Science and Technology Agency. The general targets of the project are designing molecular structure of high performance RTDT's with fluoride and siliceous functional groups, and establishing synthetic methods of the compounds that give highly protective interfacial layers on surfaces of metals, rubbers and plastics. In NRIM we take part in clarifying the mechanism of corrosion inhibition and the nature of chemical bonding between metals and RTDT's. Thiol radicals (-SH) are

known to react readily with copper and other metals following strong chemisorption. When metals are treated in solutions of properly selected triazinedithiols with variety of hydrophobic substitution groups (represented by R), stable and protective surface films are expected to be formed. In the second year of the project our concern is focused on the performance of highly sophisticated RTDT's with fluoride functional groups and the effect of conventional RTDT's on copper corrosion.

Copper specimens were electrochemically treated in several RTDT solutions with various radicals (-R), such as $-N(C_4H_9)_2$, $-N(CH_2CH{=}CH_2)_2$, -SH, $-N(n\text{-}C_8H_{17})_2$, $-NHC(CH_3)_2CH_2C(CH_3)_3$, $-N[CH_2CH(CH_3)_2]_2$, $-NHC_{18}H_{35}$, $-N(CH_2C_6H_5)_2$, $-N[CH_2(C_2H_5)CH(CH_2)_3CH_3]_2$, and $-NC_7F_{15}CH_2CH_2CH{=}CH_2$. The treated metal specimens were then subjected to the characterization of surface layers and evaluation of corrosion resistance. We have also studied the electrochemical behavior of copper in aqueous solutions of triazinedithiols for the purpose of obtaining the optimum electrolysis conditions for surface treatment. The highest protection was attained when copper was treated potentiostatically at the potential of current peak, Ep. We evaluated the corrosion resistance of anodized copper by electrochemical methods. Potentiokinetic polarization curves in 3% NaCl showed that corrosion current was suppressed with increasing number of carbon in the hydrophobic radicals, such as $-N(n\text{-}C_8H_{17})_2$, $-N[CH_2(C_2H_5)CH(CH_2)_3CH_3]_2$, $-NC_7F_{15}CH_2CH_2CH{=}CH_2$.

The performance of thiols as a corrosion inhibitor has been evaluated for a special type of localized corrosion of copper, the case of so-called "ant-nest" corrosion that occurs in wet acetic or formic acids. The performance of thiols as an inhibitor was improved with increasing number of carbon in hydrophobic radicals; e.g., such radical as $-N[CH_2(C_2H_5)CH(CH_2)_3CH_3]_2$ showed the highest performance. Among the groups of the same C number, iso-structure showed better performance than normal structure.

Using RTDTs with such derivative group as $-N(n\text{-}C_8H_{17})_2$ we studied the performance of RTDTs as a corrosion inhibitor as functions of concentration and electrode potential in surface pretreatment. In solutions containing these types of inhibitors, anode current peak was relevant in potentiokinetic polarization curves at a potential around 0.38 V vs. SCE. This anodic current maximum corresponded to the polymerization of RTDTs. The peak potential (Ep = 0.38 V vs. SCE) was thus selected for the anodization treatment of copper in the hope that the optimum performance be available for corrosion protection. Copper samples treated at Ep showed the highest water-repellent property and the highest corrosion inhibition efficiency.

Keywords: triazinedithiole, corrosion, inhibitor, copper

Mechanical Properties

(40) Effect of Cryogenic Temperature and Gas-Environment on Deformation and Fracture Behavior

T. Ogata and T. Yuri, Mechanical Properties Division

[April 1996 to March 1999]

To promote the application of clean energy and space technology, there is a project of constructing large scale facilities to transport and store liquid hydrogen. It is very important to evaluate the mechanical properties of the materials including weld metals to keep the reliability of large scale structures used at cryogenic temperatures and in hydrogen gas environment. It is required to comprehend the mechanical properties such as continuous data of fracture toughness from room temperature to liquid helium temperature, and the clarification of effects of hydrogen-gas environment at low temperatures on deformation and fracture behavior of structural materials for the design of structure and selection of materials. Especially, hydrogen embrittlement at low temperatures in the large scale structures of stainless steels is an important subject. In this study, we are going to establish the testing technique of tensile, impact properties, and fracture toughness to evaluate the effects of low temperature and gas environment from room temperature to liquid helium temperature, and investigate the effects of microstructure, grain size, δ-ferrite, and hydrogen gas environment on tensile, impact, fatigue properties, and fracture toughness of austenitic stainless steels from room temperature to cryogenic temperature.

Keyword: structural material, stainless steel, cryogenic temperature, hydrogen embrittlement

(41) Remaining Life Prediction of Weldment for FBR by Creep Damage Evaluation

Monma, Failure Physics Division

[April 1996 to March 2001]

Although the accumulated microstructural damage to the weldment of FBR components by creep exposure is considered to be rather small, but the quantitative evaluation of creep damage in welded joints is little known. In this study we plan to develop techniques to measure the degree of creep damage in welded joints for FBR. So far we have investigated the nature of the local variability of creep properties in weld metal in weldment of ferritic and austenitic stainless steels. The effect of thermal cycling and plastic constraint during welding procedure on the mechanical properties of the welded joint is complicated. A triaxial state in stress takes place by creep loading and non-equilibrium heterogeneous microstructure would constantly change during creep loading. The materials examined are welded joints of modified 9Cr-1Mo and 316FR steels. They are primary candidates of structural components for the future large-scale FBR. In the previous research we focused on the test temperature at 550℃, but we will extend it higher temperature up to 650℃ so that meaningful acceralation can be achieved to save the test duration.

In addition to the conventional creep testing of weldment, we plan to look into the quantitative evaluation of creep damage. The particular techniques being considered are the microstructural changes in the size and the distribution of precipitates Also examined will be the change of local variability in the elastic moduli of weld metal through the sound velocity. A simulation software will be developed to integrate the observation of microstructural changes and modeling of the damage processes. Ultimately we aim to develop a nondestructive evaluation method of creep damage in weldment which can be applied in-service inspection for the future FBR.

Keywords: creep damage, FBR, microstructural change, welded joint

(42) Effect of the Interfacial Damage on Mechanical Properties for Ti-Based Matrix Composites

C. Masuda, Failure Physics Division

[April 1996 to March 1998]

Silicon-carbide (SiC) fiber reinforced titanium alloy matrix composites are attractive for structural applications, such as gas turbine engines, and so on. Because of their high specific modulus and strength, and good stability at high temperature. There are many reports on the fabrication methods and mechanical properties of those composites. It is well known that the major problem during processing is fiber degradation due to the unavoidable nature of active reaction behavior between the fiber and matrix, that is, the reaction layer thickness was related to the degradation of mechanical properties. The effect of the reaction layer thickness on the mechanical properties could not be deduced by the micromechanics, because the mechanical properties of reaction layer could not be obtained.

It is very important to discuss the effect of reaction layer on the mechanical properties, and to detect the interfacial degradation and inner damage in composites for the evaluation of mechanical properties for metal matrix composites.

This subject is started this year for the following objectives,

1) The mechanisms of interfacial degradation

2) The development of non-destructive evaluation techniques to the detect the interfacial degradation

3) The basic study to detect the macroscopic inner damage in composites

Final target is the development of the new composites to reduce the interfacial reaction.

Keywords: Ti-based composite, Interfacial damage, Mechanical property, Damage evaluation method

(43) NRIM Creep Data Sheets Project-V

H. Irie, Environmental Performance Division

[Aprl. 1996 to March, 2001]

The objectives of this project are to obtain 10^5h data of heat-resistant metallic materials in creep rupture and deformation behaviour, which will be published as NRIM Creep Data Sheets in order to contribute to fundamentals of ensuring safety and reliability of structural components in high temperature plants and machines, to investigate long-term creep deformation behaviour and creep rupture properties, and to develop an evaluation of long-term creep rupture strength at high temperature.

This project has been carried out since 1966 and is still being continued in order to obtain further long-term creep testing data of domestic steels and alloys. In this new project-V which has been started this year, the change in microstructure during creep deformation will be observed, using stored up large amount of tested specimens until now and also stress relaxation behaviour of typical metallic bolts and so on will be measured. Both data will be published as photograph collection and relaxation data sheets respectively in addition to the creep testing data sheets. Further more, the

large accommodation of data in creep deformation will be analyzed and predominant factors on long-term creep strength will be made clear.

At the first stage of this project, following research programs will be carried out.

1) Long-term creep rupture and deformation testing will be being continued using Cr-Mo steels and also stress relaxation data of 12Cr steel bolt and so on will be collected, resulting in publication of new or revised creep data sheets,

2) On the analysis of creep deformation behaviour under application of the modified θ projection method, the concept of inherent creep strength, and Iso-stress method for prediction of long-term life, predominant factors in creep strength and transition process will be made clear, using large amount of data stock of ferritic heat-resistant steels such as 2.25Cr-1Mo steel,

3) Systematic analysis of microstructure during creep deformation and evaluation of accumulation process of creep damage using 300 series stainless steels, a new publication of collection of microstructure with already published creep data will be done, and

4) Evaluation of long-term creep strength at 900°C of nickel base super alloy In738LC for reliability of ultra-high temperature plant will be carried out.

Keywords: datasheet, heat-resistant steel, heat resistant alloys, creep rupture, creep deformation, stress relaxation

(44) Ductile versus Brittle Behavior of Structural Steels

S. Matsuoka, Environmental Performance Division

[April 1996 to March 1998]

Many steel structures were damaged on Hanshin-Awaji great earthquake of January 17, 1995. One typical example was the buckling of steel columns in highways and another was the brittle fracture of steel box columns in high-rise buildings. Such a difference in damage modes is closely related to the ductile versus brittle behavior of structural steels.

In this study, Charpy impact tests and fracture toughness tests are carried out for various structural steels such as SS400, SM490B or SHY685 in order to investigate the effect of test temperature, sheet thickness and test speed on the ductile versus brittle behavior. Fracture surfaces obtained are analyzed with a scanning tunneling microscope, STM, and atomic force microscope, AFM, in order to clarify the mechanisms of ductile and brittle fractures in a nanoscopic scale.

Keywords: steels, earthquake, ductile fracture, brittle fracture, STM, AFM

(45) Improvements of High Temperature Properties in Materials for High/Ultra-High Temperature Use

T. Tanabe, Environmental Performance Division

[April 1996 to March 1999]

Materials for high temperature use.

The aims of this study are to clarify the effects of microstructures on the creep rupture properties of TiAl intermetallic compounds and to develop the alloy system with high performance in high temperature creep rupture properties as well as in room temperature ductility. Ti-49 at.% Al and Ti-51 at.% Al are selected to investigate the effects, because various microstructures can be obtained through heat treatments. Microstructures include the γ grain size, lamellar grain size, morphology of α_2 phase and so on. Creep rupture tests will be carried out in the temperature range from 1023 to 1373 K in air, in vacuum and in high purity helium environment. Addition of third element to the alloy system will be considered to develop the satisfactory materials.

Materials for ultra-high temperature use.

The purpose of this study is to develop new plasma facing materials based on the mixtures of the ultra-high melting point materials. The selected materials are W,Ta, Hf, carbides and borides and the mixtures will be fabricated powder-metallurgically from the powders of the elements. Using an electron beam heating apparatus, thermal shock tests will be carried out to investigate the shock resistance of the mixtures and their fracture and/or erosion behaviors. Study on thermophysical properties of the materials before and after irradiation in JMTR will be performed in collaboration with Tohoku University (Oarai branch).

Keywords: intermetallic compound, TiAl, creep, plasma facing material, thermal shock resistance.

Related Papers

1. T. Tanabe, I. Mutoh, and M. Nakamura, "Effect of Environment and Microstructure on the Creep Rupture Behavior of TiAl Alloy Ti-46Al", *Book of Abstracts, 7th ICM*, (1995): 43–44.
2. M. Fujitsuka, I. Mutoh, T. Tanabe, and T.

Shikama, "High Heat Load Test on Tungsten and Tungsten containing Alloys", *J. Nucl. Mater.*: in press.

(46) Stability of Tetragonal Phase and Mechanical Propertiesof Transformation-Toughened Zirconia at High Temperature

F. Abe, Environmental Performance Division
[April 1996 to March 1999]

Stress-induced martensitic transformation from tetragonal to monoclinic phase near a proceeding crack tip is responsible for the high fracture toughness of partially stabilized zirconia such as ZrO_2-Y_2O_3, ZrO_2-MgO and ZrO_2-CaO alloys. Therefore, the stability of tetragonal phase affects transformation-induced toughening and can be controlled by several microstructural and chemical factors such as tetragonal particle size, composition of stabilizing elements, grain size, lattice defects and so on.

The purpose of the present research is to investigate the stability of tetragonal phase and its effect on mechanical properties for transformation-toughened zirconia over the temperature range between room temperature and 1200°C. The dynamic process of tetragonal to monoclinic transformation will be examined by measuring the change in elastic moduli, especially shear modulus, during transformation at high temperature. The elastic moduli will be measure based on an ultrasonic pulse sing-around method which causes no mechanical damage of the specimens. The effect of microcracks on the stability of tetragonal phase will be examined by means of transmission electron microscopy before and after the transformation. High-temperature fracture stress σ_f and fracture toughness K_{IC} will be examined by four-point bending test and the effect of the stability of tetragonal phase on the mechanical properties will be discussed. High-temperature Vickers hardness will be also measured to obtain hardness and K_{IC} as a function of temperature during continuous heating and cooling of the specimens.

Keywords: zirconia, fracture stress, toughness, tetragonal phase, transformation

47 Cycle Deformation in a Corrosive Environment

R. Hamano, Mechanical Properties Division
[April 1994 to March 1997]

The growth of fatigue crack nucleated along the slip bands of PSBs or PLBs occurs over two successive propagation stages - Stage I (shear mode) and Stage Ⅱ (normal mode). The past data on the effect of environments n crack growth in Stage Ⅱ fatigue region have been reported in previous works. Comparatively little attention has been paid to the effect of hydrogen-related environments on Stage I crack propagation and the transition of crack growth from Stage I to Stage II.

We present experimental results suggesting that the early transition of fatigue crack growth from Stage I to Stage Ⅱ in a hydrogen environment is a potential index for hydrogen-related embrittlemen and discuss whether the early transition of the stages of fatigue crack growth is caused by the localized transition of the stages of fatigue crack growth is caused by the localized deformation or the decohesion at a notch root, carrying out fatigue tests on specimens of iron single crystals and precipitation hardened Aluminum alloy in laboratory air with or without water vapour and in a 3.5% NaCl aqueous solution.

Fatigue tests were performed on a closed loop servo-hydraulic machine, using a sinusoidal wave and a load ratio of 0.1. The testing temperature was 293±1 K. A frequency of 15Hz in laboratory air with a relative humidity of about 50% and a frequency of 1Hz in a 3.5% NaCl aqueous solution were employed. After fatigue testing, fracture surfaces were observed with scanning electron microscope(SEM).

The observation of the early transition of fatigue crack growth from Stage I to Stage Ⅱ and the appearance of striations on the fracture surfaces in a 3.5% Nalc aqueous solution suggests that secondary slip plays an important role in the transition of fatigue crack growth and the fatigue crack grows by the operation of two more slip systems leading to macroscopically brittle (transcrystalline) fractures bisecting the two active slip planes. It seems reasonable to propose that the dominant, hydrogen-related fatigue cracking is hydrogen-assisted strain localization ahead of notch root and requires subsequent crack propagation in two more slip systems to explain the suppression of Stage I growth.

The reason why the existence of hydrogen occluded in materials activates slip multiplication might be considered based on: (1) enhancement of dislocation sources, and (2) an increase in mobile dislocations and in mobility of screw dislocations together with hydrogen atoms accumulated to the crack tip.

Keywords: stage I fatigue crack, stage II fatigue crack

Related Paper

1. R. Hamano, "In the Transition of Fatigue Crack Growth from Stage I to Stage II in a Corrosive Environment", *Met. Mater. Trans.* A, 27A(1991): 471–476.

48 Generalized Rule and Guide for Use of Fatigue Data

S. Nishijima, Failure Physics Division
[April 1995 to March 1997]

The authors have been conducting a series of projects since 1975 to establish standard reference data on the fatigue properties of Japanese materials for machines and structures. The program of work has been accomplished most successfully in March 1995 with the publication of 83 Data Sheets.

The present research aims at the presentation of generalized rules found in different fatigue properties that can be explained from view point of fundamental mechanisms of fatigue and, therefore, that are most important for adequate use of those fatigue data. It is, in other words, to offer a guide for understanding the change in properties of different materials and for applying the data to engineering requirements. Selected data from related Data Sheets are collectively analyzed to be fit to theoretical models, for some cases, or additional experiments are performed to verify theories, for the other cases.

The effort to show the generalized rule on fatigue property data has actually been continued in the previous Fatigue Data Sheet Project. The outputs have been published in Japanese as Fatigue Data Sheet Technical Documents, Table 1, and will be completed further by the present two-year program.

Table 1 NRIM Fatigue Data Sheet Technical Document

No.	Subjects	Issued
1	Fundamental Fatigue Property for Carbon, Cr and Cr-Mo Steels	1981
2	Fatigue Strength for Welded Joints of High Strength Steels	1983
3	Crack Growth in Arc-Welded Butt-Joints of High Strength Steels	1984
4	Strain Rate Effect in Low Cycle Fatigue of Alloy Steels at High Temps.	1985
5	Fundamental Fatigue Property of JIS Steels for Machine Structures	1989
6	High Cycle Fatigue of Alloy Steels at Elevated Temperatures	1990
7	High Cycle Fatigue Property of Carburized Steels	1992
8	Fatigue Crack Propagation for Welded Joints of Structural Steels	1995
9	High Cycle Fatigue Property of Hard Steels	1995
11	Time/Temp Effect in High Cycle Fatigue of Steels at Intermediate Temps.	1996
12	Time-Dependent High Temperature Fatigue of Steels and Alloys	1996
13	Fatigue Property of Aluminum Alloys for Welded Structures	1996
14	Intermediate Temperature Fatigue of Steels for Welded Structures	(1997)
15	Low/High Cycle Fatigue Properties of Steels and Aluminum Alloys	(1997)
16	Intermediate Temperature Fatigue of Steels for Pressure Vessels	(1997)
17	Elastic Moduli of Steels for Machine Structures	(1997)

Keywords: fatigue, steels and alloys, aluminum alloys, welded joints, NRIM fatigue data sheets

49 Long-Term Creep-Fatigue Properties of 316FR Stainless Steel for Fast Breeder Reactor

K. Yamaguchi, Failure Physics Division
[April 1995 to March 2000]

The 316FR stainless steel has been developed as a candidate material for fast breeder reactor of twenty first century. For the structural design of components of the reactor, evaluation of fatigue life data for the 316FR steel is important to represent the temperature- and strain rate-denpendences of the fatigue life design curves. Because the main components of the reactor are subjected to cyclic thermal stresses due to start-up and shut-down of the system. One of the objects in this research is to apply a parametric analysis for evaluating the fatigue life data, and to predict the fatigue life at very slow strain rate up to 10^{-8}/sec. This method was developed by the author and was successful to apply to many kinds of conventional engineering heat resisting materials at the strain rate up to 10^{-5}/sec. The testings are now running at 500, 550 and 600°C under the strain rates of 10^{-3}, 10^{-4}, 10^{-5} and 10^{-6}/sec.

Second is to evaluate monotonic creep and cyclic fatigue properties for modified 316FR steels which is now developing by a steel maker and fabricators. So the testing data would be useful to the materials design. In the first half of this research sixteen heats of the materials with different chemical compositions varing the elements such as C, N, Mn, P, Ni, and Cr are being tested. In the second half a prediction method of the fatigue life will be developed by using the data of monotonic creep rupture properties such as creep rupture ductility.

This research is performed in collaboration

with Mitubishi Heavy Industry Ltd., Nippon Steel Corp. and The Japan Atomic Power Co.

Keywords: low cycle fatigue, fast breeder reactor, 316 FR stainless steel

Related Paper

1. K. Yamaguchi, K. Kobayashi, K. Ijima, and S. Nishijima, "Parameter Analysis for Time-Dependent Low-Cycle Fatigue Life", *Trans. ASME, J. Eng. Mater. Tech.*, 116(1994): 479–482.

50 Study on Transient Behaviour of Deformation and Fracture at the Elevated Temperature

F. Abe, Environmental Performance Division
[April 1994 to March 1997]

Complex transient behaviour which does not obey classical form, is observed on both creep deformation and creep crack growth of heat resistant steels and alloys at the elevated temperature.

Creep deformation and creep crack growth are influenced by the changes in microstructure of materials. This study aims at giving a role of microstructural change in the transient behaviour at the elevated temperature.

Creep deformation behaviour and the effect of thermal ageing prior to creep test on that has been investigated on the carbon steel. Complex creep deformation behaviour which reveals several peaks and local minima in creep strain rate, that differ from classical one which consists of transient, steady-state and tertiary creep stages, has been clearly observed on the steel without prior ageing. Such anomalous creep deformation behaviour, however, has never been observed on the prior aged steels. Almost common creep deformation behaviour has been observed for the prior aged steels, independent of ageing time. It has been concluded that the anomalous creep deformation behaviour is caused by decrease in creep strength due to microstructural change and the common creep deformation behaviour of the prior aged steels corresponds to the inherent creep strength property of the steel.

The evaluation of creep crack growth behaviour at early stage is the very complicated problem. The theoretical transition time from small scale yielding condition to transient creep and steady-state creep condition was calculated on several materials. The calculated results have been compared with experimental observations. The predicting method of crack opening displacement rate at transient and steady-state stage from creep curve of round bar specimens was studied.

Keywords: creep deformation, inherent creep strength, creep crack growth, microstructural change

Related Papers

1. K. Kimura, H. Kushima, F. Abe and K. Yagi,"Effect of Thermal Ageing on The Complex Creep Deformation Behaviour of Carbon Steel and It's Inherent Creep Strength": submitted to Tetsu-to-Hagane: in Japanese.
2. M. Tabuchi, K. Kubo, and K. Yagi, "Effect of Specimen Thickness on Creep Crack Growth Properties of 1Cr-Mo-V steel": submitted to *J. Soc. Mat. Sci. Japan*: in Japanese.

51 Characterization of Creep-Damaged Microstructure of Stainless Steels by Computer Aided Quantitative Metallography

F. Abe, Environmental Performance Division
[April 1995 to March 1998]

The purpose of the present research is to characterize the creep-damaged microstructure of heat resisting steels and alloys by means of computer aided quantitative metallography and to analyze the creep damage process in the materials based on the characterized microstructure. The characterization of the creep-damaged microstructure has been carried out at different levels of creep strain with emphasis on the distribution of creep voids and precipitates along grain boundaries.

We have applied ion sputtering techniques to etching for a variety of heat resisting steels and alloys. Although microstructure examination of the materials is usually carried out after etching by chemical method, high skill is require for chemical etching to produce clear microstructure and reproducible microstructure is not easily obtained. The etching of small test pieces was carried out in the vacuum chamber of a microsputtering apparatus for 1Cr-1Mo-0.25V ferritic steel, type 316 stainless steel and Ni base superalloy Inconel 713C after creep rupture testing. The etching of large boiler tubes of 2.25Cr-1Mo ferritic steel and type 321 stainless steel after long-term service in plants was carried out using a specially-designed microsputtering apparatus, where the vacuum chamber was attached to the outer surface of boiler tubes, and then replicas were successfully produced. The etching by Ar-ion sputtering produced clear microstructure for all the materials

at an anode voltage of 0.8-1 kV, discharge current of 6 - 10 mA and sputtering time of 5 - 15 min, irrespective of different chemical compositions and different history of the materials. We could characterize grain boundaries, creep voids and precipitates such as carbides and σ phase. It is concluded that the present method requires less skill and reproducible microstructure is easily obtained.

Keywords: creep-damaged microstructure, computer aided metallography, stainless steels

Related Papers

1. H. Tanaka, F. Abe, K. Yagi, E. Nishikawa, and T. Sugita, "Etching for Microstructural Examination by Ion Sputtering", *Report of the 123rd Committee on Heat-Resisting Metals and Alloys, Japan Society for Promotion of Science*, 37(1996): 23–29: in Japanese.
2. F. Abe, "Creep and Creep rate Curves of a 10Cr-30Mn Austenitic Steel during Carbide Precipitation", *Metall. Trans.*, 26A(1995): 2237–2246.

52 Relationship between Fatigue Crack Propagation and Cyclic Deformation of Small Specimens

A. Ohta, Environmental Performance Division
[April 1994 to March 1997]

The fatigue crack propagation property is usually evaluated by the relationship between the fatigue crack propagation rate, da/dn, and the range of stress intensity factor. The property deteriorates with the stress ratio. However, the property saturates in the very high stress ratio condition. In these high stress ratio conditions, the fatigue crack opens in the whole range of stress. That is, the whole range of the stress intensity factor coincided with the effective range of stress intensity factor. Therefore, the property for these high stress ratio condition is determined to be the fundamental fatigue crack propagation property.

This fundamental fatigue crack propagation property for steels, A5083 aluminum alloy and Ti-6Al-4V titanium alloy which received STA heat treatment was measured by two of the maximum load hold fatigue crack propagation tests. The duplicate tests lend the confirmation of the unique property in different stress ratio conditions.

The fundamental fatigue properties for different materials become superior with the Young's modulus, E, when the properties were compared with the relationship between the fatigue crack propagation rate, da/dn, and the range of stress intensity factor, ΔK. However, the fundamental fatigue crack propagation properties for different materials become unique in the relationship between the fatigue crack propagation rate, da/dn, and the range of strain intensity factor, $\Delta K/E$. This means that the fatigue crack propagation is controlled by the elastic strain range around the crack tip.

However, the property only for titanium alloy which was annealed was superior to that for the above mentioned unique property.

In order to reveal the superior properties for the titanium alloy annealed, the cyclic deformation of small smooth specimens was measured by keeping the maximum stress to be the yield strength of material. The mean value of the cyclic strain saturated in the early period of test for the most of materials which have unique da/dn-$\Delta K/E$ relationship. However, the mean value of the cyclic strain increases for the whole period of test. These deformation properties suggest that the fatigue crack of titanium alloy annealed closes even for the maximum load hold fatigue crack propagation test.

Keywords: fatigue crack, fatigue properties, cyclic deformation

53 Fatigue Strength Evaluation of Welded Joints in Synthetic Sea Water by $\sigma_{max} = \sigma_y$ Test

A. Ohta, Environmental Performance Division
[August 1995 to March 1998]

The fatigue strength obtained with small welded specimens by a usual test condition of R=0 is higher than those for large welded beams.

The difference of fatigue strength among specimen sizes occurs from the difference of residual stress. That is, in welded beams a high tensile residual stress of the yield strength in magnitude exist. Thus, the fatigue strength of welded beams do not vary with stress ratio, because the maximum stress is kept to be the yield strength by the shakedown. While, the fatigue strength of small specimens decreases with the increase of stress ratio, because the small specimens contain slight residual stress and the maximum stress increases with the stress ratio.

In order to overcome the difference, a new fatigue testing method simulating the stress condition in welded beams by keeping the maximum applied stress to be the yield strength was developed. It was confirmed that the fatigue

strength obtained by the new testing method with small welded specimens gave the same fatigue strength of welded beams in air at room temperature.

In this investigation, the new testing method is applied in the synthetic sea water condition.

The NK-KA32 steel of which yield strength was 403 MPa was used. The specimen was boxing fillet welded joints. The width of small specimen was 120mm; the thickness, 10mm; and the length, 800mm. The environment control chamber was bonded on the specimen after the specimen was pulled up to the mean value of applied stress. This process avoided the leak of synthetic sea water due to the separation of chamber from the specimen surface. The temperature of synthetic sea water saturated with oxygen was 40°C.

The welded beams were 1,600mm in length, 240mm in width and 400mm in height. Whole of these specimens were put into a steel chamber filled with synthetic sea water. The condition of synthetic sea water was same as in the case of small specimens.

Fatigue tests were performed with sinusoidal waveform at 0.17 Hz. The axial load was applied by keeping the maximum stress to be the yield strength on small specimens, and bending moment at R=0 was applied on welded beams.

Fatigue tests were performed up to 1×10^6 cycles. The fatigue strength for both specimens successfully coincided with each other even in synthetic sea water condition.

Keywords: Welded Joint, Fatigue Strength, Residual Stress, Sea Water

Related Papers

1. A. Ohta, Y. Maeda, and N. Suzuki, "Fatigue Strength of Butt-Welded joints under Constant Maximum Stress and Random Minimum Stress Conditions", *Fatigue & Fracture Engng. Materials & Structures* , 19(1996): 265–275.
2. A.Ohta, Y. Maeda, S. Machida, and H. Yoshinari, "Fatigue Crack Propagation in Welded Joints under Random Loadings in the Splash Zone", *Weld. World*, 35(1995): 391–394.

54 Fatigue Behavior of Brittle Materials at Elevated Temperatures

G. Choi, Mechanical Properties Division

April 1992 to March 1996

The development of ceramics is being watched with knee interest, because they are very promising as structural components for engineering applications where metallic materials are not available. Since many of them are subjected to static and cyclic loading at elevated temperatures for prolonged periods, it is important to understand fatigue behavior at elevated temperatures. Nevertheless, there are very few studies on static and cyclic fatigue behavior. of ceramics at elevated temperatures.

It is known that cyclic fatigue behavior at room temperature is affected by factors such as fracture toughness, environment, stress ratio and variable amplitude loading. However, it is uncertain whether these factors affect cyclic fatigue behavior at elevated temperatures.

In this study, static and cyclic fatigue behavior in normally sintered silicon nitride and pure alumina ceramics were investigated over a range of room temperature to 1200−C. Fatigue tests were conducted on a servo-hydraulic machine, using specimens with single edge precrack introduced by bridge indentation method. It was found that static and cyclic fatigue crack growth rates increase as temperature increases, but cyclic fatigue effect decreases with the increase of temperature. Such static and cyclic fatigue behavior are closely related to the decrease of fracture toughness with increasing temperature and viscous flow of glass phase at a high temperature.

Keywords: cyclic fatigue, static fatigue, fracture toughness, ceramics

Related Papers

1. G. Choi, S. Horibe, and Y. Kawabe "Cyclic Fatigue in Silicon Nitride Ceramics", *Acta Metall. Mater.*, 42(1994): 1407.
2. G. Choi, "Cyclic Fatigue Crack Growth in Silicon Nitride: Influence of Stress Ratio and Crack Closure", *Acta Metall. Mater.*, 43(1995): 1489.

55 Study on Deformation and Fracture of Structural Materials at Cryogenic Temperatures

K. Nagai, Mechanical Properties Division

[April 1993 to March 1996]

S-N curves at cryogenic temperature were determined for the alloys such as SUS316LN austenitic stainless steel, 9%Ni steel, Ti-5Al-2.5Sn alloy, Ti-Fe-O alloy, and A2219 aluminium alloy.

Fatigue crack initiation behavior was investigated in terms of its microstructural origins. The initiation of fatigue crack at subsurface occurred more often at lower temperature. The

subsurface or internal initiation is attributable to the cracking of specific microstructure by localized cyclic deformation. The size and location of the initiation crack varied from alloy to alloy; for the SUS316LN the size was largest among the alloys studied and the distribution was uniform and for the Ti-5Al-2.5Sn alloy the size became smaller and the distribution became more localized near the surface. Multiple fatigue tests in the Ti-Fe-O alloy clarified no interrelation among the size, the location and the number of cycles to failure.

The effect of an increase in frequency from 4 Hz to 20 Hz on fatigue behavior at 4 K was investigated for the SUS316LN and the Ti-5Al-2.5Sn ELI alloy. The 20 Hz S-N curve was identical to the 4 Hz one in the long life regime (more than 10^5 cycles to failure). Hence it can be concluded that the increased frequency of 20 Hz is allowable for the determination of the fatigue behavior in long life regime.

The total operation time of the cryogenic fatigue testing machine installed in 1980 attained ten thousand hours in 1994. Presumably this is the world record among the active cryogenic fatigue testers.

Keywords: cryogenic temperature, fatigue strength, crack initiation

Related Papers

1. K. Nagai, T. Yuri, O. Umezawa, K. Ishikawa, Y. Ito, and T. Nishimura,"High Cycle Fatigue Properties of Ti-6Al-4V Alloys at Cryogenic Temperatures", *Titanium'92, Science and Technology*, edited by F.H.Froes and I.Caplan, The Minerals, Metals & Materials Society, (1993): 1827–1834.
2. K. Ishikawa, T. Yuri, O. Umezawa, K. Nagai, and T. Ogata, "Fatigue Testing and Properties of Structural Materials at Cryogenic Temperatures", *Fusion Engineering and Design*, 20(1993): 429–435.
3. O. Umezawa, T. Ogata, T. Yuri, K. Nagai, and K. Ishikawa, "Review of High Cycle Fatigue Properties of Structural Materials at Cryogenic Temperatures", *Advances in Cryogenic Engineering Materials*, 40(1994): 1231–1238.

56 Assessment of Strength and Structural Materials Databases for Weldment in FBR (Fast Breeder Reactor) Components

Y. Monma, Failure Physics Division
[April 1991 to March 1996]

The local variability of creep deformation in welded joints is investigated to ensure the structural integrity of the primary components of The FBR (fast breeder Reactor). Narrow-gap welded joints of 50mm thick plates for a ferritic 2.25Cr-1Mo steel and two austenitic stainless steels, 304, 316FR (0.01C-0.07B-18Cr-11Ni-2Mo), were prepared. Full-thickness welded joint specimens were subjected to creep tests at 550°C using 50t creep testing machines in NRIM. It was confirmed that the creep-rupture strength of 316FR steel is about 100MPa more than that for the conventional 304 steel at 500°C and 10,000h. Both 304 and 316FR steels the creep-strength of weld metal show considerable local variability in the direction of the plate thickness: The resistance to creep deformation is more pronounced in the heart of the weld metal. Since the weld metal near the surface of the plate is much weaker than the heart one, the crack to lead fracture takes place from surface portion of the weld metal. And, thus welded joint fails in the weld metal.

Another interesting observation we made for the creep of welded joint is that the initiation of fracture in the welded joint of 2.25Cr-1Mo steel seems to start from fine grain region of the heat affected zone (HAZ), particularly where front and back side of multi-layer beads meet. Although it was widely recognized that the creep rupture occurs predominantly in HAZ for ferritic steel weldment and it is along coarse grain region, but the true initiation of the crack begins in finer grain region in HAZ. We believe he observation leads us to have insight into the analysis of the Type IV creep cracking of welded joints in ferritic steel.

Keywords: creep, database, FEM, stainless steel, welded joint

57 NRIM Creep Data Sheet Project-IV

K. Yagi, Environmental Performance Division
[April 1991 to March 1996]

One of the major objectives of the NRIM Creep Data Sheet Project is to obtain 10^5 h-creep rupture strength data for principal heat resisting steels and alloys including welded joints which were produced in Japan. NRIM has been conducting the Project since 1966. The test data have been published as a series of NRIM Creep Data Sheets. In fiscal year 1995, we published two Sheets (CDS No.1B on 1Cr-0.5Mo steel and CDS No.42 on 18Cr-12Ni-Mo steel) and one technical document. The technical document provides total test plan, materials details, guidance on creep testing

procedure, data generation, data analysis using time-temperature parameter method, microstructure examination in the Project. It represents the state-of-art for creep testing and data acquisition in NRIM, and the information will be of interest to a much wider range of users.

In parallel with the testing and publishing program, we have made researches on long-term creep and rupture behavior of heat-resisting steels and alloys. Complex creep deformation behavior which reveals several peaks and local minima in creep rate curves has been investigated on carbon steel from a viewpoint of "Inherent Creep Strength" concept. Complex phenomena has disappeared by aging prior to creep test. Mechanism of complex creep deformation behavior, which is based on decrease in creep strength due to microstructural changes and advent of inherent creep strength, has been proposed. Heat-to-heat variation of long-term creep strength property observed for 12Cr steel has been investigated by creep curve analysis based on a modified θ-projection concept and by microstructure examination. Heat-to-heat variation of the creep rupture strength properties was described by the difference in the parameter α which represents an acceleration in creep rate at tertiary stage. The magnitude of α correlated with the recovery of excess dislocations during creep. The effects of long-term creep deformation and applied stress on γ-γ' microstructure have been investigated for a polycrystalline Ni base superalloy, Inconel 713C at 1000°C. Higher stresses were needed to form a rafted γ' structure. The stress dependence of γ-γ' microstructure should be taken into account for evaluation of long-term creep strength property.

Keywords: long-term creep, stress relaxation, microstructural evolution

Related Papers

1. H. Kushima, K, Kimura, K. Yagi, and K. Maruyama, "Long-term Creep Strength Property and Microstructural Stability of 12Cr Steel", *Tetsu-to-Hagane* (J. Iron and Steel Inst. Japan), 81(1995): 214–219: in Japanese.
2. H. Nagai, K. Kimura, F. Abe, and K. Yagi, "Effect of Stress on Morphology of γ'-phase and Creep Strength Properties of Inconel 713C", *Tetsu-to-Hagane* (J. Iron and Steel Inst. Japan), 81(1995): 667–672: in Japanese.
3. K. Kimura, H. Kushima, K. Yagi, and C. Tanaka, "Effects of Minor Alloying Elements on Inherent Creep Strength Properties of Ferritic Steels", *Tetsu-to-Hagane* (J. Iron and Steel Inst. Japan), 81(1995): 757–762: in Japanese.
4. K. Yagi and F. Abe, "Ageing and Life Prediction of Metallic Materials" *J. Japan Soc. for Simulation Technol.*, 15(1996): 3–13: in Japanese.

58 Toughness Improvement of Ceramics and Brittle Steels by Control of Precipitation and Phase Transformation

F. Abe, Environmental Performance Division

[April 1993 to March 1996]

The purpose of the present research is to investigate the microstructural evolution and to improve toughness by microstructural control for partially stabilized zirconia ceramics and neutron-irradiated martensitic steels.

The transformation behavior from tetragonal to monoclinic phase has been investigated for a ZrO_2-9.7mol%MgO by means of dilatometry and transmission electron microscopy. The transformation from the t- to the m-phase occurred in the two distinct stages during cooling; the low- and high-temperature stages at around 600 and 1100 K, respectively. The factors for control of the transformation were discussed by taking into account of the effect of diffusion-controlled microstructural evolution and trans-formation-induced microcracks. The effect of volume fraction of the constituent t- and m-phases on fracture toughness KIC has also been investigated for the ZrO2-9.7mol%MgO by indentation method. The volume fraction was changed from Vm = 0 to 1, where Vm is the volume fraction of the m-phase, by heat treatments at high temperature. The K_{IC} gradually increased from 4-5 MPa $\sqrt{m}$ at Vm = 0 to 7 MPa $\sqrt{m}$ at Vm = 1. It should be also noted that the K_{IC} was inversely proportional to the Vickers hardness, similar to metallic materials.

Keywords: toughness, zirconia ceramics, martensitic steel, phase transformation

Related Papers

1. F. Abe, S. Muneki and K. Yagi, "Control of Tetragonal/Monoclinic Transformation in a ZrO_2-9.7mol%MgO", *Proc. 4th Japan Intern. SAMPE Symp.*, (1995): 293–298.
2. S. Muneki, F. Abe and K. Yagi,"Effect of Heat Treatments on KIC of a MgO Partially Stabilized Zirconia", *Proc. 4th Japan Intern. SAMPE Symp.*, (1995): 446–451.
3. F. Abe, S. Muneki and K. Yagi, "Kinetics of Tetragonal to Monoclinic transformation and

Microstructural Evolution in a MgO Partially Stabilized Zirconia", *Fourth EURO Ceramics*, 2(1995): 399–406.
4. F. Abe and H. Kayano, "Evaluation of Embrittlement of Martensitic 9Cr-WVTa Steels by Instrumented Impact Testing Using 1/3 Size Specimens", *Proc. IEA/JUPITER Joint Symposium on Small Specimen Test Technologies for Fusion Research*, (1996): in press.

Measurement and evaluation

(59) Applicability of Photoaccoustic Spectroscopy Technique for Measurement of Thermal Diffusivity of Thermoelectric Materials

M. A. Okamoto, 5th laboratory, Physical Properties Division.
[April 1996 to March 1997]

Recently, photoaccoustic spectroscopy (PAS) has been applied to a wide field of industry and research. This technique is a quite simple and convenient one whose principle is mainly based on the characteristic of the magnitude of thermal diffusivity of the specimen material in the case of low frequency illumination. However, very few studies have been reported on that of thermoelectric materials, for which sensitivity of several percent is ordinarily required over a comparatively wide range of temperatures. On this view point, the present study aims to examine the applicability of the PAS technique how to get a reliable value of thermal diffusivity within the required error. Another merit of this technique is that the thermal characterization of the target material is expected to extend to the optical characterization at the same time using the same specimen.

The present study to be made employs a gass-microphone technique, and the experimental equipment consists of He-Ne laser (30mW), Xenon lamp (350W) and stainless PAS cell (0.5～1 cm3).

Keywords: thermal diffusivity, photoaccoustic spectroscopy, thermoelectric material

(60) Monitoring and Control of Thermal Plasma

K. Hiraoka, Advanced Materials Processing Division
[April 1996 to March 1999]

The aim of the new program is to analyze and control the state of thermal plasmas for the application to new materials processing. Arc discharge ,laser and their combination techniques are utilized. Two main subjects are summarized as follows.

(1) Formation of stable arc plasma under a reduced pressure atmosphere

Vaporization behavior and current density distribution on the melting anode surface will be analyzed in low pressure gas tungsten arcs. A high response monitoring method of the current distribution on the molten pool will be discussed on the basis of computer techniques and the measurement of the potential distribution of the anode plate. Furthermore, the states of metal vapors in the low pressure plasma will be analyzed from the spectroscopic measurements.

(2) Formation of stably controlled laser plasma. and its application to materials processing

We demonstrated in the previous work that a large and stably induced laser plasma can be formed by irradiating focused laser beam onto an arc plasma. The plasma stands still in space by absorbing laser power even if the arc is shut off. In the present program, we will investigate how to control the state of the plasma at various mixed gas atmospheres to apply it to a new chemical reaction plasma processing.

Keywords: arc discharge, laser, plasma, spectroscopy, probe measurement, vaporization, mixed gas

(61) Application of in-situ Strain Measurement by the Laser Speckle Method

Y. Muramatau, Advanced Materials Processing Division
[April 1996 to March 1999]

Non-contact strain measurement using the laser speckle method is characterized by its high-responsibility and high-accuracy. We have been examining its applicability to the in-situ strain measurement during local heating such as welding in thin stainless steel plates. We already proved in the previous research that it was possible to do the in-situ strain measurement for almost all period in a thermal cycle even if the measuring point was in a high temperature range.

In the new research, however, we have to clarify the strain behaviors in several parts of heating line, for examples, the starting point and the crater. To detect the strain behavior in the deposited zone or the heat affected zone should be

important for getting the information for the high and low temperature defects. We will also execute the measurement for those areas.

The peeling off of the sprayed coating films from the base materials by the thermal stress or strain is another subject in our research. Many strain curves in the surface of the base material were already detected by the laser speckle method. Some kinds of sprayed coating films will be selected and examined their specific characteristics of peeling off considering the strain curves obtained in the previous research.

Keywords: laser speckle method, dynamic strain, in-situ strain measurement, high temperature, austenitic stainless steel, plasma spraying, peeling off, coating film

(62) Development of Fundamental Technologies for Excited Neutral Beams

Y. Yamauchi, High Resolution Beam Research Station

[April 1996 to March 2003]

The electronic states of surfaces play significant roles in chemical reactions and crystal growths on surfaces of materials. The excited neutral beams are promising probes to get information from exactly outmost surfaces rather than electron or photon beams. Fundamental technologies to generate excited neutral beams are being developed.

In spite of the fact that photoelectron spectra or electron-excited secondary electron spectra include the information on the outmost layer, photons and electrons penetrate through the outmost layer and reach to more deeper layers. Those spectra contain the information on deeper layers where the ejected electrons are generated. Thus some ambiguity remains whether any features of spectra are originated from the outmost layer or the deeper layers. On the other hand excited neutrals also may release their internal energy to the surface electrons. The slow neutrals with a kinetic energy of several tens meV are reflected by the potential which comes from the surface atoms and never reach to the deeper layers. The ejected electrons pick up only the information on the electronic state outside of the top-most layer. Therefore slow excited neutrals are essentially sensitive to the electronic state of adsorbed molecules or states spatially extended wave function from the surface to the vacuum. Further the spin selected neutral beams enable us to understand surfaces more precisely.

The present project includes two kinds of technologies, i.e., generating techniques for excited neutral beams and detecting techniques for secondary particles ejected from irradiated surfaces. As regarding to the beam forming, a beam system creating high density neutral beams under a clean vacuum environment, exciting atoms by electron impacts, removing ions and high Rydberg atoms, selecting the velocities, and polarizing the electron spins of atoms is being developed. Means to measure the energy angular distribution and the spin polarization of ejected low energy electrons are also being investigated.

Keywords: neutral beam, metastable atom, excited neutral, surface

63 Study on Flat and Mirror-Finishing by Glow Discharge Plasma Using Rare Gas

M. Saito, Materials Physics Division

[April 1995 to march 1997]

It is very difficult to obtain the mirror-finishing surface for metals and semiconductors by the plasma-etching(dry-etching) technique, whereas their clean surfaces are easily prepared by this method. In order to overcome the difficulty of this technique, the gas mixtures consisting of the rare gases such as Ar/Ne, Ar/Kr and Ne/Kr was investigated.

The direct current glow discharge plasma was used in this study on steel samples. The surface roughness of the samples was measured with a surface profilmeter. The surface roughness obtained as Rmax =1μm by the Ar/1 vol. % Ne mixture was better than that obtained as Rmax=1.7μm by pure Ar. In addition, when the Kr/Ne mixture was used instead of the Ar/Ne mixture, the surface roughness(Rmax=0.7μm) was improved significantly compared with that of the Ar/Ne mixture. However, since the mirror-finishing less than Rmax=0.3μm by the above-mentioned gas mixtures is not developed yet, the other gas mixtures are investigated.

Keywords: Mirror-finishing, direct current glow discharge, mass spectrometry, rare gas

64 Improvement of Resolution in EPMA X-Ray Image

M. Fukamachi, Materials Physics Division

[April 1995 to March 1997]

EPMA is an instrument to reveal distribution of

chemical compositions in local surface area of solid specimen. The size of region producing characteristic X-ray by the irradiation of electron beam is of the order of micron meters. The spatial resolution of EPMA is taken as in the order of this size. In the analysis of EPMA, the identification of chemical compounds is one of the important application. In order to reveal the existence and to identify the compounds smaller than the probe size of electron beam, the computer image analysis was applied to analyze the relation among the chemical concentrations of elements in pixels composing X-ray image. The relation between concentrations of elements in each pixel are plotted. The patterns formed by the plotted data are analyzed to obtain the ratio of concentration among the elements. The ratio is compared with those of possible chemical compounds to identify the small compounds contained in pixels.

The method is applied to reveal the distribution of small inclusions in steel such as MnP and FeS with the electron-probe size 1μm~10μm. The compounds of the size from 1/10 to 1/30 of the region of X-ray generation are identified and their distributions on specimen surface are shown as a map.

65 Fundamental Study on Advanced Techniques of Physical Characterization of Metallic Materials and Their Application

R. Hasegawa, Materials Physics Division
[April 1994 to March 1996]

Advanced techniques and systems for the characterization of metallic materials by routine physical analysis are studied.

Electron probe microanalyzer (EPMA)

A data-analysis system based on computer image processing was established. Main component analysis of a Ti-Ni alloy was carried out to test the resolution of concentration of the system. Plane analysis, which can get a large amount of data at a time, was superior in precision and working time to the conventional spot analysis. The method was applied to the analysis of a Ti-Ni shape-memory alloy film made by sputtering. The concentration distribution of the main component elements was clarified over a large area (15 x 50 mm), as well as a relation between chemical compositions and preparation conditions of the films.

High resolution transmission electron microscope (HRTEM)

A digital high-resolution electron microscope system was constructed to observe atomic images of metallic materials. The system consists of a 200 kV transmission electron microscope, a series of camera system involving a lens, an imaging plate and a slow scan CCD and a PIX system for imaging plates. In order to prove the high-resolution of the system, the structure of the austenite-martensite phase interface of a 5% martensitic transformed Fe-Ni-Mn alloy was studied. An interface with well lattice fitting and few dislocations was found out for a fine martensite grain of about 30 μm long and 3μm wide.

Scanning electron microscope (SEM)

An automatic data-analysis system was built up to analyze the electron channeling pattern (ECP) images obtained with a scanning electron microscope. The system aims to be a powerful tool to analyze the crystal orientation of fine grains of scores μm in diameter. Degree of analysis was defined as the number of the measurements in which correct analysis was carried out. It reached above 90% for cubic crystals, but was not so high for tetragonal and hexagonal crystals. A data-input which involves the atomic positions in lattice coordinate is being examined to improve the ability of the system.

Keywords: EPMA, HRTEM, SEM

66 Research on the Development of Chemical Analysis and Characterization Techniques for Metallic Materials

R. Hasegawa, Materials Physics Division
[April 1994 to March 1997]

Taking account of the recent progress of metallic materials, studies were carried out on the expansion of the kinds of the elements to which instrumental analytical methods are applicable, as well as on the improvement of the detection limits and precision.

Elemental analysis I

(1) A direct determination procedure without matrix separation was established for trace Pb, Mn and Co in refractory metals (V, Nb and Hf) by graphite furnace atomic absorption spectrometry (GF-AAS). Detection limits of the procedure were 0.18 pg for Pb, 3 pg for Mn and 12 pg for Co.

(2) Fluoride separation-molybdosilisic acid blue spectrophotometry was applied to the determination of trace Si in high-purity aluminum.

When a sufficiently large amount of hydrofluoric acid was added, it was possible to detect sub- ppm silicon.

Elemental analysis II

(1) Simultaneous determination procedures of 17 trace impurity elements in titanium and those in titanium disilicide were established using inductively coupled plasma-atomic emission spectrometry (ICP-AES) after cation exchange separation.

(2) An extended torch was applied to end-on measurement in ICP-AES and a highly sensitive spectrometric method due to the significant decrease of background emission was established for the 24 elements which have emission lines in the range of 220 to 770 nm.

Solid analysis I

(1) In order to clarify the formation mechanism of the matrix ions (divalent, dimer and argide) which cause the spectral interference in glow discharge mass-spectrometry (GD-MS), 30 kinds of high-purity metals were discharged and ion beam intensities were measured.

(2) Total reflection X-ray fluorescence spectrometry (TR-XRF) was applied to the solution analysis of high purity copper. Using a solution from which copper had been removed by electrolysis, ng/g trace impurity elements were successfully determined.

Solid analysis II

Determination of trace oxygen in lead and solder by the inert-gas fusion method was studied. Optimum oxygen extraction conditions obtained for PbO and SnO_2 were unsatisfactory for the determination of trace oxygen in the metals.

Keywords: GF-AAS, ICP-AES, GD-MS, TR-XRF, Gas analysis

67 Modeling and Evaluation of Advanced Materials—A Coordinated Interlaboratory Research

S. Nishijima, Failure Physics Division

[April 1992 to March 1996]

This work aims at the development of models describing the behavior and properties of selected advanced materials of high performance. It covers also the establishment of rationalized test methods for advanced materials, as a part of the international research cooperation known as Versailles Project on Advanced Materials and Standards (VAMAS).

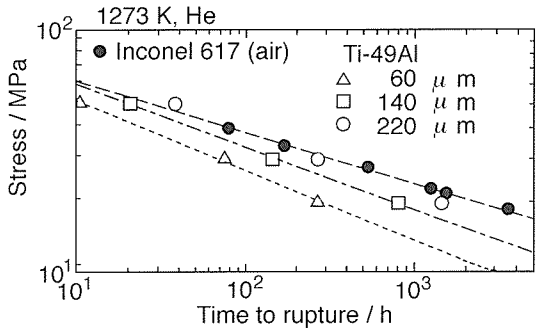

Fig. 1 Creep strength of Ti-49Al with different grain sizes, 60(△), 140(□), and 220(○) μm, respectively

The work is part of a big coordinated research project of the Science and Technology Agency. NRIM takes initiative with its 35 research staffs to harmonize the efforts of more than 50 other groups from industrial, university and national laboratories.

Intermetallic Compounds

Titanium aluminides are light-weight and heat-resisting material expected for space vehicle applications. Creep and fatigue behavior at elevated temperatures is important to be studied in detail.

Material was elaborated in NRIM, typically for a composition of Ti-49at%Al, and hot extruded to be a bar of 18mm in diameter. Creep rupture tests were conducted in pure He at 1273K for specimens with different grain sizes adjusted by heat treatments. It was found that the strength was higher for materials with larger grain sizes. Figure shows that the creep strength can be about the same with Inconel 617 when treated appropriately.

Similar researches are in progress on Metal Matrix Composites (MMC) in collaboration with Mitsubishi Heavy Industries and Tokyo University, in one hand, and on Ceramic Matrix Composites with Toshiba Corporation and Tokyo Institute of Technology, on the other hand.

International Project VAMAS

There are 16 Task Working Areas (TWA), spreading from metals, polymers and ceramics, and their composites, as well, to test methods and problems related to materials classification and data. NRIM offers international chairpersons for 3 TWAs respectively on: superconducting materials, cryogenic structural materials and materials property databases. Leading members are also from NRIM for 5 TWAs: method of evaluating MMC, method of creep crack growth test, method of low cycle fatigue test, method of surface chemical analysis, and method of mechanical evaluation of very thin films.

Keywords: advanced materials, property

evaluation, modeling, VAMAS project, interlaboratory testing

Related Papers

1. K. Hashimoto, S. Kajiwara, T. Kikuchi, and M. Nakamura, "Effect of Temperature on Tensile Properties of TiAl Base Alloys", *Scripta Metall. Mater.*, 32(1995): 417–422
2. Y. Yamauchi, N. Kishimoto, and T. Ikuta, "Nondestuructive Characterization of Materials VI", *Microtomography Using Conventional X-ray Sources*, eds. R.E. Green, Jr. et. al., (1994): 129, Plenum Press.

68 Fundamental Study for Electromagnetic Evaluation of Materials

I. Uetake, Failure Physics Division

[April 1994 to March 1997]

Flaws in structural materials decrease remarkably the materials strength. The detection of eventual flaws and material degradation is especially important for the security of important structures such as reactor pressure vessels and/or large constructions. In this study the basic phenomena of electromagnetic evaluation method is investigated.

In alternating magnetic flux leakage testing method, we clarified an evaluation technique by vector locus change which is described with amplitude and phase of magnetic flux leakage. This evaluation technique can detect flaws with higher accuracy than usual detection method using only signal amplitude. A magnitude of locus change part increases with an increase of flaw depth and the phase of peak point at the vector locus change has lag with an increase of magnetization frequency. The application of high frequency magnetization field makes it difficult for magnetic flux to penetrate into material, therefore the magnetic flux concentrates on the surface of material. It was also confirmed that the dependency of magnetization frequency on magnetic flux leakage is large in a shallow flaw but small in a deep flaw.

Keywords: non-destructive evaluation, materials evaluation, electromagnetic method, magnetic flux leakage testing, surface flaw

69 Nanoscopic Materials Damage Evaluation

S. Matsuoka, Environmental Performance Division

[April 1994 to March 1996]

It is important to examine the materials damage in the vicinity of crack tip or grain boundary to improve the reliability of structural materials. Recently, the damage in small-size structural components has also become a subject of much concern, as seen from an example of the stress- or electro-migration for aluminum thin-film conductors in the technology of integrated circuits.

This research has been conducted to develop the materials damage evaluation technique in the nanoscopic region. The damage of metallic materials such as fatigue and creep, including the stress- and electro-migration for aluminum thin-film conductors, is investigated by a scanning tunneling microscope (STM) and atomic force microscope (AFM) which has two excellent abilities of atomic-scale imaging and nano-

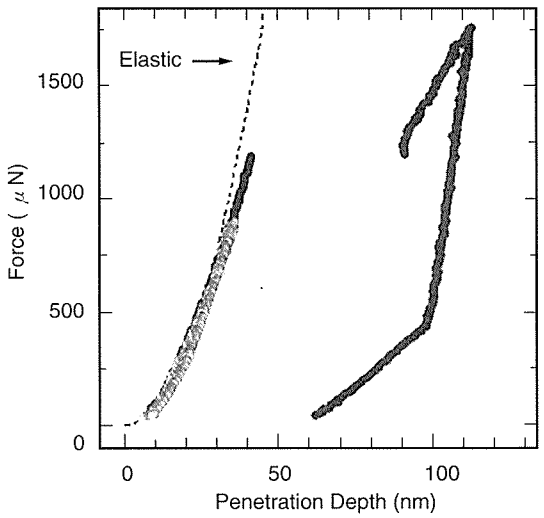

Fig. 1 Force-penetration depth curve on (001) plane of tungsten single cristal.
(a) Electrochemically polished surface

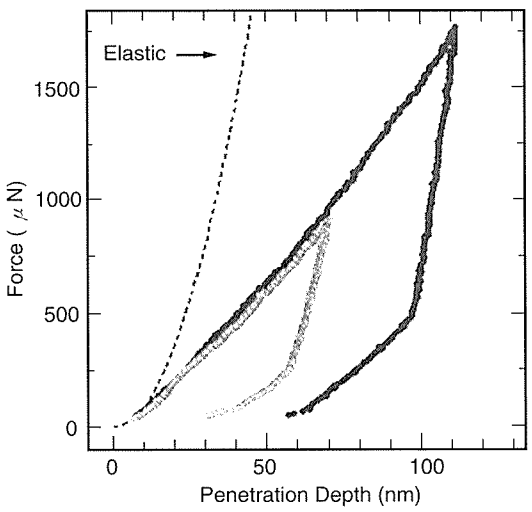

Fig. 1 Force-penetration depth curve on (001) plane of tungsten single cristal.
(b) Alumina polished surface

fabricating. On the basis of AFM, in particular, a nano-indentation method is developed to measure the elastic modulus, yield stress and hardness ahead of the crack tip or on the surface of thin films.

In the resent year, nanoindentaion tests were conducted for a tungsten single crystal, using AFM ultra-micro hardness measurement tester which has been developed by ourselves. Figure 1 shows force-penetration depth curves on (001) plane of tungsten. The solid curve in the figure is the elastic force-penetration depth curve calculated by FEM. For the specimen surface electro-chemically polished(Fig. 1(a)), the experiment showed the elastic behavior at the lower force and coincided to the calculation. The pop-in which corresponds to the upper and lower yield phenomenon in the BCC metal and the plastic behavior occurred at the higher force. Finally, the residual penetration depth from which the hardness is determined remained at the fully unloading. For the specimen surface polished by alumina particles (Fig. 1(b)), on the other hands, the pop-in behavior disappeared and the relevant yield force drastically decreased. This is because the compressive residual stress is introduced during alumina-polishing.

Keywords: materials damage, STM, AFM, molecular dynamics

70 Chemical Analysis of Organotin in Marine Environmental Samples

H. Okochi, Team of Director of Special Research
[April 1991 to March 1997]

The solid phase extraction(SPE) for sediment samples have been systematically investigated. The recoveries of tributyltin(TBT) and triphenyltin(TPT) were better in 0.12 M HCl, while those of dibutyltin(DBT) and diphenyltin(DPT) were better in 1.20 M. The recoveries were compared between the SPE using 0.6 M hydrochloric acid(HCl) / 40 ml methanol(MeOH) / 60 ml H_2O and the SPE at first with 0.12 M HCl / 40 ml MeOH / 60 ml H_2O and then with the effluent readjusted at 1.2 M HCl. The intensity (cps) ratios by measuring with micellar liquid chromatography / ICP mass spectrometry (MLC / ICP-MS) were as follows : TPT ; 14,579 / 15,726, TBT ; 11,612 / 11,970, DPT ; 241 / 1,670, DBT ; 1,315 / 6,465. The recovery of Organotin compounds(OTCs) decreased with the increase of the drying time by Ar flow in SPE. When using 100 % MeOH for eluting OTCs, the content of MeOH in the eluate became ca.85 % at 1 min drying time. When evaporating, 100 % MeOH gave poor recoveries while 85 % MeOH gave better recoveries. The temperature control at 35 ℃ is very important at evaporation.

The optimum conditions for extracting OTCs from sediments have been investigated. When extracting with MeOH, the addition of HCl was not adequate for TBT, while it gave better recoveries for DBT. Accordingly, a two steps extracting procedure was selected as follows ; Take 0.5 g or 1.0 g of a sediment(dry). Add 20 ml of MeOH and shake for 60min and then centrifuge for 45 min using a high speed cooling centrifuge. Then add 20 ml of MeOH and 2 ml of 12 M HCl and repeat the same procedure. The recovery tests were TBT(97 %), TPT(98), DBT(92) and DPT(91).

The SPE of TBT and TPT in shellfish samples has been also established. The interference of the lipid in OTCs extracts could be removed without a clean-up procedure by changing it to micelle with tris(hydroxymethyl)aminomethane dodecylsulfate(TDS) and SPE at pH 10±0.25. The recoveries of TBT and TPT were ca.96～97 %. The NIES SRM No.11 "*fish tissue*" was analyzed by the established procedure, that is SPE / MLC/ ICP-MS.

Atomic absorption spectrometry(AAS) of OTCs was comparatively studied among AAS, hydride generation AAS and graphite furnace(GF)-AAS without changing to inorganic tin. In GF-AAS the stabilized temperature platform furnace technique was applied with Ni matrix modifier.

Keywords: organotin, solid phase extraction, sediment, shellfish, LC /ICP-MS, GF-AAS

Related Paper

1. K. Sato, M. Kohri, and H. Okochi, "The speciation of organotin compounds in sea water by miceller liquid chromatography/ICP-MS", *Bunseki Kagaku*, 44(1995): 561–568.

71 Understanding of the Mechanism of High Temperature Superconductivity

K. Hirata, 1st Research Group
[April 1995 to March 2000]

Discovery of the high temperature superconductors(HTS) has stimulated the fundamental physics to understand the superconductivity and the electronic state of their normal state, as they have higher critical temperatures and the superconductivity happens in the oxide materials. The BCS theory could explain well the superconductivity in the conventional metal or intermetallic superconductors by the phonon-

electron interaction. Extending the BCS theory, or, considering the non-phonon interaction theory, many models to explain the superconductivity have been proposed such as RVB(resonating valence bonds) model, antiferromagnetic spin fluctuation model, bi-polaron model, charge fluctuation model, etc.. At the beginning, the reliable experimental results were not always obtained so that many kinds of models were proposed. Recently, high quality single crystals have been grown and the reliable data have been accumulated by measuring the samples with the matured handling and techniques. Understanding of the superconducting and the normal state of the HTS has been progressed. For example, the normal state of the HTS has been found to be a anomalous metal state with the separation of spin and charge measured by the high-resolution angle-resolved photoemission, the voltage-current characteristics and Raman spectroscopy. The symmetry of the superconducting gap has been found to be d-wave symmetry by the angle-resolved photoemission study, tri-crystal Josephson junction measurement and the nuclear magnetic resonance study. From these results, the proposed models have been selected. One of the purposes of this research is to understand the mechanism of the superconductivity.

The other aim of this research is to understand the characteristic phenomena observed in the HTS in a magnetic and an electric field, which mainly come from their layered structures, composed of the superconducting CuO_2 layers sandwiched with the insulating or less-conductive layers. The electrons or holes are confined into a quasi-two-dimensional state, which causes the electronic state to be anisotropic. The Josephson effect has been found as an intrinsic nature of these materials in the voltage-current characteristics. The magnetic phase diagram of the HTS shows also quite different features from those of the conventional superconductors. Understanding these characteristics and analyzing them, the new functional devices will be proposed.

Keywords: high temperature superconductors, mechanism of superconductivity, magnetic & electronic properties

72 Study on the Vortex Pinning Mechanism in High Temperature Superconductors

K. Hirata, 1st Research Group

[April 1995 to March 2000]

Physical properties of high temperature superconductors(HTS) have been studied intensively after the discovery of HTS. The distinct features of these materials have been recognized, compared with the conventional metal or intermetallic superconductors such as high critical temperature, high critical current density, high upper critical magnetic field. For the application of these materials, it is really essential to use these materials at liquid nitrogen temperature 77K. However, the high upper critical current density, for example, is reduced under a magnetic field, and is decreased to become comparable to the value of the conventional superconductors at 77K. Superiority to the conventional superconductors can be found in using these materials only at liquid He temperature. The reason is that there have been found no pinning centers to be effective at 77K or higher temperatures, on one hand. But, on the other hand, most of the obstacles come from the nature of the HTS themselves, for example, two-dimensional electronic state, large anisotropy, short coherence length, etc. Therefore, it is of necessity for the application of the HTS to understand the physical properties of the HTS single crystals.

This research program aims to introduce the effective pinning centers by understanding the pinning mechanism in these superconductors. First of all, we have to know the intrinsic properties of high quality single crystals; magnetic and electronic properties. We will develop our crystal growth techniques with various methods. Based on the fundamental study on the high quality single crystal, we will introduce the pinning centers, artificially, such as defects (dislocations, columnar defects by ion irradiation, other phase, etc.), impurity, and so on. The influence of these defects to the pinning will be understood experimentally as a function of the number of defects, the defect structure, temperature, magnetic field, etc. and will be analyzed theoretically. From these results, we will find the key parameters for the effective pinning, and the pinning centers will be applied in a real system.

Keywords: high temperature superconductors, vortex pinning,vortex dynamics

73 In-situ TEM Observation and Structural Analysis of High Tc Superconductors for Fusion Reactor at Low Temperature

T. Kimoto, 1st Research Group

[April 1994 to March 1999]

Few principles for the development of high Tc superconductors for fusion reactors have been found because the mechanism of their superconduction has not been understood so far. The image resolution limit of a transmitted electron microscope (TEM) is extremely low at low temperatures because of specimen drift due to unstable temperature control and specimen vibration due to the evaporation of liquid helium. The first objective of our research is to improve the resolution limit of TEM imaging at low temperatures in order to observe O and Cu atoms in high Tc superconductors near or above Tc where abnormal lattice distortion occurs which could reveal the mechanisms of their superconduction. The other objective is to develop the method to examine the LRO parameter in the microscopic region of high Tc superconductors and the analytical method to measure the abnormal lattice distortion from the convergent beam electron diffraction (CBED) pattern.

In 1995, the improvement of TEM imaging at low temperature was tried by the short-time imaging with the high-speed CCD camera system with microchannel plate (MCP) which was developed for the first time in the world in 1994. The shortest exposure time in the high-speed CCD camera system is 50 nano-sec. We used the TEM imaging of lattice image of (Bi, Pb)$_2$Sr$_2$Ca$_2$Cu$_3$O$_{10}$ (Bi2223) for this trial. It was found that the single snapshot of short-time imaging is effective to some extent for the improvement of TEM imaging at low temperature in the case of slow specimen drift and specimen vibration. As expected, however, the reduction of signal and noise (S/N) ratio due to the smaller number of electrons for imaging prevents us from getting a image of clear contrast.

To resolve the problem of the reduction of S/N ratio, the hardware or computer system for the special image processing of "shift and addition" of many short-time exposed images taken continuously was developed in 1995. The computer is sun SPARCstation 20 model 514MP whose main memory is 384 MB. The combination of the developed computer system and the high-speed CCD camera system enable us to take continuous snapshot of TEM imaging at the speed of about 5 frames / sec to the maximum number of 160 frames for the 2.1 MB image data. The software for the special image processing of "shift and addition" will be developed in 1996.

It was found from the analysis of CBED pattern that the abnormal temperature dependence of lattice constant occurs at the temperature range of 200 - 230 K in a single crystal of Bi$_2$Sr$_2$CaCu$_2$O$_8$ (Bi2212). The same abnormal temperature dependence of (115) lattice spacing at 200 - 230 K in the Bi2212 was observed in the X-ray diffraction experiment. Since it was confirmed by the high resolution TEM imaging at room temperature that the Bi2223 single crystal has a good crystal structure with few lattice defects, the observed temperature dependence of lattice constant (or abnormal lattice distortion) at 200 - 230 K is thought to be the essential phenomenon for Bi2212.

Keywords: resolution limit of TEM at low temperature,high Tc superconductors, short-time TEM imaging, MCP, CCD camera, signal and noise (S/N) ratio, single snapshot, continuous snapshot, image processing of "shift and addition"

74 Study on Deformation and Fracture of Materials under Irradiation

J. Nagakawa, 2nd Research Group

[April 1993 to March 1998]

Changes in mechanical properties induced by the irradiation with energetic particles are critically important for the structural materials of nuclear application. It influences significantly the endurance of structural components. In this research project, deformation and fracture of materials under irradiation has been studied experimentally and theoretically. During the fiscal year 1995, the following research activities were accomplished.

The synergistic stress/strain loading of alternate and constant type, associated with start-up/shutdown and steady operation, respectively, under irradiation is characteristic of the nuclear reactor materials. In-beam experimental apparatus and technique to study the material's response to such a condition have been developed in the present research project. In 1995, equipment for ion-beam control and monitoring has been completed. The whole system was connected to the NRIM compact cyclotron accelerator and a series of preliminary irradiation testing have been carried out. In the course of this trials, it was realized that the strain measurement range for the high sensitivity mode was too small, i.e., about 0.4 mm, for austenitic steel samples that deform to a rather large amount. An innovative mechanism consisting of two high sensitivity LVDT's and a computer for control was developed, which can cover a very wide strain range of more than10 mm without sacrificing its high sensitivity.

Nuclear reaction products like helium are expected to be introduced abundantly in the fusion reactor materials under 14MeV neutron

irradiation.Helium atoms were implanted in Fe-25%Ni-15%Cr austenitic steel using cyclotron at 650°C to 50 atomic ppm. A newly installed PEELS was used to examine the microstructure of this alloy, and helium was detected in tiny cavities of about 40 nm in diameter. These cavities, or helium-filled "bubbles", especially those formed at the grain boundaries are believed to influence the fracture properties by deteriorating the coalescence of neighboring grains or by initiating a crack.

Keywords: irradiation, radiation damage, deformation, fracture

75 Fundamental Research on Flexible Structure and Machine Systems Using Advanced Materials

N. Shinya, 5th Research Group
[April 1995 to March 1997]

In order to realize flexible structures and machines which have abilities to respond to environmental changes, it is necessary to develop advanced materials provided with the functions of sensors and actuators. For manifestation of the multi-function in advanced materials, utilization of peculiar functions of interfaces in materials is very useful. In this work fabrication and measurement techniques of artificial material interfaces are developed, and properties of various artificially-fabricated interfaces are evaluated.

Powder particle manipulation technique

For the preparation of the artificial interfaces, powder particle manipulation techniques using a microprobe are being studied. By controlling voltage of about 10V between a tungsten microprobe and a metallic substrate, powder particles can be easily absorbed to and desorbed from the probe. Moreover, by applying high voltage of 10kV, powder particles can be welded onto the substrate and other powder particles. Using these techniques, devices for measurements of interface properties are being fabricated.

Measurements of interface properties

It is well known that the Shottky effect is found at interfaces between metals and semiconductors. The so-called Shottky effect can be used for manifestation of the current-voltage characteristic of varistors. For the purpose of a new type varistor development, the current-voltage characteristic at interface between a gold particle and a polypyrrole (a conductive polymer) was measured. The measured non-linear current-voltage relation suggested that the interfaces between metals and conductive polymers can be used for superior varistors.

Keywords: interface, particle manipulation, multi-function

76 Development of Analytical Techniques for Characterization of Nuclear Materials Using New Generation Synchrotron X-Rays

K. Sakurai, High Resolution Beam Research Station
[April 1993 to March 1997]

The new synchrotron radiation (SR) facility, SPring-8 is scheduled to provide the first light in 1997. The brightness in X-ray region will be highest in the world, and therefore, scientists will be able to study new phenomena which have not been observed so far because of the faint signals. Another benefit from the SPring-8 is high energy X-rays, typically, 40-100 keV, where any other appropriate X-ray source has not been available. Both features of new synchrotron radiation are very attractive from a view of materials characterization.

Chemical state analysis of small quantity specimen by fluorescence detection of absorption edge shifts using a total reflection support. (Use of collimated strong X-rays)

The position of the absorption edges, which are the minimum energy to excite inner shell electrons, is slightly affected by the chemical environment. We developed a technique for chemical state analysis based on the measurement of the edge shifts by X-ray fluorescence detection using SR at the Photon Factory, KEK. One of the most important advantages is high sensitivity, and chemical state of trace metals in the order of ppm or ng in the solid can be analyzed. The extension of the technique to small quantity specimen like a liquid drop is also important. In the present study, a total reflection mirror (Si wafer) is employed as a sample support to reduce the scattering background further. The oxidation numbers of trace metals (1 ~ 5mM, Fe, Se etc.) in a liquid drop (3μl) have been successfully determined under the total reflection condition. Further sensitivity improvement and industrial/biomedical application are future task using strong photon flux from the SPring-8.

High energy X-ray fluorescence analysis (Use of high energy X-rays)

X-ray fluorescence analysis of heavy metals with high energy K lines is very promising. In the present study, the signal to background ratio has been studied in detail, and we have found that quasi-monochromatization of the primary X-rays is effective to improve the detection limit.

Keywords: synchrotron radiation, chemical state analysis, X-ray fluorescence, materials characterization

Related Paper

1. M. Harada and K. Sakurai, "Narrow pulse shaping for high-counting-rate X-ray measure-ments", *Rev. Sci. Instrum.*, 67(1996): 615.

77 Development for Unification System of Materials Scientific Database for Materials Properties Prediction

M. Nihei, Computational Materials Science Division

[Apr. 1995 to Mar. 2000]

Researches with a view of developing new evaluation technologies of materials through the utilization of the materials scientific databases are being conducted. For this purpose, the prototype of the new unification system utilizing a networking environment and treating many different type of materials scientific database, which are on many different sites bound with network systems such as INTERNET, is developed.

It is well known that there are many different types of materials scientific databases such as fact data, visual data, equations and knowledge data. Therefore the mutual utilization of these materials scientific databases is considered to be difficult in general. On the other hand, it was already found in the previous research that the empirical systematization approach based on the combining the scientific and empirical understanding using the materials strength database was powerful tools for the fatigue life prediction of many heat treated structural steels. To extend this approach for the other materials properties, more different types of scientific database will be needed.

This research has an aim to solve this problem of the mutual utilization of scientific data through the development of the new unification system of materials scientific database. In this year, the development of the prototype system for the unification was conducted. Figure 1 shows the

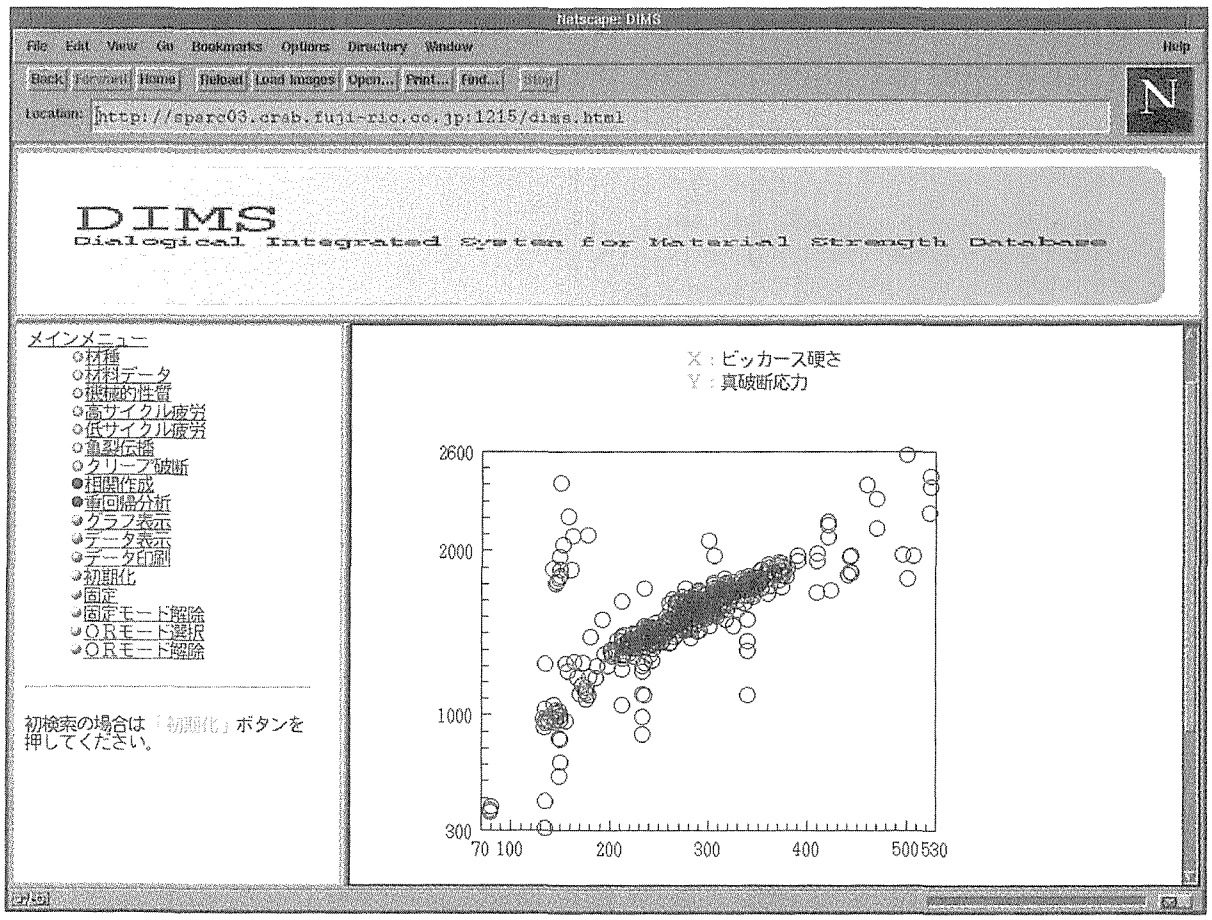

Fig. 1

X-ray fluorescence analysis of heavy metals with high energy K lines is very promising. In the present study, the signal to background ratio has been studied in detail, and we have found that quasi-monochromatization of the primary X-rays is effective to improve the detection limit.

Keywords: synchrotron radiation, chemical state analysis, X-ray fluorescence, materials characterization

Related Paper

1. M. Harada and K. Sakurai, "Narrow pulse shaping for high-counting-rate X-ray measure-ments", *Rev. Sci. Instrum.*, 67(1996): 615.

77 Development for Unification System of Materials Scientific Database for Materials Properties Prediction

M. Nihei, Computational Materials Science Division

[Apr. 1995 to Mar. 2000]

Researches with a view of developing new evaluation technologies of materials through the utilization of the materials scientific databases are being conducted. For this purpose, the prototype of the new unification system utilizing a networking environment and treating many different type of materials scientific database, which are on many different sites bound with network systems such as INTERNET, is developed.

It is well known that there are many different types of materials scientific databases such as fact data, visual data, equations and knowledge data. Therefore the mutual utilization of these materials scientific databases is considered to be difficult in general. On the other hand, it was already found in the previous research that the empirical systematization approach based on the combining the scientific and empirical understanding using the materials strength database was powerful tools for the fatigue life prediction of many heat treated structural steels. To extend this approach for the other materials properties, more different types of scientific database will be needed.

This research has an aim to solve this problem of the mutual utilization of scientific data through the development of the new unification system of materials scientific database. In this year, the development of the prototype system for the unification was conducted. Figure 1 shows the

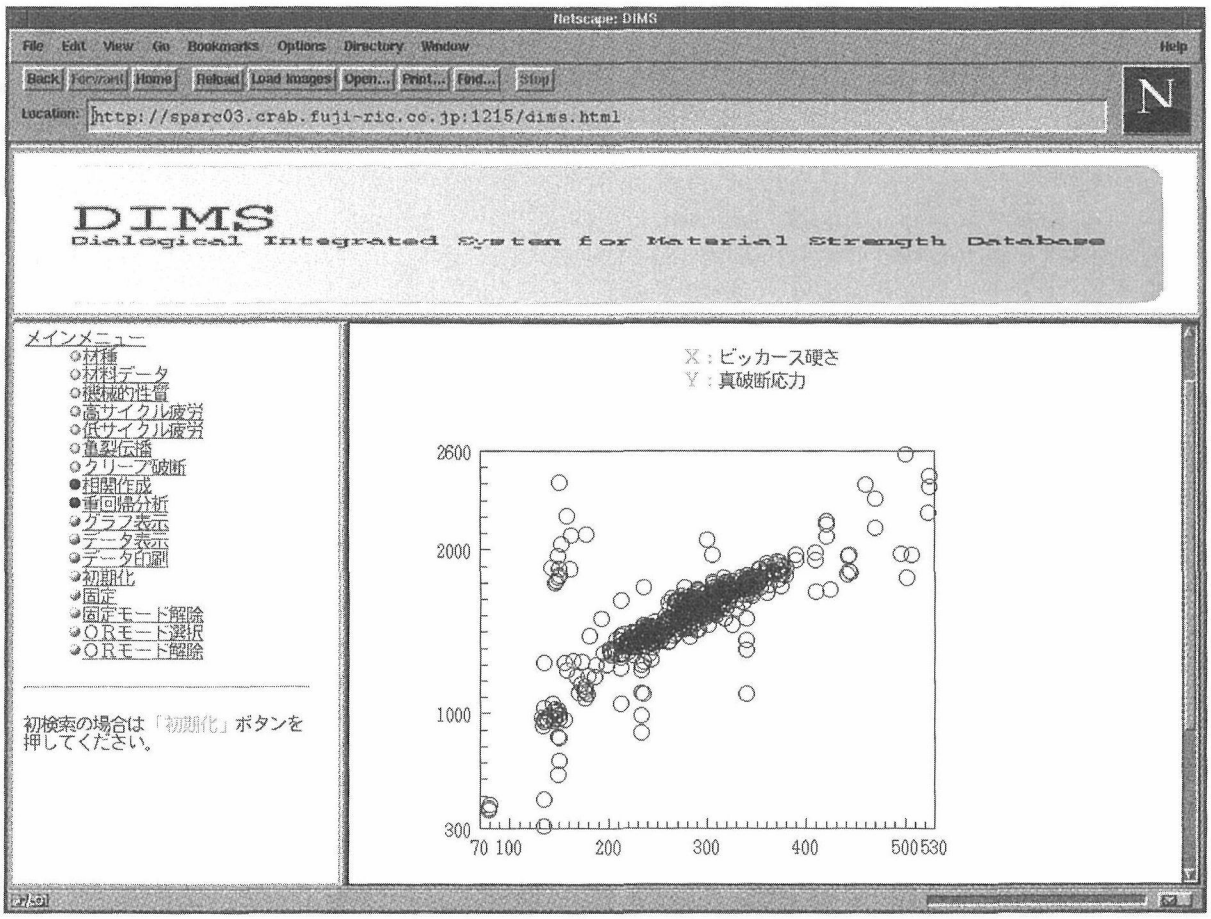

Fig. 1

operating image of the developed system through the LAN environment. The systematization approach using this developed unification system is also being conducted for the time-dependent creep rupture properties for heat resistant steels.

Keywords: materials properties prediction, database, networking

78 Study on Detection and Evaluation of Radiation Damages in Extreme Particle Fields

N. Kishimoto, High Resolution Beam Research Station

[April 1992 to March 1999]

Hybrid particle fields of ion and photon exert strong interactions with materials and are potent not only to detect elementary processes but to explore novel properties of materials. Especially if both high energy and high density of ion and photon are attained, unexplored non-equilibrium effects will be expected, by virtue of their contrasting effects of momentum, energy, excitation modes. The extreme particle field is also an important aspect for practical environments of high energy devices, such as fusion reactors, MHD generators etc. The main purpose of this research program is to detect and evaluate non-equilibrium processes of materials in the extreme particle fields, associated with radiation damage.

The key technology to attain the extreme ion field has been an ion injector of high current and low emittance, particularly the negative ion source for the tandem acceleration. A high-current negative ion injector of plasma-sputter type has been successfully developed and ion currents of 3 mA have become available for Cu, Ni, Si and C at a sufficiently low emittance. After optimizing the beam characteristics, we are moving on to the next phase of MeV acceleration, that is, construction of tandem accelerating tubes, a Schenkel-type voltage multiplier, a switching magnet, an SF_6 tank etc. Of the technological issues, the most important at present is control of the space charge effects, from the injector to the accelerating tube. After analyzing the beam optics, a lens effect of the accelerator tube has turned out to be important and a device of potential adjustment was installed. As compared to the ordinary machines, not only the power supply was significantly intensified but also the diameter of accelerating tubes and the divider current were enlarged.

The generator of extreme particle fields has thus arrived at the important milestone and the next step is the beam line and the in-situ characterization system in F.Y. 1996.

Keywords: extreme particle field, high current, negative ion source, in-situ measurement

Related Papers

1. N. Kishimoto, H. Amekura, and T. Saito, "Resonant Creep Enhancement of Austenitic Stainless Steels Due to Pulsed Irradiation at Low Doses", *Fusion Eng. & Design*, 29(1995): 391.
2. H. Amekura, N. Kishimoto, and T. Saito, "Photoconductivity Evolution Due to Carrier Trapping by Defects in 17 MeV Proton Irradiated Silicon", *J. Nucl. Mater.*, 77(1995): 4984.

79 Thermal and Electrical Properties of II–IV and V–VI Thermoelectric Semiconductors

I. A. Nishida, Physical Properties Division

[April 1993 to March 1996]

Thermoelectric(TE) materials have been widely used for the direct energy conversion systems. These materials convert thermal energy to electric power with quick response and without noise and mechanical vibration. Recently, the thermoelectric generators are mainly used for the electric source in the sea, space, and polar regions, and the thermoelectric cooling systems are mainly used for the precise temperature control in the semiconductor processing, optical and electronic devices. Therefore, it is important to develop TE materials with high efficiency.

The TE materials with high efficiency are given by the three characteristic, i.e., high thermoelectric power α, high electric conductivity σ and low thermal conductivity κ. For the TE materials with very low values of κ, such as the case of $Bi_{2-x}Sb_xTe_{3-y}Se_y$, $Pb_{1-x}Sn_xTe$ and $Mg_2Sn_{1-x}Ge_x$, it is very difficult to obtain the reliable value of κ, which is necessary for developing TE materials.

In this study, a technique for the precise measurement of κ was established by means of the static comparative method, and the details of measurement and analytical method for PAS(Photo Acoustic Spectroscopy) were explained.

Keywords: thermal conductivity, thermoelectric property, energy conversion, $Bi_{2-x}Sb_xTe_{3-y}Se_y$, $Pb_{1-x}Sn_xTe$, $Mg_2Sn_{1-x}Ge_x$

Related Papers

1. H. T. Kaibe, Y. Tanaka, M. Sakata, and I. A. Nishida, "Anisotropic Galvanomagnetic and Thermoelectric Properties of *n*-Type Bi_2Te_3

Single Crystal with the Composition of a Useful Thermoelectric Cooling Material", *J. Phys. Chem. Solids*, 50(1989): 945–950.
2. Y. Noda, T. Sugawa, I. A. Nishida, and K. Masumoto, "Preparation and Thermoelectric Properties of $Mg_2Sn_{1-x}Ge_x$", *Proc. 12th Int'l. Conf. Thermoelectrics, Yokohama, Japan*, November (1993): 142–144.

80 Energy Conversion Materials Fabricated with Functionally Graded Structure

I. A. Nishida, Physical Properties Division
[April 1993 to March 1996]

Thermoelectric(TE) materials have been widely used for the purpose of direct conversion of thermal energy to electric power without noise and mechanical vibration. For a given TE material system with homogeneous carrier concentration, the optimized figure of merit Z can be obtained only in a narrow temperature range. The TE conversion efficiency η has been comparatively small. Temperature range for the optimized Z can be shifted by changing the carrier concentration. The larger value of η will be obtained if the TE material has the continuous change of carrier concentration along the thermocouple leg, i.e., functionally graded material(FGM). The effective value of η is estimated to be more than 2 times lager at a temperature difference of 1000K. In addition, Z can be increased by controlling the composition and the grain size of FGM, because the lattice contribution to thermal conductivity can be decreased by phonon scattering at the lattice defects such as crystal distortion and grain boundary.

An effective maximum power for the three layered FGM of n-type PbTe with different electron concentrations was found to be larger by 11% than one for the optimized homogeneous material.

Keywords: energy conversion, thermoelectric materials, functionally graded materials(FGM)

Related Paper

1. I. A. Nishida, "Highly Efficient Thermoelectric Materials in FGM Program", *Proc. Japan-Russia-Ukraine Int'l. Workshop on Energy Conv. Materials(ENCOM 95)*, Sendai, Japan, January (1995): 1–10.

81 Self-Organizing Information-Base System Used for Creative Research and Development

K. Hoshimoto, Materials Design Division
[April 1992 to March 1996]

In the domain of metals and alloys one can never find any two species that have precisely identical internal structure even if the chemical composition and outer shape are the same; which means that one can not specify the object exactly in the database of materials properties. Therefore the specification of materials has inevitably somewhat ambiguity. Specialists create new materials by combining basic theories, factual data and qualitative knowledge with their full skill and experiences, while the information on materials today is increasing day by day beyond the quantity which one person can deal with. To support researchers working in such a tangled world, an information base system that supports constructions and exploration of an space in metallurgy was implemented. Information about materials development inevitably includes ambiguities because, in most cases, it is obtained empirically. Use of natural language is, therefore, important to transmit materials information. The developed system interprets technical papers on metallurgy and constructs information space semi-automatically. It consists of two sub-systems which are called METIS(METallugy papers Intelligent Surveyors) and KE(Knowledge Editor) respectively. METIS adopts a naive natural language processing, and KE adopts both syntactic and semantic analysis technologies. In the system domain knowledge is represented using an instance-oriented and script-based method.

The heart of METIS is a packet of domain specific knowledge called KP(Knowledge Pieces) in which procedures for extracting and structuring technological information are embedded. They have four principal facilities, i.e., to select sentences, to extract features, to structure information by merge and to structure information by intersection. METIS extracts technological information from technical papers on metallurgy written in a mark-up language, by a naive natural language processing specified by keywords or key phrases embedded in KPs which are classified into various categories in materials development such as alloys, test procedures, materials processing, materials properties, etc.. Product of METIS is a variety of summaries and surveys such as structured technical summary, as well as visualization of similarities, differences of relevant papers, and cause-effect relations.

There are difficulties in construction of information space from natural-language texts and much more efforts are required to understand extracted information that can be retrieved from conventional system by keyword matching with full text. KE enables to construct information

space semi-automatically by semantically understanding the contents of articles and facilitates to provide the retrieved information by semantic analysis of queries. KE represents knowledge on metallurgy by a set of objects together with a set of relations between them. It also supports detection of unknown objects in papers and enables them to be stored into information space by communicating with users. KE provides two interactive facilities for exploring into information space; one is the natural language query based on semantic understanding and the other is the navigation of the relations between objects.

It was found, through experiments, that the system could be applied to other research domain(s).

Keywords: self-organizing, information-base, materials design, dictionary, knowledge converter

Related Paper

1. K. Hoshimoto, "Development of a Knowledge Base System for Computer-Assisted Alloy Design", Advanced Materials '93, III, *Proceedings of the Symposium of the 3rd IUMRS Int. Conf. on Advanced Materials*, Tokyo, (1993): 173–176.

82 A Comparative Study of Nanostructure Characterization Techniques

K. Hono, 3rd Research Group

[April 1995 to March 1996]

There is an increasing interest in synthesizing nanostructured materials in anticipation of the appearance of novel properties which arise by the reduction of the physical dimensions of microstructural features such as grain size, various phase domains and precipitate particles. Recent examples nanostructured materials include nanocrystalline soft and hard magnets, granular magnetic materials, and ultrahigh strength nanocomposite aluminum alloys. These examples indicate that the synthesis of nanostructured alloys can lead to the development of new materials with unconventional magnetic, electric and structural properties.

In order to understand the mechanisms involved in the emergence of the novel properties from the nanocrystalline microstructures, it is essential to characterize the microstructures in less than a nanometer resolution. The microstructural characterizations of metallic materials are performed mainly by transmission electron microscopy, electron and x-ray diffraction methods. These techniques are effective to determine the crystal structure and grain sizes. However, nanoscale quantitative analysis of local chemical compositions has been inaccessible by these conventional techniques. In particular, it is extremely important to measure the local chemical concentration changes of light elements in less than a nanometer scale resolution for understanding the microstructures of nanocrystalline magnetic materials. The conventional analytical methods, such as analytical electron microscope, has a significant drawback in detecting light elements quantitatively. An atom probe field ion microscope (APFIM) is an combination of field ion microscope and a time-of-flight mass spectrometer with a single atom detection capability. It can determine the chemical compositions of alloys with an atomic resolution. Furthermore, recent development of three dimensional atom probe (3DAP) made it possible to visualize individual atoms in a three dimensional real space with an extremely high spatial resolution (<0.2 nm). By employing both APFIM and 3DAP, it will be possible to visualize behaviors of alloying elements during the microstructure evolution in an atomic spatial resolution. However, the atom probe technique lacks ability to determine crystal structures. It is therefore strongly desired that various advance microanalytical tools are used complementarily for characterizing critical microstructures of metallic materials in less than a subnanometer resolution.

For this purpose, the most advanced microstructural characterization techniques available at the National Research Institute for Metals were employed for nanostructure characterizations of some selected metallic materials. For structure analysis, high resolution electron microscopy (HREM) and x-ray diffraction have been used. Small angle x-ray and neutron scattering (SAXS and SANS) have been employed for characterizing dimensions of nanoscale heterogeneities in materials. For analysis of local chemical concentration changes, modern electron microscopes with an energy dispersive x-ray spectroscope (EDXS) and an electron energy loss spectroscope (EELS), APFIM, and 3DAP have been utilized. In order to elucidate the role of minor solute additives, extended x-ray absorption fine structure (EXAFS) analysis and APFIM have been performed. Based on these results, comprehensive discussions on the mechanisms of the nanoscale microstructure evolution have been made for better understandings of the mechanisms of nanostructure evolution.

Keywords: atom probe, transmission electron microscope, small angle scattering, APFIM, TEM,

HREM, SAXS, SANS, nanostructure, microstructure, phase transformations

Related Papers

1. K. Hono, E. Abe, T. Kumagai, and H. Harada, "Mechanism of ultrafine lamellar structure formation in Ti-48at.%Al alloy", *Scripta Mater*, 35(1996): 495–499.
2. K. Hono, Y. Zhang, A. Inoue, and T. Sakurai, "APFIM studies of nanocrystallizations of amorphous alloys", *MRS Proceedings*, 400(1995): 203–208.
3. K. Hono, "Subnanometer scale microstructural characterization by a three dimensional atom probe", *Materia Japan*, 35(1996): 267–274.

83 Correlation between Plasma Parameters and Evaporation in Free-Burning Arcs

K. Hiraoka, Advanced Materials Processing Division

[April 1993 to March 1996]

Main results of this program had been shown in NRIM Research Activities 1994 and 1995. In this report, firstly, temperature distributions in argon arcs were discussed by several kinds of light spectroscopy measurements. It has been shown in other researchers' results that the temperatures (ionization temperature) of arc plasma estimated by Fowler-Milne (Off-axis) method and ArII/ArI relative intensity ratio method are higher than that (excitation temperature) by Boltzmann plot method. The temperatures were measured in detail by these methods. The experimental results led to the conclusion that the ionization temperature was equal to the excitation temperature in high current argon arcs. Furthermore, it was theoretically concluded that the measured data error had a remarkably bad influence on the temperature determination at the plasma region above 10,000K in Boltzmann plot method.

Secondly, to prove the effect of alloy elements on the anode behavior, GTA welding was carried out on the anode plate which was spread with the powder of some materials, and the characteristics of the arc voltage and the melting phenomena of the anode plate were discussed. It was found that the spread materials which caused a marked decrease in the arc voltage and the weld pool size were chemical compounds with the alkaline metal and the halogen. On the other hand, it was found that the materials which caused an increase in the arc voltage and the pool size were compounds with the element on the right side from the center of the periodic table and the halogen or element of the oxygen group. These results supported the conclusion that it was possible to estimate the degree of influence of those materials from the relative position of each chemical element in the proposed coordinate system with the ionization potential and the vapor pressure.

Keywords: arc plasma, spectroscopy, temperature, alloy element, arc voltage, melting phenomena

84 In-situ Measurement of Local Strain in High Temperature Range of Material and Detection of Defects by the Laser Speckle Method

Y. Muramatsu, Advanced Materials Processing Division

[April 1993 to March 1996]

We have been examining the applicability of the laser speckle strain measurement to the welding process. We already proved that it was possible to do the in-situ strain measurement in a high temperature range such as in welding using the laser speckle measurement.

In 1995, we mainly executed the measurements to detect the information during phase-transformation in some kinds of steels. A 9%Ni steel and a mild steel were used for the purpose because their strain behaviors during transformation are quite different. A SUS304 plate was also used to make comparisons with above steels.

A moving heat source of Gas Tungsten Arc (GTA) was applied on a rectangular thin plate and the strains were detected on the bottom surface of the plate. We clearly detected the strains during phase-transformation for several conditions of the heat input. The strain curves in the 9%Ni steel showed anisotropic behavior according to the measuring direction. The typical transformation curve, so-called S-curve was observed only in the perpendicular direction against the heating line, in the 9%Ni steel. In the experiments with the mild steels, however, we could not find out such tendencies. The restraints in the rectangular plate and the transformation temperature strongly affect these strain behaviors.

Moreover, the expansion during transformation in the 9%Ni steel plate in the perpendicular direction against the heating line exceeds greatly the values of the stress-free specimen with increasing the heat input. Some degree of the transitional tensile stress is expected to appear when the transformation starts and the stress acts

on the transformed part and stretches it like as the superplasticity.

We could detect clearly these strain behaviors using the laser speckle method, and we confirmed the usefulness of the laser speckle strain measurements in an actual welding process.

Keywords: laser speckle method, dynamic strain, in-situ strain measurement, high temperature, phase-transformation, 9%Ni steel, mild steel, austenitic stainless steel

85 Research on Quantitative and Intelligent Nondestructime Evaluation Techniques for Materials and Structures of High Reliability, Stage II

C. Masuda, Failure Physics Division

[April 1994 to March 1996]

In this research, it is planned to develop the nondestructive measurement technique and systems based on ultrasonic techniques to evaluate the properties of the metal matrix composites. This research is sponsored by STA and supported by members of various institutions, universities and companies. The previous stage (Stage 1) of this project was the development of the advanced ultrasonic measurement techniques and supporting procedures, using the ultrasonic spectrum analysis, velocity measurement with a scanning ultrasonic microscope, the laser-ultrasonic technique and computer simulation for ultrasonic wave propagation. In the Stage II produced two major results, as follows.

(1) Evaluation of microstructures in metal matrix composite by analyzing the ultrasonic frequency response

The frequency response analysis technique has been widely approved in the quantitative measurement of microstructual parameters such as grain size in a steel and shape factor of graphite in a cast iron. By improving this technique, higher accuracy has been achieved through this work. Theoretical analysis indicated the influence upon frequency spectrum of different factors, such as specimen surface roughness, thickness of ultrasonic couplant, sound field and input pulse wave form.

In the Stage II, the analysis by the technique clarified mechanisms of the wave form inversion of the tip echo of flaw reflector and the peak frequency shift of spectrum of sound directivity characteristics. Further improvement of the technique has been achieved in this work. The analysis by the technique also clarified the mechanism of the wave form variation in total reflection of a vertically polarized shear (SV) wave.

The frequency response analysis technique was applied to evaluate the microstructure in aluminum alloy matrix composites reinforced by the SiC whiskers (0.5 and 1.0μm in diameter) with the volume fractions of 0, 10, and 20%. Distribution of reinforcement can be evaluated by measuring the relative energy loss of transmitted ultrasound in the specimen thickness of 3 mm in C scan mode. The C scan images in 3 mm × 3 mm area clearly showed that the values of relative energy loss linearly increased with increasing the volume fraction on semi- logarithm paper. The slope of the linear relationship in case of SiC whisker of 0.5 mm in diameter is lower than that of 1 mm in diameter. Moreover, this technique was applied to detect the inner fiber in the aluminum alloy matrix composite and it was suggested that it was very useful to evaluate the microstructures in metal matrix composites.

(2) Evaluation of structures in metal matrix composites using laser ultrasonic techniques.

In the Stage I, the noncontact ultrasonic imaging system was developed using laser ultrasonic techniques. In this year, the SiC fiber reinforced Al matrix composite was inspected using the imaging system. The composite specimen includes SiC fibers with 140 μm in diameter and 35μm depth below the surface. It had been expected to obtain the intensity image of the fibers, but no contrast corresponding to the fiber appeared on the image. To analyze this result, a computer simulation technique was employed to visualize ultrasonic propagation in the specimen. The computer simulation technique characterized by the applicability for 3-dimensional, anisotropic, and combined material conditions, had been developed in the Stage I. From the calculation, it was clarified that intensity modulation of transmitting ultrasound caused by the fibers was weak in comparison with the modulation caused by voids, and traveling time through the specimen became shorter because ultrasonic velocity in the SiC fiber was twice as fast as that of the Al matrix. From the experiment and calculation, it was indicated that the ultrasonic imaging using traveling time might be required for the detection of the SiC fiber. Already, the ultrasonic imaging using traveling time had been realized in the system. However, the application to the SiC fiber specimen would require improvement of signal to noise ratio of ultrasonic detection.

Using the computer simulation technique developed in the stage I, the calculation for ultrasonic generation by laser beam scanning was

also examined and it is succeeded to visualize longitudinal, shear and surface waves generated in conjunction with scanning velocity of laser beam at the specimen surface. In the calculation, thermal stress caused by laser absorption was considered as external force affecting the motion of the quantified material into the simulation technique. This visualization would be useful for analysis of the ultrasonic waves generated by laser scanning.

The techniques for the frequency response analysis and the visualization of wave propagation were developed in this work as mentioned above. These techniques were very useful to evaluate the reinforcement distributions and its sizes in the aluminum alloy matrix composites. It is suggested that the fundamental techniques were established in this work and it is very important to apply to evaluate the more complex structural composites.

Keywords: Nondestructive Evaluation, Frequency response, Laser-ultrasonic, Composite materials, Computer simulation, Anisotropic microstructure

86 Application of Rutherford Backscattering and Particle Induced X-Ray Emission Analyses to Material Science

K. Nakamura, 1st Research Group
[April 1995 to March 1996]

For one year project named "Bilateral International Joint Research", we have carried out cooperative research project with Institute of Physics, Slovak Academy of Science. In this project, we aimed to develop high resolution Rutherford backscattering (RBS) technique to analyze thin film multilayer and surface roughness of oxide superconductor films. For this purpose we also utilized small angle X-ray diffraction (SAXRD) and Scanning atomic force microscope (AFM) to investigate multilayer modulation period and surface roughness to confirm the RBS results.

For multilayer samples, W/Si, $W_{1-x}Si_x$/Si and Co/Si/W/Si which have been prepared by UHV electron beam deposition at Institute of Physics (Slovakia) are investigated. These multilayers are well known to be used as mirrors for soft X-ray optics. The results obtained in Slovak side is that the W/Si multilayers show superconductivity up to 4.2 K (Tc of bulk W=0.012 K). This result is similar to Mo/Sb multilayer in which Tc increased with increasing modulation wave length. Thermal stability of these multilayers was also studied by applying eximer laser annealing and the resultant films were characterized by SAXRD, AFM and μ beam RBS. For μ beam RBS, we applied grazing in and grazing out geometry with the angle of 5 degree using beam diameter of 50 -100 (m and current of 10 nA of He^{2+} of 2 MeV. We succeeded to get depth resolution of 1 nm for W, which is about 10 times better than the normal angle RBS analysis.

Keywords: RBS, AFM, SAXRD, Multilayer, thin films

Related papers

1. Y. Asada and K. Ogawa, "Superconductivity of Mo/Sb Multilayered Films", *Solid State Comm.*, 60(1986): 161.
2. R. Sandrik, V. Bohac, K. Nakamura, A. Ishii, I. Orlic, S. M. Tang, and F. Watt, "The Study of the Structural Stability of Multilayer Systems by RBS and PIXE Microbeam Methods", *Nucl. Instr. and Methods in Phys. Res.*, B104(1955): 519–523.

Simulation and theory

87 Development of Knowlegde Database for High-Tc Superconducting Materials

Y. Asada, Computational Material Science Division
[April 1995 to March 2000]

We have already developed numerical database for high-Tc oxide superconductors. It is already opened publicly via network. All the data in it are extracted from the papers reported in journals. The papers contains many useful informations as well as numerical data. These informations are written in text style in Abstract, summary or conclusion. It is desirable that researchers employed in designing new products and searching new materials retrieve these informations from database and apply them to their purposes.

In this project we study how to store the informations and how to construct knowledge base for high-Tc superconductors. The knowledge base contains the information induced by processing the data from numerical database: empirical relations between physical properties. Conclusions and informations obtained in studies of Multi-core project are also included in the knowledge base.

We developed Tc-prediction system for Y123-system by using Neural Network method. Neural Network was constructed using the data obtained by retrieving from the numerical database "SUPERCON". The system predicts that Ca in Y-site have a valuable effect for high-Tc materials and Tc is

higher than that of $YBa_2Cu_3O_7$ if we choose Ca- and O-content the best. The system will be used for knowledge acquisition from the numerical database.

Keywords: oxide Superconductors, database, knowledge base, net work

Related Paper

1. Y. Asada and E. Nakada, "Database Development in Assistance of New Superconducting Materials", *J. Jpn. Soc. Information and Knowledge*, 5(1995): 57: in Japanese.

88 Establishment of Multidimensional Evaluation of Human Senses for Materials Design

Y. Kurihara, Materials Design Division

[April 1994 to March 1997]

Recently, there are increasing demands for materials developments from new aspects such as environment consciousness, amenity, and so on. When we investigate such new needs, most of information are provided mainly by language and human senses. Thus, the target of this study is to construct a quantitative evaluation method which can incorporate sensory information into materials design.

For this purpose, we inquired of 81 persons from 20 to 50 yearsold about the relationship between human sense and technical terms for materials properties such as mechanical, chemical and physical ones using a relationship matrix. Three characteristic vectors representing "warmth", "cleanliness" and "splendidness" were extracted from multivariate statistical analysis on collected sensory data. From the present analysis, it is concluded that we understand and express materials properties in comparison with functions and properties of human beings. In other words, most of materials represent the functions of human beings.

As the next stage of this study, we have constructed a database which correlates various kinds of materials properties with functions of human beings by a relationship matrix. This relationship matrix will be applied to find needs for new materials and effective uses of materials properties.

Keywords: human senses, materials properties, relationship matrix, multivariate statistical analysis, function of human beings

Related Papers

1. Y. Kurihara, T. Kaneko, M. Fujita, K. Hosimoto, and C. Tanaka, "An Application of Human Sense to Materials Development", *Symposium on Sensory Inspection*, (1995): 93–98.
2. Y. Kurihara, T. Kaneko, M. Fujita, K. Hosimoto, and C. Tanaka, "An Application of Quality Function Deployment to Establishment of Material Needs Finding System", *Symposium on Sensory Inspection*, (1995): 215–220.

89 Theory of Thermal Reaction on Solid Surfaces

T. Ohno, Computational Materials Science Division

[April 1994 to March 2000]

The thermal reactions on solid surfaces play important roles in various surface processes including epitaxial growth, etching, and catalysis. The purpose of this work is to clarify theoretically the thermal reaction processes on several solid surface systems such as semiconductor surfaces and metal surfaces. The analysis is based on the density-functional electronic theory within local-density approximation, which provides a powerful tool to determine the dynamical behavior as well as the stable atomic arrangement of solid surfaces.

The structural stability and optimum atomic arrangement of the Ga-rich GaAs(001)-(4x2) reconstructed surface has been theoretically investigated. This work shows that the stable Ga-rich GaAs(001) surface consists of two Ga dimers on the top layer and another Ga dimer at the third layer and that the calculated surface charge distributions are in good agreement with the observed scanning tunneling microscopy images.

Recently, we have investigated the adsorption of chlorine molecules on the reconstructed GaAs(001) surfaces. Chlorine is one of the most important halogens used in the semiconductor etching processes. The stable geometries of the chlorinated GaAs(001) surfaces have been determined theoretically, which are consistent with recent temperature programmed desorption measurements.

Keywords: structural stability, chemisorption, reaction, solid surface

Related Papers

1. T. Ohno, "Energetics of As Dimers on GaAs(001) As-Rich Surfaces", *Phys. Rev. Lett.*, 70(1993): 631–634.
2. T. Ohno, "Barrierless Dimer Breaking at Semiconductor Surfaces by Chlorine Atoms", *Phys. Rev. Lett.*, 70(1993): 962–965.
3. T. Ohno,"Chlorination of Ga-Rich and As-Rich

Reconstructed GaAs(001) Surfaces", in *Proc. 22nd International Conference on the Physics of Semiconductors*, ed. D.J. Lockwood(World Scientific Publishing, 1995): 545–548.

90 Thermodynamic Analysis of Transition Process from Metastable to Stable Phases

H. Onodera, Computational Materials Science Division

[April 1994 to March 1997]

The crystallization process of sputter deposited $Ti_{48}Al_{52}$ amorphous alloy was studied by high resolution transmission electron microscopy (HRTEM) and X-ray diffraction. An unknown phase having spherical morphology precipitates in amorphous matrix in the early stage of crystallization. Electron diffraction patterns from this phase can be identified by the primitive cubic or tetragonal structures with the lattice parameter of a(=c)=0.69nm.

Liquid-amorphous transition process of Ti-Al alloys were investigated by using molecular dynamics techniques with the Embedded Atom Method. The simulation could reproduce the experimentally observed concentration range (40-85at%Al) for amorphization. Structure analyses of the amorphous alloys indicate that the basic building blocks for the amorphous phases of Ti-Al system should be icosahedral clusters with Al-atom in their center.

Coating of HfC on W powder was tried by a fluidized bed CVD as a new process to manufacture sintered W-Hf-C alloys. A HfC coated layer of 8nm thickness is obtained by a fluidized bed CVD at 1553K for 900s, which corresponds to 0.4mol% of HfC in bulk. Preliminary experiments were also performed to establish CVD conditions for coating of SiO_2 or SiC on Fe powder.

Keywords: metastable phase, amorphous, molecular dynamics, thermodynamic analysis, CVD

Related Papers

1. T. Abe, S. Akiyama, and H. Onodera, "Crystallization of Sputter Deposited Amorphous Ti-52at%Al", *ISIJ Int.*, 34(1994): 429.
2. T. Tagaki, "Coating of HfC on Tungsten Powder by Fluidized Bed CVD", *J. Japan Inst. Metals*, 59(1995): 1157.
3. M. Shimono and H. Onodera, "Molecular Dynamics Study on Amorphization of Ti-Al Alloys", *Proc. of CMSMD'96, Japan*, (1996): 215.
4. M. Ohnuma, T. Abe and H. Onodera "Crystallization of Sputter Deposited Amorphous Ti-52at%Al Alloy", *MRS Symposium Proc. Series*, 400 (1996).

91 Computational Analysis of Mechanical Property and Structural Design of Materials Taking Microstructures into Account for Atomic Power Plants

H. Shiraishi, 2nd Research Group

[April 1994 to March 1999]

The creep damages and irradiation damages will initiate and grow in materials of atomic power plants during use, however these micro structural changes are disregarded when plants are designed. This research aims to develop the evaluation program of mechanical properties taking microstructures into account by using FEM, micro-mechanics and damage mechanics. The designing methods of most suitable material structures based on inverse analysis are also studied. The parallel computing method by using multiple CPU are introduced.

We have indicated that creep crack growth behavior have been dependent on microscopic creep fracture mechanism from the long-term creep crack growth tests. The growth rate of wedge-type intergranular crack and transgranular crack could be predicted from fracture mechanical C* value and material's creep ductility. The growth rate of cavity-type intergranular crack was accelerated as the creep damage density ahead of the crack tip increased and could not be predicted from creep ductility. In order to clarify the effect of damaged zone, we are developing the FEM program which simulates the growth of creep voids and cracks based on the local critical strain criterion. The predicting method of crack growth rate from the creep constitutive equation under cavity type fracture mode would be discussed.

The FEM program to simulate the He embrittlement has been developed. The effect of size and density of He bubbles and work hardening exponent on tensile properties were discussed. The critical size and spacing of bubbles at which He embrittlement appeared were clarified from this simulation.

Keywords: FEM simulation, Creep damage, Creep crack growth, He embrittlement

Related Paper

1. M. Tabuchi, K. Kubo, and K. Yagi, "Evaluation of Creep Crack Growth Rate in Terms of Creep

Fracture Mechanism for 316 Stainless Steel": submitted to *9th Int. Conf. on Fracture.*

92 Development of Virtual Experimental Technologies for Material Design

M. Nihei, Computational Material Science Division

[April 1995 to March 1998]

The coordinated research program of the Science and Technology Agency(STA) to develop the virtual experimental technologies for materials design is being carried out from April 1995. Over twenty researchers participate in this program. This research program aimes to promote the computational science of Japan in the region of material science and to develop the new material design technology through the realization of a virtual experimental system using the computer technologies such as supercomputings, databases and network systems. This research program consists of four parts, the first principal computational approach, meso-scopic material structure prediction using the statistical thermo-dynamics and/or monte-carlo calculation, modeling and simulation of material properties such as strength and development of a virtual experimental system by integration of computer technologies.

In this research program, NRIM is conducting the following three research projects.

1.Calculation of atom transfer on a material surface by Ab Initio molecular dynamics(Car-Parinello method).

This research aims to develop the Ab Initio computing method based on the density functional theory to analyze physical phenomena such as chemical response on the solid surface, thermal atom transfer such as diffusion. In this research, the force acting on the atom is simulated by the first principle calculation.

2.Material design of heat-resistant alloys by statistical thermo-dynamics calculation.

In this research, the statistical thermo-dynamics calculation method is being improved for the material design. The Cluster Variation Method(CVM) using a phenomenological interatomic potential (L-J potential) is employed for the calculation of the equilibrium state in multi-components Ni-base superalloys.

3.Modeling and simulation for the prediction of material strength.

This aims to develop the simulation method for strength, fracture and damage process of materials. The molecular dynamics is being applied for nano-scopic materials evaluation such as the nano-indentation and the combination method using the solid-state mechanics and the fact database is also developed. In this research, the realization of a virtual consultant system is also tried for a use of material design researchers.

Keywords: computational simulation, modeling, virtual experiments

Ferrous materials

(93) A Study of the Deformation and Fracture Mechanism of the High Strength Metal Matrix Composites

H. G. Suzuki and Y. Tsubokawa, Mechanical Properties Division
[April 1996 to March 1999]

Steel frames and steel-reinforced concretes have never been so terribly broken in Japan as they were by Hanshin-Awaji Great Earthquake. Particularly, there were brittle fractures on the steel bars of the high-rise buildings and buckling deformation on the oil tanks. For high strength materials, most of them are steel, the studies of the brittle fractures have been tied up until the 1970's. Quantitative studies are not sufficient concerning the deformation and fracture at base metal and welding joint, where the high speed and restricted deformation happened during this earthquake. Moreover, the strength is incompatible with the toughness and/or ductility on the real steel, i.e., the higher the strength we want, the lower the toughness and/or ductility we receive.

The present study aims at the compatibility between the high strength and high toughness and/or ductility in the light of metal matrix composites, including:
(1)Fundamental study of the strength of ferrous materials to clarify the deformation and fracture mechanism at restricted and high speed deformation and to obtain the fundamental knowledge for developing the high strength and high toughness material through the microstructural control
(2) Creating some basic knowledge for developing the structural composites with high physical properties

Keywords: strength, deformation, composite

94 Fundamental Research for Intelligent Materials (Formation Process and Recovering Method of Creep Damage)

N. Shinya, 5th Research Group
[April 1994 to March 1999]

In this work, high temperature damage formation process and healing method of the damage are being studied for creating self-healing materials.

Creep damage formation process

Using the electron Moiré method, the micro creep deformation such as grain boundary sliding, coarse slip and localized strain in pure copper and 321 stainless steel specimens have been measured. The results show that the local deformation after secondary creep is non-uniform, while the deformation up to beginning of secondary creep is comparatively uniform, and the high longitudinal tensile strain and transverse compressive strain are formed at the same area. This strain distribution has a close relationship to grain boundary sliding and grain boundary properties.

Healing of Creep Damage

For the purpose of healing creep damage and life extension on heat resisting steels, a sintering mechanism of cavities and precipitation behavior of stable compounds on cavity surface are studied.

The progressive sintering of the cavities due to some treatments (compressive creep, hot isostatic pressing and annealing) is monitored using highly sensitive density measurement technique. The results show that sintering rates under compressive creep are rapid and depend proportionally on compressive creep rate, whereas annealing causes only slight sintering. Therefore compressive creeps remove completely the cavities and extend the rupture life considerably.

Cavity surface coated by precipitation of a stable compound like BN is expected to suppress the surface diffusion and the cavity growth remarkably. The austenite stainless steel with high B, high N and low S showed the precipitation of BN on cavity surface, rare formation of cavity, extended rupture time and high rupture ductility. It is thought that these properties are due to the precipitation of BN.

Keywords: Intelligent Materials, electron Moiré method, creep deformation, self-healing of creep cavity, life extension

Non-ferrous materials

95 Relationships between Fatigue Softening/Hardening Behavior and TEM Structure of Titanium Alloys

T. Kainuma, Mechanical Properties Division
[April 1994 to March 1997]

The change of the width or area of the hysteresis loop during the fatigue testing of materials at constant stress amplitude is taken usually as a measure of dynamical changes in mechanical properties. By testing at stress amplitudes higher than yield stress, fatigue hardening only takes place in alloys as well as pure metals (decrease in the width of hysteresis loop). While at stress amplitudes lower than the yield stress, fatigue softening occurs. Details of fatigue softening behavior have been reported for the materials such as aluminum(1), copper(2), silver and iron(3). The aim of this work is to reveal the mechanisms of fatigue softening and hardening behavior of titanium alloys in connection with the characteristics of crystal structures, using transmission electron microscope (TEM).

Fatigue softening and hardening behavior

We determined at first the specimen shape most suitable for tension-compression fatigue testing, then examined the crystal structure dependence of fatigue softening and hardening behavior using Ti-3Al-8V-6Cr-4Mo-4Zr alloy(β-type titanium alloy, Ti-3-8-6-4-4), pure titanium(α-type) and Ti-6Al-4V alloy($\alpha+\beta$ type). Also examined the stress retio(R=-1, R=0.1) dependence of fatigue softening and fatigue hardening behavior using β-type titanium alloy and pure titanium. The experiments for the fatigue softening and hardening phenomena were carried out on work-hardened and annealed materials, respectively. Following are the main results. (1)In fatigue testing of annealing materials, fatigue hadening behavior of β-type titanium alloy was more remarkable than pure titanium (α-type). (2)In fatigue testing of cold working materials, the fatigue softening behavior of β-type titanium alloy taked place more remarkable then pure titanium(α-type).

Relation between fatigue behavior and electron microscopic structure

The TEM observation has been aimed to reveal the mechanisms of fatigue softening and hardening in the β-type titanium alloys. At low and intermediate cyclic stress ranges(stress ratio R=-1) in annealing materials dislocation loops, loop patch (dislocation loop cluster) and network of dislocation cells are observed. At larger cyclic stress levels equiaxed subgrains and elongated subgrains are appeared. As cold working TEM structure are exhibited high density tangle dislocation structures. On the other hand, TEM structure of fatigue softening are changed equiaxed and elongated subgrains with low dislocation density.

Keywords: Ti-3-8-6-4-4, pure titanium, Ti-6A1-4V, TEM structure, fatigue softening, fatigue hardening

Related Papers

1. J. C. Grosskreutz and P. Waldow, "Substructure and Fatigur Fracture in Aluminum", *Acta Metallurgica*, 11(1963): 717–724.
2. K. V. Rasmussen and O. B. Pedersen, "Fatigue of Copper Polycrystals at Low Plastic Strain Amplitudes", *Acta Metallurgica*, 28(1980): 1467–1478.
3. H. J. Roven and E. Nes, "Cyclic Deformation of Ferritic Steel-I. Stress-Strain Response and Structure Evolution", *Acta metall. mater.*, 39(1991): 1719–1733.

Intermetaric compouds

(96) Fundamental Research on New Wear Resistance Materials of TiAl Based Composites

S. Ikeno, Physical Properties Division
[April 1996 to March 1998]

TiAl has charateristics of high specific strength and high melting points, but lack of ductility at room temperature. Efforts to improve the ductility of TiAl at room temperature have been made by many researchers.

Wear resistance of TiAl is also higher than that of ordinary metals. However it is necessary to increase the surface hardeness and lower the friction coefficient to use as a wear resistance material. In order to increase the wear resistance of TiAl, two kinds of TiAl based composites, i.e., TiAl- Ti_2AlN and TiAl- MoS_2, were prepared in this study.

Ti_2AlN in TiAl is stable at 1273 K. Therefore, Ti_2AlN is suitable as hardening particle for TiAl based composites. A mixture of TiN powder and TiAl powder is hot-pressed at 1473K - 1573K. Ti_2AlN particles are formed by the reaction of TiN and TiAl, and distributed homogeneously in the composite. The composite of TiAl- Ti_2AlN has been developed for a high-temperature sliding or rotating parts material in aero-space.

A mixture of MoS_2 powder and TiAl powder was hot-pressed and reacted each other. MoS_2 particles on the surface decreased the friction coefficient of the composite of TiAl- MoS_2. The composite of TiAl- MoS_2 has been developed for a sliding or rotating

parts material in high vaccum systems.

Keywords: TiAl, Ti_2AlN, MoS_2, intermetallic compound,composite, wear resistance

(97) Mesoscopic Structure Control and Properties of Intermetallic Compounds

M. Nobuki, 3rd Research Group
[April 1996 to March 2000]

Mesoscopic structure and fine microstructure controls are paid attention as a method of materials development for structural alloys of the next generation. We have initiated overall research systematically connected with (1) processing, (2) characteristic evaluation and (3) detailed structure analyzing.

The objectives of our work with respect to TiAl gamma base and trialuminide intermetallic alloys in titanium system are as follows:

(a) Preparation of nonequilibrium phase alloys utilizing a rapid cooling method and a vapor deposition method, etc. and detailed analysis of the microstructure in these alloys will be carried out.

(b) The microstructure change by chemical composition fluctuation or multiple alloying will be investigated. The elucidation of microstructure formation process and development of mesoscopic structure control method from the view point of the phase transformation will be also performed.

(c) The clarification of morphology in the grain structure and dispersion of precipitation phase will be done. Development of the mesoscopic structure control method utilizing plastic working such as isothermal forging will be carried out.

Highly functional properties and new characteristic properties will be investigated based upon the mesoscopic structure control. The relation between mesoscopic structure and chemical composition, phase transformation, plastic working, etc. and the relation between material properties and mesoscopic structure will be also systematically elucidated.

Keywords: intermetallic compounds, microstructure, phase transformation, thermomechanical processing, mechanical properties, TEM analysis

98 Diffusion in Ordered Alloys and Preparation of Composition Gradiented Materials

H. Sasano, Physical Properties Division
[April 1995 to March 1998]

One of purposes of this research program is to make clear diffusion mechanism and phase stability in ordered alloys such as NiAl, TiAl and Ti_3Al. This year the interdiffusion coefficient in TiNi was measured by a chemical transportation technique in a closed tube using transporting medium of aluminum chloride gas. The coefficient is extraordinary low in the composition range between 46 and 54 atomic percent aluminum. The result implies the existence of a miscibility gap in a NiTi single phase region.

Another purpose of the program is to develop the fabrication method of composition gradiented materials of ordered alloys. If the composition is delicately changed along the longitudinal direction of the material, we can obtain the material possessing unique properties. We tried to control the concentration of titanium in Ni-Ti binary alloys by regulating of heating temperature of nickel plate specimens and mixture of titanium and ammonium chloride placed in a closed alumina tube independently. It was found that titanium concentration in TiNi shape memory alloys could be precisely controlled by this method.

Keywords: ordered alloy, diffusion, chemical transportation, shape memory alloy

99 Hydrogen Behaviors at Interfaces in Alloys

C. Nishimura, Physical Properties Division
[April 1995 to March 1998]

Hydrogen-trapping behaviors in $L1_2$-ordered Ni_3Al have been investigated using thermal desorption spectroscopy(TDS), in order to obtain fundamental data to clarify the mechanism of environmental embrittlement in $L1_2$-ordered intermetallics. Boron-free, equiaxed polycrystals of Ni_3Al were used for samples. The samples were prepared, starting from a ductile bar of Ni_3Al which was grown by floating zone unidirectional solidification (FZ-UDS), by recrystallizing cold rolled sheets. Tritium was electrochemically charged in advance to the measurement. Heating rate was 5K/s. The thermal desorption spectrum exhibited two distinct peaks, at 363K and 458K. This result shows that the samples contain the two different types of trapping site for hydrogen. One possibility is that the grain-boundaries in Ni_3Al trap hydrogen more strongly than the interstitial sites. It is speculated that environmental embrittlement in Ni_3Al is caused by the moisture-induced hydrogen which segregates at grain boundaries, promoting intergranular fracture.

Hydrogen permeation behaviors of magnesium

alloys have been investigated in order to obtain fundamental data on hydrogen-absorption characteristics of the alloys. Magnesium alloy investigated here was Mg-1.54Al-0.65Zn-0.05Mn mass%. Alloy membranes were palladium-plated by evaporation in vacuum. Hydrogen permeation was performed in the equipment with ultra high vacuum system in the temperature range 423-498K. Hydrogen diffusion in the Mg alloy is not slow: hydrogen diffusivity of the alloy is comparable to that of palladium. On the other hand, hydrogen permeability of the alloy is rather small. The values of hydrogen permeability in the temperature range investigated are around 10^{-12} mol of $H_2 \cdot m^{-1} \cdot s^{-1} \cdot Pa^{-1/2}$, which are smaller than that of palladium by nearly 4 orders. The hydrogen solubility calculated from the obtained data was consistent with the previous results determined by the resistmetric study. The present result suggests that the addition of alloying elements which enhance the hydrogen solubility is effective in improving the hydrogen absorption kinetics of magnesium alloys.

This research was performed in collaboration with the Institute of Industrial Science, the University of Tokyo.

Keywords: hydrogen, intermetallics, grain boundary, interface, trapping

100 Improvement of Mechanical Properties of Intermetallic Compounds by Crystal Growth Control

T.Hirano, Chemical Processing Division
[April 1992 to March 1997]

The objective of this study is to improve the mechanical properties of intermetallic compounds by crystal growth. We have found that unidirectional solidification using a floating zone method remarkably enhances the room-temperature ductility of Ni_3Al without addition of alloying elements such as boron. We call this method FZ-UDS. Stoichiometric Ni_3Al exhibits more than 60% tensile elongation at room temperature. It is found that FZ-UDS can enhance even the ductility of Al-rich Ni3Al which can not be ductilized by the addition of alloying elements, indicating that FZ-UDS is a new promising method to improve the brittleness of intermetallic compounds.

In this study three subjects are stressed. First, crystal growth technique is developed in detail. Columnar-grained structure which is closely related to the large ductility of Ni_3Al is obtained by selecting the growth rate, depending on the deviation from the stoichiometry. Second, the solidified columnar structure is characterized, paying attention to the grain boundary structure and segregation. It is found that this structure consists of low energy grain boundaries. Third, the mechanical properties and deformation behaviors are studied.

Keywords: unidirectional solidification, floating zone method, Ni_3Al, room-temperature ductility

Related Papers

1. T. Hirano and T. Mawari, "Unidirectional Solidification of Ni_3Al by a Floating Zone Method", *Acta metall. mater.*, 41(1993): 1783–1789.
2. T. Mawari and T. Hirano, "Effects of Unidirectional Solidification Conditions on the Microstructure and Tensile Properties of Ni_3Al", *Intermetallics*, 3(1994): 23–33.
3. T. Watanabe, T. Hirano, T. Ochiai, and H. Oikawa, "Texture and Grain Boundary Character Distribution (GBCD) in B-Free Ductile Poly-crystalline Ni_3Al", *Mater. Sci. Forum.*, 157–162(1994): 1103–1108.

101 High Performance Materials for Severe Environments-I (Microstructure and Properties of Intermetallic Compounds with High Specific Strength)

M. Nakamura, 3rd Research Group
[April 1990 to March 1997]

Light-weight, heat-resisting intermetallic compound TiAl is a candidate for a structural use in severe environments for a space plane etc., and the knowledge of various properties of TiAl base alloys is required for a practical use in such an environment. In this research program, the mechanical properties are systematically studied for TiAl base alloys whose composition and microstructure are well controlled, and then the fundamental methods to control microstructure which gives the optimum properties for a practical use to materials are discussed.

TiAl base alloys with Sb addition from 3 to 9 at.% were prepared by argon arc melting, and unidirectionally solidified using a floating zone furnace. The effect of the Sb-rich phase on yield strength at 1373 K was studied. In the alloy with the addition of Sb above 6 at.%, the proeutectoid Sb-rich phase was particulate, and no elongated Sb-rich phase were observed. The alloys with a small amount of Sb exhibited the elongated, fibrous phase with an aspect ratio of more than 10 in the central part of the directional solidified specimens. The alloys with the fibrous Sb-rich

phase exhibited the tensile strength above 200MPa at 1373 K, but many specimens exhibited premature failure and no elongation even at 1373 K. As many pores were observed near the fracture surface, and was considered to cause the premature failure, the directionally solidified alloys were HIPed at 1473 K, and then tested in tension at 1373 K. Thus, one of the HIPed alloys exhibited the tensile strength of higher than 240 MPa, and the elongation above 10%.

The microstructure control of TiAl base alloys was carried out using a thermo-mechanical processing, and the high temperature strength was examined. In order to obtain high strength at high temperatures, solid solution and precipitation hardening, and microstructure control are required. Based on previous results, the microstructure and mechanical properties of TiAl alloys with the addition of Si, V, Zr, Nb, Hf and Sn were studied. The alloys were HIPed at 1470 K and isothermally forged at both 1470 and 1530 K, followed by heat-treatment at 1370~1670 K. In the forged alloys, recrystallized grains with a grain size of smaller than 10μm accompanied with a small amount of fine second phase particles were observed, and no lamellar grains were observed. After heat-treatment, the microstructure consisting of equiaxed γ grains with a grain size of about 55μm and the fine second phase particles along the γ grain boundaries was obtained. Thus, the isothermal forging and heat-treatment above 1570 K are available for the microstructure control of these alloys. The heat-treated alloys exhibited the yield strength of 1.4 times higher than binary alloys, but they hardly had room temperature elongation.

The microstructure change caused by quenching from the α phase field, and then aging at high temperatures was investigated for Ti-48 at.% Al. When the aging temperature exceeded a critical temperature, the equiaxed γ grain structure with the plate-like α_2 phase in the γ grain interiors and the particulate α_2 phase along the grain boundaries was obtained. The latter phase was formed independent of the aging temperature, and coarsened remarkably as the aging time increased. Meanwhile, the thickness of the former phase (about a few to some tens nm) hardly changed. EPMA measurement showed the composition difference between the matrix γ phase and the plate-like and particulate α_2 phase. Although the composition change of the particulate α_2 phase is caused by the rapid diffusion along the γ grain boundaries, that of the plate-like one may be controlled by the short-distance diffusion.

The microstructure of the rapidly cooled Ti-48 at.% Al was also observed using high resolution electron microscopy, and new local atomic arrangement with a B19 structure was confirmed in the unmassively transformed region by fine structure analysis.

The oxidation behavior at 1173K and tensile properties at room temperature were studied for aluminized TiAl base alloys.

Keywords: Intermetallic Compound, TiAl, Sb, Microstructure, elongation, thermomechanical processing, GAR, high temperature strength

Related papers

1. K. Hashimoto, M. Nobuki, H. Doi, E. Abe, and M. Nakamura, "High Temperature Strength and Room temperature Ductility of TiAl Base Alloys with Antimony", Proc. Int. Symp. on Gamma Titanium Aluminides, ed. by Y-W. Kim, R. Wagner, and M. Yamaguchi, *TMS*, (1995): 761–770.
2. M. Nobuki, D. Vanderschueren, and M. Nakamura, "High Temperature Mechanical Properties of Vanadium Alloyed γ Base Titanium-Aluminides", *Acta Metall. Mater.*, 42(1994): 2623–2632.
3. T. Kumagai, E. Abe, M. Takeyama, and M. Nakamura, "Reaction Process of $\alpha \rightarrow \gamma$ Massively Transformation in Ti-Rich TiAl Alloy", *Mat. Res. Soc. Symp. Proc.*, 364(1995): 181–186.

102 Fundamental Study on the Search for Advanced Materials

T.Hirano, Chemical Processing Division

[April 1995 to March 1996]

In order to develop advanced materials we studied the mechanical properties of aluminides, Ni_3Al, and the electrical properties of silicides, $BaSi_2$.

Ni_3Al exhibits a positive temperature dependence of the yield stress which is known as the yield stress anomaly. The mechanical properties have been extensively studied, but there are few data on the single crystals with stoichiometric composition. It is because it is difficult to grow them due to the peritectic reaction during solidification. We have successfully grown large single crystals by floating zone method. This binary, stoichiometric single crystals exhibited strain-rate independence of the flow stress, which is different from that of non-stoichiometric alloys. This suggests that the deformation is controlled by dislocation multiplication.

So far it is known that there are three different

polymorphs in $BaSi_2$, orthorhombic, cubic, and trigonal phases. The first one is normal phase and the latter two are high-pressure ones. We found the fourth high-pressure phase (called $BaSi_2$ (IV) hereafter) by in-situ X-ray measurements under high-pressure and high-temperature conditions. $BaSi_2$ (IV) can be quenched to normal pressure and room-temperature. The electrical resistivity showed a positive temperature dependence, suggesting that $BaSi_2$ (IV) is a metal. It also shows a superconducting transition at 6.3K similar to tetragonal $BaSi_2$.

Keywords: Ni_3Al, single crystal, mechanical properties, $BaSi_2$, high-pressure phase, electrical properties

Related papers

1. M. Demura and T. Hirano, "Stress Response by the Strain -Rate Change in Binary, Stoichiometric N_3Al Single Crystal", *Phil Mag. Lett.*, 75(1997): 1103.
2. M. Imai and T. Hirano, "Electrical Resistivity of Three Polymorphs of and P-T Phase Diagram", *Mat. Res. Soc. Symp. Proc.*, 402(1996): 567.

103 Basic Research on Intermetallic Compounds for Structural Applications

M. Nakamura, 3rd Research Group

[April 1993 to March 1996]

TiAl base intermetallic compounds have become of major interest as a candidate for high temperature structural applications. Although they have advantages of high melting point, high strength at high temperatures, high elastic moduli and reasonable oxidation resistance, improvement of both room temperature ductility and strength at high temperatures is required.

Stoichiometric TiAl and Ti-53at%Al alloys were tested in tension in a temperature range from room temperature to 773 K in order to study the brittle-ductile transition behavior in elongation. The elongation increased from 1% at room temperature to about 3% at 473 K for the stoichiometric alloy, while the increase of elongation was observed at about 573 K for the Al-rich alloy. The transition temperature increased by 100 K in the Al-rich alloy compared with the stoichiometric γ single phase alloy. This result was discussed using "the evaluation method of phase stability of TiAl phase" which has already been proposed and in which lattice constants measured by x-ray diffraction and atomic radii are taken account of. It may be concluded that the increase of the transition temperature in the Al-rich alloy is due to the difficulty of mechanical twinning caused by the increase of the binding force between Ti and Al atoms in the Al-rich TiAl phase.

The knowledge of creep behavior at high temperatures is also required for high temperature structural applications, but there are not many researches on tensile creep behavior of TiAl base alloys. Thus, the creep rupture test was carried out at 1273 K in a vacuum of 3×10^{-5} torr for Ti-46at%Al alloys with a fully lamellar ($\gamma+\alpha_2$) structure (grain size: 1500 μm), γ+ lamellar structure (350 μm) and γ + lamellar structure (150 μm), and the effect of the microstructure on the creep rupture behavior was studied. The results are as follows. (1) The rupture life is the shortest in the alloy with the smallest grain size. (2) In a high stress region, the alloy with a grain size of 350 μm exhibited the longest rupture life, while, (3) in a low stress region, the fully lamellar structure exhibited the longest one. In the high stress region, the fully lamellar structure ruptured at the elongation less than 10%, because of the brittle intergranular fracture, while, in the low stress region, it exhibited the elongation of about 50%, because of the dynamic recrystallization of the lamellar structure. The alloy with the smallest grain size exhibited the elongation of more than 100%, and the chisel point fracture was always observed.

The microstructure control of TiAl base alloys was studied for improvement of mechanical properties at high temperatures using a thermomechanical processing. It is known that a large aspect ratio of grains improves remarkably high-temperature strength. Thus, the recrystallization structure which was obtained with a zone annealing method using a high frequency induction furnace was studied for Ti-47/48 at%Al alloys. The alloys were at first isothermally forged repeatedly in order to obtain a fine equiaxed grain structure, and then recrystallized using a zone annealing method. The result indicates that the recrystallized grains with the grain aspect ratio (GAR) of more than 15 was obtained, if the annealing temperature, zone speed and temperature gradient were well controlled. The longitudinal direction of the elongated grains was randomly oriented. The yield strength of the elongated grain structure increased with increasing GAR at 1273 K, and was estimated to be about 1.6 times higher for the alloy with GAR of 1.5 than for the equiaxed grain structure alloy.

The wear properties of TiAl base alloys were studied. The wear resistance of two alloys, i.e. Mn containing TiAl and Sb-containing TiAl was compared at room temperature using a Ohgoshi-type wear testing machine. The Mn-containing

alloy with a fully lamellar structure (grain size of 60 μm) had the Vickers hardness (Hv) of 260 to 320. The addition of Mn resulted in the increase of specific wear rate, and thus the decrease of wear resistance. Dislocation structures were observed in the portion below the friction surface. The Sb-containing alloy consisted of γ, α_2 and the Sb-rich phases, and showed 330 to 560 Hv. As the content of Sb increased, the hardness largely increased, the specific wear rate decreased and the wear resistivity was improved. Although the hardness was as high as 550 Hv, the alloy with a large amount of the α_2 phase exhibited the decrease of the wear resistance. This result is different from that in a binary alloy with a large amount of the α_2 phase, that is, the increase of the α_2 phase resulted in the improvement of the wear resistivity for a binary alloy. Mechanical twinning was observed in the portion below the friction surface, and the twinning deformation may explain this difference.

The resistance to thermal shock of W and W-Re alloys with a high melting point was also studied for much higher temperature structural applications using a electron beam heating apparatus.

Keywords: intermetallic compound, TiAl, elongation, creep behavior, grain morphology control, thermal shock, W alloys

Related papers

1. M. Fujitsuka., I. Mutoh, H. Nagai, and T. Tanabe, "Thermal shock behavior of metal-ceramics mixtures for ultrahigh temperature use", *Proc. of the 3rd Japan Int. SAMPE Symp. "Advanced Materials-New Processes and reliability"*, ed. T. Kishi, N. Takeda, and Y. Kagawa, , SAMPE, Chiba, Japan (1993): 641–646.
2. K. Hashimoto, S. Kajiwara, T Kikuchi, and M. Nakamura, "Effect of Temperature on Tensile Properties of TiAl Base Alloys", *Scripta Metall. Mater.*, 32(1995): 417.
3. S. Ikeno, M. Siota, M. Nobuki, and M. Nakamura., "Wear Properties of Oxide Dispersion Strengthened Nickel Alloys", *J. Mater. Sci.*, 30(1995): 4401.

Composite

104 Development of High Strength Metal Base Composites with Excellent Physical Properties by the Advanced Bronze Method

Dr. H. G. Suzuki, Mechanical Properties Division
[April 1994 to March 1997]

High strength materials with excellent physical properties, such as electrical conductivity, are strongly demanded by many fields of modern industries. In order to meet this demand, we applied the Bronze Method (also named as Tachikawa Method), which is originally developed for the production of brittle Nb_3Sn superconductive materials, to produce a kind of Cu in-situ composites. In this composite, the content of secondary element is much higher than its solubility in the Cu matrix. Then by heavy cold working, the dendrites of secondary element can be deformed into the in-situ reinforcing elements of fibers or ribbons. Correspondingly, the strength of the material is greatly improved. Furthermore, the good electrical conductivity of the composites can be obtained by an optimum combination of cold working and aging treatments.

By this method, now we have successfully developed a low cost Cu-Cr in-situ composite with tensile strength as high as 850MPa, and electrical conductivity as good as 75%IACS. The microstructural evolution of the composite has also been characterized systematically by means of optical metallography, scanning electron microscopy, analytical transmission electron microscopy, high resolution electron microscopy and computer image simulation. It is found that Cu incorporates into Cr and forms nanosize Cu-rich clusters during cold-rolling process, while screw dislocations line-up along the longitudinal direction of the reinforcing elements. In addition, by X-ray texture structure analysis, the preferential elongation direction of the Cr dendrites is determined to be <011>.

Now we are carrying out a more profound investigation on the deformation mechanism, aging mechanism and other theoretical topics concerning the in-situ composites. At same time, extensive efforts are also devoted to the exploration of other kinds of Cu-based and Fe-based composites with even higher strength and better physical properties, through incorporation of in-situ composite processing techniques with other advanced materials processing techniques. The commercialization of our results to industrial mass production is also under consideration.

Keywords: In-situ composite, Bronze Method, high strength, high conductivity

Related Papers

1. H. G. Suzuki, K. Adachi, T. Takeuchi, and Y. Jin, "Process Optimization of High Strength and High Conductive Cu-Cr In Situ Metal Matrix Composites", Int. Sym. on Adv. Mater. and

Techno. for the 21st Century, *ASM/JIM/ISIJ/MMIJ, Honolulu, USA*, (1995): 206.
2. Y. Jin, K. Adachi, T. Takeuchi, and H. G. Suzuki, "Microstructural evolution of a heavily cold-rolled Cu-Cr in-situ metal matrix composite", *Mater. Sci. Eng.*, A212(1996): 149–156.
3. S. Tsubokawa, T. Takeuchi, and H. G. Suzuki, "Microstructure of Cr Fiber in Cu-Cr In-situ Composite", *Jap. Inst. Metal.*, 35(1996): 472.
4. Y. Jin, K. Adachi, T. Takeuchi and H. G. Suzuki, "Cu precipitation in Cr ribbon of Cu-15wt%Cr in-situ composite", *Appl. Phys. Lett.*, accepted.
5. K. Adachi, T. Takeuchi, and H. G. Suzuki, "Plastic Deformation Mode of Cr Phase in the Cu-Cr Composite by Cold Rolling": submitted to *Jap. Inst. Met.*

105 High Temperature Strength and Fracture of Reinforced Oxide- and Nitride-Base Ceramics

K. Hiraga, Mechanical Properties Division
[April 1995 to March 1997]

Though polycrystallin ceramic materials are typically brittle at room temperature, most of them show plasticity at high temperatures under the aid of grain boundary sliding accommodated by matter transport through and/or across the boundaries. Concurrent damage accumulation occurs by cavitation and/or diffusional crack growth, both of which are related closely to the above-mentioned deformation mechanisms. The basic information of such deformation and damage process, which are quite different from those at lower temperatures, are important when the materials are used in high temperature machinery. The present study is conducted to examine the high temperature deformation and fracture of whisker-reinforced nitrides and particle- dispersed oxides. The special attention is placed on the constitutive behavior and cavitation damage of reinforced composites at relatively low tensile stresses ($\sigma/E \sim 10^{-4}$), at temperatures higher than 1400 K.

Keywords: creep, cavitation, toughening microstructure

106 Thermal Stability of Intermetallic Compound Matrix Composites Reinforced with Fibers

Y. Shinohara, Physical Properties Division
[April 1993 to March 1997]

Heat resistive materials which can be used above 1373K are essential to the developments of the space-plane, the fusion reactor and the high-efficient turbine engine. TiAl intermetallic compounds have higher strength and toughness than metals and ceramics at elevated temperatures. TiAl matrix composites reinforced with fibers are promising for structural materials above 1373K.

Reinforcements for TiAl matrix are SiC, B and W fibers. B and W fibers are tougher than SiC fibers, while are more reactive with TiAl. If good protection layers are developed, B and W fibers can be applied for TiAl matrix. When protection layers has insufficient shear stress, roughening of fiber surface is effective in transferring stress from fibers to matrix. In this study, the following subjects have been investigated to develop good protection layers for TiAl matrix and to improve stress transfer from fibers to matrix:

Formation of BN and TiB_2 protection layers and optimization of layer thickness

B fibers were coated with Ti by using PVD method, and were heat treated to form TiB_2 layers on the surfaces. The fiber strength was decreased with increasing the layer thickness. It is due to the heterogeneous formation of TiB_2 and the pits of fibers by the formation of TiB_2. The thin layer of less than 1μm is desirable to prevent fiber strength from decreasing.

W fibers were coated with BN by slurry method, and TiAl matrix were reinforced with the BN-coated fibers. BN protection layer showed good performance for suppressing the interfacial reaction.

Effect of surface morphology on the strength of W fiber

The surface of W fiber was successfully roughened by oxidizing method. It is obvious that the optimized roughness can keep the original fiber strength and transfer stress sufficiently from fibers to matrix.

Keywords: TiAl matrix composite, B fiber, W fiber, protection layer, BN, TiB_2

107 Development of Porous Ceramics Impregnated with Ionic Conductive Materials

H. Nakamura, Environmental Performance Division
[April 1995 to March 1998]

Recently, research works on solid high ionic conductor have been mainly focused on oxygen

ion conductor such as ZrO_2, proton conductor such as $SrCeO_3$ and sodium ion conductor such as β-Al_2O_3.

One of the reasons why no other solid electrolytes have been developed as high ionic conductor is that cracks caused by grain growth or voids along grain boundaries tend to initiate in the sintered materials prepared for the solid electrolyte.

The objective of this study is to develop a new type of solid electrolyte in which grain boundaries or voids are extremely decreased by impregnation of liquid compounds (M_2O - B_2O_3 - M_2SO_4, M = Li,Na,K) into the porous oxides. Subsequently,its electrical properties will be evaluated by the measurement of electrical conductivity, the investigation of polarizing behavior and the determination of charge carrier. Furthermore, the thermal characteristics will also be evaluated using various thermal analysis methods.

Keywords: ionic conductor, solid electrolyte, charge carrier, electrical conductivity

Materials for mechanical application

108 High Temperature Mechanical Properties of Particulate Reinforced Titanium-Based Metal Matrix Composites

M. Hagiwara, Mechanical Properties Division

[April 1994 to March 1997]

Titanium alloys are attractive materials for aircraft and automobile applications due to their high strength/weight ratio. However, the service temperature is limited to 600°C due to a degradation of tensile strength, creep resistance, thermal stability and environmental resistance. Moreover, Ti alloys exhibit lower stiffness and poor abrasion-related properties than nickel-based alloys. The dispersion of ceramic particulates such as TiB into Ti matrix is expected to overcome these drawbacks. These particulates metal matrix composites (MMC's) have isotropic properties and can be processed more cheaply using the conventional near net shape methods. However, mechanical property data available for these types of MMC's is still lacking.

This research program has been aimed to produce Ti-based particulates MMC's using the advanced powder metallurgy (P/M) processes such as blended elemental and rapid solidification techniques. Firstly we have discussed the processing conditions in more detail. Secondly, Ti-based MMC's such as P/M Ti-6Al-2Sn-4Zr-2Mo/5 ~ 20TiB,Ti_3Al/10TiB and Ti/TiC have been produced using the best processing conditions obtained, and high temperature mechanical properties, especially creep and fatigue, have been evaluated quantitatively.

Keywords: particulate-reinforced, titanium, MMC's, mechanical properties, powder metallurgy

Related Papers

1. M. Hagiwara, S. Emura, Y. Kawabe, N. Arimoto, and S. Mori, "Properties of P/M Processed Titanium Alloy/Particulate Composite", *Metallurgy and Technology of Practical Titanium Alloys*, ed. S. Fujishiro, TMS, (1994): 363–370.
2. M. Hagiwara, S. Emura, Y. Kawabe, and S. J. Kim, "In-Situ Reinforced Titanium-Based Metal Matrix Composites", *Synthesis/Processing of Lightweight Metallic Materials*, ed. F. H. Froes, TMS, (1995): 97–106.

109 Design of Refractory Superalloys

H. Harada, Computational Materials Design Division

[April 1995 to March 2000]

The temperature capability of the Ni-base superalloy has been improved by 400 ℃ since it was introduced in 1945; the capability of the latest single crystal superalloys is approaching 1100 ℃. However, it is obvious that there will be a limitation which comes from the melting points (~1350 ℃) of the Ni-base superalloys.

In this project we design "Refractory Superalloys" which are defined by us as alloys with fcc/$L1_2$ coherent microstructures similar to Ni-base superalloys and yet with considerably higher melting points. A computer model based on statistical thermodynamics calculation is employed in the alloy design. Metallic elements with high melting points, such as Ir and Rh, has been examined experimentally for possible use as the base metal in the refractory superalloys. It has been shown that both Ir and Rh can be precipitation hardened by $L1_2$ phase to exhibit high yield strengths at ultra-high temperatures, e.g., 220MPa at 1800℃ for Ir-15at%Nb alloy. Characterization of the micro-structure and evaluation of the ultra-high temperature creep strength/oxidation resistance are being carried out.

Keywords: computer modelling, refractory superalloy, creep strength, Iridium, Rhodium

Related Papers

1. Y. Yamabe, Y. Koizumi, H. Murakami, Y. Ro, T. Maruko, and H. Harada, "Development of Ir-base Refractory Superalloys", *Scripta Materialia* , 35(1996): 211–215.
2. Y. Yamabe-Mitarai, Y. Koizumi, H. Murakami, Y. Ro, T. Maruko, and H. Harada, "Rh-base Refractory Superalloys for Ultra-high Temperature Use", *Scripta Materialia*, 36(1997): 393–398.

110 Effect of Particulate Distribution on the Mechanical Properties of Ti-Based Particulates Composites

M. Hagiwara, Mechanical Properties Division

[April 1995 to March 1996]

Titanium-based particulates-reinforced composites (MMC's) have a strong application potential for aerospace and automobile industries due to their low density, high specific strength and attractive high temperature strength. However, the effect of particulate morphology such as diameter, width, dimension and aspect ratio on the mechanical properties is not fully understood. In the present study, Ti/TiC MMC's with different diameter of TiC particulates were produced. The fundamental relationship between particulate diameter and tensile properties were then examined.

The Ti/TiC MMC's were produced by mechanical alloying pure titanium powder and fine carbon powder in a high energy planetary ball mill and subsequent HIP'ing at 1273K under 200MPa pressure. TiC diameter were found to be varied from 2μm to 20μm depending on both applied energy during ball milling and annealing temperature after HIP'ing. The finer TiC particulates were formed by increasing the applied energy and decreasing the annealing temperature. The tensile strength and ductility showed higher values for MMC's with smaller diameter of TiC particulates. For example, with decreasing TiC diameter from 14.0μm to 5.9μm, the corresponding tensile strength increased from 850MPa to 925MPa, and elongation increased from 1.8% to 6.4%.

Keywords: titanium, particulate composites, mechanical alloying, tensile property

Related Paper

1. M. Hagiwara, S. Emura, Y. Kawabe, and S. J. Kim, "In-Situ Reinforced Titanium-Based Metal Matrix Composites", *Synthesis/Processing of Lightweight Metallic Materials*, ed. F. H. Froes, TMS,(1995): 97–106.

111 Intelligent Structural Materials

S. Matsuoka, Environmental Performance Division

[April 1991 to March 1995]

Recently, a new material concept, known as intelligent material or smart material, has been proposed and developed to establish the reliability of engineering structures such as air crafts, space structures and nuclear power plants. The intelligence of the material is defined as self-detectability for environmental changes and feasibility of sensing, processing and actuating.

In this study, fundamental research has been carried out in order to impart the intelligent functions to the metallic materials for structural use. Small cavities which do not deteriorate the mechanical properties exist in the materials. An attempt has been made to implant the sound-emitted material, phase-transformed material or surface-film-controlled material into the cavities. The implantation could make the material possible to self-sense and self-restore the damage during operation. A nanotechnology based on a scanning tunneling microscope (STM) and atomic force microscope (AFM) has also been developed to evaluate the intelligent functions of the materials from atomic scale viewpoint.

Y_2O_3 particles in Fe-20Cr alloy, Pb particles in two stainless steels, SUS304 and SUS403, and a small addition of Zr in Fe-27Cr-35Ni alloy have been found to arrest the long fatigue crack growth at elevated temperatures. In the current year, Y_2O_3 and Pb particles and Zr addition also showed the arrest function in the short fatigue crack growth near the notch root at elevated temperatures. Accordingly, Y_2O_3 and Pb particles and Zr addition increased the fatigue limits of notched specimen at elevated temperatures, as compared with those for host materials.

Keywords: intelligent materials, materials damage, self-sensing, self-restoring, nanotechnology

Materials for electronics application

112 Structure Control and Electromagnetic Properties of High Temperature Superconductors

K. Togano, 1st Research Group

[April 1993 to March 1997]

The purpose of this study is to establish the basic

technologies to control the structure of high temperature superconductors (HTSC) in synthesizing them by melt or vapor process. The relation between the structure and electromagnetic properties is also studied to understand the vortex state and pinning mechanism of HTSC. The informations obtained here are feedbacked to the processes to optimize their parameters. Following four subjects are being studied.

Relation Between Microstructure and Critical Current

Comprehensive works on the microstructure and phase changes during the partial melting process for $Bi_2Sr_2Ca_1Cu_2Ox$(Bi-2212) are being carried out in this subject. In order to improve the mechanical properties of Bi-2212/Ag composite tape, the addition of elements such as Mg and Ni to Ag substrate tape is studied. Coils were made by using the Bi-2212/Ag alloy composite tape and tested to generate magnetic field.

Elucidation of Electromagnetic Behavior

The purpose of this subject is to establish a new concept of mixed state of HTSC. Large and high-quality single crystals of Bi-2212 were prepared by zone melting technique with the infrared image furnace, which were used for precise measurements of resistivity change and microwave response. These results were analyzed in connection with the phase change of vortex state and intrinsic Josephson junction. We have also succeeded to fabricate single crystals of new intermetallic compound superconductors of borocarbide system.

Structure Control by Thin Film Synthesis

By using alternative sputtering technique, we succeeded in preparing metastable structures up to n=7 of $Bi_2Sr_2Ca_{n-1}Cu_nO_x$ and superlattices composed of structures with different n. The Tc change of the superlattices suggested us that the superconductivity is governed by the averaged hole concentration of the mother structures with different n. We are also challenging the synthesis of metastable structure of borocarbide new intermetallic compound.

Microstructure Control by Vapor Deposition Technique

Studies on the texture control of $Y_1Ba_2Cu_3O_x$ thin film are being carried out to overcome the weak link problem of this material. We have succeeded in obtaining three dimensionally controlled crystal orientation for YSZ buffer layer on a Hastelloy tape using a modified bias sputtering technique. The YBCO film deposited on this buffer layer shows in-plane alignment, resulting in a large improvement of transport critical current density. Other materials are also being examined for buffer layer.

Keywords: structure control, melting process, vapor process, mixed state

113 Effect of High Energy Ion Irradiation on $Bi_2Sr_2CaCu_2O_x$ and $YBa_2Cu_3O_y$

H. Kumakura, 1st Research Group

[April 1995 to March 1999]

A columnar defect introduced by high-energy heavy-ion irradiation is one of the most effective flux pinning centers in high-T_c oxide superconductors. In this program, 180MeV Cu^{11+} irradiation was performed on $Bi_2Sr_2CaCu_2O_x$(Bi-2212) and $YBa_2Cu_3O_y$(Y-123), and the obtained results were compared each other.

Samples were grain oriented Bi-2212 and Y-123 thick films. 180MeV Cu^{11+} irradiation was performed at 100K with fluence of 10^{11}-3×10^{13} ions/cm^2 using the Tandem accelerator at the Japan Atomic Energy Research Institute. Critical current density J_c and pinning characteristics were evaluated from the hysteresis in D.C. magnetization curves. The increase in the J_c values by the irradiation, $J_{c,\ after\ irrad.} - J_{c,\ before\ irrad.}$ is comparable for both superconductors at low temperature region. At high temperatures, on the other hand, columnar defects introduced by the irradiation were much more effective as pinning centers in Y-123 than those in Bi-2212. This indicates that the defects introduced by the irradiation act as much more effective pinning centers in Y-123 than in Bi-2212. Before the irradiation, the flux pinning force density F_p versus magnetic field curve of Bi-2212 was much different from that of Y-123. After the Cu^{11+} irradiation, this large difference of the F_p-B curves between Bi-2212 and Y-123 was still observed.

The decay of magnetization was measured as a function of time. The decay of magnetization increased with temperature and magnetic field for both non-irradiated and irradiated oxides. The decay of magnetization of Bi-2212 is much larger than that of Y-123 not only for non-irradiated samples but also for irradiated samples, suggesting that the decay of magnetization depends more sensitively on the material rather than on the kinds of pinning centers. This difference of the decay of magnetization between

Bi-2212 and Y-123 becomes larger with increasing temperature and magnetic field.

All these results mentioned above indicate that the defects in Y-123 are more effective as pinning centers than those in Bi-2212. This difference can be understood in terms of the difference in two-dimensionality of the oxides.

This research was performed in collaboration with the Japan Atomic Energy Research Institute.

Keywords: critical current density, flux pinning, two dimensionality

Related papers

1. Y. Kazumata, S. Okayasu, H. Kumakura, and K. Togano, "Bi-2212 films and tapes irradiated by 120MeV oxygen ions", *Physica* C, 235-240(1994): 2825–2826.
2. H. Kumakura, K. Togano, N. Tomita, E. Yanagisawa, S. Okayasu, and Y. Kazumata, "Comparative study on 180MeV Cu^{11+} irradiation effect on textured $YBa_2Cu_3O_x$ and $Bi_2Sr_2CaCu_2O_y$", *Physica*, C251(1995): 231–237.
3. X. Gao, Y. Kazumata, H. Kumakura, and K. Togano, "Effects of 230MeV Au^{14} irradiation on $Bi_2Sr_2CaCu_2O_x$", *Physica*, C250(1995): 325–330.

114 Development of Superconducting Magnet for Magnetic Separation

H. Kumakura, 1st Research Group

[April 1995 to March 1999]

Magnetic separation is a promising method as a separation technique in many technological fields such as steel industry, mining industry, nuclear fuel recycle, and so on. The fields available with conventional electromagnets are limited to 1 Tesla by the saturation of iron. In addition, the creation of large field volumes is costly in terms of copper, iron and electric power. For these reasons, superconducting magnets for magnetic separation is proposed. However, the use of liquid helium reduces the advantage of the superconducting separator magnets. Oxide superconductors with critical temperatures much higher than those of metallic superconductors are very promising from this point of view. Operation at higher temperatures using a cryocooler or liquid nitrogen significantly reduces cryogenic costs. In this research program, we will develop a high-T_c oxide superconducting separator magnet. In 1995, we developed small bismuth-based oxide superconducting magnet and tested it using cryocooling system .

Bismuth-based oxide superconductor/silver composite tapes were fabricated by the combination of slurry-coating method and melt-solidification method. The tape conductors were wound into small pancake coils with outer diameter of 50mm, and fixed with epoxy resin. Four pancake coils were stacked and connected in series. This magnet was set at the cooling stage of the Gifford-McMahon(GM) cryocooler, and tested at temperatures from 10 to 80K in a zero bias field. Four coils show almost equal critical current density J_c at all temperatures. J_c at 10K was as high as $2 \times 10^5 A/cm^2$. J_c decreased with increasing temperatures. However, the decrease of J_c was not crucial up to 40K. This result suggests that a bismuth oxide superconducting magnet can generate 1-2 Tesla at 20-40K where the cryocooler can be efficiently used. The result indicates a great possibility of bismuth oxide superconductors for the magnetic separation magnets.

In 1996, we will make a larger magnet and define the specification of the prototype magnet.

Keywords: bismuth oxide superconductor, magnet test, cryocooling

Related Paper

1. N. Tomita, M. Arai, E. Yanagisawa, T. Morimoto, H. Kitaguchi, H. Kumakura, K. Togano, T. Kiyoshi, K. Inoue, H. Maeda, K. Nomura, and J.C. Vallier, "Development of Superconducting Magnets using Bi-2212/Ag Tapes", *IEEE Trans. Appl Superconductivity*, 5(1995): 520–523.

115 Characterization and Application of Superconducting Thin Films Synthesized by Atomic Layer-by-Layer and Epitaxial Growth Methods

K. Nakamura 1st Research Group

[April 1995 to March 2000]

In the preceding project on high Tc superconductors, we have investigated on the application of atomic layer-by-layer deposition technique to the growth of Bi and Y based superconducting films, and the application of a modified bias sputtering technique to the preparation of in-plane textured buffer layers on metallic substrate for the epitaxial growth of YBCO thick films. In the present project we attempt a further development based on the above mentioned results. In the atomic layer-by-layer growth we are investigating surface and inner defects and are aiming to get a controlled surface

morphology in the atomic scale. For example, in the Bi system, we are investigating the effect of various deposition conditions in the sputtering and laser ablation deposition techniques on the formation of various defects. These defects observed in the as-deposited films include intergrowth and other stacking faults, surface roughness including particle formation, and island growth including screw dislocation in YBCO films.

In order to developed in-plane aligned YBCO films, a new technique named "plasma beam assisted deposition (PBAD)" is proposed to grow buffer layers on long tape or large area substrates. Furthermore, using modified PBAD processes, we are trying to fabricate textured films simultaneously on one side or both sides of plural pieces of tape substrates. The results indicates that PBAD is one of the most promising potential techniques towards future large scale application of YBCO films.

Keyword: atomic layer epitaxy, superlattice, oxide superconductor, Boro-carbide superconductor, textured buffer layer, microwave cavity, high temperature plasma

Related Papers

1. T. Hatano, A. Ishii, and K. Nakamura, "Charge transfer enhancement on Tc in $(Bi_2Sr_2Ca_3Cu_4O_{12+\delta})$ $(Bi_2Sr_2CaCu_2O_{8+\delta})$ superlattices", *J. Appl. Phys.* 79(1996): 2556–2573.
2. J. Ye and K. Nakamura, "Relaxation of crystallographic defects of $YBa_2Cu_3O_{7-\delta}$ thin films by heat treatment and its effect on Tc", *Physica C*, 254(1995): 113–123.
3. J. Ye and K. Nakamura, "Defects in $YBa_2Cu_3O_{7-\delta}$ YBCO thin films and their influence on Tc", *MRS Symposium Proceedings*, 401(1996): 429–434.
4. M. Fukutomi, S. Kumagai, and H. Maeda, "Fabrication of $YBa_2Cu_3O_y$ thin films on textured buffer layers grown by plasma beam assisted deposition": to be published in *Australia J.Physics*.

116 Stabilities of Superconducting Materials

H. Wada, High Magnetic Field Station

[April 1994 to March 1999]

The main purpose of this study is to define stabilities of superconducting materials under various conditions they may experience when wound to superconducting magnets. Stabilities of new, promising superconducting materials including high-temperature oxide superconductors are examined in terms of temperature, magnetic field and magnetic field and mechanical stress/strain.

In fiscal year 1995 temperature dependence of critical currents of new Nb_3Al multifilamentary wires fabricated by rapid heating and quenching process was studied. Critical currents were considerably decreased with increasing temperature. In the magnetic field of 12 T a critical current density of $6\times10^8 A/m^2$ at 6K was decreased to $8\times10^7 A/m^2$ at 10K. Magnetic field dependence of critical currents were nearly the same in the temperature range of 6K to 16K tested. Furthermore, upper critical fields were evaluated on the basis of critical currents vs. magnetic field data. For the optimized wire upper critical fields were 2.0 T, 8.9 T, 15.9 T and 22.9 T for 16 K, 13 K, 10 K and 6 K, respectively. The upper critical field of about 25 T at 4.2 K may be estimated from the extrapolation of these values. It is higher than that of conventionally processed Nb_3Al wires and comparable to that of practical $(Nb,Ti)_3Sn$ wires. Measurements of superconducting properties under mechanical stress/strain of present Nb_3Al wires are to be planned.

Keywords: Nb-tube processed Nb_3Al wires, critical current, critical field temperature dependence

117 Development of 1 GH_Z NMR Spectrometer

H. Wada, High Magnetic Field Research Station

[April 1995 to March 2001]

High *Tc* oxide superconductors (HTS) are expected to be able to induce much higher magnetic fields than low *Tc* metallic superconductors (LTS) when used at 4.2 K. We have initiated a program in which we will develop a 1 GHz superconducting NMR spectrometer including a 23.5 T superconducting magnet; such magnet must be constructed using HTS coils in combination with LTS coils. In fiscal year 1995, preliminary design work of the NMR system was done, together with the development of high performance metallic superconductors and small HTS coils to be used for the NMR magnet in the system.

In our design the LTS coils are operated in persisting mode at a field of 21.1 T in a 150 mm diameter bore. The HTS coil is expected to generate an additional field of 2.4 T in a 51 mm room temperature bore. The cryostat shall be composed of two vessels. This enables parallel development of the LTS and HTS coils, and we can later replace the HTS coil easily when necessary.

The LTS coils in outer vessel is cooled with atmospheric superfluid helium at 1.8 K, while the inner HTS coil vessel is filled with liquid helium.

Development of high performance metallic superconductors is one of the key issues of this program. LTS coil conductors need to have high yield strength as well as high critical current density in order to be wound compact. A Nb_3Sn conductor reinforced with Ta was newly developed. Its 0.2 % yield strength was 358 MPa at 4.2 K. This is the highest value ever reported on the reinforced monolithic Nb_3Sn conductors.

Since HTS coil development requires a lot of technological challenges, we have performed R&D studies on small HTS coils as the first step. A Bi-2212 coil made of double-pancakes generated an incremental field of 1.8 T in a backup field of 21 T. The total field of 22.8 T in fully superconducting state is a new world record.

Keywords: NMR spectrometer, high field magnet oxide superconductor

Related Papers

1. K. Inoue, T. Kiyoshi, A. Sato, H. Aoki, K. Itoh, H. Wada, H. Maeda, R. Ogawa, Y. Kawate, K. Takabatake, T. Horiuchi, J. Kida, and K. Higuchi, "Development Project of 1 GHz NMR Spectrometer", *Proc. ICEC16/ICMC*, (1996): 1103–1106.
2. K. Itoh, M. Yuyama, T. Kiyoshi, T. Takeuchi, K. Inoue, H. Maeda, T. Miyatake, and M. Shimada, "Development of NbTi and Nb_3Sn Conductors for 1 GHz NMR Spectrometer", *ibid*, 1735–1738.
3. T. Kiyoshi, K. Inoue, M. Kosuge, K. Itoh, M. Yuyama, and H. Maeda, "NRIM R&D Program on HTS Coils for 1 GHz NMR Spectrometer", *ibid*, 1099–1102.

118 Development of High Strength/High Conductivity Materials for High Field Magnets

K. Inoue, High Magnetic Research Station

[April 1995 to March 1998]

In this study we are developing new high-strength/high conductivity materials for resistive high-field magnets, such as Bitter-type magnets, polyhelix-type magnets, and non-destructive pulsed magnets. Recently we successfully developed a new Cu-Ag microcomposite alloy, which is composed of Cu-based alloy matrix and Ag-based alloy filaments, has a promising combination of high mechanical strength (0.7-1.1 GPa) and high electrical conductivity (75-83 %IACS) at room temperature. Intermediate annealing two or three times at about 350-450°C during cold-working is very effective to improve not only its mechanical strength but also its electrical conductivity through the deposition of solute elements (Ag in the Cu-based alloy matrix and Cu in the Ag-based alloy filaments). This year we optimized the fabrication process of Cu-Ag microcomposite alloy to obtain ultra-high strength as well as high conductivity. Heavily cold-drawn with repeating the intermediate annealing, the mechanical tensile strength increased effectively without severe decay of conductivity. In this optimized process the Cu-24wt%Ag were cold drawn up to a total drawing strain of $\eta = 5.8$ with intermediate annealing 5 times at 330-430°C. The drawing reduction ratios are defined as terms of logarithmic strain by $\mu = \ln (A_0/A)$, where A_0 and A are the initial and reduced cross section areas, respectively. Tensile strength of 1.5 GPa has been realized in the Cu-Ag alloy while its conductivity is about 65 %IACS at room temperature. Furthermore, the wire can be wound to small diameter without surface microcracking. However, it needs much more effort to wind the ultra-high strength wire into pulsed high-field magnets because of its large spring-back force.

Keywords: Cu-Ag microcomposite alloy, high strength/high conductivity, high-field conductor material

Related Papers

1. Y. Sakai, K. Inoue, and H. Maeda, "New High-Strength, High-Conductivity Cu-Ag Alloy Sheets", *Acta Metall. Mater.*, 43(1995): 1517–1522.
2. S. I. Hong, M. A. Hill, Y. Sakai, J. T. Wood, and J. D. Embury, "On the Stability of Cold Drawn Two-Phase Wires", *Acta Metall. Mater.*, 43(1995): 3313–3323.

119 Microstructure and Electromagnetic-Characteristics Studies on V_3Si Multifilamentary Superconductors

T. Takeuchi, High Magnetic Field Station

[April 1994 to March 1997]

A V_3Si multifilamentary conductor has been developed as a new A15-type AC superconductor. V_5Si_3 layers are preferentially formed between the bronze matrix and V_3Si filaments at the early stage of diffusion reaction. The resistivity of V_5Si_3 is ~15 μΩcm at 4.2 K, which is expected to be high enough to separate the filaments from each other for electromagnetic decoupling. The combination of adjusting the total proportion of V to Si in the

Cu-Si/V composite to ~3 and reducing V filaments to ~1 μm enables the completion of the reaction in a short time; the initially formed V_5Si_3 appropriately decomposes the mostly V3Si probably without grain growth is produced to achieve a high overall J_c (1.3×10^9 A/m^2 at 5 T). In order to investigate the flux pinning mechanism, the angular dependence of the pinning force density F_p with respect to magnetic field direction was examined in detail with a flattened multifilamentary conductor. From the analogy to Nb_3Sn conductors, both the grain boundary and S (superconductor:V_3Si) - N (normal conductor: V_5Si_3, (Cu-Si), V) interface are believed to act as effective pinning centers. However, it is so far difficult to separate and evaluate the individual contribution as long as the wire specimen is used. On the other hand, in the flattened conductor, S-N interface are parallel to the conductor surface and columnar grains of V_3Si are grown perpendicular to the surface. Thus, two kinds of F_p peaks appear when fluxoids and the conductor surface make angles of $n\pi$ and $(2n+1)\pi/2$ (n: integer), demonstrating actually the existence of two kinds of pinning centers. We have evaluated the peak height of F_p by considering the interface density, and thus concluded that an elemental pinning force of S-N interface is 2-3 times larger than that of grain boundary pinning.

Keywords: flux pinning, ac loss, V_5Si_3, image analysis

Related Paper

1. T. Takeuchi, Y. Nemoto, K. Itoh, Y. Iijima, M. Kosuge, K. Inoue and H. Maeda, "Superconducting Properties of V_3Si Multi-filamentary Conductor": to be published in *Adv. Cryo. Engine.* 42(1996).

120 Fabrication of High Strength Oxide Superconducting Wires for High Magnetic Field Applications

Y. Tanaka, High Magnetic Field Station
[April 1995 to March 1997]

Bi-2223 high temperature oxide superconductors are of great interest for high current and high magnetic field applications such as power transmission cables and high field magnets. Producing conductors with high critical current density, J_c, high critical current, I_c, long lengths and high mechanical strength are practically essential to realize these applications. It has generally been thought in oxide superconfuctors that the Jc property is strongly dependent on the oxide microstructures such as many kinds of precipitate particles, dislocation, crystal defects introduced by particle irradiation techniques or transformation during heat treatment. In the present work Bi-2223 superconducting tapes were prepared by the powder-in-tube technique using Ag-10at%Cu alloy sheaths with and without a small amount of doping elements such as Ti, Zr or Hf. The Ag-10at%Cu alloy sheath enables to increase the mechanical strength by two to three times as that of pure Ag sheath. The doped samples have exhibited high critical current density, Jc due to a modified grain structure of Bi-2223 phase. Micrograph examinations on these samples revealed large and plate-like Bi-2223 grains at the sheath/core interface along with a more dense and aligned microstructure inside, especially for the Ti and Hf dopings. The effect enhancing the formation of Bi-2223 phase is more significant for the AgCu alloy sheath with higher Cu concentration. Higher volume fraction of the Bi-2223 phase was obtained for the doped samples with an improved texture, resulting in generally higher J_c. Distributions of doped elements are being analyzed with respect to microstructural defects.

This research was performed in collaboration with Sumitomo heavy industries Co. Ltd.

Keywords: Bi-2223 tape, powder-in-tube technique, element addition, high-Jc

Related paper

1. M. Ishizuka, Y. Tanaka, and H. Maeda, "Superconducting properties and micro-structures of Bi-2223 Ag-Cu alloy sheathed tapes doped with Ti, Zr or Hf", *Physica*, C 252(1995): 339–347.

121 Evaluation of Long Oxide Superconductor Wires

K. Itoh, High Magnetic Field Research Station
[April 1995 to March 2000]

To realize a magnet made of a high-temperature oxide superconductor, it is indispensable to have a long wire with high quality and homogeneity. We often use short-length specimens cut from the different positions of the whole length of a wire to check the quality and homogeneity. However, such technique does not only waste a wire but also disable to use it for magnet winding.

In this study we develop techniques to measure superconducting properties such as the critical current, ac losses, thermal and electro-mechanical properties, of a long wire without giving any damage to the wire. In addition, we develop measurement techniques on a coil shaped

specimen, and compare the results with those obtained by the techniques on short- and long-length specimens. Such comparison would be useful for the development of wire fabrication and winding techniques.

Keywords: oxide superconductor, evaluation, measurement technique, long length

122 Study on the New Intermetallic Compound Superconductor

K. Togano, 1st Research Group
[April 1995 to March 1996]

Recent discovery of a new family of borocarbide intermetallic superconductors of $[RE]_1T_2B_2C_1$, where RE=rare earth elements and T=Ni, Pd, Pt, attract again the interest in intermetallic compounds as a possible road to high temperature superconductivity. The study on the physical properties already starts for Ni systems (RE-Ni-B-C), whose single phase can be easily synthesized by conventional methods. However, the YPd_2B_2C compound, which shows the highest transition temperature Tc of 23K, can never be formed from nominal composition of 1221 by conventional melting methods. It can be formed only from the nominal composition of around $YPd_5B_3C_{0.3}$, therefore the material synthesized is composed of multiple phases. From several experimental results on the phase diagram,we speculate that the 1221 phase is formed by peritectic reaction which exists far from the liquidus curve and is stable only at high temperature region above 1,000°C.

In this study, we investigated the effect of rapid quenching on the formation of YPd_2B_2C compound. The ingot with nominal composition of 1221 prepared by a conventional arc melting showed no sign of superconductivity. Quenching was done by arc melting a small piece of the sample and splashing the droplet onto a copper substrate by argon gas jet. The quenched sample showed apparent superconducting transition at about 22K. On the other hand, the liquid quenching of $YPd_5B_3C_{0.3}$ resulted in a complete disappearance of superconductivity. This is due to the complete suppression of 1221 equilibrium peritectic reaction. This result indicates that the 1221 liquid was largely supercooled and the 1221 phase was directly formed from the supercooled liquid. We also succeeded to synthesize the metastable $LuPd_2B_2C$ phase by the liquid quenching, which showed Tc of 15K.

The materials prepared by the liquid quenching are still multiple phases, however, the experiments demonstrated that the metastable 1221 phases can be formed from supercooled liquid.

Keywords: superconductor, borocarbide, liquid quenching

123 Application of Cu-Ag Alloy Plates to Extremely High-Field Magnets

K. Inoue, High Magnetic Field Research Station
[April 1995 to March 1996]

Cu-Ag alloy plate, newly developed at NRIM, is composed of Cu-based alloy matrix and Ag-based alloy micro-filaments, and a promising material for resistive high-field magnets due to the useful combination of high mechanical strength and high electrical conductivity. Bitter-type water-cooled magnet is one of the hopeful applications of the Cu-Ag alloy plate. National High Magnetic Field Laboratory has the most powerful DC power supply and the most powerful water-cooling system for operating water-cooled magnet. In addition there are many excellent magnet designers having much experience to fabricate Bitter-magnets in NHMFL. For evaluating the new material as the conductive material in Bitter-type water-cooled magnet, we performed the present collaboration study with NHMFL.

According to the design proposed by NHMFL, we fabricated Cu-Ag alloy plates with optimizing the fabrication conditions and send them to NHMFL. At NHMFL the Cu-Ag alloy plates were processed into Bitter-plates, assembled into a Bitter-type water-cooled magnet and then tested with using the most powerful power source and water-cooling system. On February, 1996 we successfully generated steady magnetic fields up to 34 T in a clear bore of 32 mm. This value is a new world record of steady magnetic field generated by an entirely water-cooled magnet. The result has demonstrated the great value of Cu-Ag alloy plate as the conductor material in Bitter-type water-cooled magnet. The previous record were performed by a Bitter-type water-cooled magnet with using Cu-Be alloy plates, of which conductivity are about half of the Cu-Ag alloy plates. The excellent properties of Cu-Ag alloy plate are the main causes of this success.

This research was performed in collaboration with National High Magnetic Field Laboratory.

Keywords: Cu-Ag alloy, Bitter-type magnet, water-cooled magnet

Related Papers

1. Y. Sakai, K. Inoue, and H. Maeda, "New High-Strength, High-Conductivity Cu-Ag Alloy Sheets", *Acta Metall. Mater.*, 34(1995): 1517–1522.
2. Y. Sakai and H. J. Schneider-Muntau, "Ultra High-Strength, High-Conductivity Cu-Ag Wires": to be published in *Acta Mettal. Mater.*

124 Development of High-Jc Bi-Oxide Superconducting Wires

Y. Tanaka, High Magnetic Field Research Station
[April 1995 to March 1996]

Bi-2223 tapes using Ag-Cu alloy sheath doped with Ti, Zr or Hf have been fabricated by the powder-in-tube technique in order to increase mechanical strength along with improved Jc property. Ag-10at%Cu alloy tubes doped with Ti. Zr or Hf, by an amount of less than 1 at% have been prepared and filled with Bi-2223 powder to make composites. All these composites were rolled to thin tapes after swaging and drawing and then submitted to heat treatment to form Bi-2223 superconducting phases. Microstructures, superconducting properties and mechanical properties have been measured by XRD, SEM, HRTEM, SQUID, 4-probe resistive measurement and micro- Vickers hardness.

It is observed that Ag-7～10at%Cu alloys have mechanical strength with 2 to 3 times larger than that of pure Ag and show no decrease in Tc or Jc properties of the Bi-2223. As for the effect of the doping Ti, Zr or Hf into the AgCu alloy sheaths it is found that the addition with less than 0.1 at% increases the Jc remarkably, especially for Ti and Hf dopings. In the doped samples larger and plate-like Bi-2223 grains are formed which seem to be strongly responsible for the high Jc property observed due to an improved texture and electrical connections between grains. Furthermore, it is suggested that a new kind of flux pinning center is introduced into the Bi-2223 crystalline lattice of the Hf doped sample according to the results by SQUID measurements. Studies on microstructures by high resolution transmission electron microscopy have been continued.

This research was performed in The Bilateral Joint Research by Special Coordination Funds Promoting for Science and Technology (FY1995).

Keywords: Bi-2223 tape, powder-in tube technique, element addition, hig h-Jc

Related Papers

1. Y. Tanaka, M. Ishizuka, H. Maeda, and T.Hashimoto, "Influence of doping Ti, Zr or Hf into Ag-Cu alloy sheath of Bi-2223 tapes", *ICEC16/ICMC*, Kitakyusyu, Japan, (1996): May 20–24.

Magnetic Materials

125 Research on Quantum Magnetic Properties and Spinic Functions of Mesoscopic Magnetic Materials

I. Nakatani, T. Furubayashi, H. Mamiya, and T. Taniyama
[April 1996 to April 2002]

The objective of the project is to explore the basic research, technology, and applications of novel magnetic materials with mesoscopic sizes. In all sort of fundamental phenomena in magnetism, there exist corresponding characteristic lengths, e.g., distance of exchange interaction, distance of magnetic dipole interaction, magnetic domain size, spin diffusion length, and so on. The project includes three types of magnetic materials with mesoscopic sizes of dimensions in around 100nm, 10nm and 1nm regime, respectively. This work has two main components.

First, there is a exploration of fabrication method for mesoscopic magnetic materials. These are electron-beam nanolithography to fabricate nanostructure of ferromagnetic substances with dimensions in several hundreds nm or sub-100nm, syntheses of magnetic colloids (magnetic fluids) of ferromagnetic iron-nitride particles, 10nm or sub-10nm in diameter, dispersed in liquid of mineral oil, and preparations of nanogranular magnetic materials that ferromagnetic fine particles, several nm or 1nm in size, are embedded in solid matrix of insulator.

Second, there is the challenge that one can explore mesoscopic magnetic phenomena, from classical to the quantum limit. A new field that has come to be called "spin-polarized transport" is now growing. Although its roots are in the quantum description of solids, only recently new fabrication techniques for sophisticated materials described above allow to make wide-spread studies of the phenomenon and the development of device applications.

Keywords: mesoscopic magnetic material, quantum magnetic properties, spinic function

126 Basic Research for Development of Intelligent Materials Aimed at Interactions between Atoms or Molecules

I. Nakatani, Physical Properties Division
[April 1993 to March 1996]

The objective of the project includes studies on ultramicro fabrication techniques for magnetic substances and on magnetic quantum effects originated by the ultramicro structures. The research area is divided into three area corresponding to characteristic length of mesoscopic phenomena: These are mesoscopic magnetic substances with sizes of around 100nm, 10nm and 1nm in dimensions.

Electron-beam nanolithography and micromagnetic properties of nano-structured ferromagnetic materials(100nm class)

A novel reactive-ion-etching method for magnetic materials has been investigated and developed in the course of this project. This method has an ability of the key technology of micro-fabrications of magnetic substances. By applying the method, ferromagnetic Fe-Ni thin wire arrays with 250nm width and space were successfully fabricated.

Colloid of ferromagnetic fine particles (magnetic fluids) (10nm class)

Magnetic relaxation phenomena of the iron-nitride magnetic fluids are studied. It was clarified that the magnetic relaxation process of the magnetic fluids can be explained by the Néel-type relaxation added by dipole interaction between the particles. Superparamagnetic properties and magnetic relaxation were studied on 4 different types of iron-nitride magnetic fluids with different particle diameter from 6 to 10 nm. The relationship between viscosities of the magnetic fluids and volume fractions of solid particles was made clear.

Nanogranular magnetic materials (1nm class)

Nanogranular magnetic materials, Fe particles with 2nm in diameter embedded and well dispersed in insulating SiO_2 or MgF_2 matrix, were prepared by co-evaporation in ultrahigh vacuum system. The giant magnetoresistance (GMR), reaching 6.2% at 78K, was observed. It has been elucidated that the GMR effect is due to spin-polarized electrons tunneling between the Fe particles.

Keywords: intelligent material, magnetic material, ultramicro fabrication, mesoscopic phenomenon

Related Papers

1. I. Nakatani, "Ultramicro Fabrications on Fe-Ni Alloys Using Electron-Beam Writing and Reactive-Ion Etching", *IEEE Trans. Magn.* 32(1996): 4448–4451.
2. I. Nakatani, "Fabrications of Thin Wire Arrays or Fine Particle Arrays of Permalloy by Electron-Beam Nanolithography and Their Magnetic Properties", *Materia Japan*, 35(1996): 854–857.
3. T. Furubayashi and I. Nakatani, "Magnetic and Transport Properties of Granular Fe-MgF_2Films", *Mater. Sci. Eng.*, A, 217-218(1996): 307–309.
4. T. Furubayashi and I. Nakatani, "Giant Magentoresistance in Granular Fe-MgF_2Films", *J. Appl. Phys.* 79(1996): 6258–6260.
5. H. Mamiya and I. Nakatani, "Effect of Cooling Field on Magnetic Relaxation for an Iron-Nitride Fine Particle System", *J. Appl. Phys.* (1997): in press.
6. H. Mamiya, M. Onoda, T. Furubayashi, and I. Nakatani, "Structural and magnetic studies on vanadium spinel MgV_2O_4", *J. Appl. Phys.*, (1997): in press.

127 Fabrications and Spinic Functions of Mesoscopic Magnetic Materials

I. Nakatani, T. Furubayashi, H. Mamiya, and D. Kim

[April 1995 to April 1996]

The objective of the project includes studies on ultramicro fabrication techniques for magnetic substances and on magnetic quantum effects originated by the ultramicro structures.

The research area is divided into three areas corresponding to characteristic length of mesoscopic phenomena. These are mesoscopic magnetic substances with sizes of around 100nm, 10nm and 1nm in dimensions.

Electron-beam nanolithography and micro-magnetic properties of nano-stuructured ferromagnetic materials(100nm class)

A novel reactive-ion-etching method for magnetic materials has been investigated and developed in the course of this project. This method has an ability of the key technology of micro-fabrications of magnetic substances. By applying the method, ferromagnetic Fe-Ni thin wire arrays with 250nm width and space were successfully fabricated.

Colloid of ferromagnetic fine particles (magnetic fluids) (10nm class)

Magnetic relaxation phenomena of the iron-nitride magnetic fluids are studies. It was clarified that the magnetic relaxation process of the magnetic fluids can be explained by the Néel-type relaxation added by dipole interaction between the particles. Superparamagnetic properties and magnetic relaxation were studies on 4 different types of iron-

nitride magnetic fluids with different particle diameter form 6 to 10 nm. The relationship between viscosities of the magnetic fluids and volume fractions of solid particles was made clear.

Nanogranular magnetic materials (1nm class)

Nanogranular magnetic materials, Fe particles with 2nm in diameter embedded and well dispersed in insulating SiO_2 or MgF_2 matrix, were prepared by co-evaporation in ultrahigh vacuum system. The giant magnetoresistence (GMR), reaching 6.2% at 78K, was observed. It has been elucidated that the GMR effect is due to spin-polarized electrons tunneling between the Fe particles.

Keywords: mesoscopic magnetic material, electron-beam lithography, magnetic fluid, granular material

Related Papers

1. I. Nakatani, "Ultramicro Fabrications of Magnetic Materials by Electron-Beam Lithography," *Magn. Soc. Jpn.*, 19(1995): 831–839.
2. T. Furubayashi and I. Nakatani, "Magnetic Properties of Iron Fine Particles in Fe-MgF_2 Composite Films," *J. Magn. Magn. Mater.* 140-144(1005): 393–395.
3. T. Furubayashi and I. Nakatani, "Magnetic Properties of Granular Fe-SiO_2 Films," *J. Korea Magn. Soc.* 5(1995): 474–477.
4. H. Mamiya and I. Nakatani, "Dynamical Magnetic Properties of Iron-Nitride Magnetic Fluids," *J. Korea Magn. Soc.* 5(1995): 815–818.

Opto-materials

(128) Single Crystal Growth of New Nonlinear Optical Materials by Means of Controlling Crystal Symmetry

M. Sato, Physical Properties Division
[April 1996 to March 1999]

Single crystals for nonlinear optical materials are important for frequency modulation devices. It is usually required for this purpose that single crystal should have asymmetry. However, it is generally difficult to grow single crystals having crystal asymmetry even if new materials are discovered. It would be possible to obtain single crystals having crystal asymmetry by means of the substitution of constituent elements for another elements in order to form the asymmetry surroundings of substituent elements in micro scale. In this work, single crystal growth of these materials having crystal asymmetry will be tried by the Czochralski method from their melts and the crystal quality will be improved by means of controlling the crystal growth conditions. Furthermore, the optical property of the crystals will be evaluated using the single crystals grown.

In this year, $BaAl_2O_4$ substituted Al for B will be targeted on and synthesized polycrystalline sample. The nonlinear optical properties using SHG (second harmonic generation) intensity will be investigated.

This research is performed in collaboration with the Institute for Materials Research, Tohoku University.

Keywords: frequency modulation, crystal asymmetry, substitution

Material for energy application

(129) Energy Conversion Materials Fabricated with Composite Structures

I. A. Nishida, Physical Properties Division
[April 1996 to March 1999]

Thermoelectric(TE) materials have been widely used for the direct energy conversion systems. These materials convert thermal energy to electric power with quick response and without noise and mechanical vibration. Recently, the TE generators are mainly used for the electric source in the sea, space, and polar regions, and the TE cooling systems are mainly used for the precise temperature control in the semiconductor processing, optical and electronic devices. Therefore, it is important to develop TE materials with high efficiency.

The TE materials with high efficiency are given by the three characteristics, i.e., high Seebeck coefficient α, high electric conductivity σ and low thermal conductivity κ. The good TE materials can be found in the semiconducting compounds, alloys and their mixtures with very low values of the phonon thermal conductivity κ_{ph}, such as $Bi_{2-x}Sb_xTe_3$ and $Pb_{1-x}Sn_xTe$. The κ_{ph} is reduced by the phonon scattering of the deformation field in the crystal grains, grain boundary in the sintered bodies and composite materials.

In this study, the several preparation techniques and thermoelectric properties of TE materials with a composite structure are examined, and also the optimum composite structure for good TE materials is explained.

Keywords: energy conversion, thermoelectric materials, composite materials, thermoelectric material

Related Paper

1. H. T. Kaibe, Y. Tanaka, M. Sakata, and I. A. Nishida, "Anisotropic Galvanomagnetic and Thermoelectric Properties of *n*-Type Bi_2Te_3Single Crystal with the Composition of a Useful Thermoelectric Cooling Material", *J. Phys. Chem. Solids*, 50(1989): 945–950.

(130) Effect of Aging Degradation on Localized Corrosion of Structural Materials for Light Water Reactors

Y.Katada, Failure Physics Division
[April 1996 to March 2000]

The objectives of this research as one of the nuclear safety researches are to investigate the interaction between aged structural materials and the initiation of local corrosion such as stress corrosion cracking, corrosion fatigue in high temperature water, and to restrain the enlargement of local damage in weld joints by using a laser method.

Interaction between aged materials and local damage

Stress corrosion cracking tests and corrosion fatigue tests are conducted for aged materials such as temper embrittlement simulated by heat treatment, hydrogen embrittlement by cathodic treatment and so on. These tests are carried out to investigate the initiation of the local damage from the view-point of microscopic aspect by means of SEM, AFM, EDX and so on.

Restraint of enlargement of local damage by laser method

Weld joints of structural components including weld metal and heat affected zone (HAZ) are considered to be more sensitive than base metal for aging degradation because of the discontinuous micro structure, residual stress, segregation and so on.

Synthetic aged weld metal and HAZ will be produced by high heat input TIG arc welding and/or heat treatment and will be homogenized by rapid solidification treatment with a high power carbon dioxide laser up to 6 kW. Micro structure, segregation at the grain boundary, corrosion resistance and so on, of the rapid solidified layer will be investigated. At the same time a laser speckle method of high resolution with respect to place and time will be applied to solidified and/or HAZ to investigate the stress and strain behavior during laser treatment. Finally the recovery of damaged zone will be evaluated from the point of corrosion resistance.

Localized corrosion map

Localized corrosion map will be developed mainly in the field of high temperature water in terms of stress corrosion cracking data, electrochemical data, corrosion fatigue crack growth data, low cycle fatigue data and so on. The corrosion map will be useful for material selection in engineering design and for high accurate prediction of material damage.

Keywords: aging degradation, localized corrosion, light water reactor, laser, rapid solidification treatment

(131) Influence of Nuclear Transmutations on Low Activation Structural Materials for Fusion Reactor Application

N. Yamamoto, 2nd Research Group
[April 1996 to March 2001]

Reducing radio-activation of materials has been strongly desired for nuclear fusion reactor systems from the viewpoint of waste management and environmental safety. It is especially important for advanced reactors like prototype and DEMO reactors which succeed to an experimental reactor such as ITER (International Thermonuclear Experimental Reactor), due to much higher doses expected in those reactors. Since such activation occurs most extensively in structural materials used for first wall/blanket applications, a great concern has been paid to lowering the degree of activation in these materials. At the same time those materials must withstand severe fusion environments, such as heavy neutron irradiation, and maintain material integrity. Therefore the development of high performance and low activation structural materials has been recognized as one of key issues in the progress of fusion reactors.

In this study the influence of transmutational elements, which are generated in the materials through nuclear reactions, on the properties of low activation candidates has been investigated in order to estimate their capabilities and to gain significant insight for future material development. The emphasis is focussed on the effect of gas elements (helium and hydrogen) on the mechanical properties, because these elements are known to be able to cause remarkable

deterioration. The materials intensively studied in this research are low activation ferritic steels and vanadium alloys, promising candidates for prototype and DEMO reactors. Helium and hydrogen will be implanted in the sample materials by ion bombardment with NRIM compact cyclotron. The technique of post implantation mechanical testing (e.g. creep and tensile tests) will be chiefly adopted for the evaluation, owing to its high efficiency, accuracy and simplicity. Fractographical examination and microstructural observation on the fractured specimens will also be carried out to provide the link between mechanical properties and microstructures.

This fiscal year the half part of the high vacuum creep testing equipment which is utilized for post implantation experiments will be constructed and the methodology of the testing will be established through tests on unimplanted specimens. The preliminary modeling of phenomena will also be started as well.

Keywords: helium embrittlement, hydrogen embrittlement, ferritic steel, vanadium alloy

132 Research on Fundamental Science of Frontier Ceramics

K. Hiraga, Mechanical Properties Division
[April 1995 to March 1997]

This study aims at obtaining systematic bases for the microstructural design of advanced oxide-base ceramics for superplastic forming and for high temperature machinery.

Although the requirement for high temperature plasticity is opposite between superplastic materials and heat resistant ones, the performance of both materials depends on the same factors such as morphologies, nanometer-sized structures, and chemistry of interfaces. It is because the factors closely relate to the grain boundary sliding accommodated by intergranular matter transport and the nucleation and growth of intergranular defects, which are the common elemental processes of high deformation and fracture in both materials. For the advanced microstructural design, therefore, it is essential to understand systematically how the factors govern the elemental processes and to establish new advanced methods for controlling these microstructural factors. For this purpose, we have promoted tight cooperation between the micromechanisms of high temperature material performance under tensile loading and highly qualified material synthesis by colloidal processing using nanometer-sized oxide powders.

First we analyzed damage accumulation in a pure tetragonal zirconia during superplastic tensile deformation. The analysis revealed the most of damage introduced up to moderate strains of about 200 % to arise from the growth of preexistent intergranular defects. From this results, we tried to reduce the density of the defects by colloidal processing. We controlled the dispersion of nanometer-sized zirconia powders in colloidal solution based on the relationship between the surface potential of the powders and the pH-value of the solution. The processing followed by pressure filtration enable us to get sintered bodies with higher densities and with finer grain size of about 0.2 μm as compared with those obtained by usual dry processing. As expected from the analysis, the resultant materials showed higher superplastic tensile ductilities than that of the usual one. The cooperative work on the microstructural control of fine-grained zirconia and alumina base materials containing intergranular glassy phases or second phase particles is also in progress.

Keywords: colloidal processing, oxide ceramics, interface, microstructural control, high temperature, deformation and fracture mechanisms

133 Fundamental Study of Microstructures and Properties to Develop High Performance Materials for Severe Environment (II-High Temperature Intermetallic Compounds)

T. Yamagata, Materials Design Division
[April 1990 to March 1997]

The project is a part of a national research project to develop high temperature intermetallic compound such as Niobium Alminide. In this project, the target was fixed on mechanical properties of 3% elongation at room temperature and 75 MPa tensile strength at 2073K. High temperature strength, in general, strongly depends on the homologous temperature. In this project, homologous temperature corresponds to 0.9 of melting point of Nb_3Al. It is necessary, therefor, to rise the melting point of Nb_3Al phase by the addition of high melting point refractory element, such as Ta, Mo, W. Nb_3Al, on the other hand, is a typical brittle material, so that, ductile Nb+brittle Nb_3Al two phase alloys equilibrated at 2073K were searched in binary and Nb-Al-X ternary systems. Two phase alloys were obtained in Nb-18Al, Nb-4Ta-18Al, Nb-4W-18Al alloys. Effective alloying elements to rise melting point were searched for by the incipientmelt-structure observation method. Arc

melt specimens were heat treated at 2073K~ 2400K for 2hr in vacuum, Mo, Ta, W were effective elements.

These two phase alloys were melted to 3Kg ingots by high frequency scarmelt method. After 2hr heat treatment at 2073K in vacuum, $4\phi \times$ 10mm compression specimens were machined and mechanical properties were evaluated. At room temperature, very few deformation was observed and at 2073K, 23 MPa 10% compression deformation strength were obtained in Nb-18Al-4W alloy. Addition of 4 at% Mo improved the strength up to 31Mpa.

Keywords: Nb_3Al+Nb two phase structure, compression strength at 2073K

134 Development of Third Generation Nickel-Base Single Crystal Superalloys

T. Yamagata, computational materials science Division

[April 1994 to March 1997]

A single crystal (SC) superalloy with balanced intermediate and high temperature creep strengths was designed by using NRIM Alloy Design Program (ADP) with help of Cluster Variation Method (CVM) computer program based on statistical thermodynamics. The design condition was as follows; alloy density to be less than 8.9, solution heat treatment window to be larger than 40°C, lattice misfit to be negative at high temperatures but not beyond certain extent, creep rupture lives both at 900°C-392MPa and at 1040°C-137MPa to be longer than 1000hrs, etc.

An alloy with a multi-chemical composition, TMS-75, having 3wt% Cr, 5wt% Re, etc, was selected as the best through the programs and was cast to SC bars. The SC bars were successfully solution heat treated by a simple two-step heating at 1300°C for 2 hrs and at 1320°C for 5hrs, followed by a two-step aging treatment, first at 1150°C for 4hrs and second at 870°C for 20hrs.

Creep tests at temperatures ranging from 900 to 1150°C showed that the alloy has a good balance of creep strengths over this temperature range compared with other Re containing alloys like CMSX-10; typical rupture lives at 900°C-392MPa, 1000°C-245MPa and 1100°C-137MPa being 1000hrs, 330hrs and 220hrs, respectively. A laboratory scale hot corrosion test using Na_2SO_4-25%NaCl salt mixture at 900°C showed that the alloy has a very good hot corrosion resistance as well.

Design and development of further superior SC superalloys are being conducted.

Keywords: single crystal, superalloy, alloy design, creep strength, hot corrosion resistance

Related Papers

1. H. Murakami, Y. Yamagata, and H. Harada, "The influence of Co on creep deformation anisotropy in Ni-base single crystal superalloys at intermediate temperatures": accepted for publication in *Science & Engineering A*, May 1997.
2. T. Kobayashi, Y. Koizumi, S. Nakazawa, H. Harada, and T. Yamagata, "Design of a high rhenium containing single crystal superalloy with balanced intermediate and high temperature creep strengths": to be presented at the 4th International Charles Parsons Turbine Conference, 4-6 Nov. 1997, Newcastle, UK (The Institute of Materials).

135 Real-Time Investigation on Surface Reactions and Defect Growth Processes under Irradiation

M. Kitajima, 2nd research Group

[April 1994 to March 1999]

We are studying on reaction dynamics of material surface under irradiation of ions, plasma, molecular beams and light. The purpose of this research is to elucidate dynamics of the irradiation-activated surface reactions including surface damage process and to develop the fast analytical techniques with emphasis of real-time observation of dynamic process. Investigations on cluster reactions in gas phase and with surface is also targets. From this viewpoint, we have started studies on reactive scattering of molecular beam with solid surfaces using a resonance enhanced multiphoton ionization (REMPI) spectroscopy, in order to get direct information on molecular dynamics during surface chemical reaction. In the REMPI measurements, the desorbing molecules from the surface are ionized with a tunable UV light, introduced into the TOF chamber and detected by a multichannel plate. We obtained internal state distributions of the SiO and GeO molecules desorbing from Si and Ge surfaces, respectively, in reaction with O_2 beam. The REMPI result gives a clue for further development of the study on surface chemical reaction dynamics, and the techniques obtained here will be applied to the studies on cluster reactions. Plasma-solid interactions are also being studied by using in situ real-time ellipsometry. A strong sample bias dependence of growth rate of very thin oxide film in oxygen plasma has been found and its temperature dependence is being examined.

Recently we have started an application of this technique to determine the threshold energy of sputtering for metal films. With Raman spectroscopy, we have obtained the first experimental evidence of the existence of hydrogen molecules in crystalline silicon. A basic study on technique of transient Raman scattering for ion-irradiated crystals is now in progress.

Keywords: irradiation, surface reaction dynamics, growth process of surface defect, real-time observation

Relate Papers

1. K. G. Nakamura and M. Kitajima, "Reactive scattering of O_2 with the Si(111) surface: Resonance enhanced multiphoton ionization of SiO," *J. Chem. Phys.*, 102(1996): 8569–8573.
2. K. Ishioka, K. G. Nakamura, and M. Kitajima, "Phonon confinement in GaAs by defect formation studied by real-time Raman measurements," *Phys. Rev.*, B52(1995): 2539–2542.
3. M. Kitajima, I. Kamioka, K. G. Nakamura, and S. Hishita, "Oxidation rate and surface-potential variations of silicon during plasma oxidation," *Phys. Rev.*, B53(1996): 3993–3999.
4. M. Kitajima, "Real-time Measurements of Chemical Reaction and Damage Processes of Surfaces," *Proc. Int. Symp. on Material Chemistry, 1996*(1996): 87–94.

136 Research on Utilization Technique of "Data-Free-Way" System for Nuclear Materials

M. Fujita, 2nd Research Group

[April 1995 to March 2001]

Data systems having huge material database and effective computer utilized tools are required for the alloy design or selection of advanced nuclear materials. However there are limitations in storing numerous material properties into the database and developing a variety of tools for material design in each research laboratory. Under the cooperation among National Research Institute for Metals (NRIM), Japan Atomic Energy Research Institute (JAERI) and Nuclear Fuel Development Corporation (PNC) with different special field, the pilot distributed database system for development of nuclear materials called "Data-Free-Way" has been built since 1990. The project on the second stage was started in 1995 under the cooperation among NRIM, JAERI, PNC and Japan Information Center of Science and Technology (JICST). The aim of this project are to store the data in the database and to develop useful computer utilized tool for data analysis and simulation codes for various phenomena under irradiation environments.

To supply the information for designing and selection of nuclear materials, some trials were made on World Wide Web (WWW) used to send information to Internet. Several databases and tools in the WWW provided the function as follows: 1) Factual database, 2) Full text file, 3) Alloy design tool for Ni-base superalloy, 4) Simulation for nuclear transmutation. It was shown that the WWW server system is powerful and attractive to supply the material information.

Keywords: Data-Free-Way, distributed database, advanced nuclear materials, data share, transmutation

Related Paper

1. M. Fujita, Y. Kurihara, M. Shindo, N. Yokoyama, Y. Tachi, S. Kano, and S. Iwata, "A Computer Network System for Mutual Usage Four Databases of Nuclear Materials (Data-Free-Way)", *Proc. Int. Sympo. Mat. Chem, Nuclear Env.*, Tsukuba, (1996): 675–884.

137 Material Synthesis to Control of Magneto-Thermal Properties by Changing Distance between Magnetic Ions

M. Sato, Physical Properties Division

[April 1993 to March 1996]

Several nanocomposite magnetic materials were synthesized by sol-gel processing. Nano-composites containing 10-20 wt% Fe were prepared by adding the appropriate amounts of an aqueous solution of ferric nitrate to a 50 mol% solution of tetraethoxysilane and ethanol, with a few drops of HF added as a catalyst. The nanocomposite containing 12 wt% Gd was also prepared by the similar processing without the catalyst. The magnetization measurements show the paramagnetic behavior between 4.5 and 77 K. This suggests the evidence of nano-scale magnetic composites, especially for Fe base sample.

Anisotropic magneto-thermal properties of Czochralski-grown $RAlO_3$ (R: Dy, Ho and Er) single crystals having orthorhombic system were measured for magnetic refrigerants along each crystal axis direction. Larger magnetic entropy changes were obtained for single crystals of $ErAlO_3$ along {001} direction and $DyAlO_3$ along {010} direction than those for single crystals of $Dy_3Al_5O_{12}$ and $Gd_3Ga_5O_{12}$ along <111> direction which were used for the current magnetic

refrigeration system to produce liquid helium below 20 K.

Single crystals of BaB_2O_4 having low-temperature (β) phase could be grown by the Czochralski method using a Pt tube as a seed (along particular crystallographic direction when a β-phase single-crystal seed was mounted inside the tube and the β-α phase transformation was prevented before seeding).

This research was performed in collaboration with the Institute for Materials Research, Tohoku University.

Keywords: magnetic refrigerants, nanocomposite, orthorhombic system, anisotropy, low-temperature phase

Related Papers

1. H. Kimura and R. S. Feigelson, "Phase formation of BaB_2O_4 from melts in graphite crucible", *Journal of Alloys and Compounds*, 234(1996): 187–192.
2. H. Kimura, T. Numazawa, M. Sato, V. V. Kochurikhin, K. Shimamura, and T. Fukuda, "Optical Absorption-Spectra of Czochralski Grown $(Dy_{1-x}Gd_x)_3Ga_5O_{12}$ and $Dy_3(Ga_{1-y}Al_y)_5O_{12}$ Garnets Relating Unstable Spiral-shape Growth", *Crystal Research and Technology*, 31(1996): 301–306.

138 Effect of Crevice on Low Cycle Fatigue Behavior of Pressure Vessel Steel in High Temperature Pressurized Water

T, Ishihara, Failure Physics Division

[April 1995 to March 1996]

The objective of this cooperative research is to clarify the effect of crevice on low cycle fatigue behavior of a low alloy pressure vessel steel in high temperature water by means of experimental and analytical procedures.

Low cycle fatigue behavior

Effect of crevice on low cycle fatigue behavior was investigated in high temperature water by using smoothed round bar specimens with a pair of split collar made from the same material. The tests were conducted under a wide range of dissolved oxygen (DO) concentration from 10 ppb to 4000 ppb in order to clarify the relation between the effect of crevice and DO concentration. As a result, it was found that fatigue lives with crevice were longer than those without crevice. This trend was more striking with decreasing total strain range. From the results of optical observation of the specimen surface after the tests it was found that in the case of without crevice many corrosion pits of about 50 μm in diameter were observed and a small crack was recognized at the root of each pit, while few corrosion pits were observed in the case of with crevice.

Analytical evaluation of water chemistry in crevice

Behavior of several parameters related to the water chemistry in crevice such as pH, corrosion potential and DO concentration were analyzed by using two-dimensional mathematical model, which was developed taking into account the pumping effect by cyclic loading, diffusion of various ionic species, law of conservation of mass in crevice. Analytical results were compared with the experimental results by using CT specimens in NaCl solution resulting in the analytical results being reasonable. Corrosion potential and pH in crevice were decreasing with approaching to the center of the crevice.

This research was preformed in collaboration with Institute of Corrosion and Protection of Metals, Academy of Science in China.

Keywords: crevice, low cycle fatigue, high temperature water

139 Environmental Degradation of Structural Materials for Light Water Reactors

Y. Katada, Failure Physics Division

[April 1991 to March 1996]

The purpose of this research is to clarify the elemental process of environmentally assisted cracking (EAC) of structural materials for light water reactors in high temperature water and to systematize the related data for prediction of damage of structural components. In this year, following two items were conducted:

Interaction between stress corrosion cracking and corrosion fatigue

Three kinds of corrosion tests by using compact tension specimens of sensitized stainless steel were conducted in high temperature water: (a) fatigue crack growth tests at a constant stress ratio, (b) slow strain rate tests and (c) combined tests of (a) with (b). As a result, crack growth rate of (a) was higher than that of (b) by about 10 times, while crack growth rate of (c) was higher than those of (a) plus (b) by 3 times, which meant the existence of additional interaction effect due to the combined test mode. From the observation by

SEM of the fracture surface obtained by the combined test mode (c), intergranular cracking and striation-like pattern were observed at the same fracture surface.

Dissolution behavior of MnS inclusion in high temperature water

Dissolution behavior of MnS inclusion in high temperature water under crevice condition was conducted at various temperature from room temperature to 561K. As a result, amount of dissolution of MnS increased with increasing temperature, and MnS inclusion was completely dissolved at 561K.

After the test, the depth of dissolved MnS inclusions at various temperature was measured by an atomic force microscope (AFM). Based on the measured data by AFM a new procedure was proposed for prediction of dissolution rate of MnS at 561K from the dissolution rate at lower temperature less than 523K.

Keywords: stress corrosion cracking, corrosion fatigue, stainless steel, high temperature water

Materials for environmental performance

(140) Fundamental Study on the Processing for Ecomaterials

Halada, Ecomaterials Research Team
[April 1996 to March 1998]

ECOMATERIALs, which have high recyclability and give less environmental load to the eco-sphere without deteriorating their properties, are expected to be coming materials adapting to the sustainable development. ECOMATERIALs have superior properties in the each following indexes. 1) Expanding the human' frontiers, 2) Co-existing with eco-sphere, and 3) Optimizing the amenities: This study is a case study on processing to develop material into ecomaterial.

Preparation of fiber reinforced porous Fe-Fe composite composed from SCIFER (highly drawn iron fiber) and Fe powder was investigated as an attempt of production of ECOMATERIAs by P/M technology. This Fe-Fe composite is expected to have high recyclability because the microstructure of SCIFER reinforces the matrix without using any alien material nor any alloying elements. In order to utilize the cold-worked structure of SCIFER, sintering temperature was limited under 450°C. UFP (ultra-fine powder) of Fe was used for the acceleration of sintering in lower temperatures. SCIFER fiber and Fe-powder were covered and embellished with Fe-UFP by wet dispersion method. Sintering behavior of embellished SCIFER and Fe powder mixture was examined, and raptured microstructures were observed. Fe-Fe composite had 30kg/mm2 of Fracture resistance strength by sintered at 400°C, while sintered Fe-powder had 10.3kg/mm2 by sintered at the same temperature. SEM observation showed that Fe-UFP improved the interconnection of SCIFER fiber and Fe powder at lower temperature.

Adding to the recyclability and property, energy consumption and other environmental burdens to produce the material ought to be discussed in order to develop the Ecomaterials. MLCA(Materials environmental Life-Cycle analysis) will be applied and modified.

Keywords: ecomaterials, recyclability, Fe-Fe composite, powder processing, materials environmental life-cycle analysis

Related Papers

1. K. Halada, K. Minagawa, S. Ohno, H. Okuyama, and N. Itsubo, "Porous Fe-Fe Composite as an Environment Conscious Materials (ECO-MATERIAL)", *Advances in Powder Metallurgy & Particulate Materials*, 1996,(1996): to be published.
2. K. Ijima and K. Halada, "Environmental Life-Cycle Analysis", *Boundary*, 12, No.1(1996): 42–45: in Japanese.

[141] Study on Design and Assessment Technology foı Ecomaterials

K. Yagi, Environmental Performance Division
[April 1993 to March 1996]

Global environmental problems originate from strains existing in a large amount of materials and energy consumption. Although man-made materials have supported the society bringing advantages and conveniences to human life, they also impose a wide variety of burdens on the environment through each and every step of production, processing, consumption, usage, recycling and disposal. Ecomaterials which would harmonize with the environment and minimize environmental load have to be developed as a new concept of materials design and materials technology. In this project, the study on three subjects as follows are being conducted.

Construction of Ecomaterials Data Base

The development of assessment method for environmental load through the life cycle of materials is a very important subject in this research. The objective of this work is to construct basic database and their frame in order to establish a new ecobalance evaluation method in which environmental load and materials properties are evaluated. A new evaluation method named MLCA(Materials environmental Life-Cycle Analysis) was established, and the data of the environmental load of materials were accumulated.

Structural Design of High Temperature Solid Solution Alloys

Ecobalance of heat resistant ferritic steels can be improved by the minimum alloying through saving energy and mineral resource. In the present study, the optimum ferrite compositions has been sought through maximizing M-C atomic pair concentrations which control the long term creep strength of ferritic steels. The maximum M-C pair concentration was obtained in a Fe-0.002at%C-0.91at%Mn-1.6at%Ni-0.01at%Mo alloy. The creep rupture life of the alloy is estimated to be .55 million h at 88MPa/773K from the previously reported regression equation, suggesting that the long term creep strength of ferritic steels can be improved by the optimization of chemical compositions.

Fracture Criterion for Multiphase Structure

Simple system alloy is a potential candidate for inherently recyclable material.Al-Si alloy is one of the simple system alloys which contain only high Clark-number elements and are composed of plural phases. The Al-Si alloy is a two-phase alloy used generally in as-cast condition. However, the alloy is hardly deformable due to easy cracking by plastic deformation. This study elucidates the applicability of thermo-mechanical treatment for enhancing the ductility. A cyclic treatment of slight straining and annealing makes the microstructure five times finer than the as-cast condition. The thus treated material deforms more than 99% and shows two times strength with a higher ductility.

Keywords: evaluation of environmental load, ecomaterials database, structural design of solid solution alloys, recyclable materials design, multiphase structure

Related Papers

1. K. Harada, "MLCA(Materials environmental Life Cycle Analysis) for ECOMATERIALS", *Proc. Intnl. Conf. on EcoBalance*,(1994): 288–293.
2. K. Nagai, "A design concept for recyclable materials with high quality, Advanced Materials'93,V", *Trans. MRS-J*, 18A(1994): 139.
3. H. Onodera, T. Abe, M. Ohnuma, K. Kimura, M. Fujita, and C. Tanaka, "Effect of minute solute elements in the ferrite matrix on the inherent creep strength of carbon steels", *Tetsu-to-Hagane*, 81(1995): 821–826: in Japanese.

142 Fundamental Study on Creation of Micro Stereom Fabrics by Powder Technology

Halada, 5th Research Team

[April 1993 to March 1996]

Minerals of biological origin have the micro-structure to perform functions efficiently. It is well-known that spicules or echinoderms have three dimensional framework or porous structures, e.g. microperforate, labyrinthic, retiform fascicular etc., to perform efficient mechanical properties. We have started this study as a first step with an ambitious to acquire or mimic the design and construction of materials of natural origin in the field of the inorganic materials technology.

Powder technology is noteworthy technology to create the mimetic microstructure of natural materials, because the powder can be divided to small elemental particles and can be synthesized under optional controllings. Prediction of microstructures and stereom morphologies of sintered materials is important to design such microstructures. One part of this study is that on arrangement; to develop the way of prediction for the microstructure and the stereom morphology of sintered materials.

The feature of powder particle is also important as the element of synthesis. Embellishment of particles with finely controlled qualities is expected to enlarge the possibility of the design of stereom fabrics. The second part of the study is that on assembling; to inquire the way of combination of various type of particles and to inquire the production method of appropriate powder or embellished particles for assembling. The embellishment technology was applied to porous Fe-Fe composite which is one type of recyclable composite, and the mechanical property of the porous Fe-Fe composite was examined.

Keywords: powder, porosity, sintering, structure control, ecomaterial

Related Papers

1. N. Itsubo, K. Halada, K. Minagawa, and R. Yamamoto, "A Trial for Eco-Materials; Possibility of Manufacturing of Fe-Fe Composite", *Funtai oyobi Funmatsuyakin*, 41, No.11(1994): 1361–1366: in Japanese.
2. H. Okuyama, S. Ohno, K. Minagawa, and K. Halada, "Study on the Creation of Micro-Porous-Shere by Ultrafine Particles", *Funtai oyobi Funmatsuyakin*, 40, No.12,: 1174–1178: in Japanese.

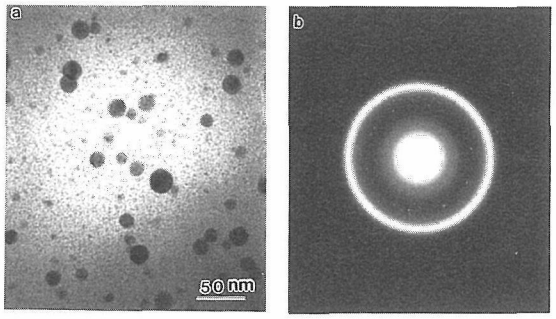

Fig.1 Bright-field image (a) and selected area electron diffraction pattern(b) of a melt quenched (AlCuV+20wt%Pb) showing nanoscale Pb particles embedded within the AlCuV amorphous matrix.

Bio-Materials, etc.

(143) Fabrication and Fundamental Studies on the Materials with Nano-Mesoscopic and Nonperiodic Structures

A. P. Tsai, 3rd Research Group
[April 1996 to March 2001]

In this year, we have been starting three topics; (1) fabrication of the nanoparticles in immisicble system, (2) Growing single decagonal quasicrystal, (3) study on rheology of amorphous alloys.

Nanoscale Pb particles embedded in amorphous metallic matrix

Most of nanocrystalline materials were prepared by the crystallization of the amorphous alloys. In the previous process, to obtain a structure with dispersion of nano scale particles isolated in the matrix is impossible. Since the Pb is immiscible to Al, Cu and V, we employed melt-quenching technique to fabricate a composite structure consisting of nanoscale Pb-particles homogeneously dispersed within an amorphous matrix in an alloy with composition $Al_{75}Cu_{15}V_{10}$-20wt%Pb. X-ray and transmission electron microscopic examinations revealed that the particles had spherical shape in the amorphous matrix.

In Fig. 1(a), a bright-field image and the corresponding selected area diffraction pattern of amorphous AlCuV containing a dispersion of Pb-particles are revealed. In the low magnification micrograph(a) the Pb-particles uniformly dispersed in the amorphous matrix are revealed. In Fig. 1(b), it could be noted that the shape of the particles was almost that of a perfect sphere, and the size distribution was estimated to be between a few nm to 20 nm. In some particular cases, planar defects were clearly observed running across the Pb particles; this has been observed in Fig. 1(a). In the corresponding selected area diffraction pattern, in addition to the halo-ring due to the presence of the amorphous phase, a few dim spots forming a ring, corresponding to [111] zone of the lead structure could be recognized. Since the Pb atom is immiscible to the matrix and the matrix is an amorphous phase(without grain boundary), the characteristics of nanoscale Pb particle are measurable. We are now studying the melting-solidification behaviors and superconductivity for the nanoscale Pb particles.

Growth of single decagonal quasicrystal

Current interest of study on quasicrystals has been focussed on the structure and physical properties from a single quasicrystal. This has been achieved in icosahedral Al-Pd-Mn alloy where single grain with a size of centimeter was obtained. Studies on resistivity, magnetic properties and neutron scattering for the single icosahedral quasicrystal have been extensively studied. On the other hand, only a few works concering to the preparation of single decagonal quasicrystal have been reported. The sizes of the single decagonal quasicrystals were about ~1mm and their quality were not good enough for structural analysis. We have grown a single decagonal quasicrystal with a size of 5 mm in an Al-Ni-Co alloy, by floating-zone method. The single quasicrystals have been characterized by Laue back scattering as well as precession camera and verified to have high perfection in structure. Figure 2 reveals a pattern showing 10mm symmetry taken by the precession camera along a 10 fold zero layer. Detailed characterizations are in progress.

Rheology of amorphous alloys

Oxide and fluoride glasses are known to have significant glass transition and stable supercooled liquid region before crystallization. Structural relaxation and glass transition for these glasses

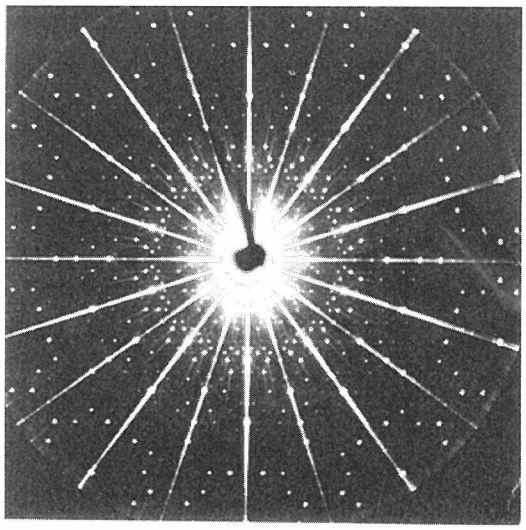

Fig.2 Diffraction pattern taken by a precession camera along ten-fold axis from an Al-Ni-Co single decagonal quasicrystal prepared by floating-zone method.

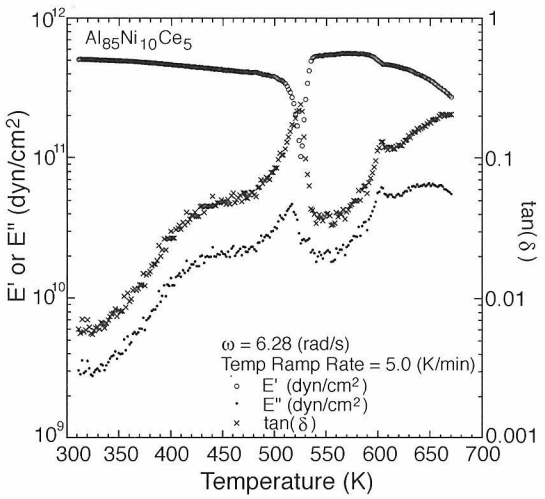

Fig.3 Viscoelastic measurement performed by the oscilating forced method for an Al-Ni-Ce alloy. E': storage modulus, E'': loss modulus and tan(∂): Internal friction.

have been comprehensively studied from the view point of rheology. Since most amorphous alloy rarely showed such a significant glass transition or stability against crystallization, nature of glass transition in amorphous alloys is mostly unknown. Recently, a large number of amorphous alloys revealing clear glass transition and supercooled liquid have been discovered in metallic alloys. Especially, these alloys show high glass formability which allows to produce a bulk amorphous alloy with large size scale. Thus, the glass transition in amorphous alloys is remarkably important. The amorphous alloys behave like *elastic solid* below the glass transition while at sufficiently high temperatures they have the properties of *viscous fluid*. Thus, to realize the inherent nature of the glass transition for the amorphous alloys the viscoelastic measurements are required.

Al-based amorphous alloys are a new group of unique materials, because they show the low specific gravity and high tensile strength. In this study, we employed a forced oscillation method to measure the dynamic mechanical properties of storage(E') and loss(E'') moduli in Al-based amorphous alloys. Fig. 3 shows temperature-dependent mechanical properties of E', E'' and tan δ for an $Al_{85}Ni_{10}Ce_5$ amorphous alloy. The measurement was performed at a heating rate 5K/min and a frequency of 6.28 rad/s. A hump observed in E'' and tan ∂ around 400K is correlated with structural relaxation. Furthermore, a drastic change observed in the three parameters around 500K is caused by the glass transition. In order to clarify the details, the measurements of frequency scan and time scan for the glass transition are in progress.

Keywords: nanocrystalline materials, quasicrystal, amorphous alloy

144 Spectroscopic and Electrochemical Investigation of the Metal Complexes with an Unusual Electronic Structure

H. Isago, Chemical Processing Division
[April 1994 to March 1997]

The fabrication of molecular devices, where one molecule functions as one device, is one of the most attractive and challenging themes in current and future science. Some materials in biological systems, such as proteins (including enzymes), can be considered as well-designed molecular devices. In numbers of such materials in biological systems, unusual electronic structures have often been observed. Therefore, it is a key step for the fabrication of molecular devices to find out compounds with an unusual electronic structure. In this meaning, metal complexes are particularly of interest as model compounds for such materials in biological systems because numbers of such materials contain some metal ion(s) in their reaction centers which have an unusual electronic structure.

We have investigated some metal complexes of phthalocyanine, which have attracted much attention as a group of new advanced materials in recent years. For example, it was found in this laboratory that bis(phthalocyaninato)lanthanoids(III) complexes exhibited remarkable electro-chromic properties in organic solvents and in solid state as thin films. In these compounds, unlike usual molecular compounds, a hole is created in the complex

molecule. This work is intended to understand the unusual electronic structures of the above mentioned bis(phthalocyaninato)lanthanoids(III) complexes from the viewpoints of π-π interaction between the two cofacial phthalocyanine chromophores mainly by using spectroscopic, electrochemical, and spectro-electrochemical techniques. Furthermore, we will try to prepare previously unknown antimony-phthalocyanine complexes. It is because that antimony is stable in trivalent oxidation state and has a close ionic radius to those of lanthanoids(III), and hence, bis(phthalocyaninato)antimony(III), which has a hole in the molecule, is expected to form.

The results of this work will serve not only for the fabrication of molecular devices but also for further understanding of supramolecular chemistry.

Keywords: Metal Complex, Antimony, Phthalocyanine, Electronic Structure

145 Fundamental Study on Biocompatibility of Materials

M. Sumita, Biomaterials Research Team
[April 1994 to March 1999]

Towards 21st century, the aged society the progresses, and requirements for affluent quality of life are getting stronger. The number of the aged and the physically challenged implanted in their bodies increase. It is important that artificial organs and medical devices exist and function in their bodies without any trouble for many years until they die. Release of metallic ions and debris from materials implanted in body should be avoided, because they always or infrequently cause carcinogenicity, physical deformity enhancement and allergies. Unexpected failure of artificial organs and medical devices implanted also should be avoided, because the reluctant re-operation forces the patient physical and mental pains. Therefore, non toxicity, adhesion to tissue, control in bioreaction caused by foreign bodies, sufficient resistance to corrosion and wear, and long fatigue life are considered as necessary characteristics for the used in vivo conditions.

As metallic materials had the higher strength and the higher toughness than all of the other materials, 316L stainless steel, Co-Cr-Mo alloy, Ti-Al-V alloy etc. have experimentally been used as biomaterials, though those alloys had been developed for other applications. Therefore, a capability exists in development of other materials with higher biocompatibility than those being used as biomaterials. The research conducted here is the accumulation of fundamental data to develop new biomaterials, which are superior in bio-compatibility in living bodies.

The content of the present research subject is as follows:

(1) Quantitative evaluation and systematic interpretation of cytotoxicity of biomaterials.
(2) Measurements of cell adhesion force to various materials and observations of cell response to mechanical stimulation by a modified atomic force microscope.
(3) Measurements of corrosion, wear, fatigue, and fretting fatigue properties of biomaterials under a quasi-biological environment.
(4) Reliability tests and standardization of artificial hip joints by a simulator having been developed.
(5) Durability tests of bone plates and artificial hip joints in animal bodies, being carried out by cooperative researches.

Keywords: biomaterials, cytotoxicity, cell adhesion force, durability tests, bio-simulator, in vivo tests

Separation and synthesis

(146) New Continuous Steelmaking Process

A. Fukuzawa Chemical Processing Division
[April 1996 to March 1998]

Today, basic oxygen steelmaking furnace(BOF) is a dominant process which converts pig iron produced in the blast furnace to steel. Among many kinds of processes in the steel industry, BOF is the only one process which keeps batch type operation process. Over a quarter century ago, various types of continuous steelmaking processes were proposed and examined by using tons of hot metal. However, none of them was realized directly in industrial scale, since it was in the midst of developing era of BOF. However, an idea or technology of continuous steelmaking is succeeded now in the continuous desiliconization or continuous dephosphorization process in front of blast furnace. However, an expectation to the continuous steelmaking still exists because demands for higher productivity and lower man power are becoming stronger in these days.

Here, a new continuous steelmaking process is proposed to solve these problems. The characteristics of the new one is in one trough type oxygen bottom blowing furnace, that is, by setting blowing nozzles at certain interval in the bottom of the furnace steelmaking reactions can be divided by the bubble curtain without changing the furnace. This will bring the reduction of heat loss and man power, and simplification of layout. This year water model experiment is going to be carried out to simulate the mixing characteristics in the bath.

Keywords: continuous steelmaking, steelmaking, oxygen bottom blowing, trough type furnace

147 Processing and Development of Isotopically Controlled Materials(ICM)

T. Noda, High Resolution Beam Facility
[April 1992 to March 1996]

Materials composed of isotopically selected elements realize the essential solution of subjects such as induced activity, He embrittlement, and compositional change caused by reactions with energetic particles.

The objectives of the program are (1)R&D of in-situ ICM processing facility(ICMPF) utilizing infrared multi-photon decomposition reaction, (2)search of working materials for isotope separation, (3)development of in-situ synthesis of isotopically controlled SiC, Si_3N_4, BN etc. and (4)development of ceramics and their composites with advanced properties.

The isotope separation experiment using Si_2F_6 was conducted under the irradiation of pulse infrared laser at 930-985cm^{-1}. SiF_4 with condensed ^{29}Si and ^{30}Si was produced at 944-967cm^{-1} while ^{28}Si was concentrated in the residual Si_2F_6. The natural Si is composed of 92.23% of ^{28}Si, 4.67% of ^{29}Si and 3.10% of ^{30}Si. The optimum separation of each isotope mainly depends on the wavenumber of CO_2 laser. $^{30}SiF_4$ of 43.3% and $^{29}SiF_4$ of 12% at maximum could be continuously obtained with a yield of 4% at 951.20cm^{-1} and 10% at 956.20cm^{-1}, respectively. In the present study the efforts to concentrate ^{28}Si in the residual Si_2F_6 was made using a long cell, 60mm in diameter and 200mm long, with NaCl windows at both inlet and outlet ends of the laser beam. The addition of inert gas such as He, Ar, and Kr to Si_2F_6 was effective to increase the ^{28}Si concentration. The maximum concentration of 99.7% at 952.923cm^{-1} with a yield of 5.4% was obtained.

The SiF_4 and Si_2F_6 enriched with ^{28}Si, ^{29}Si or ^{30}Si is being transformed to Si flake using a plasma CVD technique.

The simulation code, IRAC, calculating transmutation was improved by combining with a neutron transport calculation code and introducing multi-step reactions to predict more precisely the transmutation of materials including ICM. Chemical vapor infiltration process to obtain SiC composite with a high purity and a stability against temperature and neutron or ion irradiation is being developed. It was required to use crystalline SiC fiber.

Keywords: isotopically controlled materials, ICM processing facility, isotope separation, chemical vapor infiltration

Related papers

1. H. Suzuki, H. Araki, and T. Noda, "Si Isotope Enrichment by infrared Laser", *Proc. 6th ICSCM*, (1995).

2. H. Araki, T. Noda, H. Suzuki, F. Abe, and M. Okada, "Effect of Pyrocarbon Pre-Coating on the Mechanical Properties of CVI Carbon fiber/SiC Composites", *J. Nucl. Sci. Technol.*, 32(1995): 369–371.

Gaseous Process

(148) Development of Advanced Shape Memory Thin Films by Sputtering

A. Ishida, 3rd Research Group
[April 1996 to March 2000]

Since 1993, we have been successful in showing that sputter-deposited thin films of Ti-Ni display perfect shape memory effect, perfect superelasticity and two-way shape memory effect. These successes have made a shape memory thin film attractive for a microactuator and stimulated interest in the sputter-deposited thin film of Ti-Ni.

In this research subject, we try to produce a high performance shape memory thin film. Such an advanced film will be obtained in several ways. One of the ways to improve the shape memory effect is addition of the third element to Ti-Ni alloys. The third elements such as Cu and Pd will reduce thermal hysteresis of shape memory effect, leading to quick response of a microactuator. This effect is well known in bulk specimens, but it is difficult to use this effect in thin films because of difficulty in controlling the film composition. Therefore we have to establish the way of controlling the film composition. This is also important even in Ti-Ni binary alloy thin films. Another interesting approach to the improvement of the shape memory effect is to utilize an unstable structure formed in sputter-deposited thin films. Ti-rich Ti-Ni thin films after annealing at 773K for 1h were found to contain fine distribution of Ti_2Ni precipitates in a Ti-Ni grain. This structure cannot be obtained in bulk specimens and gives us the opportunity to improve the shape memory effect. Such a fine structure is likely to increase the recovery force, leading to an increase in the work output of a microactuator.

Keywords: micromachine, shape memory, Ti-Ni, Sputtering

Related Papers

1. A. Ishida, A. Takei, and S. Miyazaki, "Shape Memory Thin Film of Ti-Ni Formed by Sputtering", *Thin Solid Films*, 228(1993): 210–214.
2. A. Ishida, M. Sato, A. Takei, and S. Miyazaki, "Effect of Heat Treatment on Shape Memory Behavior of Ti-rich Ti-Ni Thin Films", *Trans JIM*, 36(1995): 1349–1355.

149 Development of Shape Memory Thin Films Formed by PVD Method

A. Ishida, 3rd Research Group
[April 1993 to March 1996]

Micromachines such as micromanipulators and fluid microvalves are expected to be used in the near future in various fields such as biotechnology, medicine and the semiconductor industry. However, in order to achieve such a micromachine, the development of an effective microactuator is essential. Recently the shape memory thin films have begun to attract considerable attention as one of such promising actuators.

Since 1993, we have been successfully characterizing the shape memory effect, superelasticity and two-way shape memory effect of the sputter deposited thin films. A Ti-51at. %Ni thin film after annealing at 773K for 1h showed a perfect shape memory effect with a maximum recovery force of 500MPa and a transformation strain of 4%. These values are almost equivalent to those of bulk specimens, indicating the great advantage of a shape memory thin film as an actuator. Furthermore, this film exhibited a perfect shape memory effect even after 100 thermal cycles under a load of 240MPa. Also, this thin film showed a perfect superelasticity at room temperature. The two-way shape memory effect was obtained in the Ti-51at. %Ni thin film by age-treatment at 673K for 100h under constraint. This film was found to change its shape reversibly and repeatedly with a 1.5V battery. This property is desirable for a microactuator since any bias force is not necessary. As described above, Ti-51at. % Ni thin films displayed almost the same shape memory behavior as bulk specimens. In contrast, Ti-49at. %Ni thin films showed different shape memory behavior from bulk specimens. This composition film showed good shape memory effect compared with bulk specimens. This difference comes from different structures. Thin films of Ti-49at. %Ni contain fine distribution of Ti_2Ni inside a Ti-Ni grain, whereas Ti_2Ni precipitates form along the grain boundary of a Ti-Ni grain in bulk specimens.

Keywords: micromachine, shape memory, Ti-Ni, Sputtering

Liquid state process

(150) Manufacture Processing of Recyclable Simple-System Alloys

A. Sato, Advanced Materials Processing Division
[April 1996 to March 2001]

It is very important for protecting the terrestrial environment to reduce energy and resources used in industries. Recycling of metallic materials can contribute greatly to the reduction of both energy and resources. The law of promotion of utilizing regenerated resource (The law of recycling) urges to contrive frameworks and materials for an easy recycling after their consumption. But metallic materials used for automobiles, for example, worsen materials regenerated, and the regenerated materials can not be used and have to be abandoned as a solid waste after several times of recycling. The main reason why regenerated materials have to be abandoned is elements and additives which have harmful effects on recycling of metallic materials. Materials, therefore, have to be easily recyclable. On the other hand, the properties of materials must be the same to those of materials with elements and additives which have harmful effects on recycling.

This research is consisted of four sub-themes, and the objectives are as follows:

Multi-phase complex materials.

a) High damping alloys of easy recyclability.
High damping alloys should be developed to substitute for vibration absorbing steel sheets whose macromolecular plastic sheets sandwiched sheets prevent steels from recycling.

b) Sintered ferrous alloys of easy recyclability.
Copper is usually added to sintered ferrous materials to improve their mechanical properties. But copper is one of the worst elements for recycling of ferrous materials. High strength sintered ferrous materials should be made by surface treatment of powders.

Materials without harmful additions for recycling.

(c) Cast aluminum alloys of easy recyclability.
Grain refining elements, such as Na, Sr, Sb, are used to refine the grain structure of aluminum castings. Because those elements worse the regenerated materials, a new solidification processing should be developed.

(d) Free cutting steels of easy recyclability.
Free cutting steels used nowadays contain Pb, but Pb is very harmful to recycling of steels. Hence, free cutting steels without Pb should be developed.

Keywords: environment, recycling, high damping alloy, powder metallurgy, spray deposition, free cutting steel, fine-grain material, composite

151 Basic Study on Refining of Molten Metal and Controlling of Solidification by Electromagnetic Force

A. Fukuzawa, Chemical Processing Division
[April 1994 to March 1997]

A cold crucible type levitation melting method using high frequency electric power is known as a non-contacting melting method. Therefore, this melting method is advantageous for melting high purity metals, chemically reactive metals and refractory metals.

In these several years, we have made various kinds of trials using the cold crucible type non-contacting induction furnace and we have obtained many fundamental results concerning the cold crucible.

Another advantage of this melting method is that it has the ability of separating inclusions from the molten metal, because magnitude of electromagnetic force working toward the molten metal is different from that of inclusions due to the difference in physical properties between metal and inclusions. So, the optimum levitating conditions for separating inclusions from molten metal, such as the shape of the cold crucible, high frequency coil and the electric output power have been sought to obtain materials with excellent quality. The study on separating mechanism and separating rate of oxide inclusions from molten titanium are now progressing.

Keywords: cold crucible, levitation melting, electromagnetic force

152 Solidification in the Strong Magnetic Field

A. Fukuzawa, Chemical Processing Division
[April 1995 to March 1998]

In the dendritic crystal growth, there exists Seebeck current between the top and the base of dendrites caused by the temperature difference. The current is very weak, however, in the strong magnetic field it would be possible to induce

Lorentz force in the solidification front, and make the flow in the liquid metal trapped in the dendrite region. From this effect, it can be expected to make a homogeneous composition ingot from the surface to center of the ingot with finer grain size. With the idea mentioned above the research work will be carried out by using a 10 Tesla superconducting magnet. In this fiscal year, by setting a furnace to melt and solidify low melting point alloys in the magnet, the solidification behavior of Sn and Al alloys will be investigated. The effect of magnetic field on the grain growth is also going to be examined.

Keywords: dendrite growth, strong magnet, Seebeck effect, Lorentz force

153 Investigation on Nucleation and Crystal Growth Mechanism under Heterogeneous Ambient Phase

T. Fujii, Chemical Processing Division
[April 1994 to March 1996]

The purpose of the present study is to obtain the fundamental knowledge for controlling the following crystal growth processes, which occur in the circumstances containing other solid phases of foreign particles.

1)Nucleation and crystal growth with peritectic reaction.

2)Nucleation in solid state reaction and exaggerated grain growth.

Recently, high J_c values have been obtained in the bulk specimens of high T_c oxide superconductors fabricated by means of peritectic solidification process. However, the growth mechanism of these crystals and the role of peritectic reaction in the growth process have not been revealed. In the first subject, we intend to clarify such a growth mechanism on $YBa_2Cu_3O_x$ crystals which melt incongruently at 1000℃ through the metallographic observation and the measurement of growth parameters on the quenched specimens grown at various temperatures.

Investigation will also be made on salicylic acid-acetamid system, in which a peritectic compound with the composition of 1:1 ratio forms at 65℃. It is possible to observe in situ the crystal growth process by means of optical microscopy in this experiment.

In the second subject, we aim to develop the theory of the normal and abnormal grain growth process so as to apply it to the growth of single crystals of intermetallic and ceramic materials as well as metallic materials.

Keywords: Nucleation, crystal growth, peritectic reaction, secondary recrystallization, exaggerated grain growth

154 Basic Technology Development of Materials Processing in a Short-Duration Microgravity Environment

A. Sato, Advanced Materials Processing Division
[April 1995 to March 1997]

A study on double combustion synthesis apparatus

Combustion synthesis is a production process to produce chemical compounds from elemental powders in a short time using the heat of formation of component elements. The main purpose of the study is synthesizing high performance intermetallic compounds using short time micro-gravity environment. The short time double combustion synthesis apparatus was developed in order to conduct the experiment of combustion synthesis in microgravity. The micro-gravity is achieved by dropping the experimental apparatus. The experiments were carried out using the same combustion synthesis apparatus in order to compare the 1G and micro G results exactly. The velocities of propagation of combustion synthesis were measured by two sets of W-Re thermocouple.

Study on the synthesis of high temperature superconductors

This research program is focused on two topics; wettability measurement for molten-Bi-Sr-Ca-Cu-O/Ag-substrate and synthesize of superconducting meta-stable Y-Pd-B-C phase from large-super-cooled liquid. Wettability measurement for Bi-Sr-Ca-Cu-O/Ag was performed in 1G and short duration microgravity environments. Sample of about 10mg of Bi/Sr/Ca/Cu=30/23/10/34 was melted on pure silver substrate by using infra-red image furnace. Wettability angle was determined by analyzing video images. For Y-Pd-B-C system, as the superconducting YPd2B2C phase is meta-stable, it is advantageous to utilize large super-cooling state. Rapid solidification with different cooling rates; solidification on water-cooled copper block and the splatter quench technique, were examined. Superconducting YPd2B2C phase is not formed in the former case. It can be obtained only with the splatter quench technique with the higher cooling rate.

Keywords: microgravity, combustion synthesis, intermetallic compounds, superconductor

155 Solidification Processing for Particle Dispersed Unidirectionally Grown Composites

A. Sato, Advanced Materials Processing Division
[April 1994 to March 1997]

The destruction of metallic materials is greatly affected by the crystal structure of materials. In order to improve the mechanical properties of materials, structure controlling techniques, such as grain refining, unidirectional solidification, single crystal growth, are applied in manufacturing of materials. Other methods are composites whose reinforcing particles or fibers prevent the propagation of cracks in materials. Particle dispersed composite materials can be manufactured by solidification processing at the lowest cost. It is very important that properties of particle dispersed materials can be improved by controlling the structure of matrix alloys. The purpose of this study, therefore, is to obtain basic knowledges and fundamental techniques to make particle dispersed unidirectionally grown composites.

The powder metallurgy technique is used to prepare samples. Because the behavior of a particle/particles at the solidification interface between liquid and solid is most important to make materials solidified unidirectionally with particles dispersed uniformly, properties of powders of alloys and ceramics should be already-known. Powders of aluminum and alumina are mixed mechanically in stainless steel pots set on a planetary ball-mill. Aluminum can be handled easily due to its low melting point. Sintered samples of 11.3mm in diameter and 10mm in thickness of Al-(0~20)vol%Al_2O_3 could be made to use in experiments of solidification processing.

Keywords: solidification, solidification processing, unidirectional solidification, composite, particle dispersion

Related Paper

1. Y. Osawa, G. Aragane, S. Takamori, and A. Sato, "Manufacture of Al_2O_3 particle dispersed Al alloys with pellets alloyed mechanically", *Proceedings of Japanese Foundry Engineering Society, 128th Meeting* , (1996.5.27~28): 121.

156 Metastable Phase Solidification from Undercooled Liquid by Inducing External Nucleation Seed

S. Tsukamoto, Advanced Materials Processing Division
[April 1993 to March 1997]

Metastable metallic materials produced from deeply undercooled melts can provide some interesting properties. The aim of the investigation is to elucidate the role of nucleation during the solidification of undercooled melts and to develop a new technique for producing metastable bulk materials using an electromagnetic levitation melting and an external seeding.

Two kinds of stainless steels with different solidification modes of primary ferritic (type 316) and austenitic (type 310S) were undercooled up to 230 K using the electromagnetic levitation melting. However, no sign of metastable phase solidification was observed in both materials. In the electron beam surface melting, on the other hand, the solidification mode of type 316 changed from primary ferritic to austenitic with increasing cooling rate or undercooling. The distinct difference between the levitation and the electron beam processes is the presence of the solid substrates which may allow epitaxial growth or heterogeneous nucleation in the latter case. In the electron beam process, the phase selection is mainly determined by the kinetics of growth which is favoured for austenite. In the levitation process, on the other hand, it may be determined by the kinetics of nucleation which is favoured for ferrite.

During the above experiments, determination of the primary solidified phase was not always easy, because solid phase transformation took place after the solidification. A new system was developed to analyse the primary solidified phase easily. The electric power was shut down within 200 ms after the recalescence event to quench the sample in low temperature melts. The temperature increase during the recalescence was also measured using a high time-response pyrometer. The external seeding with a thin Fe-Ni austenitic needle was attempted onto undercooled 316 melts to form metastable austenite. However, it was not successful, because strong surface flow of the levitation melted sample prevented a good contact between the sample and the needle. Then, we are trying another seeding method where the nucleation seed of ultra fine particles is produced in the levitation chamber.

This research was performed in collaboration with Research Development Corporation of Japan and University of Cambridge.

Keywords: solidification, undercooling, metastable phase, electromagnetic levitation, stainless steel

Related papers

1. S. Tsukamoto, H. Harada, and H.K.D.H. Bhadeshia (Unv. of Cambridge), "Metastable

Phase Solidification in Electron Beam Welding of Dissimilar Stainless Steels", *Mater. Sci. Eng.*, A178(1994): 189–194.
2. S. Tsukamoto and O. Umezawa, "Metastable Alloy Phase Formation from Undercooled Steel and Ti-Al Melts": to be published in *Mater. Sci. Eng.*

Solid state process

(157) Study on Combustion Synthesis

Y. Kaieda, Chemical Processing Division
[April 1996 to March 1999]

Most intermetallic compounds are conventionally produced by the processes including high frequency induction vacuum melting and casting. It is difficult to control accurately the chemical components of intermetallic compounds produced by the conventional process. Homogeneous intermetallic compound is produced by the industrial process including a combustion synthesis method, which is a newly developed manufacturing process in this institute. The chemical components, the impurities industrially produced by the process are revealed. These properties are vitally important when the combustion synthesis method is applied to an industrial mass production process for producing intermetallic compounds.

The fundamental study to reveal the reactions in combustion synthesis is carried out. The propagation of the reaction front and the synthesis process of the materials synthesized through the reaction are also studied. Investigation by the thermal analysis with rising temperature at constant speed and/or in alternating speed is carried out to reveal the conditions for the initiation of the reaction, the propagation and the synthesis. The influence of pressure and convection on the phenomena in the reaction process of the system containing gaseous phase or liquid phase is studied using a high gaseous pressure apparatus.

The selection of the combinations of elements, which is focused in the present study, will be investigated. The system of the combination that might exhibit the effect of convection and pressure during the reaction and synthesis process is selected considering the system that performs the effect of liquid and gaseous phase. The system of elements, in which the safety during the experiment is assured, is selected.

Keywords: combustion synthesis, TiNi

(158) Heterogeneous Structure Design for High Plasticity and Wide Applicability of Simple System Alloys

K. Nagai, 3rd Research Group
[April 1996 to March 1997]

Mechanical properties can be generally controlled by changing microstructures. In the present study, a high density and fine dispersion of second phase in the matrix is going to be designed using a thermo-mechanical processing on some two phase alloys.

The basic idea is mentioned in the following.

Microscopic distribution of second phase:

When the second phase is deformable, plastic work of the sample leads to a decrease in the second phase spacing.

When the second phase is undeformable, the plastic work causes the second phase cracking and finer distribution.

Role of the second phase as pinning site in deformation of matrix:

The second phase is a site for localized deformation and a pinning site for dynamic recovery of the matrix.

The marked increase of plastic strain in the matrix introduces dynamic recovery and recrystallization into very fine microstructure.

Al-Si alloy is a typical cast material. The heavy cold-work produces sever cracking in the eutectic and/or hyper-eutectic Al-Si cast materials. Then, we have developed a new thermo-mechanical processing with multiple combination of limited strain and annealing to make the alloys deformable. An eutectic Al-Si alloy is composed of Al-rich matrix and coarse primary Si phases. By a given amount of cold-working a primary Si cracks into a few pieces and decreases the size. The voids formed by the cracking heal up by the annealing. A series of these treatments results in a fine microstructure. The fine structure sample shows the excellent plasticity such as 99% in reduction. The tensile strength is higher than twice strength of the as-cast. The above idea will be applied for alloy systems such as Al-Fe, Fe-C, and so on.

Keywords: cold-working, fine microstructure, high plasticity, high strength

[159] Metallurgical Analysis of Micro-Machining Region

S. Yamamoto, Advanced Materials Processing Division
[April 1993 to March 1996]

Aiming at the miniaturization of the mechanical system, the effect of them metallurgical factor on the micro-machining are analyzed, data on micro-machinability of the various materials are accumulated.

The relation of data on micro-machinability and that on machinability in usual cutting work of the various material required in this year. Cracks and exfoliations are generated in usual cutting work at the machined surface region of TiAl intermetallic compound materials. In order to solve those problems, and it micro-machining works are also examined.

The cutting resistance increases as the hardness of a work material increases in a general tendency. But, this result is reverse to the usual cutting data, because the heat quantity effects greatly on the cutting resistance in the usual cutting. The machined surface region of the TiAl intermetallic compound sound,1) in a high cutting speed area, 2) by using a sharp cutting edge and 3)by the micro-machining. In other words, 1) the plasticity of TiAl in chip shear region starts in this temperature range, 2),and 3) the stress in cutting region decreases and suppress cracks and exfoliations.

Keywords: micro-machinability, metallic material, TiAl intermetallic compound, cutting resistance

Powder processing

(160) Oxidation Behavior of TiAl Intermetallic Compounds Produced by Powder Metallurgical Techniques

Y. Muramatsu, Chemical Processing Division
[April 1996 to March 1997]

TiAl has received considerable attention as a low density, high strength, creep resistant material for high-temperature applications. However,this material has not yet been used industrially because of its brittleness at temperatures below 900K and poor oxidation resistance at temperatures exceeding 1000K. Therefore, improvements of these properties are main problems for practical uses of this material.

This study concerns the oxidation behavior of TiAl compounds produced by powder metallurgical(P/M) techniques, conventional sintering and HIPing. Isothermal and cyclic oxidation tests will be carried out in air and oxygen atmospheres for compounds containing a third element such as niobium, molybdenum or tungsten. Effects of residual pores and the third element on oxidation resistance will be examined. Structures of oxide scales together with the phenomenon of spalling will also be examined in order to clarify the mechanism of oxidation resistance. The final purpose of this study is to develop P/M TiAl compounds resistant to oxidation at temperatures of 1000K and higher without sacrificing their inherent good mechanical properties.

Keywords: TiAl intermetallic compound, powder metallurgy, oxidation resistance

(161) Characterization of Photocatalytic Properties of Ultrafine Particles Synthesized by Plasma Processing

S. Ohno, Chemical Processing Division
[April 1996 to March 1998]

It is well known that the ultrafine particles (UFP) have many excellent physical and chemical properties. In particular, UFP of oxide semiconductors is a very promising material as a photocatalyzer.

In this study, various oxides and composite (oxide/metal) UFP synthesizes by the plasma processing such as an arc plasma technique (reactive plasma-metal reaction) and a RF-plasma CVD. Then the photocatalytic property of the UFP characterizes by the photodecomposition of water.

(162) Synthesis and Utilization of Mesoporous Materials

Y. Sakka, Chemical Processing Division
[April 1996 to March 1999]

Two types of porous materials are used for fabricating nanocomposite, heterogeneous phases, biomimetic materials, etc. One is synthesized by consolidating fine powders through a colloidal processing. The other is microporous materials with layered perovskite structures, which are synthesized by a sol-gel processing or solid state reaction.

The colloidal processing is a useful tool for preparing mesoporous materials with desired pore size distribution. An important factor is to control the interparticle interaction in liquid. Infiltration of metal solutions into the porous materials and sintering result in the advanced materials.

Intercalation or ion-exchange reaction in host materials (antimony oxide, vanadium oxide, etc.) results in a novel electronic material which is not

synthesized by heating at high temperatures. The reaction is influenced by the micro-pore size of the host-material. Determination of the reaction mechanism is conducted and effect of the pore size on the electronic properties is studied.

Keywords: soft chemistry, micro-pore, colloid, sol-gel process, antimonic acid

163 Coatings Formation by Powder Deposition Processes

S. Kuroda, Advanced Materials Processing Division
[April 1995 to March 1997]

Coatings with thickness over 50 μm are highly demanded in various industries. The most successful process in this category has been a family of thermal spray processes. Thermally sprayed coatings have been used mostly for surface protection but recent applications include more functional areas such as biomedical implant, electric heaters and radiators, and catalytic cleaners. Our group has worked on plasma spray in the past 10 years to clarify the mechanism of coating formation. This research has two objectives. The first is to extend the study on thermal spray. Special emphasis will be placed to clarify the bonding between sprayed splats, which plays a key role in the development of the microstructure of sprayed deposits. Effects of the substrate temperature, spraying environment, the velocity and temperature of particles before impact on the inter-lamellar bonding will be studied systematically. The other is to develop a new process to deposit thick coatings with improved properties, such as less porosity. Finer powders than those usually used for thermal spray are electrified and deposited onto a substrate. A possibility to consolidate the deposit by a CO_2 laser is under investigation.

Keywords: thick coatings, spray deposition, electrification

Related Papers

1. S. Kuroda and T. W. Clyne, "The Quenching Stress in Thermally Sprayed Coatings", *Thin Solid Films*, 200(1991): 49–66.
2. S. Kuroda, T. Dendo, and S. Kitahara: "Quenching stress in plasma sprayed coatings and its correlation with the deposit microstructure", *J. Thermal Spray Technol.*, 4(1)(1995): 75–84.

164 Development of Particles Assembly Technology for Integration of Functions

N. Shinya, 5th Research Group
[April 1992 to March 1997]

For creation of intelligent materials, technologies for systematization and integration of multiple material functions should be developed in advance.

Systematically coordinated multiple functions will lead to manifestation of intelligent functions, such as self-repair, self-diagnosis, feedback and so on, which can respond to environmental conditions.

In order to provide materials with the systematically coordinated multiple functions, a new approach is made through a development of particles assembly technology in this work. Each particle has a primitive function such as sensor, processor and actuator. Therefore coordinations and systematizations of these primitive functions may be realized through three dimensional particles arrangement. For the arrangement it is necessary to develop the technology which make it possible to assemble several kinds of particles according to micro-structural designs for the manifestation of the coordination and systematization. As key technologies for the three dimensional particles assembly, a fabrication of particle's ordered mixtures and a particle manipulation using a micro-probe in addition to the particle arrangement using an electron beam are being studied. The ordered mixtures of semiconductive $BaTiO_3$ particles and metallic indium particles were prepared by the electrification method. These complex particles showed a good positive temperature coefficient of resistivity by only packing without sintering. For the particle manipulation, a tungsten micro-probe method was developed, and it was confirmed that particles can be easily manipulated one by one and welded each other by controlling the voltage between the probe and the substrate.

Keywords: intelligent materials, multiple functions, particle assembly

165 Study on Solid State Chemical Reaction, Its Propagation and Meterials Syntyesis

Y. Kaieda, Chemical Processing Division
[April 1993 to March 1996]

The fundamental study to reveal the reactions between solids, solid and liquid, and solid and gas

is carried out. The propagation of the reaction and the synthesis process of the materials synthesized through the reaction are also studied. The field of the study covers not only the grasp of the phenomena but the comprehensive understanding of the chemical reaction, the heat transfer, the mass transfer and the other aspects of the synthesis of materials in the solid phase system.

The selection of the combinations of elements, which is focused in the present study, will be investigated. The system of the combination that might exhibit the effect of convection and pressure during the reaction and synthesis process is selected considering the system that performs the effect of liquid and gaseous phase. The system of elements, in which the safety during the experiment is assured, is selected.

Investigation by the thermal analysis with rising temperature in constant speed and/or in alternating speed is carried out to reveal the conditions for the initiation of the reaction, the propagation and the synthesis. The influence of pressure and convection on the phenomena in the reaction process of the system containing gaseous phase or liquid phase is studied using a high gaseous pressure apparatus.

Combustion syntheses of mixture of Ni and Ti powder are carried out in a 100kg batch scale. The synthesized materials were worked to be wires. The wire samples were examined by a measurement of thermal analysis.

Keywords: combustion synthesis, TiNi

166 Sintering of TiAl Intermetallic Compounds

Y. Muramatsu, Chemical Processing Division
[April 1993 to March 1995]

TiAl intermetallic compounds were prepared by sintering mixed powder compacts of TiH_2 and $TiAl_3$ in varying sintering temperatures. Sintered compounds were further densified by HIPing at 1470K and 202MPa for 3.6ks without canning. The densification due to HIPing was examined. The hardness and oxidation behavior of HIPed compounds were examined and compared to those of wrought TiAl compounds.

The density of HIPed compounds increased with an increase of sintered density, and saturated when the relative density exceeded 94%. The room-temperature hardness varied with sintering temperature, and increased with increased sintering temperature. The temperature dependence of hardness was similar to that of wrought compounds. Homogeneous lamellar structural compounds showed higher high-temperature hardness than duplex structural compounds. The oxidation behavior was dependent on the microstructure. Homogeneous lameller structural compounds showed excellent oxidation resistance as compared with duplex structural compounds. In comparison with wrought compounds, HIPed compounds showed better oxidation resistance.

Keywords: TiAl, powder metallurgy, high temperature hardness, oxidation resistance

Related Paper

1. Y. Muramatsu, T. Ohkoshi, and H. Suga, "High Temperature Hardness and Oxidation Resistance of Sinter-HIPed TiAl", *J. Japan Inst. Metals*, 59(1995): 754–760: in Japanese.

167 Characterization of Composite Ultrafine Particles

S. Ohno, Chemical Processing Division
[April 1994 to March 1996]

It is well known that the ultrafine particles (UFP) have many excellent physical and chemical properties. Further, the composite UFP formed by combining between foreign particles in the region of a UFP's size expect to improve the properties of UFP and to create a new function.

In this study, we synthesize the composite UFP of Ni-Zr-O systems by a RF-plasma CVD technique, and then characterize photocatalytic properties of the UFP by the photodecomposition of water. The UFP of Ni-Zr-O systems prepared by the RF plasma CVD is composed of the following fore phases: monoclinic ZrO_2, tetragonal ZrO_2, NiO and metallic Ni. It was found that the UFP of Ni-Zr-O systems has a maximum photocatalytic activity for the decomposition of water at the composition of about 2mol%NiO.

Keywords: ultrafine particle, composite UFP, RF-plasma, Ni-Ti-O UFP, photocatalytic property, photodecomposition

168 Synthesis and Characterization of Advanced Materials Utilizing Colloidal Dispersed Systems

Y. Sakka, Chemical Processing Division
[April 1993 to March 1996]

Key developments in processing of fine powders are (1) synthesis of fine powders with controlled sizes, shapes and chemistries, (2) consolidation techniques to control pore volume and pore size

distribution, and (3) the role of powders and compacts on the evolution of microstructures during sintering. Although many kinds of techniques in preparing fine powders have been reported, little efforts have been paid on the consolidation of fine powders. In this study, the emphasis will be on the second and third development.

Colloidal processing of nano-sized powders (Al_2O_3, ZrO_2, etc.) is conducted to obtain consolidate the powders with controlled pore sizes. The most important factor is how to disperse the powders. Well-dispersed suspensions are prepared by controlling pH and/or adding appropriate amount of stabilizer such as polyacrylic acid, etc. Electro-discharge sintering is applied to obtain the advanced materials. In this procedure, the powders are heated by instaneous high electric pulsed power application under uniaxial pressure. Characterization of the synthesized materials is another subject. The gas (especially H_2, H_2O, CO and CO_2) sorption-desorption experiments of metal-ceramics nanocomposite particles are conducted for characterizing the catalytic properties.

Keywords: colloid, fine powder, sintering gas desorption, nanocomposite

Related Papers

1. Y. Sakka, D. D. Bidinger, and I. A. Aksay, "Processing of Silicon Carbide-Mullite-Alumina Nanocomposite", *J. Am. Ceram. Soc.* 78(1995): 479–486.
2. S. Hong, K. Ozawa, and Y. Sakka, "Electro-Discharge Sintering of (Fe,Co)-B and Ni-B Amorphous Ultrafine Powders Prepared by Chemical Reduction", *J. Jpn. Soc. Powder and Powder Metall.* 42(1995): 323–329.
3. Y. Sakka and S. Ohno, "Hydrogen Sorption-Desorption Characteristics of Mixed and Composite Ni-TiN Nanoparticles", *Nano-structured Mater.* 7(1996): 341–353.

Joining

(169) Diffusion Bonding of Stainless Steel and Metals of Group IV–VI

T. Kasugai, Advanced Materials Processing Division

[April 1996 to March 1999]

It is difficult to apply fusion welding processes, such as an arc welding or an electron beam welding, to dissimilar metals joining because a large amount of brittle metallic compounds form in the weld metals. On the other hand, the size of metallic compounds and diffusion layer in dissimilar metal joints can be easily controlled by a solid state diffusion bonding.

The basic metallurgical knowledge on the dissimilar metal bonding zone has been scarce until now, and it is difficult to estimate the size/kind of metallic compounds at the bonding zone based on phase diagrams. The diffusion process in the bonding zone of dissimilar metals, moreover, is not simple, but a few negative diffusion or up-hill diffusion phenomena have been observed[1].

In this study, joinability of the diffusion bonding of stainless steels and metals of group IV ~ VI , the formation of metallic compounds in the bonding zone of these steels and metals, and diffusion processes are investigated in connection with the periodic table.

Keywords: Diffusion bonding, Stainless steel, Group IV metals, Group V metals, Group VI metals, Metallic compound

Related Paper

1. T. Kasugai, K. Ei, and H. Irie: "Diffusion Bonding of Zr and Stainless Steel", *J. of High Pressure Institute of Japan*, 33(1955)5, 237–244: in Japanese.

(170) Brazing Experiment under Microgravity Using Parabolic Orbital Rocket

K. Sasabe, Advanced Materials Processing Division

[April 1996 to March 1998]

Near future, the construction of the space station will begin. The space station will be a permanent, multipurpose manned facility and utilized for a very long period. It will be useful, therefore, to prepare joining technique to be used on the space station in future.

Brazing is one of the most expected technique as a joining method in space environment. It was thought generally that micro gravity would be the ideal condition for brazing because capillary flow during brazing is not disturbed by gravity. It was however clarified by our recent study that the brazing mechanism under micro gravity is not so

simple as it was thought before. The most important factor for brazing under micro gravity is to fill brazing gap completely, which depends on the control of initial behavior of capillary penetration, i.e. meniscus must be formed at the place expected strictly by controlling of temperature distributions.

We are going to carry out a brazing experiment under microgravity using a parabolic flight rocket. The test specimens are prepared to verify our theoretical predictions about the relationships of meniscus formation mechanisms and temperature distributions during brazing under microgravity.

We will use sleeve joints of thin wall tubes as specimens. The material of the tube is stainless steel (SUS 316) and the filler alloy is a Ag-Cu eutectic+0.2 Li alloy (JIS BAg-8A).

Keywords: brazing, microgravity, capillary penetration, temperature distribution

171 Influence of Surface Composition on Joining of Materials

K. Sasabe, Advanced Materials Processing Division

[April 1995 to March 1998]

Ion bombardment has several effects on a joining surface; not only cleaning, but ion implantation and surface roughening. The relationship between each effect and joint properties is not clarified yet. On the other hand, hydroxyl radical and thermal oxide on the surface accelerate the joining process of silicon. The bonding mechanism is not clarified yet.

The aim of this study, in joining of metals, is to investigate; i) the relationship between each effect and joint properties, ii) effect of gases on a joining surface. The aim, in joining of silicon, is to investigate; i) the effect of hydroxyl radical and thermal oxide on a surface, ii) the difference in bonding mechanism between metals and silicon.

Joining of metals

In this study, we carry out the diffusion joining using a clean surface with little defects. We investigate the effect of an adsorptive on joining properties.

Joining of silicon

In order to clarify parameters that affect mechanical and electric properties of joint, we investigate the relationship between surface adsorptives and joint properties using a clean surface in an ultra high vacuum atmosphere. It is expected that oxygen in a material affects disappearance of surface adsorptives, so we also investigate the relationship between behavior of surface adsorptives and joint properties of CZ silicon in different oxygen concentration.

Keywords: joining, adsorptive, silicon

172 Fundamental Research on Brazing and Electron Beam Welding in Space Environment

K. Sasabe, Advanced Materials Processing Division

[April 1994 to March 1996]

The characteristic phenomena of molten metal flow during brazing and EB welding have been studied as fundamental research for the establishment of joining techniques in space.

Research on brazing

It was thought generally that micro gravity would be the ideal condition for brazing because capillary flow during brazing is not disturbed by gravity. However, it was clarified by our study that the brazing mechanism under micro gravitation is not so simple as it was thought before.

We have studied on the relationships between meniscus formation mechanisms and temperature distributions during brazing of the sleeve butt joints of thin walled pipes as a typical model for brazing in space environment.

Our analysis of penetration mechanisms using the thermal conductivity theory proved that the formation mechanisms of meniscus preceding capillary penetration are the points to be specially considered. Based on the results of analysis, we proposed 7 types of specimens for the micro gravity experiments using a parabolic orbital rocket TR-1A #5. By this micro gravity experiment, we expect to get information to establish the guidelines of design and construction of brazing joints in space environment.

Electron beam welding

Considering usage of electron beam welding in space, the lower accelerating voltage is desirable. So an accelerating voltage of 20kV was selected and the welding were carried out. The minimum diameter under this voltage was about 1.3mm and penetration depth was 1mm/10mA when the welding was carried out in drilling mode and at low welding speed of 3mm/sec. Then the electron beam of 100mA could weld a steel of 10mm in thickness. In this case, sulfur content in steel effected only the surface bead, that is the surface region above the neck portion, and the penetration depth did not change. If sulfur content was less than 50ppm, the bead width was wide and the neck located near the surface. However the width of fusion zone was very shallow. When sulfur was

more than 50ppm, the neck moved toward inside and the bead width became narrower. But at sulfur content of more than 100ppm, the fusion zone in the steel tended to be parallel. When the melting process by electron beam was of heat conduction mode from the surface heat source as arc welding, lower sulfur content induced wide and shallow bead and thick material could not be welded. More than 50ppm sulfur content resulted in deeper penetration and with narrow width. The influence of sulfur content on shape of fusion zone was investigated and analyzed with respect to molten metal flow by a high speed video and 16mm movie.

Keywords: Brazing, EB Welding, Micro gravity, Simulation, Sulfur

173 Corrosion of Dissimilar Metals Joints in Reactor Fuel Reprocessing Plants

H. Irie, Advanced Materials Processing Division
[Apr. 1991 to Mar. 1996]

Dissimilar metals joints are to be used in a new reactor fuel reprocessing plant in Japan. The joints composed of austenitic stainless steels and valve metals are made by solid state joining. It is necessary for the safety of plant to assure sufficient high corrosion resistance against condensed nitric acid involving active fission products. The objectives of this project are to obtain a satisfactory joint between zirconium and stainless steel or titanium and stainless steel with enough strength and corrosion resistance.

According to the research results carried out until last year, a satisfactory diffusion joint of zirconium and stainless steel with a strength level of pure zirconium could be accomplished, using annealed tantalum foil inserted into joint surfaces, which could depress formation of brittle intermetallic compounds layer and accomplished full contact of interfaces. A direct bonding of titanium and stainless steel could be obtained in vacuum diffusion bonding with cleaning of surface by the ion sputtering method.

In this year, corrosion properties of above solid state diffusion bonded joints were investigated by measuring macroscopic corrosion speed in 3N-HNO_3 with 0.1gCr^{6+}/l at 60°C and microscopic electrochemical potential distribution. Corrosion at the first stage at 1440h depended strongly upon the finished surface state and occurred locally near the bonding interface. However longer-term corrosion occurred in stainless steel in the grain boundary corrosion manner and the bonded interface was not selectively corroded. This result indicated good property of corrosion of the diffusion bonded joint. The local stress and strain distributions across the bonded interface were also measured by the laser speckle method using a tube type joint by the above bonding method.

Keywords: diffusion bonding, zirconium, tantalum, titanium, austenitic stainless steel, corrosion, nitric acid

Composite process

(174) Micro Structure Control with Plastic Deformation under Mashy State

T. Dendo, Advanced Materials Processing Division
[April 1996 to March 1998]

Processing under semi-solid or semi-molten state i.e. mashy state has attracted the attention as an exotic technique for refinement of the micro structure and/or for creation of new composite materials. In the procedure of the above processing, plastic working is mostly inevitable. Plastic working under mashy state in which solid and liquid phases coexist, however, induces unfavorable problems such as segregation due to the flow of the liquid component and/or difficulty of the shape retention.

Against the background mentioned above, this study starts from this fiscal year, and consists of two sub-themes; one is to make some attempts so as to solve the above problems, and to examine their feasibility; and another is to explore the preferred orientation in the crystalline introduced by plastic deformation under mashy state in order to develop the new method of texture control.

Keywords: mashy state, plastic working, deforming behavior, preferred orientation

175 Forced Infiltration Process for Making Composite Structures

T. Dendo, Advanced Materials Processing Division
[April 1992 to March 1996]

Forced infiltration technique is applied to two different processing purposes in this theme.

The first is to manufacture a sort of metal-ceramic composite by infiltration under the semi-molten state. Through this process, two types of composite can be obtained; one is of a porous ceramic compact having a metal-ceramic-composite layer near its surface; another is of a ceramic compact joining with a metal layer which is the solid component in the semi-molten

state. The infiltrating metals employed are Pb-Sn alloys which have a wide region of the semi-molten state. The porous compacts used are made of alumina powder. Infiltrating behavior and morphology of the structure in the composite layer were investigated in relation to the process parameters such as volume fraction of solid, porosity of ceramic compact, infiltration pressure and so on. As for the joining pieces, it was confirmed that a durable bond between metal and ceramic was gained as a result of the optimum processing conditions.

The second is to synthesize intermetallic compounds by forced infiltration of molten aluminum into a porous titanium preform. Through this process, three kinds of Ti-Al compounds are synthesized i.e., Ti_3Al, TiAl and $TiAl_3$. Fraction and distribution of them are mainly affected by the thermal conditions such as pre-heating temperature and pouring temperature. At lower processing temperature, $TiAl_3$ and un-reacted Ti are seen, whereas TiAl and Ti_3Al are observed at higher temperature. On the other hand, effects of grain size and relative density of the Ti-powder preform on synthesizing behavior are explored.

Keywords: forced-infiltration, joining, semi-molten state, ceramic, intermetallic compound

Related Papers

1. T. Shirota, T. Hashimoto, M. Nakamura, H. Doi, T, Kimura, and T.Dendo, "Synthesis of Ti-Al Intermetallic Compounds by Reaction during Pressure Infiltration", *Proc. 43th Join.Conf. Tech. Plast.* , (1992): 483–486: in Japanese.
2. T. Dendo, T. Shirota, and M. Kiuchi, "Pressure Infiltration under Semi-molten State for Making Composite Layer Structure", *Proc. 4th Int. Conf. Tech. Plast.*, (1993): 194–199.
3. T. Shirota, T. Dendo, and M. Kiuchi,"Infiltrating and Joining Processes under Semi-molten State for Making Metal-Ceramic Composite", *Proc. 3rd Int. Conf. Proces. Semi-soli. Alloy. Comp.*, (1994): 407–415.
4. T. Shirota, T. Dendo, and M. Kiuchi,"Infiltrating and Joining Processes under Semi-molten State for Making Metal-Ceramic Composite", *Journal of the JSTP*, 36(1995): 961–966: in Japanese.

Process with aid of beam technology

176 Study on the Efficiency of Resonance Photoionizatio Process

Y. Ogawa, Chemical Processing Division

[April 1995 to March 1998]

Laser resonance photoionization continues to be popular in many research fields and the process may find a wide variety of applications. In this process,atoms are selectively pumped from their ground state to an intermediate excited state and subsequently the excited atoms are ionized by direct photoionization. The ions generated are then extracted from a photoionization induced plasma by an externally applied electric field. One of the important factors in evaluating the process performance is the overall ion yields, which is restricted by two conditions: small bound-free transition cross-section in the ionization scheme and space charge limitation in the plasma.

The objective of this study is to improve the overall efficiency of the resonance photoionization process. The reaserch is composed of the following two subjects.

1. Investigation for autoionizing levels or highly excited Rydberg levels to achieve the efficient photoionization of atoms via bound-bound transitions.
2. Measurement of plasma characteristics to elucidate the ion extraction behavior from the plasma.

Keywords: resonance photoionization, photo-ionization induced plasma, autoionizing level, Rydberg level, plasma characteristic

Related Paper

1. Y. Ogawa et al., "Laser Material Purification of Neodymium", *J. Jpn. Inst. Met.* 55(1991): 545–552.

177 Annealing of α'-Martensite Under Magnetic Field for Synthesis of $Fe_{16}N_2$

H. Shinno, Advanced Materials Processing Division

[April 1995 to March 1998]

Because of very large magnetic moments, $Fe_{16}N_2$ is an attractive material used for magnetic recording devices, but it is hard to fabricate a material with a large volume fraction of $Fe_{16}N_2$. This nitride has been synthesized by a long time annealing of α'-martensite at low temperature, in order to avoid decomposition of α'-martensite into α-Fe and other nitrides. The transformation rate and the final volume fraction of $Fe_{16}N_2$ was small, since annealing temperature was lower than 473K.

In this study, we attempted to synthesize $Fe_{16}N_2$ by nitrogen ion implantation into sputtered Fe films and post annealing under magnetic field. It is expected that magnetic field will distort an Fe lattice and reduce the potential barrier for nitrogen

diffusion along interstitial sites of Fe lattice.

A preliminary experiment of annealing under magnetic field was performed. A 50 nm thick Fe film was sputter deposited on a MgO(100) substrate and coated with 30nm thick Cu, in order to prevent nitrogen escape from the surface. 120keV N_2^+ ions and 80keV N_2^+ ions were implanted up to $7.5 \times 10^{20} m^{-2}$ and $5 \times 10^{20} m^{-2}$ respectively. Then the film was coated with 90nm thick Cu. X-ray diffraction analysis showed that almost all Fe film transformed to α'-martensite. The film was annealed at 423K for 3.6ks under magnetic field of 1.3T parallel to the film plane. But X-ray diffraction did not show clear evidence of existence of $Fe_{16}N_2$. It is considered that annealing temperature was too low and duration was too short in this experiment. Further systematic study has been under way.

Keywords: $Fe_{16}N_2$, ion implantation, annealing under magnetic field

Related Paper

1. H. Shinno, K. Saito, and M. Uehara, "Synthesis of $Fe_{16}N_2$ by means of nitrogen ion implantation into Fe thin films", *Proceedings of the 10th symposium on surface layer modification by ion implantation*, Tokyo, (1994): 17–23.

178 Analysis/Evaluation of Atomic Scale Compositional Change in Materials Due to the Radiation Damage

K. Furuya, High Resolution Beam Research Station

[April 1995 to March 1999]

Radiation damage in materials is characterized by the atomic displacements associated with the destruction of crystalline structure, transmutation by nuclear reaction and radiation induced solute segregation by the irradiation of energetic particles such as neutrons and ions. Many types of defect clusters are supposed to be produced by this atomic process and the resultant microstructure generally become complicated with the formations of dislocation loops, voids and so on. In addition, enhanced diffusion associated with these defect reactions results in the local change in the concentration of solute atoms, the segregation at grain boundaries and surfaces, and the precipitation of secondary phases. For the basic understanding of radiation damage and compositional changes, an analytical TEM which consists of 1 MeV electrons with two ion accelerators, energy dispersive X-ray spectroscopy (EDS) and energy loss spectroscopy (EELS), so-called "SUBNANOTRON", is used in this research. At the first stage, the hardware of the EDS was developed to be operated at 1000 kV and the behavior of electron irradiated defect clusters in 316 stainless steel was investigated in this year.

The EDS spectra have been measured from 400 kV to 1000 kV. The general shape of the spectra didn't change at all accelerating voltages tested. As increasing the accelerating voltage, a little increasing of the dead time and of the background noise below 1 keV were observed. However the combination of the high resolution electron microscopy (HRTEM) with EDS at 1000 kV is considered to be very powerful for in-situ analysis.

The electron irradiation induced defects in 316 stainless steal have also been investigated by the atomic scale imaging. The defect clusters were observed on two apparent {111} planes in HRTEM along [110] projection, but were difficult to detect in the bright field images due to the slight diffraction contrast. The details in the structural morphology of these defects was compared with the results of image simulation, in which the models of various kinds of defects were proposed. The defect clusters and the local composition change by ion beam irradiation will be investigated as a next step.

Keywords: radiation-damage, SUBNANOTRON, analytical TEM, EDS

179 Study on Evaporation Process by High Energy Density Beams

H. Irie, Environmental Performance Division

[April 1992 to March 1996]

The CO_2 laser has been widely used as an energy source of material processing. One of main problems of the processing is that the interaction among laser beam, metal vapour and gases produces a laser induced plasma. Once the plasma forms, it absorbs or scatters the laser beam and leads to a reduction in heat input or power density. It is very difficult, however, to measure the distributions of electron density and temperature of the plasma to elucidate the interaction between the laser and the plasma, because they change very rapidly during the laser processing.

In the present study, formation of large and stably induced laser plasma has been attempted to analyse the characteristics of the laser plasma. A focused laser beam was irradiated onto an arc plasma generated in a horizontal direction. Assist gas of Ar was flown through a coaxial nozzle of 5

mm in diameter. With an adequate coupling of laser power and the flow rate of the assist gas, the plasma stood still in space between the nozzle and the arc plasma. Once the plasma formed in the space, it continued to exist by absorbing laser power even if the arc was shut off. This plasma is large and stable enough to analyse the characteristics of the plasma.

The absorption coefficient of the plasma was measured using a power probe. Distributions of the electron density was evaluated by measuring the infrared radiation from the plasma. Temperature distributions in the plasma were calculated numerically from the value of the electron density on an assumption that the plasma was in local thermodynamic equilibrium. The maximum value of the electron density and the temperature of the plasma were 2.0×10^{17} cm^{-3} and 18000 K, respectively. The absorption coefficient of the plasma had an approximately constant value of 0.6 cm^{-1} independent of the laser power. The results were well explained on the basis of inverse Bremsstrahlung. Furthermore, this stable plasma can be used as an energy source of a new thermal plasma materials processing.

This research was performed in collaboration with Ibaraki University.

Keywords: high energy density beam, laser, laser induced plasma, absorption, electron density, temperature distribution

Related Papers

1. S. Tsukamoto, K. Hiraoka, Y. Asai, H. Irie, M. Yoshino, and T. Shida, "Characteristics of Stably Induced Laser Plasma", *Proc. ICALEO'96*, (1996): to be published.
2. S. Tsukamoto, K. Hiraoka, Y. Asai, H. Irie, M. Yoshino, and T. Shida,"Formation of Stably Induced Laser Plasma and Its Characteristics", *Proc. 6WS*, (1996): to be published.

[180] Joint Research on the Structure and State Analysis of Metastable Liquid and/or Solid Gas Atom Clusters

K. Furuya, High Resolution Beam Research Station

[April 1995 to March 1996]

Understanding of the behavior of implanted atoms which make nonequilibrium phase is interesting because of the physical point of view as well as the application point of view. For example, in the case of rare gas atoms clusters precipitated as crystals in metals and semiconductors, the inhomogeneity of atom structures and of electron state density results in the unique-properties of materials. In this study, the investigation of the microstructures of implanted ions into the crystalline materials at an atomic scale has been performed as a joint research with Argonne National Laboratory (ANL).

The assignment of this collaboration work is as follows. The Al specimens for high resolution electron microscopy (HRTEM) were prepared in NRIM by electrochemical polishing. Then rare gas ion such as Xe^+ and Kr^+ were implanted into the specimens by using the NEC-650kV accelerator in Tandem-Facility at ANL with accelerating voltage of 25-35 kV. The HRTEM and compositional analysis was done by SUBNANOTRON (JEM-ARM-1000) with EDS.

A great many precipitates in Al with the size of 1-5nm in diameter were observed. EDS analysis showed stronger peak of Xe at these precipitates than that of at Al matrix. The extra spots in electron diffraction patterns appeared with the same orientation of the matrix. These results showed that the existence of Xe in the precipitates which have a FCC structure and 50% larger lattice spacing than that of Al. The details of the structure were investigated by HRTEM. The moiré pattern of Xe precipitates in every 3 Al fringes (2 Xe fringes) appeared and they had a polyhedron structure. According to these results, the model of Xe precipitates was proposed and image simulation has been performed with Al crystal including the polyhedron Xe-precipitates. The physical properties and the behavior of Xe-precipitates will be investigated for clarifying the formation mechanism of nonequilibrium nanocrystals in solids.

Keywrods: precipitation of rare gas, HRTEM, image simulation

Processing in special environment

(181) Fundermental Studies on Microbial Reactions with Inorganic Compounds

A. Aoki, Failure Physics Division

[April 1996 to March 1998]

Certain species of microorganism accelerate the aqueous oxidation of metals and inorganic compounds. These are called **chemolithotrophic bacteria** and have played an important role in mining to extract metal valuables from ore. Much effort has been done to clarify and control the potential usefulness of microbiology in this field. However, the interfacial process of the interaction

between the microorganism and the inorganic compound is still not sufficiently understood. To clarify this ambiguous point, as a first step, we are investigating the characteristics of the microbial reaction of the oxidation of the inorganic compounds. **Thiobacilus ferroxidans**, a typical microorganism of the chemolithotrophic type, is applied in this study. A few grams of powdered metal sulfide are put into a "9K medium" of pH 2.2 and about 10^6 cells/ml of the microorganism is subsequently added. The reaction is carried out at 30°C in air. Redox potential, pH and metal ion concentrations are measured during a run and the results obtained are discussed by referring to the control. First we found that the redox potential change was proportional to the number of the bacteria, which increases according to the progress of oxidation. This result shows that the microorganism significantly influences the oxidising reaction. Furthermore, the solid phase formed at the sulfide surface will be characterized by using XRD,IR and EDX, and also the corroded surface of the sulfide will be observed by using SEM and AFM.

Keywords: chemolithotrophic bacteria, Thiobacillus ferrooxidans, interfacial process, redox potential, AFM, IR

182 Study of Regenerator for Ultra-Low Temperatures

A. Sato, T. Numazawa, F. Matsumoto , and H. Nagai, High Magnetic Field Station
[April 1995 to March 1998]

This study is focused on a key component of a new refrigeration system which provides various temperatures lower than 1 K by the super fluid helium Stirling cycle. Several regenerator materials which have high heat capacity in the temperature range below 2 K are investigated. Some kinds of magnetic materials show specific heat anomaly and magneto-caloric effect related to magnetic phase transition or Shottoky anomaly. In particular, some rare-earth garnets are very useful because of high entropy properties and low transition temperatures. The specific heats of $(DyGd)_3Ga_5O_{12}$ system have been measured. The heat capacity is about four times larger than that of $Dy_3Ga_5O_{12}$ above 0.5 K. This magnetic material will be one of most candidates as the regenerative materials between 0.5 K and 1 K. A test apparatus for the regenerator is under construction. This apparatus will be used for measurements on heat exchange rate between the regenerator materials and ^{3}He-^{4}He gas, and heat conduction loss. Cycle simulations will be done by using the experimental parameters.

Keywords; low temperatures, regenerator, helium

Related Papers

1. Thermal Properties of $(Dy_xGd_{1-x})_3Ga_5O12$ Garnet Single Crystals.
2. T. Numazawa, H. Kimura, A. Sato, H. Maeda, K. Shimamura, and T. Fukuda, Advances in Cryogenic Engineering-Materials, 42(1995): in press.

183 Development of Magnetic Separation Control System

T. Ohara, Strong Magnetic Field Research Station
[April 1995 to March 2000]

Progress in applied superconductivity technologies has resulted in the development of superconducting (sc) magnets with excellent operability. One of the promising application fields is magnetic separation. The primary advantages, those being energy saving, compact size, and increased speed becomes visible only after the system is superconductorized. The full-scale application of this process will also contribute greatly to the preservation of global environments.

We will develop the key system technologies of application of high Tc sc magnets to magnetic separation. We proposed the concept of magnetic chromatography which can separate chemically similar but magnetically dissimilar materials, such as lanthanide and actinide elements. Our rough numerical simulation illustrated the fractionation process, and suggests the potential of separating very weak paramagnetic materials which we have not been able to deal with through the conventional High Gradient Magnetic Separation (HGMS) techniques. We have developed more accurate simulation code by using COMPACT 3D to get precise information on design limit.

In order to minimize the quantity of sc wire used in sc HGMS systems, we developed two computational techniques to simulate the magnetic field created by sc solenoids: a detailed numerical model, and a simplified graphical method. We used the numerical model as a standard of comparison to evaluate the accuracy of the graphical method. The evaluated error in the graphical determination of sc wire volume was less than 4.6% in hypothetical systems for purifying dissolved fission products in nuclear reprocessing.

Comparing with the case where an HGMS filter and an sc solenoid have the same length, our optimization technique shows that a large amount of wire reduction is possible.

We conduct this research in collaboration with the Electrotechnical Laboratory, AIST, MITI.

Keywords: fine particles, high gradient magnetic separation, magnetic chromatography

Related Papers

1. T. Ohara, S. Mori, Y. Oda,Y. Wada; and O. Tsukamoto, "Feasibility of Magnetic Chromatography for Ultra-Fine Particle Separation", *Trans. IEE of Japan*, 116-B(1996): 979–986.
2. T. Ohara, K. Kaiho, and T. Kiyoshi "Optimization of a Superconducting Solenoid for High Gradient Magnetic Separation Systems", *IEEE Trans. Magnetics*, 32(1996): 5103–5105.

Publications

❒ Papers published in 1995

Characterization/Properties

Electronic and nuclear properties

1. K. Hirata, K. Kadowaki, and T.Mochiku, "Anomalous Non-Linear Effect of the C-Axis I-V Characteristics in Single Crystalline $Bi_2Sr_2CaCu_2O_{8+\delta}$ Under Magnet Fields", *Advances in Superconductivity*, 1(1995): 563–566.

2. T. Furubayasi and I. Nakatani, "Magnetic Properties of Glanular Fe-SiO Films", *J. Korean Magnetics Society*, 5(1995): 474–477.

3. H. Mamiya and I. Nakatani, "Dynamical Magnetic Properties of Iron-Nitride Magnetic Fluids", *J. Korean Magnetics Society*, 5(1995): 815–818.

4. T. Naka, T. Matsumoto, *Y. Okayama, *N. Môri(*Univ. Tokyo), †Y. Haga, and †T. Suzuki (†Univ. Tohoku), "Magnetization at High Pressure in Cep", *J. Magnetism and Magnetic Mater.*, 140–144(1995): 1253–1254.

5. H. Amekura and T. Masumi, "Reconfirmation with Discussion of Anomalies in Photo-conductivity of Cu_2O at Low Temperatures", *J. Phys. Soc. Jpn.*, 64(1995): 2684–2696.

6. H. Kitazawa, *T. Okada, *Y. Kobayashi, *F. Abe(*RIKEN), and †Y. Noro(†Hitachi. Ltd), "Huge Hyperfine Magnetic Field of ^{61}Ni in Spinel Chromites $Cu_{0.9}Ni_{0.1}Cr_2O_4$ and $Co_{0.9}Ni_{0.1}Cr_2O_4$, *Phys. Lett. A*, 209(1995): 241–245.

7. *Y. Saito, *K. Inomata(*TOSHIBA), †A. Goto, †H. Yasuoka(†Univ. Tokyo), S. Uji, T. Terashima, and H. Aoki, "Magnon-Excitation Contribution to the Interface Magnetization in Co/Cu Superlattice", *Phys. Rev B*, 51(1995): 3930–3932.

8. T.Sasaki, *Andrew. M. Rappe, and *Steven. G. Louie(*Univ. California), "Ab Initio Soft-Core Pseudopotential Calculations of Magnetic Systems", *Phys. Rev B*, 52(1995): 12760–12765.

9. T. Naka, T. Matumoto, and *N. Môri(*Univ. Tokyo), Magnetic States of α-and γ-Ce at High Pressure, *Physica B*, 205(1995): 121–126.

10. K. Kadowaki, H. Takeya, K. Hirata, and T. Mochiku, "Magnetism and Superconductivity in ReT_2B_2C," *Physica B*, 206(1995): 555–558.

11. T. Naka, T. Matsumoto, *Y. Kanke (*NIRIM), and †K. Murata(†ETL), "Magnetization and Hall Effect Under Pressure in NaV_6O_{11}", *Physica B*, 206&207(1995): 853–855.

12. S. Nimori, G. Kido, and *T. Suzuki(*Univ. Tohoku), "The De Haas-van Alphen Effect Measurements of Tmsb with High Magnetic Fields, *Physica B*, 211(1995): 148.

13. *S. Katano, T. Matsumoto, *T. Funahashi (*JAERI), †J. Iida, †M. Tanaka (†Ochanomizu Univ.), and **J. W. Cable(**Oak Ridge Natl. Lab), "Crystal and Magnetic Structure of Stoichometric YFe_2O_4", *Physica B*, 213(1995): 218–220.

14. S. Uji, T. Terashima, H. Aoki, *J. S. Brooks, *R. Kato, *H. Sawa, *S. Aonuma, and *M. Kinoshita (*Univ. Tokyo), "Fermi Surface and Obsence of Oddditional Mass Enchancencnt Near the Insulating Phase in $(DMe\text{-}DCMQI)_2Cu$", Solid State Commun., 93(1995): 203–207.

15. H. Mamiya and *M. Onoda(*Univ.Tsukuba), "Electronic States of Vanadium Spinels MgV_2O_4 and ZnV_2O_4", *Solid State Commun.*, 95(1995): 217–221.

16. T. Terashima, H. Takeya, S. Uji, K. Kadowaki, and H. Aoki, "De Haas-van Alphen Oscillations in the Normal and Superconducting States of the Boro-carbide Superconductor YNi_2B_2C", Solid State Commun., 96(1995): 459–463.

17. T. Terashima, S. Uji, H. Aoki, M. Tamura, *M. Kinoshita (*Univ.Tokyo), and †M.Tokumoto (†Electrotechnical Laboratory), "Reexamination of Angle Dependent", Magnetoresistance Oscillation in θ-$(BEDT\text{-}TTF)_2I_3$, *Synthetic Met.*, 70(1995): 845–846.

18. T. Terashima, S. Uji, H. Aoki, M. Tamura, *M. Kinoshita(*Univ. Tokyo), and †M. Tokumoto (†Electro-technical Laboratory), "The Shubnikov-de Haas Oscillations and a Small Closed Orbit in θ -$(BETD\text{-}TTF)_2I_3$", *Synthetic Met.* , 70(1995): 847–848.

19. S. Uji, T. Terashima, H. Aoki, J. S. Brooks, *R. Kato, *H. Sawa, *S. Aonuma, *M. Tamura, and *M. Kinoshita(*Univ. Tokyo), "Fermi Surface and Cyclotron Mass in $(DMe\text{-}DCNQI)_2Cu$ System", *Synthetic Met.*, 70(1995): 1075–1076.

Atomistic arrangement

20. T. Hatano and K. Nakamura, "Superconductivity in Superstructure of Bi-based Oxide thin Film", *Advances in Superconductivity VI* (1995): 877–882.

21. N. Kishimoto, H. Amekura, and T. Saito, "Resonant Creep Enhancement in Austenitic Stainless Steels Due to Pulsed Irradiation at Low Doses", *Fusion Eng. and Design*, 29(1995): 391–398.

22. M. Imai and T. Hirano, "Electrical Resistivity of Metastable Phases of $BiSi_2$ Synthesized Under High Pressure and High Temperature", *J. Alloys Compounds*, 224(1995): 111–116.

23. H. Amekura, N. Kishimoto, and T. Saito, "Photoconductivity Evolution Due to Carrier Trapping by Defects in 17MeV-Proton Irradiated Silicon", *J. Appl. Phys.*, 77(1995): 4984–4992.

24. K. Nakamura and T. Hatano, "Analysis of Intergrowth Structure and Growth Model of $(Bi_2Sr_2CuO_\gamma)m(CaCuO_2)m'$ Superlattice by Alternate Deposition, *J. Appl. Phys.*, 77(1995): 6402–6410.

25. J. Ye, *T. Shishido, *T. Sasaki, and *S. Fukuda (*IMR), "Are-Melting Synthesis and Properties of Perovskite-Type $HoRh_3$", *J. Chem. Soc. Jpn.*, 9(1995): 703–706.

26. J. Ye and K. Nakamura, "Oxygen Deficiency and Cation Disorder in $YBa_2Cu_3O_{7-\delta}$ Superconducting Thin Films", *J. Crystallogr. Soc. Jpn.*, 37(1995): 112–117 : in Japanese.

27. H. Amekura, N. Kishimoto, K. Kono, and T. Saito, "Irradiation Temperature Dependence of Residual Defects in 17MeV-Proton Bombarded Silicon", *Materials Science Forum*, 196–201(1995): 1159–1164.

28. *H. Takahashi, *N. Môri (*Univ. Tokyo), T. Matsumoto, †T. Kamiyama, †K. Oikawa, †I. Ohta, †H. Asano (†Univ. Tsukuba), **S. Ikeda, **N. Watanabe (**KEK), ††M. Itoh, and ††H. Yamauchi (††ISTEC), "Development of a high-pressure cell for the neutron powder diffractometer(HRP) at KEK", *Phisica B*, 213&214(1995): 1028–1030

29. A. Matsushita, *Y. Yamada (*Univ. Nagoya), †N. Yamada (†Univ. Electro-Communications), **S. Horii (**Univ. Nagoya) and T. Matsumoto, "Effects of Pressure on the Electrical Resistivities of $PrBa_2Cu_4O_8$ and $Pr_2Ba_4Cu_7O_{15-\delta}$",*Physica C*, 242(1995): 381–384.

30. M. Imai, K. Hirata, and T. Hirano, "Superconductivity of Trigonal $BaSi_2$", *Physica C*, 245(1995): 12–14.

31. J. Ye and K. Nakamura, "Relaxation of Crystallographic Defects in $YBa_2Cu_3O_{7-\delta}$ Thin Films by Heat Treatment and its Effects on Tc", *Phisica C*, 254(1995): 113–123.

32. J. Ye and K. Nakamura, "Cation Disordering and Oxygen Deficiency in $YBa_2Cu_3O_{7-\delta}$ Thin Films", *Proc. 8th CIMTEC*, (1995): 203–210.

Phase transformation and micro structures

33. S. Tukamoto and N. Koguchi, "Surface Reconstruction of Sulfer-terminated GaAs (001)Observed Burning Annealing Process by Scanning Tunneling Microscopy", *J. Cryst. Growth*, 150(1995): 33–37.

34. T. Hirata, "Raman Active Modes and the Tetragonal-monoclinic Phase Transition in ZrO_2 Doped with 12mol%CeO_2", *J. Phys. Chem. Solids*, 56(1995): 951–957.

35. *A. Vevecka, H. Ohtsuka, and *H. K. D. H. Bhadeshia (*Univ. Cambrige), "Plastic Accommodation of Martensite in Disordered and Ordered Iron-Platinum Alloys", *Mater. Sci. Technol.*, 11(1995): 109–111.

36. T. Kikuchi, S. Kajiwara, and *Y. Tomota (*Ibaraki Univ.), "Microscopic Studies on Stress-induced Martensite Transformation and Its Reversion in an Fe-Mn-Si-Cr-Ni Shape Memory Alloy", *Mater. Trans. JIM*, 36(1995): 719–728.

37. S. Kajiwara, "Velocity of the Austenite-martensite Interfaces in Reverse Martensitic Transformation in Fe-Ni-C Alloys", *Materials Characterization*, 34(1995): 105–119.

38. *B. Strnadel(*Technical Univ. of Ostrava), S. Ohashi, H. Ohtsuka, **T. Ishihara (**Yokohama Univ.), and †S. Miyazaki (†Univ. of Tsukuba), "Cyclic Stress-Strain Characteristics of Ti-Ni and Ti-Ni-Cu Shape Memory Alloys", *Materials Science and Engineering*, A202(1995): 148–156.

39. *B. Strnadel(*Technical Univ. of Ostrava), S. Ohashi, H. Ohtsuka, **S. Miyazaki(**Univ. of Tsukuba), and †T. Ishihara (†Yokohama Univ.), "Effect of Mechanical Cycling on the Pseudo-elasticity Characteristics of Ti-Ni and Ti-Ni-Cu Alloys", *Materials Science and Engineering*, A203(1995): 187–196

40. M. Yata, K. Nakamura, and *K. Ogawa (*Yokohama City Univ.), "Self annihilation of

Surface Precipitates on Compound Films by Alternate Impinging of Molecular Beams", *Phys. Rev B*, 51(1995): 2473–2478.

41. H. Ohtsuka, S. Kajiwara, T. Kikuchi, T. Ishihara, and Nagai, "Growth Process and Microstructure of ε Martensite in an Fe-Mn-Si-Cr-Ni Shape Memory Alloy", *Proc. Int. Conf. on martensitic Transformation*, 1995, *Lausanne, J. Physique IV*, 5(1995): C451–455.

42. T. Kikuchi, S. Kajiwara, and *Y. Tomota (*Ibaraki Univ.), "Formation Process of Lamella Structures by Deformation in an Fe-Mn-Si-Cr-Ni Shape Memory Alloy", *Proc. Int. Conf. on martensitic Transformation, 1995, Lausanne, J. Physique IV*, 5(1995)C8-445–450.

43. K. Hashimoto, M. Nobuki, H. Doi, E. Abe, and M. Nakamura, "High Temperature Strength and Room Temperature Ductility of TiAl Base Alloy with Antimony", *Proc. Int. Sympo. Gamma Titanuim Aluminides*, (1995): 761–770.

44. T. Kumagai, E. Abe, *M. Takeyama (*Tokyo Inst. Tech.), and M. Nakamura, "Reaction Process of α→γ Massive Transformation in Ti-rich TiAl Alloy", *Proc. MRS*, 364(1995): 181–186.

45. F. Abe, M. Muneki, and K. Yagi, "Kinetics of Tetragonal to Monoclinic Transformation in a MgO Partially Stabiliged Zirconia", *Proc. 4th Euro Ceramics*, (1995): 399–406.

46. F. Abe, M. Muneki, and K. Yagi, "Control of Tetragonal/Monoclinic Transformation in a ZrO_2-9. 7mol% MgO", *Proc. 4th Jpn. Inst. SAMPE. Sympo.*, (1995): 293–298.

47. F. Abe, M. Muneki, and K. Yagi, "Transformation of Tetragonal to Monoclinic Phase in MgO-Partially-Stabilized-Zirconia and Y_2O_3-Tetragonal-Zirconia-Polycrystal", *Proc. 12th Japan-Korea Symposium on Advanced Ceramics*, (1995): 280–284.

48. K. Hashimoto, S. Kajihara, T. Kikuti, and M. Nakamura, "Effect of Temperature on Tensile Properties of TiAl Base Alloys with on without Manganese", *Scripta Metallurgica et Materialia*, 32(1995): 417–422.

Surface and interface properties

49. Y. Sakka, T. Uchikoshi, and S. Ohno, "Degradation Behavior of Advanced Ceramic Powder: (I)Superconducting and Tetragonal Zirconium Oxide", *Advances in Science and Technology*, 3B(1995): 1011–1018.

50. Y. Sakka, T. Uchikoshi, and S. Ohno, "Degradation Behavior of Advanced Ceramic Powder: (II)AlN and TiN Ultrafine Powders", *Advances in Science and Technology*, 3B(1995): 1451–1458.

51. M. Yoshitake, "Surface Segregation on Metal Films Driven by Surface Free Energy Reduction and Material Application of Films with Segregation", *J. Jpn. Inst. Met.*, 34(1995): 588–593: in Japanese.

52. H. Masuda, Y. Ikeda, E. Sumiyosi, and N. Washizu, "In-situ Measurements of Photo-Électron Emission at Elevated Temperature", *J. Jpn. Inst. Met.*, 59(1995): 1322–1325: in Japanese.

53. K. Ozawa, Y. Sakka, and M. Amano, "Synthesis of $LiSbO_3$ from Metal Alkoxides", *J. Jpn. Soc. Powder Powder Metall.*, 42(1995): 603-607.

54. M. Yositake and K. Yosihara, "Electric States of Segregated Metal Atom on Metal Surfaces and Potential Use for Field Emitter", *J. Vac. Sci. Technol.*, A13(1995): 2407–2411.

55. T. Ohno and T. Sasaki, "Ab Initio Study of Cl Impurity at GaAs Surfaces", *Materials Science Forum*, 196(1995): 543–548.

56. Y. Sakka, H. Okuyama, T. Uchikoshi, and S. Ohno, "Characterization of Degraded Surfaces of Al and AlN Ultrafine Powders", *Nanostruct. Materials*, 5(1995): 577–588.

57. T. Ohno, "Chlorination of Ga-rich and As-rich Reconstructed GaAs(001) Surfaces", *Proc. Int. Conf. Phys. Semiconductors*, (1995): 545–548.

58. H. Baba and T. Kodama, "Localized Corrosion of Copper in Wet Organic Acid Vapor", *Zairyo-to-Kankyo*, 44(1995): 233–239: in Japanese.

59. S. Matsushima, S. Ohashi, and T. Ishihara, "Stress Corrosion Cracking Behavior of the Fe-Base Shape Memory Alloy in High Temperature Water", *Zairyo-to-Kankyo*, 44(1995): 386–390: in Japanese.

Mechanical properties

60. K. Yagi, M. Tabuchi, and A. Saxena, "Crack Growth under Small-Scale and Transition Creep Conditions in Creep Ductile Materials", *ASTM STP1207*, (1995): 481–497.

61. R. Hamano, S. Kaise, and K. Saito, "The Effect of Mixing Treatment on Corrosion Fatigue Strength of SNCM439 Steel in a 3.5% NaCl Aqueous Solution", *Corrosion Engineering*,

44(1995): 101–110.

62. K. Nagai, "Effect of Strengthen Mechanisms on Fatigue Strength", *Frontiers in Strengthening of Steels*, (1995): 145–153: in Japanese.

63. T. Mawari and T. Hirano, "Effect of Unidirectional Solidification Conditions on the Microstructures and Tensile Properties of Ni_3Al", *Intermetallics*, 3(1995): 23–33.

64. K. Nakazawa, A. Takei, K. Kasahara, A. Ishida, and M. Sumita, "Effect of Ni-TiC Composite Film Coating on Fretting Fatigue in High Strength Steel", *J. Jpn. Inst. Met.*, 59(1995): 1118–1123: in Japanese.

65. E. Takeuchi, S. Matuoka, K. Miyahara, K. Hirukawa, and N. Nagashima, "Arrest Function in Elevated Temperature Fatugue Crack Propagation for Stainless Steels with Dispersed Lead Particles", *J. Jpn. Soc. Mech. Eng.*, 61(1995): 39–44: in Japanese.

66. I. Mutoh, T. Tanabe, T. OoBa, and K. Yagi, "Creep Rupture Behavior of Mechanically Alloyed Metals at 1373K", *J. Jpn. Soc. Mech. Eng.*, 95-2B(1995): 345–346: in Japanese.

67. Y. Maeda, A. Ohta, *S. Machida, and *H. Yoshinari(*Univ. Tokyo), "Fatigue Crack Propagation in Welded Joints in Environment Periodically Changed between Synthetic Sea Water and Ambient Air", *J. Jpn. Welding. Soc.*, 13(1995): 289–292: in Japanese.

68. C. Kan and *S. Horibe (*Univ. Waseda), "The Environmental Effect on Cyclic Fatigue Behavior in Ceramic Materials", *J. Mater. Sci.*, 30(1995), 1565–1569.

69. C. Kan, "Cyclic-Fatigue Crack Growth of Silicon Nitride under a Constant Maximum Stress Intensity", *J. Mater. Sci. Lett.*, 14(1995): 241–243.

70. N. Yamamoto, J. Nagakawa, and H. Shiraishi, "The Effect of MC and MN Stabilizer Additions on the Creep Rupture Properties of Helium Implanted Fe-25%Ni-15%Cr Austenitic Alloy", *J. Nuc. Mater.*, 226(1995): 185–196.

71. N. Maruyama, T. Kobayashi, and M. Sumita, "Fretting Fatigue Strength of a Ti-6Al-4V Alloy in a Pseudo-Body-Fluid and Quantitative Analysisses of the Substances in the Fluids", *Journal of Japanese Society for Biomaterials*, 13(1995): 14–20.

72. H. Harada, "High Temperature Metallic Materials", *Journal of Robotics Society of Japan*, 13(1995): 185–188.

73. F. Abe, "Creep and Creep Rate Curves of a 10Cr-30Mn Austenitic Steel During Carbide Precipitation", *Metallurgical and Materials Transaction*, 26A(1995): 2237–2246.

74. M. Tabuchi, Y. Nakasone, T. Ohba, K. Yagi, and T. Tanabe, "Effect of Carbon Content and Helium Gas Environment on Creep Crack Growth Properties of Ni-26%Cr-17%W-0. 1%Mo Alloy at1273K", *Metallurgical and Materials Transactions A*, 26A(1995): 383–389.

75. K. Kimura, H. Kusima, and K. Yagi, "Design for High Temperature Metallic Materials in Consideration of Environment Load", *Proc. Ecom-Conf.*, (1995): 99–102.

76. K. Kimura, H. Kushima, F. Abe, and K. Yagi, "Creep Deformation Assessment of Aged Steel Based on Inherent Creep Strength Concept", *Proc. Int. Sympo. Mater. Aging and Component Life Extension*, (1995): 459–468.

77. F. Abe, K. Kimura, E. Baba, O. Kanamaru, and K. Yagi, "Creep Curve Analysis and Creep Life Evaluation of 10Cr-30Mn Austenitic Steels", *Proc. Int. Sympo. Mater. Aging and Component Life Extention*, (1995): 1075–1084.

78. H. Nagai, K. Kimura, F. Abe, and K. Yagi, "Effect of Stress on Precipitation Morphology of γ'-Phase and Creep Strength Properties of Inconel 713C", *Tetsu-to-Hagane*, 81(1995): 61–66: in Japanese.

79. K. Nakano and K. Yasunaka, "Fracture Toughness in the Tradition Region of a carbon Steel and a Ferritic Nodular Cast Iron", *Tetsu-to-Hagane*, 81(1995): 209–213: in Japanese.

80. H. Kushima, K. Kimura, K. Yagi, and *K. Maruyama (*Univ. Tohoku), "Long-term Creep Strength Property and Microstructural Stability of 12Cr Steel" *Tetsu-to-Hagane*, 81(1995): 214–219: in Japanese.

81. K. Kimura, H. Kushima, K. Yagi, and C. Tanaka, "Effects of Minor Alloying Elements on Inherent Creep Strength Properties of Ferritic Steels", *Tetsu-to-Hagane*, 81(1995): 757–762: in Japanese.

Measurement and evaluation

82. T. Yokokawa and K. Ohno, "Accurate Measurement of Lattice Misfit Between γ and γ' Phese of Ni-base Superalloys at High Temperature", *Advances in X-ray Chemical Analysis*, 26(1995): 113–124.

83. Y. Nakasone, I. Mutoh, and T. Tanabe, "Creep Damage of Ni-base Superalloys in Helium Gas at Very High Temperatures", *Am. Soc. Mech. Eng.*, Book H00978(1995): 517–524.

84. K. Sato, M. Kohri, K. Ide, H. Ohkouchi, and *S. Hotta(*JAMSTEC), "X-ray Fluorescence Analysis of Submarine Sediment by Low Dilution Fusions and Matrix Correction Using Theoretical Alpha Coeffecients", *Bunseki Kagaku*, 44(1995): 143–150: in Japanese.

85. M. Kohri, K. Sato, K. Ide, H. Ohkouchi, and *Y. Inoue (*Yokogawa Analyticals Systems Inc), "Batch Operation for Solid Phase Extraction of Organotin Compounds in sea Water", *Bunseki Kagaku*, 44(1995): 537–542: in Japanese.

86. K. Sato, M. Kohri, and H. Ohkouchi, "Speciation of Organotin Compounds in Sea Water by Micellar Liquid Chromatography/ICP-MS", *Bunseki Kagaku*, 44(1995): 561–568: in Japanese.

87. K. Ide, H. Ohkouchi, and *S. Hashimoto (*Tokyo Univ. of Fisheries), "Determination of Total Tin in Sediments by GF-AAS", *Bunseki Kagaku*, 44(1995): 617–625: in Japanese.

88. H. Yamaguchi, M. Kiyokawa, and R. Hasegawa, "Determination of Trace Silicon in High Purity Titanium and Chromiun by Molybdosilicic Acid Blue Spectrophotometry After Fluoride Separation", *Bunseki Kagaku*, 44(1995): 647–650: in Japanese.

89. K. Inoue, Y. Sakai, M. Asano, and H. Maeda, "Cu-Ag Microcomposite Alloy and Its Application to Generate Extremely High Magnetic Field", *Cryogenic Engineering*, 30(1995): 163–170: in Japanese.

90. H. Ohkouchi, M. Kohri, K. Satou, and K. Ide, "Development of Analytical System for Monitoring of Organotin in Marine Environmental Samples", *Environmental Research in Japan*, 1(1995): 1–19: in Japanese.

91. M. Saito, "Relatine Send Relative Sensitivity Factors in Direct Current Glow Discharge mass Spectonetry Using Kr and Xe gas-Estimation of The Role of Penning Ionization", *Fveslmius J. Anal. Chem.*, 351(1995): 148–153.

92. K. Itou, M. Yuyama, and H. Wada, "VAMAS Critical Current Round Robin Test on a 2212 BSCCO Ag-Sheathed Tape", *IEEE Trans. Superconductivity*, 5(1995): 536–539.

93. K. Sakurai, "Development of High Power X-ray Generator for X-ray Adsorption Fine Structure Measurements", *Isotope News*, 11(1995): 6–7.

94. T. Kobayashi, K. Ide, S. Hasegawa, R. Hasegawa, and *K. Iwase (*Kawasaki Steel Corporation Ltd.), "Determination of Trace Elements in Titanium and Titanium Alloys by GF-AAS", *J. Jpn. Inst. Met.*, 59(1995): 290–295: in Japanese.

95. K. Miyahara, S. Matsuoka, H. Hirukawa, and N. Nagashima, "Observation of Oxide Particles and Thickness Measurement of Oxide Films by an AFM/STM Hybrid System", *J. Jpn. Soc. Mech. Eng.*, 61(1995): 581–588: in Japanese.

96. H. Hirukawa, S. Matsuoka, K. Miyahara, and E. Takeuchi, "Observation of Elevated-Temperature Fatigue Surfaces for Stainless Steel with Dispersed Lead Particles by an AFM/STM Hybrid System", *J. Jpn. Soc. Mech. Eng.*, 61(1995): 697–704: in Japanese.

97. K. Miyahara, S. Matsuoka, N. Nagashima, and *S. Mishima (*Olympus Optical Company Ltd.), "Development of a Nanoindenter on the Basic of a Atomic Force Microscope", *J. Jpn. Soc. Mech. Eng.*, 61(1995): 2321–2328: in Japanese.

98. Y. Nakasone, I. Mutoh, and T. Tanabe, "Effects of Sampling Site and Direction on the Creep Damage of Ni-Base Superalloys by the A-Parameter in Very High Temperature Creep", *J. Jpn. Soc. Mech. Eng.*, 95-2A(1995): 425–426: in Japanese.

99. M. Yoshitake and K. Yoshihara, "Reference Structure and Reference Items for Surface Analysis Spectral Database", *J. Surface Analysis*, 1(1995): 303–308.

100. K. Yoshihara and M. Yoshitake, "Construction of the Surface Analysis Network Database", J. *Surface Analysis*, 1(1995): 369.

101. K. Yoshihara, "The Progress in Quantitative Surface Analysis with Electron Spectroscopy", *J. Surface. Sci. Soc.Jpn.*, 16(1995): 18–23: in Japanese.

102. M.Yoshitake and K. Yoshihara, "The Characterization of XPS 'Secondary-Standard' Spectra for the Common Data Processing System", *J. Surface. Sci. Soc. Jpn.*,16(1995): 434–440: in Japanese.

103. K. Yamada, O. Kujirai, and R. Hasegawa, "Simultaneous Determination of Sub μg/g Levels of Nine Impurities in High Purity Iron by Horizontal Cation Exchange Resin Mini-Column and ICP-Atomic Emission Spectrometry", *Mater. Trans. JIM*, 36(1995): 56–60.

104. S. Itoh, F. Hirose, S. Hasegawa, and R. Hasegawa, "Glow Discharge Mass Spectrometric Analysis of Titanium Alloys", *Mater. Trans. JIM*, 36(1995): 664–669.

105. S. Hasegawa, T. Kobayashi, R. Hasegawa, and *K. Cho (*Korea Research Institute of Standards and Science), "Determination of Trace Amounts of Selenium in Ni-Base Heat-Resisting Alloys by Graphite Furnace Atomic Absorption Spectrometry" *Mater. Trans. JIM*, 36(1995): 1157–1162.

106. K. Ito and H. Wada, "VAMAS Activities on Establishment of Critical Parameter Measurement Methods for the Oxide Superconductors", *Proc.9th US-Japan Workshop on High-field Super-conducting Materials Wires and Conductors*, (1995): 73–76.

107. M. Yoshitake, "Ion-Induced Auger Electron Spectrometry", *Radioisotopes*, 44(1995): 280–283: in Japanese.

108. M. Saito, "A Contribution to the Study of Matrix Effects in the Analysis of Solid Samples by D.C.Grow Dischange Mass Spectrometry", *Spectrochim. Acta.*, 50B(1995): 171–178.

109. Y. Yamauchi, N. Kishimoto, and T. Saito, "Observation of TiN Coating by High Energy X-ray Microtomography", *Surface Tailoring for Steels by Dry Coating*, (1995): 41–42: in Japanese.

110. K. Yamaguchi and S. Nishijima, "High Temperature Low Cycle Fatigue Lives of Engineering Materials", *The Pipning Engineering*, 37(1995): 61–64.

111. K. Sakurai and H. Sakurai, "High Power X-ray Generation for XAFS Experiments", *The Rigaku Journal*, 12(1995): 41–45.

Simulation and theory

112. S. Nishijima, "Needs of Common Data Processing for Materials Databases", *ASTM STP Computerization of Materials Property Data*, 1257(1995): 9–19.

113. K. Nagai "Aspects for Ecomaterial in Metals", *Chemical Industry*, 46(1995): 35–39: in Japanese.

114. T. Noda and H. Takahashi, "Corrosion Controlled New Materials Production Using Transmutation Reaction under Irradiation of High Energy Particles", *J. Jpn. Inst. Met.*, 34(1995): 966–968: in Japanese.

115. T. Dan, K. Halada, and Y. Muramatsu, "Characteristics of Image Data Processing Techniques for Sessile Drop Method", *J. Jpn. Inst. Met.*, 59(1995): 846–850: in Japanese.

116. J. Nagakawa, "Calculation of Radiation induced Deformation", *J. Nucl. Mater.*,225(1995): 1–7.

117. M. Ohnuma, *J. Suzuki, *S. Funahashi(*JAERI), †T. Ishigaki, †H. Kuwano, and †Y. Hamaguchi (†Muroran Inst. Technol.), "Small-Angle Neutron Scattering Study on Fe-Cu-Nb-Si-B Nanocrystalline Alloys", *Materials Transactions, JIM*, 36(1995): 918–923.

118. H. Onodera, "Alloy Design Based on Predictions of Atom Configuration", *MTERE2*, 35(1995): 1172–1178: in Japanese.

119. M. Ohnuma, *J. Suzuki, *S. Funahashi (*JAERI),†T. Ishigaki, †H. Kuwano, and †Y. Hamaguchi(†Muroran Inst. Technol.), "Small-Angle Neutron Scattering Study on Fe-Cu-Nb-Si-B Nanocrystalline Alloys", *Physica B* 213 & 214(1995): 582–584.

120. T. Abe, H. Onodera, K. Kimura, M. Fujita, and C. Tanaka, "Effect of Alloying Elements on the Concentration of Atomic Pairs in the Ferrite", *Proc. Ecom-Conf.*, (1995): 139–141.

121. H. Onodera, T. Abe, M. Oonuma, K. Kimura, M. Fujita, and T. Tanaka, "Effect of Atom Configurations in the Ferrite Matrix on the Long Term Creep Strength of Carbon Steels", *Proc. Ecom-Conf.*, (1995): 670–673.

122. J. Nagakawa, N. Yamamoto, and Y. Murase, "Calculation of Radiation Induced Deformation in the LWR", *Proc.2nd Japan-China Sympo. Mater. Advanced Energy Systems and Fission and Fusion Engineering*, (1995): 347–351.

123. M. Shimono and H. Onodera "Molecular Dynamics Study on Amorphization of Ti-Al Alloys", *Proceedings of the First Symposium on Molecular Dynamics*, (1995): 1–6.

124. J. Kinukawa, M. Yamazaki, H. Hongou, T. Watabe, and Y. Monma, "Prediction of Creep Lifetimes for Butt-Welded Joint of Type 304 Stainless Steel by Finite Element Method in-Corporating Damage Variable", *Q. J. Jpn. Weld. Soc.*, 13(1995): 19–27: in Japanese.

125. T. Noda, "Radioactivation under High Neutron Dose", *Report on Fusion Materials for Heliotron Reactor*, (1995): 78–93: in Japanese.

126. H. Onodera, T. Abe, M. Oonuma, K. Kimura, M. Fujita, and T. Tanaka, "Effect of Atom Configuration in the Ferrite Matrix on the Long Term Creep Strength of Carbon Steels", *Tetsu-to-Hagane*, 81(1995): 821–826: in Japanese.

Ferrous materials

127. M. Hagiwara, S. Emura,*S. J. Kim(*Korea Institute of Machinery and Metals), and Y. Kawabe, "Synthesis of Low Cost BE P/M Titanium Composites", *Advanced Materials and Processing, KIMM,* (1995): 505–510.

128. H. G. Suzuki, K. Ushioda, H. Komatsu, and *K. Esaka (*Nippon Steel Corp.), "Influence of Sulfer on ALN Precipitation During Cooling After Solidification and Hot Ductility in Low Carbon Steel", *J. Jpn. Inst. Met.,* 59(1995): 373–380: in Japanese.

129. M. Hagiwara, S. Emura, Y. Kawabe, and *S. J. Kim(*Korea Institute of Machinary and Metals), "In-Site Reinforced Titanium-Based Metal Matrix Composites", *Synthesis/Processing of Lightweight Metallic Materials,* TMS, (1995): 97–106.

Intermetallic compounds

130. E. Abe, "Direct Observation of an Orded Arrangement of Atoms in Intermetallic Compound", *Boundary,* 9(1995): 15–18: in Japanese.

131. M. Nakamura, "Elastic Properties of Intermetallic Compounds", *Intermetallic Compounds-Principles and Practice,* 1(1995): 873–893.

132. H. Nakamura, Y. Ogawa, S. Kasahara, and T. Iwasaki, "Electrical Conductivity of IIa and IIIa Metal Sulfide in Solid", *Mater. Trans. JIM,* 36(1995): 1263–1270.

133. M. Nakamura, "Fundamental Properties of Intermetallic Compounds", *MRS Bulletin,* XX8(1995): 33–39.

134. E. Abe, T. Kumagaya, and M. Nakamura, "Studies on the $\alpha \rightarrow \gamma$ Phase Transformation Mechanism in Ti-48at%Al Alloy by High-Resolution Electron Microscopy", *Philosophical Magazine Letters,* 72(1995): 291–296.

135. M. Muneki, F. Abe, and K. Yagi, "Effect of Heat Treatment on KIc of a MgO Partially Stabilized Zirconia", *Proc. 4th Jpn. Int. SAMPE. Sympo.,* (1995): 446–451.

Materials for mechanical application

136. K. Nagai, "Recyclable Materials Design", *Proc. Ecom. Conf.,* (1995): 260–262.

137. Y. Yamabe, H. Koizumi, H. Murakami, Y. Ro, T. Maruko, and H. Harada ,"Development of Ir-Based Refractory Superalloys", *Report of the 123rd Committee on Heat-Resisting Metals and Alloys Japan Society for the Promotion of Science,* 36(1995): 259–264.

Materials for electronics application

138. Y. Sakai, K. Inoue, and H. Maeda, "New High-Strength High-Conductivity Cu-Ag Alloy Sheets", *Acta Metallurgica et Materialia,* 43(1995): 1517–1522.

139. H. Kumakura, "Review of HTS Wire and Cable Research in Japan", *Advances in Superconductivity,* 7(1995): 577–582.

140. H. Kitaguchi, H. Kumakura, and K. Togano, "Anomalous Current Distribution in Bi-2212/Ag Composite Superconducting Tape caused by Hall Effect", *Advances in Superconductivity* ,(1995): 891–894.

141. Y. Tanaka, *M. Ishitsuka, *T. Yanagitani (*Sumitomo Heavy Industries Co.,Ltd), F. Matsumoto, and H. Maeda, "AgCu Alloy Sheathed Bi-System Oxide Superconducting Wires", *Ceramics Internationals,* 21(1995): 349–353.

142. T. Takeuchi, *Y. Nemoto(*Univ.Tsukuba), Y. Iijima, M. Kosuge, K. Inoue, and H. Maeda, "Critical Current Density and Microstructures of V_3Si Multifilamentary Superconductors", *Critical State in Superconductors,* (1995): 253–256.

143. H. Kumakura, K. Togano, *T. Hasegawa, and *K. Kobayashi(*SHOWA Electric WIRES & CABLE Co.,Ltd), "Improvement of Superconducting Characteristics of a $Bi_2Sr_2CaCu_2O_x$/Ag Thick Film by Controlling Microstructure Under Reduced O_2 Atmosphere", *IEEE Trans. Appl. Super-conductivity,* 5(1995): 1845–1848.

144. H. Kumakura, H. Kitaguchi, K. Togano, *T. Kawasima, and *E. Muromachi(*NIRIM), "Flux Pinning and Irreversibility Fields of $(Cu_{0.5}C_{0.5})Ba_2Can\text{-}1CunO_2{+}3(n{=}3.4)$", *IEEE Trans. Superconductivity,* 5(1995): 1399–1404.

145. T. Takeuchi, K. Itou, Y. Iijima, M. Kosuge, K. Inoue, and H. Maeda, "Magnetic Properties and Microstructure of V_3Si Multifiramentary Superconductors", *IEEE Trans. Superconductivity,* 5(1995): 1785–1788.

146. T. Takeuchi, "V_3Si Conductor", *ISTEC Journal*, 8(1995): 48–50.

147. H. Kumakura, H. Kitaguchi, K. Togano, *T. Hasegawa, and *K. Kobayashi(*SHOWA Electric WIRES & CABLE Co.,Ltd), "Superconducting Properties of $Bi_2Sr_2CaCuO_y$ Tape Prepared by Continuous Heat Treatment Technique", *J. Appl. Phys.*, 34(1995): L1638–1640.

148. K. Saito, "Ion Irradiation Effects and Modification of Superconducting BiSrCaCuO Thin Films", *J. Defect Solid State*, 123(1995): 135–156.

149. H. Kitaguchi, H. Kumakura, K. Togano, T. Kiyoshi, K. Inoue, H. Maeda, *N. Tomita, and *J. Kase(*ASAHI GLASS Co.,Ltd), "Superconducting Magnet System Containing Bi-2212/Ag Coil Generates 21.8T at 1.8k", *J. Electric Mater.*, 24(1995): 1883–1886.

150. F. Matsumoto, Y. Tanaka, *T. Yanagiya, *M. Ishizuka(*Sumitomo Heavy Industries.Ltd), M. Asano, and H. Maeda, "Fabrication and Superconducting Properties of Ag-and AgCu Alloy-Sheathed Bi-2212 Superconducting Tapes", *J. Jpn. Inst. Met.*, 59(1995): 339–346: in Japanese.

151. T. Kuroda, M. Yuyama, H. Wada, K. Inoue, *K. Katagiri(*Univ. Iwate) and †H. Koguro (†Univ. Kyoto), "Effect of Neutron Irradiation on the Critical Temperature and the Critical Current in Nb-Tube Processed Nb_3Al Multifilamentary Wires", *Journal of the Atomic Energy Society of Japan*, 37(1995): 652–659.

152. G. Kido, *T. Yasui, *Y. Segawa, *Y. Aoyagi(*RIKEN), †Y. Iimura(†Univ. Agriculture and Technology), **G. E. W. Bauer(**Delft Univ.), ††I. Mogi(††Univ. Tohoku), "Excitation States in Two-Dimentional Systems of GaAs/AlAs Multi Quarter-Well Structure Under High Magnetic Fields", *Phys. Rev B*, 51(1995): 9813–9819.

153. H. Kumakura, K. Togano, Y. Kazumata, and Xinghua Gao, "Effect of 230MeV Au_{14+} Irradiation on $Bi_2Sr_2CaCu_2O_x$", *Physica C*, C250(1995): 325–30.

154. H. Kumakura, K. Togano, *N. Tomita, *E. Yanagisawa(*ASAHI GLASS Co.,LTD) and †S. Okayasu(†JAERI), "Comparative Study on 180MeVCu_{11+} Irradiation Effect on Textured $YBa_2Cu_3O_x$ and $Bi_2Sr_2CaCuO_y$", *Physica C*, C251(1995): 231–237.

155. Y. Tanaka, *M. Ishizuka(*Sumitomo Heavy Industries Co.,Ltd), and H. Maeda, "Superconducting Properties and Microstructure of Bi-2223 Ag-Cu Alloy Sheathed Tapes Doped with Ti, Zr or Hfm", *Physica C*, 252(1995): 339–347.

156. Y. Tanaka, H. Maeda, *M. Ishizuka(*Sumitomo Heavy Industries,Ltd), †L. L. He, and †S. Horiuchi(†NIRIM), "Introduction of Amorphous Disk-Layer into Bi-2212 Lattice of AgCu Alloy Sheeted Tapes and the Critical Current Properties", *Proc. European Ceramic Conference IV*, 7(1995): 255–263.

157. H. Kitaguchi, "Melting and Solidification of Oxide Superconductors in Short Durational Microgravity", *Proc. In Space 95*, (1995): 300–311.

158. H. Kitaguchi, H. Kumakura, K. Togano, *N. Tomita(*ASAHI GLASS Co.,Ltd), †N.Takeda, and †N. Igata(†Science Univ. of Tokyo), "Mechanical and Superconducting Properties of Bi-2212/Ag-Mg-Zr Alloy Composite Tapes", *Proc. 4th Japan Int. SAMPE Sympo.*, (1995): 495–500.

159. H. Kumakura, H. Kitaguchi, K. Togano, K. Inoue, H. Maeda, *T. Katou, and *N. Inoue (*HITACHI CABLE, Ltd), "Bi-2212 Pancake Coils Fabricated Alloying Dip-Coating Process", *Proc. 9th US-Jpn Workshop on High-Field Superconducting Materials Wires and Conductors*, (1995): 153–156.

Magnetic materials

160. H. Kimura and M. Sato, "Single Crystal Growth of Rare-Earth Oxides for Magnetic Refrigeration", *Current Topics in Crystal Growth Res.*, 1(1995): 329–366.

161. H. Kimura, T. Numasawa, M. Sato, *T. Ikeya, and *T. Fukuda(*Tohoku Univ.), "Properties of Czochralski Grown $RAlO_3$ Single Crystals for Magnetic Refrigeration", *J. Appl. Phys.*, 77(1995): 432–434.

162. S. Nimori, G. Kido, *H. Haga, and *T. Suzuki(*Tohoku Univ.), "Field Induced Magneti-zation of TmSb", *J. Mag. Mag. Mater.*, (1995): 140–144.

163. I. Nakatani, "Ultramicro Fabrications of Magnetic Materials by Electron-Beam Lithography", *Journal of the Magnetics Society of Japan*, 19(1995): 1.

Materials for energy application

164. *M. Okamoto(*Tokyo Inst. Tech.), M. Kitajima, †T. Mitsuhashi (†NIRIM), **Y. Kobayashi (**NIMC), ††K. Kiuchi(††JAERI), and ***S. Kano (***PNC), "Nuclear Material Research in Cross-Over Research Project", *J. Atomic Energy Soc. Japan*, 37(1995): 796–806: in Japanese.

165. K. G. Nakamura and M. Kitajima, "Reactive Scattering of with Si(111) Surface: Resonance Enhanced Multiphoton Ionization of SiO", *J. Chem. Phys.*, 102(1995): 8569–8573.

166. M. Amano, M. Nishimura, and M. Komaki, "Alloys for Hydrogen Permeation and Purification", *J. Jpn. Inst. Met.*, 34(1995): 168–172: in Japanese.

167. I. Kamioka, M. Kitajima, T. Kawabe, K. G. Nakamura, and S. Hishita, "Effect of Oxygen Ions on Plasma Oxydation of Silicon", *J. Surface. Sci. Soc. Jpn.*, 16(1995): 32–37: in Japanese.

168. K. G. Nakamura and M. Kitajima, "Rovibrational State Distribution of SiO Desorbed from a Silicon Surface During O_2 Molecular Beam Scattering", *J. Surface. Sci. Soc. Jpn.*, 16(1995): 41–44: in Japanese.

169. Y. Kobayashi, I. Kojima, S. Hishita, T. Suzuki, E. Asari, and M. Kitajima, "Damage-Depth Profiling of an Ion-Irradiated Polymer by Monoenergetic Positron Beams", *Phys. Rev. B*, 52(1995): 823–828.

170. K. Ishioka, K.G. Nakamura, and M. Kitajima, "Phonon Confinement in GaAs by Defect Formation Studied by Real-Time Raman Measurements", *Phys. Rev. B*, 52(1995): 2539–2542.

171. K. Ishioka, K. G. Nakamura, and M. Kitajima, "Reduction in Raman Intensity of Si(111) due to Defect Formation During Ion Irradiation", *Solid State Commun.*, 96(1995): 387–390.

172. F. Abe, "12Cr Steels for Nuclear Reactors", *12Cr Steels for Nuclear Application*, (1995): 222–236.

Bio-Materials,etc.

173. A. Yamamoto, N. Maruyama, T. Kobayashi, K. Nakazawa, and M. Sumita, "Fretting Fatigue Properties of Ti-6Al-4V Alloy in a Psendo-body Fluid and Evaluation of Biocompatibility by Cell Culture Method", *J. Jpn. Inst. Met.*, 59(1995): 463–470: in Japanese.

174. A. Yamamoto, T. Kobayashi, N. Maruyama, and M. Sumita, "Cytotoxicity Evaluation of Psendo-Body Fluids Used as Environment of Fretting Fatigue Tests of Metallic Biomaterials", *Proc. Jpn. Int. SAMPE Sympo.*, 1(1995): 643.

Processing

Gaseous process

175. A. Ishii and K. Nakamura, "RBS-PIXE Analysis on Thin Films of HTC Oxide Superconductors", *J. Appl. Phys.*, 64(1995): 372–373.

176. H. Araki, T. Noda, Y. Suzuki, F. Abe, and M. Okada, "Effect of Pyrocarbon Pre-Coating on Mechanical of CVI Carbon Fiber/SiC Composites", *J. Nuc. Sci. Tech.*, 32(1995): 369–371.

177. A. Ishida, A. Takei, and S. Miyazaki, "Shape Memory Thin Film", *J. Surface Finishing Soc. Jpn.*, 46(1995): 628–631: in Japanese.

178. A. Ishida, M. Sato, A. Takei, and S. Miyazaki, "Effect of Heat Treatment on Shape Memory Behavior of Ti-Rich Ti-Ni Thin Films", *Mater. Trans. JIM*, 36(1995): 1349–1355.

179. A. Ishida, M. Sato, A. Takei, and S. Miyazaki, "Shape Memory Behavior of Ti-Ni Thin Films Annealed at Various Temperatures", *Proc. MRS. Sympo.*, 360(1995): 381–386.

Liquid state process

180. N. Aritomi, *M. Takeyama (*Tokyo Inst.Tech), T. Yoshida, †T. Tsujimoto (†Ibaraki Univ.), and M. Nakamura, "Electrolytic Isolation and Quantitative of α_2 and Non-Metallic Phases in γ-TiAl Base Alloys", *Intermetallics*, 3(1995): 281–291.

181. G. Aragane, S. Takamori, Y. Osawa, and A. Sato, "Refinement of Cast Structures of Al-Si Alloy Ingots by Rheocasting", *J. Jpn. Inst. Met.*, 59(1995): 559–563: in Japanese.

182. M. Kobayashi, H. Nakamura, A. Kasahara, and M. Amano, "Effect of Potassium Addition to Lithium Antimonate on Ion Exchange Rate", *Journal of the Mining and Materials Processing Institute of Japan*, 111(1995): 949–954.

183. K. Sakuraya, T. Watanabe, S. Iwasaki, A. Fukuzawa, M. Yamazaki (Chubu Electric. Power Co), T. Take, and M. Fujita (Fuji Electric Co. R. &D. Ltd), "Levitation and Heating of Metallic Ball in Cold Crucible Simultaneously Supplied with Two Freguencles", *Tetsu-to-*

Hagane, 81(1995): 179–184: in Japanese.

184. Y. Ohsawa, G. Aragane, S. Takamori, A. Sato, *H. Haishi, and *K. Nagamori(*Shinagawa Refractories Co., Ltd.), "Effects of Ultrasonic Vibration on Solidification Structures of Cast Iron". *The Journal of the Japan Foundrymen's Society*, 67(1995): 325–330: in Japanese.

Solid state process

185. K. Kamihira, K. Honda, and T. Fujii, "Effect of Rolling Reduction on the Secondary Grain Growth in Molybdenum Sheet", *J. Jpn. Soc. Powder Powder Metall.*, 42(1995): 1190–1195: in Japanese.

186. S. Yamamoto, H. Miyaji, and *H. Nakamura (*Hosei Univ.), "Mechanisms of Poor Machinability of Austempered Ductile Iron", *Tetsu-to-Hagane*, 81(1995): 19–24: in Japanese.

Powder processing

187. Y. Kaieda, "Properties of TiNi Intermetallic Compound Industrially Combustion Synthesis", *Ad. Sym. Pro. Comp. Ad. Cer.*, 56(1995): 27–38.

188. Y. Sakka,*D.D. Bidinger, and *A. Aksay (*Univ. Princeton), "Processing of Silicon Carbide-Mullite-Alumina Nanocomposites", *J. Am. Ceram. Soc.*, 78(1995): 479–486.

189. S. Ohno, H. Okuyama, and K. Honma, "Synthesis of Ultrafine Iron Nitride Particles by Reactive Plasma-Matal Reaction", *J. Jpn. Inst. Met.*, 59(1995): 408–414: in Japanese.

190. Y. Muramatsu, K. Ohkoshi, and H. Suga, "High Temperature Hardness and Oxidation Resistance of Sinter-HIPed TiAl", *J. Jpn. Inst. Met.*, 59(1995): 754–760: in Japanese.

191. T. Itagaki, "Coating of HfC on Tungsten Powder by Fluidiged Bed CVD", *J. Jpn. Inst. Met.*, 59(1995): 1157–1164: in Japanese.

192. T. Uchikoshi, Y. Sakka, and H. Okuyama, "Pressure Filtration of Al_2O_3", *J. Jpn. Soc. Powder Powder Metall.*, 42(1995): 309–313: in Japanese.

193. S. Hong, K. Ozawa, and Y. Sakka, "Electro-Discharge Sintering of (Fe,Co)-B and Ni-B Amorphous Ultrafine Powders Prepared by Chemical Reduction", *J. Jpn. Soc. Powder Powder Metall.*, 42(1995): 323–329: in Japanese.

194. Y. Muramatsu, K. Ookoshi, and H. Suga, "Sintering of TiAl Containing Nb and Densification by HIPing", *J. Jpn. Soc. Powder Powder Metall.*, 42(1995): 611–617: in Japanese.

195. Y. Muramatsu, K. Ookoshi, and H. Suga, "Production of Tungsten Dispersion Cu-1.0Vol%W Alloy Plates and Their Mechanical Properties", *J. Jpn. Soc. Powder Powder Metall.*, 42(1995): 762–766: in Japanese.

196. K. Kamihira, K. Maiwa, K. Gotou, K. Honda, and T. Fujii, "Characterization of $YBa_2Cu_3O_x$ Superconductor Fabricated by Use of Refined Alloy Oxide Powders", *J. Jpn. Soc. Powder Powder Metall.*, 42(1995): 939–943: in Japanese.

197. *K. Sodeyama, Y. Sakka, and *Y. Kamio (*Kagashima Pref. Inst. of Industrial Tech.), "Preparation of Fine Shirasuballoons", *J. Jpn. Soc. Powder Powder Metall.*, 42(1995): 1128–1135: in Japanese.

198. Y. Sakka, "Ultrastructure Control by Colloidal Processing", *Seramikkusu*, 30(1995): 1017–1020: in Japanese.

Joining

199. T. Kasugai, K. Ei, and H. Irie, "Diffusion Bonding of Zr and SUS304L Stainless Steel", *Pressure Engineering*, 33(1995): 237–244: in Japanese.

200. T. Kasugai, K. Ei, and H. Irie, "Diffusion Bonding of Zirconium and Stainless Steel", *Proc. IIW Asian Pacific Welding Congress*, (1995): 271.

Composite process

201. S. Kuroda, T. Fukushima, and S. Kitahara, "A Study on the Microstructural Development of Plasma Sprayed Ceramic Coatings", *Elevated Temperature Coatings: Science and Technology II*, (1995): 21–30.

202. T. Shirota, T. Dendo, and *M. Kiuchi(*Univ. Tokyo), "Infiltrating and Joining Process Under Semi-Molten State for Making Metal-Ceramic Composite", *Journal of the Japan Society for Technology of Plasticity*, 36(1995): 960–966: in Japanese.

203. *L. Bianchi, †P. Lucchese(†C.E.A.), *A. Denoirjean, S. Kuroda, and *P. Fauchais (*Univ.Limoges), "Evolution of Quenching Stress during Ceramic Thermal Spraying with Respect to Plasma Parameters", *Proc. NTSC'95*, (1995).

204. S. Kuroda, "Evaluation of the Pore Structure in Plasma-Sprayed Coatings", *Proc.8th CIMTEC*, (1995): 373–380.

205. S. Kuroda and S. Kitahara, "Effects of Spray Conditions on the Pore Structure Quenching Stress in Plasma Sprayed Coatings", *Proc.14th Int.Thermal Spray Conf.*, (1995): 489–494.

Process with aid of beam technology

206. N. Sakuma and K. Hiraoka, "Heat Transport and Vaporization in Ar-He or Ar- Mixed Gas Tungsten Arcs", *J. Jpn. Welding. Soc.*, 56(1995): 104–105: in Japanese.

207. M. Kobayashi, H. Fudouzi, M. Egashira, and N. Shinya, "Particles Arrangement on Dielectric Substrates Using Electron Beam", *Proc. Int. Sympo. MIMR'95*, (1995): 205–208.

Processing in special environment

208. T. Ohara, "Applied Superconducting Technology for Preservation of Natural Environment", *Feasibility Study on Superconductivity Application Fields*, (1995): 21–28: in Japanese.

209. T. Ohara, *O. Tsukamoto, *T. Ohizumi (*Yokohama National Univ.), †S. Mori (†Univ. MIE), and **Y. Wada(**PNC), "Feasibility Study on Separation of Several Tens Nanometer Scale Particles by Magnetic FFF Technique Using SCM", *IEEE Trans. Appl. Superconductivity*, 5(1995): 311–314.

210. H. Fujii, T. Kimura, H. Kitaguchi, H. Kumakura, K. Togano, and M. Mohri (NASDA), "Fabrication of Uniform Al-Pb-Bi Monotectic Alloys Under Microgravity Utilizing the Space Shuttle: Microstructure and Superconducting Properties", *J. Mater. Sci.*, 30(1995): 3429–3434.

211. M. Tosa, A. Itakura, A. Kasahara, and K. Yoshihara, "Sample Transfer and Delivery in the XHV Integrated Process", *J. Vacuum Soc.Jpn.*, 38(1995): 821: in Japanese.

212. T. Kiyoshi, M. Asano, K. Inoue, H. Maeda, and H. Wada, "Development of High Field Magnets", *Oyo Buturi*, 64(1995): 364–367 :in Japanese.

213. T. Asano, Y. Sakai, G. Kido, K. Inoue, and H. Maeda,"Development of Wire Wound Pulsed Magnet", *Physica B*, B211(1995): 46–49.

214. T. Ohara, *S. Mori(*Univ.MIE), †Y. Oda, †Y. Wada(†PNC), and **O. Tsukamoto (**Yokohama National Univ), "Feasibility of Using Magnetic Chromatography for Ultra-Fine Particle Separation", *Proc. of IEEJ Power and Energy'95*, (1995): 161–166.

❐ NRIM Publications (Apr. 1995 to Mar. 1996)

1. Bulletin of National Research Institute for Metals, in Japanese.
   No.18(Mar. 1996)
2. Annual Report of National Research Institute for Metals, in Japanese.
   For fiscal year of 1994 (Mar. 1996)
3. Kinzaigiken News, in Japanese. Nos. 4 to 12 (1995) and Nos. 1 to 3 (1996).
4. NRIM Research Activities, in English.
   (Dec. 1995)
5. Material Strength Data Sheet, in English.
   NRIM Creep Data Sheet,
   Nos. 1B amd 42 (Mar. 1996)
   NRIM Material Strength Data Sheet Technical Document, in Japanese No.10 to 13 (Mar. 1996)
6. Guide to National Research Institute for Metals,in Japanese and in English. For fiscal year of 1995 (July 1995)

International Exchange Apr. 1995 to Mar. 1996
International Collaboration Research

❒ Research Programme

Australia

1. Study on Surface Modification of Metals with Ultra-High Temperature Heat Sources. (CSIRO)
2. Studies on Conductor Fabrication Process of High-Tc BiSrCaCuO Superconductors. (University of Wollongong)
3. Comparison of High Energy Density Beam and Arc Welding Technique for Joining Advanced Materials of both the Metal-Matrix Composite and Intermetallic Compound Types. (CSIRO)
4. Process Technology and Characterization of Advanced Metal Matrix Composites. (CSIRO)

Brazil

1. Study on Ni-Base Superalloys. (Fundacao de Technologia Industrial)

Canada

1. Damage Evaluation and Remaining Life Prediction of Structural Materials for Extended Service Operation. (Canadian Center for Mineral and Energy Technology, Energy, Mines and Resources)

China

1. Investigation of High Temperature Titanium Alloy for Application over 600°C (Northwest Institute for Non-Ferrous Metal Research)
2. Studies on Structural Control and Superconducting Properties of High Temperature Superconductors. (Institute of Metals Research, Chinese Academy of Science)
3. Fundamental Study on the Improvement of Superconductivity for High-Tc Oxides. (Northwest Institute for Non-Ferrous Metal Research)
4. Study of Local Corrosion Damage of Corrosion Resistant Alloy in High Temperature Aqueous Solution. (Shanghai Jiao Tong University)
5. Study on the Improvement of Brittleness of Ni_3Al and NiAl by Unidirectional Solidification. (Institute of Metal Research,Chinese Academy of Science)
6. Environmental Life Cycle Analysis of Materials. (Lanzhou University)
7. Study of TiAl Base Alloy. (Northwest institute for Non-Ferrous Metal Research)
8. Fundamental Research on TiAl Base Intermetallic Compounds. (University of Science and Technology Beijing)
9. Studies of Crevice Corrosion of Low Alloy Pressure Vessel Steels in High Temperature Aqueous Solution. (Institute of Corrosion and Protection of Metals)

Finland

1. Development of Superconducting Thin Oxide Coatings. (Tampere Technical University)

France

1. Superconducting and Cryogenic Magnetic Materials. (Service National des Champs Intenses, CNRS)
2. Mechanical Properties such as Fatigue and so on for Short Fiber Reinforced Metal Matrix Composites. (Conservatoire National des Arts et Metiers)
3. First Order Phase Transitions in Magnetic and Superconducting Materials at Low Temperatures. (Laboratoire Louis Neel Magnetisme, CNRS)

Germany

1. High Performance Superconducting Materials. (Kernforschungszentrum Karlsruhe)
2. Information and Documentation Panel Numerical Data.(Fachinformationszentrum Karlsruhe)
3. Designing of New Continuous Refining Process. (Haus der Technik e.v. Essen)
4. Nanoscopic Evaluation of Material Properties. (Max-Planck-Institut fur Eisenforschung GmbH, Universitat des Soarlandes)
5. In Vitro and In Vivo Biocompatibility of Materials. (Institute of Pathology, Steglity University Hospital)

India

1. Studies on Fabrication Processes for Superconducting Oxide Conductors. (National Physical Laboratory)

Italy

1. Superconducting Properties of Advanced Super-

conductors in Time-Varying Magnetic Fields. (CISE Spa, Technologia Innovative Thermophysics & Cryogenics Sec.)
2. Intercomparison of Methods and Materials for Strain Measurements at Cryogenic Temperatures. (Instituto di Metrogia "G. Colonnetti" -C.N.R)
3. Metallic Materials. (Instituto per la Technologia dei Materiali Metalici Non Tradizionzli)

Korea

1. Development of the Aluminide-Base Intermetallic Compounds for Structural Application of High Temperatures. (Korea Institute of Machinery and Materials)
2. Performance Characterization of Materials at High-Temperature. (Korea Research Institute of Standards and Science)
3. Development of Metallic Superconducting Materials. (Korea Research Institute of Standards and Science)
4. Thermoelectrics Research for Advanced Intermetallic Compounds. (Rapidly Solidified Materials Research Center)
5. Evaluation of the High Temperature Properties for Titanium-Based Particulate Composites. (Korea Advanced Institute of Science and Technology)
6. Studies on the Fabrication of Bi-2223 Superconducting Wire and its Application. (Korea Institute of Machinery and Materials)

Poland

1. Magnetization and Optics in Diluted Magnetic Semiconductors in High Magnetic Fields. (Polish Academy of Science)

Russia

1. Research on Materials Property Data Modeling. (Institute Inorganic Chemistry, Academy of Sciences)
2. Water Purification through Absorptive Dispersed Electrochemical System. (Frumkin Institute of Electrochemistry)
3. Eco-Balance Analysis in Life Cycle of Materials. (Russian Research Center for Standardization, Information and Certification of Materials)
4. Study on Electron Transport through Atomic Scale Tunnel Junctions. (Novosibirsk State University)

Sweden

1. Fabrication and Characterization of Semiconductor Quantum Dots. (Lund University)

Switzerland

1. Research and Development of High Performance Ceramic Superconducting Wires. (University of Geneve)

U.K.

1. Prediction Technology of Life and Remaining Life of Huge Structures under Service Condition and its Application to Design. (The Welding Institute)
2. Research and Development of High Performance Multifilamentary Ceramic Superconducting Wires. (University of Cambridge)
3. Investigation and Development of Highly Parallel Algorithms for Materials Science Calculations. (Kingston University)
4. Measurement and Evaluation Methods for Critical Current in High Temperature. (University of Cambridge)
5. Advancement of Levitation Melting and Refining Technology. (National Physical Laboratory)

U.S.A.

1. Research and Development on Systems and Materials for Magnetic Refrigerators. (Francis Bitter National Magnet Laboratory, MIT)
2. Databases on High Temperature Superconducting Materials. (National Institute of Standards and Technology)
3. Studies of High-Strength/High-Conductive Materials and Their Application to High-Field Magnets. (Francis Bitter National Magnet Laboratory, MIT)
4. Fundamental Studies on the Conductor Fabrication of High Temperature Oxide Superconducting Materials. (National High Magnetic Field Laboratory)
5. Evaluation Methods for Superconductors. (National Institute of Standards and Technology)
6. Developments and Applications of Extremely High-Field Magnets and Magnet Systems. (National High Magnetic Field Laboratory)
7. Study of Nanocomposites Magnetic Materials for Cryogenics. (National Institute of Standards and Technology)
8. Joint Research on the "in-situ" Analysis/Evaluation of Atomic and Microstructural Changes in Materials. (Argonne National Laboratory)
9. Fundamental Studies of Vortex State in High Tc Superconductors. (Argonne National Laboratory)
10. High Pressure Research on Strongly Correlated Electron Systems.(University of California, Davis)
11. Effect of High Magnetic Field on Solid/Solid Phase Transformations. (Northwestern

University)
12. Studies on Mechanisms of Nanoscale Microstructural Evolution in Advance Metallic Materials. (University of Virginia)
13. Study on the Mechanical Properties of Directionally Solidified Intermetallic Compounds. (Oak Ridge National Laboratory)
14. Evaluation of Thick Coatings Formed by Advanced Thermal Spray Processes. (New York State University)

❐ List of Visiting Foreign Researchers

*STA Fellowship

Country and Name	Affiliation	Term	Research Subject
Belgium			
Lieve Stockman	Nijmegen University	1996.1.8 to 1996.1.31	Quantum Phenomena Appeared on Atomic Scale Structures
Johan Vanacken	Leuven University	1995.11.11 to 1995.12.10	Study of Quantum Effect in Mesoscopic Systems
Brazil			
Jose Eduardo Goncalves Lamas	Technological Research Institute of State of Sao Paulo	1995.8.2 to 1995.9.29	Creep Test Technology and Evaluation Technology about Structure of Ni-Base Superalloys
Mario Boccalini Jr.	Technological Research Institute of State of Sao Paulo	1996.3.5 to 1996.4.10	Ceramic Mold for Directional Solidification of Ni-Base Superalloys
Canada			
William Ross Datars	McMaster University	1995.11.1 to 1995.12.28 1996.2.19 to 1996.3.9	Study of Quantum Effects in Mesoscopic Systems
Michael A. Peters	University of Cambridge	1996.3.6 to 996.5.31	Development of High Temperature NiTi Based Intermetallic Alloys
China			
Dali Mao*	Shanghai Jiao Tong University, Department of Materials Science and Engineering	1995.5.25 to 1996.11.24	Development of Magnetic and Superconducting Materials for High Field Use
Shao Qing Zhang*	Beijing Institute of Aeronautical Materials,National Key Laboratory of Advanced Composite	1996.3.8 to 1996.4.7	Development of New High-strength and High-conductivity Composite Materials
Jun Qing Guo*	Harbin Institute of Technology	1996.3.21 to 1997.5.20	Formation of Metastable Materials from Deeply Undercooled Metallic Melts
Huang Ying Kai*	University of Amsterdam	1994.4.14 to 1995.4.13 1995.5.10 to 1995.11.9	Fundamental Study of Electromagnetic Materials with Strong Electron Correlations
Yan Jin*	University of Manitoba, Dept. Mechanical and Industrial	1995.3.22 to 1996.12.21	Development of High Strength Metal Base Composites with Excellent Physical Properties by the Advanced Bronze Method
Piao Min	University of Amsterdam	1994.1.1 to 1996.12.31	Research on Effects of Lattice Defects on Phase Transformations and Precipitations of Alloys by NRTEM
Liu Jian Hong	Harbin Institute of Technology	1994.1.12 to 1995.4.30	Microstructure and Mechanical Properties of Ti_2AlNb Intermetallic Compounds Produced by the Powder Metallurgy Process
Wei Sun	Tohoku University, Institute for Materials Research	1994.11.1 to 1997.10.31	In-situ Observation and Structural Analysis of High Tc Superconduct Superconductors for Fusion Research at low Temperature
Zhao Minshou	Changchun Institute of Applied Chemistry, Chinese Academy of Science	1995.5.8 to 1995.5.11	Purification and Chemical Analysis of rare Earth Metals

Country and Name	Affiliation	Term	Research Subject
Hang Dong	Institute of Metal Research, Chinese Academy of Science	1995.11.20 to 1995.12.20	Fundamental Investigation of Effect of Particulate Distribution on the Mechanical Properties of Particulates MMC's
Mu Ying	Research Development Corporation of Japan	1995.10.1 to 1998.9.30	Fundamental Study on Biocompatibility of Metallic Materials
Bing Jun Gao	National High Magnetic Field Laboratory	1996.2.1 to 1996.2.14	Application of Cu-Ag Alloy Plates to Extremely High-Field Magnets
Ke Wei	Institute of Corrosion and Protection of Metals Academia Sinica	1996.3.1 to 1996.3.20	Effect of Crevice on Low Cycle Fatigue Behavior of Pressure Vessel Steel in High Temperature Pressurized Water
Han Yumei	Institute of Corrosion and Protection of Metals Academia Sinica	1996.1.19 to 1996.3.19	Effect of Crevice on Low Cycle Fatigue Behavior of Pressure Vessel Steel in High Temperature Pressurized Water
Wu Jiansheng	Shanghai Jiao Tong University	1996.3.28 to 1996.3.30	Structure and Mechanical Properties of Intermetallic Compounds
France			
Jean Louis Bobet*	University of Bordeaus	1994.3.1 to 1995.8.31	Thermostructural Composites Laboratory Effect of Residual Stress on Mechanical Properties for SiC/Ti-15-3 Metal Matrix Composite
Herve Rouch*	S2MC(Laboratories de Science des Surfaces et Materiaux Carbone)	1994.11.1 to 1996.7.31	Control of Surface Reaction and Synthetic Processes by "State controlled" Molecular Beams
Bernard Deconihout	Laboratoire de Microsopie Ionique URA CNRS Facultedes Sciences	1996.3.18 to 1996.3.31	Implementation of the Tomographic Atom Probe and Its Applications to Materials Science
Germany			
Christian Roth*	Techinische Universitat Clausthal	1995.3.28 to 1997.3.27	Designing of Continuous Refining Process
Knut Deppert	Department of Solid State Physics, Lund University, Sweden	1995.1.16 to 1995.11.5	Fabrication of Quantum Dots in III-V Compound Semiconductors Using MBE/STM Deposition of Metal Masks for Plasma Etching
Eckhard Steep	Grenoble High Field Magnet Laboratory	1996.2.17 to 1996.3.9	Electronic Properties in Quantum Limit
Wilfred Sigle	Max-Planck-Institute Metall-forschunge, Sttutgart	1995.12.4 to 1995.12.12	Analysis of Quantum Size Effects in Nanostructures by TEM
Mathias Goeken	University of Saarland	1996.3.18 to 1996.3.31	Modeling and Simulation for the Prediction of Material Strength
India			
Balvinder Gogia*	Panjab University, Physics Department	1995.2.5 to 1996.8.4	Study on the Single Crystal Growth of High Temperature Oxide Superconductors
Sankara Pajendran Pillai*	Indira Gandhi Center for Atomic Research Metallurgy Division	1996.1.9 to 1996.4.8	Study on Evaluation of Creap Life for Heat Resisting Steels and Alloys
Mannarathu Devasia Mathew*	Indira Gandhi Center for Atomic Research Materials Development Division	1996.1.11 to 1996.4.10	Self-healing of Creep Damage at High Temperature
Hiranmay X Pal*	Indian Association for the Cultivation of Science, Department of Materials Science	1996.1.17 to 1997.1.16	Effect of Magnetic Field on Transformation Structures and Kinetics in the fcc/bcc Martensitic Transformation
Gautam Ghosh	Northwestern University Dept. of Materials Science and Technology	1996.1.15 to 1996.2.3	Effect of High Magnetic Field on Martensitic and Bainitic Transformations in Steels
Anil R Chaurasia	Department of Physics, East Texas State University	1995.12.21 to 1996.3.19	Materials Characterization by X-ray Absorption Fine Structure
Sunil D. Deshpande	Physics Department. Goa University	1996.3.11 to 1997.3.10	X-ray Spectroscopic Studies on the Impurities in Diluted Magnetic Semiconductors

Country and Name	Affiliation	Term	Research Subject
Indonesia			
Winatapura Shaidin Didin	National Atomic Energy Agency, Indonesia	1995.7.31 to 1996.2.29	Transmission Electron Microscopy Technique and its Applications to Porous Silicon
Kazakhstan			
Askar K. Bazaev*	Institute for Metallurgy and Enrichment	1996.3.11 to 1997.5.10	Research on the Improvement of Long Term Creep Strength of Ferritic Steels based on Design of Atomic Configurations
Korea			
Sung-Joon Kim*	Korea Institute of Machinery and Materials	1994.4.2 to 1995.4.1 1996.2.1 to 1996.2.15	Structure Analysis and Fatigue Properties Evaluation of Ti-based Metal Matrix Composites
Jonghun You*	University of Texas at Dallas, Center of Quantum Electronics	1995.2.1 to 1996.1.31	The Synthesis of Superconducting Ultrathin Films by the Combined Use of Magnetron Sputtering and Ion Implantation Techniques
Choi Il Dong*	Korea Maritime University	1996.1.1 to 1996.2.18	Study on the Fatigue Improvement of the Titanium Particulates Composites
Jaimoo Yoo*	Korea Institute of Machinery and Materials	1996.2.26 to 1996.3.25	Development of Bi-system Superconducting Wire by PIT Process
Kim Dong Yup	Ssang Yong Research Center, Dept. of Elec and Magnetic Materials	1994.11.9 to 1995.11.8	Proparation and Magnetic Properties of Chemically Stabilized Iron-nitride Magnetic Fluids
Soo-Woo Nam	Korea Advanced Institute of Science and Technology	1995.7.10 to 1995.8.6	Investigation of Creep Deformation Behavior of Titanium-Based MMC's and TiAl Intermetallics
Sung-Joon Kim	Korea Institute of Machinery and Materials	1996.2.1 to 1996.2.15	Morphology Control of Reinforcing Ceramic Particulates in Titanium-Based MMC's
Choi Baing-Gyu	Korea Advanced Institute of Science and Technology	1996.1.16 to 1996.2.23	Creep Deformation and Creep Crack Growth of Heat Resisting Steels
Hyum Kyong Kim	Korea Research Institute of Standards and Science	1995.7.24 to 1995.10.14	Research on the Surface Analysis Database
Kyung-Youl Min	Osaka University	1995.10.1 to 1998.9.30	Interface Control and the Measurements of Physical Properties of Thin Film Nitrides
Nong Moon Hwang	Korea Research Institute of Standards and Science	1996.1.29 to 1996.4.25	Modeling of Order-Disorder Transformation in the b.c.c Structure by the Cluster Variation Method
Choe Seung Joo	Korea Institute of Machinery and Materials	1996.3.4 to 1996.3.30	Design of Nickel-base Superalloys
Wan-Young Maeng	Korea Atomic Energy Research Institute	1995.11.27 to 1996.3.26	Environmental Degradation of Structural Materials for Light Water Reactors
Chang Soo Kim	Korea Research Institute of Standards and Science	1996.3.10 to 1996.6.7	X-ray Structure Analysis of Advanced Materials and High Temperature Superconductor Films
Kim Young Suk	Korea Atomic Energy Research Institute	1995.12.3 to 1996.2.25	Phase Stability and Atomic Level Analysis of Zr-2.5Nb Alloy under Electron Irradiation
Lee Yong-Ho	Korea Advanced Institute of Science and Technology	1996.1.16 to 1996.2.23	Computational Simulation for Material Research
Montenegro			
Jovan Mirkovic*	Moscow State University	1996.2.5 to 1996.3.31	Fundamental Study of Electromagnetic Materials with Strong Electron Correlations
Netherlands			
Frank de Bore	University of Amsterdam	1995.10.8 to 1995.10.29	Study of Electronic Properties under High Magnetic Field
Anne de Visser	University of Amsterdam	1996.3.17 to 1996.3.23	Study of Quantum Effect in Mesoscopic Systems

Country and Name	Affiliation	Term	Research Subject
Philippines			
Barbara Dar Juan TIO	Industrial Technology Development Institute Department of Science and Technology	1995.2.6 to 1995.7.27	Japan-ASEAN Cooperation Program on Materials Science and Technology, Philippine Project on Atmospheric Corrosion (Metallic Coating)
Russia			
Dmitri Victorovich Golberg*	Max-Planck Institute fur Eisenforshung Gmbh Materials, Science	1996.3.29 to 1997.5.28	On the Study of the Mechanical Properties of the Unidirectionally Grown Ni_3Al
Marat Gaifullin	Department of Physics, Hokkaido University	1996.1.15 to 1996.3.31	Fabrication of Intrisic Josephson Function Devices and Their Evaluations
Slovakia			
Roman Sandrik	Institute of Physics Slovak Academy of Science	1995.9.25 to 1995.10.16 1996.1.8 to 1996.3.1	Application of Rutherford Back-scattering and Particle Induced X-ray Emission Analysis to Materials Science
Spain			
Jose Luis Jimenez Castells	Columbia University	1996.3.4 to 1996.3.8	Quantum Phenomena Appeared on Atomic Scale Structures
Sweden			
Magnus Persson	Chalmers University of Technology	1996.3.18 to 1996.3.27	Quantum Phenomena Appeared on Atomic Scale Structures
Switzerland			
Giovanni Grasso	University of Geneve Department de Physique de La Matiere Condensee	1995.10.16 to 1995.11.4	Development of High-Jc Bi-Oxide Superconducting Wires
Thailand			
Sermkiat Jomjunyong*	Chiang Mai University, Faculty of Engineering	1996.3.15 to 1996.6.14	Durability of Materials for Infrastructure Use in Asian Pacific Rim
Pakdi THONGCHAROEN	Department of Mineral Resources Ministry of Industry Metallurgy Division	1995.3.20 to 1995.6.8	Japan-ASEAN Cooperation Program on Materials Science and Technology, Thai Project on Atmospheric Corrosion (Organic Coating)
Chalothorn Bhamornsut	Thailand Institute of Scientific and Technological Research	1996.3.1 to 1996.3.30	Degradation of Materials by Ultra-violet Light
U.K.			
Anne F. Whitehouse*	University of Cambridge, Materials Science and Metallurgy	1996.2.9 to 1996.4.8	Development of New High-strength and High-conductivity Composite Materials
Paul J. Warren*	University of Oxford	1994.4.11 to 1995.4.10	Atom-probe Microanalysis of NiTi/Ni_2TiAl Two-phase High Temperature Alloys
Timothy Martin King*	CEC, Joint Research Center. Institute for Advanced Materials	1994.9.30 to 1996.9.29	Investigation of Key Technologies for International Sharing of Materials Property Databases and Advanced Models of Materials Behavior
Swallow Elizabeth*	University of Cambridge, Department of Materials Science	1996.1.22 to 1997.1.21	Atomic Force Microscope Study of Shape Memory Effects in Fe-based Alloys
Richard A. Doyle	IRC in Superconductivity University of Cambridge	1995.3.13 to 1995.4.10	Study of Electronic Transport Properties in Superconducting Vortex State on High Tc Superconductor Bi2212 Single Crystal
Martin P. Seah	National Physical Laboratory	1996.2.6 to 1996.2.10	Surface Analysis of Nano-Structure Materials
J. Singleton	Oxford University	1995.8.14 to 1995.9.1	Quantum Oscillations in Two Dimensional Electron Systems
Robin J. Nicholas	Oxford University, Clarendon Laboratory	1996.3.24 to 1996.3.31	Study on Effective Masses of Curriers in Wide-Gap Semiconductors Using Very High Magnetic Field
Howard G. Read	Center for Tsukuba Advanced	1996.1.4 to 1996.3.31	Atom Probe Microanalysis of Metallic

Country and Name	Affiliation	Term	Research Subject
	Research Alliance, University of Tsukuba		Materials
Colin J. Humphreys	University of Cambridge, Department of Materials Science and Metallurgy	1996.3.21 to 1996.3.31	Nano-analysis of High Temperature Alloys
Andrew Piers Horsefield	University of Oxford	1996.2.19 to 1996.2.27	Analysis of Quantum Size Effects in Nanostructure by TEM
Wei Yao Liang	Cambridge University	1995.8.22 to 1995.8.26	Participation in the Multicore Project Symposium on Superconducting Materials
Henry Winand	University of Cambridge	1996.2.9 to 1996.4.8	The Development of Cu-Cr in-situ Composite
Uklaina			
Svetlana Alexandrovna Vitusevich	Uklaina Academy of Science	1996.3.7 to 1996.3.15	Quantum Phenomena Appeared on Atomic Scale Structures
U.S.A			
John T. Grant	University of Dayton	1996.2.5 to 1996.2.14	Surface Analysis of Nano-Structure Materials
J. S. Brooks	National High Magnetic Field Laboratory	1995.6.3 to 1995.6.24	Fermi Surface Studies of Organic Conductors
William Gilbert Clark	University of California at Los Angels	1996.2.18 to 1996.2.24	Study of Quantum Effect in Mesoscopic Systems
John Goodwin Vandegrift	University of Alabama in Huntsville	1995.6.29 to 1995.8.12	Melting and Solidification of Particle Dispersion Alloys Mainly, the Effect of Bubble Motion on the Dispersion will be Investigated
Lance L. Miller	Ames Laboratory, Condensed Matter Physics, Iowa State University	1996.1.29 to 1996.2.20	Study on the New Intermetallic Compound Superconductors
Robert C. Birtcher	Argonne National Laboratory	1996.2.13 to 1996.3.15	Structural and State Analysis of Liquid and/or Solid Gas Clusters by TEM
Charles W. Allen	Argonne National Laboratory	1996.2.13 to 1996.3.14	Analysis of Quantum Size Effects in Nanostructures by TEM
Christopher J. Gilbert	Department of Materials Science and Mineral Engineering, University of California, Berkeley	1995.6.29 to 1995.8.12	Research on Fatigue Crack Growth in Alumina
Robert James Bastasz	Sandia National Laboratories	1996.1.31 to 1996.3.19	Reaction Processes of Plasma /Surface Interactions
James Robert Engstrom	Cornell University, School of Chemical Engineering	1996.2.26 to 1996.3.16	Chemical Dynamics of Solid Surface and Microscopic Structure

❐ List of Visitors

T:Tsukuba Site M:Meguro Site

Nationality and Name	Affiliation	Site	Date
U.S.A			
Dr.Crystal H.Newton	ASTM E-49Committee	T	Apr. 1995
Prof.D.K.Finnemore	Iowa State University Ames Laboratory	T	Apr. 1995
Mr.John Bell and his party	DIST Deputy Secretary & Chief Science Adviser	T	May. 1995
Dr.Richard Gann his party	NIST	T	Jun. 1995
Director. David T Shaw his party	State University of New York	T	Oct. 1995
Dr.Sordlet and his party	Iowa State University Ames Laboratory	T	Feb. 1996
China			
Dr.HAM En-Hou and his party	Institute of Corrosion of Protection of Metals	T	Apr. 1995
Senior Research Engineer. FANG XIANG WEI and his party	Shanghai Research Institute of Materials	T	Apr. 1995
Prof.Ma Ju-sheng and his party	Qing Hua University	T	Jun. 1995
Deputy Director.Xiong Guo Xing and his party	Dalian Institute of Chemical Physics	T	Sep. 1995
Deputy Director.SHI Pei-hua and his party	Shanghai Nuclear Engineering Research of Design	M	Nov. 1995
Prof.WENG YUQING and his party	Central Iron & Steel Research Institute Ministry of Metallurgical Industry	T	Dec. 1995
Director.KE Wei and his party	Institute of Corrosion and Protection of Metals	T	Mar. 1996
Korea			
Director.Chang Shik Shin and his party	Research Institute of Industrial Science & Technology	T	Sep. 1995
Senior Reserecher. YIM CHANG HEE and his party	Pohang Iron & Steel Co. Ltd.	T	Dec. 1995
Mr.JUNG CHUL SHIN and his party	Research Institute of Industrial Science & Technology	T	Mar. 1996
Itaria			
Mr.Monica Zamboni and his party	University of Southampton	T	Aug. 1995
Dr.G.N.Babini and his party	Research Institute for Ceramic Technology	T	Mar. 1996
Germany			
Researcher.Gerd.Rudiger.Tillack his party	BAM	T	May 1995
Director.Hermann Krockel	Institute for Advanced Materials	T	Sep. 1995
Dr.Beyer his party	Degussa AG	T	Oct. 1995
India			
Associate Professor. G.Anantha Krishna and his party	Indian Institute of Science	T	Sep. 1995
France			
Dr.B.Barbara his party	CNRS Laboratoire Louis Neel	T	Aug. 1995
Miss.Emmanuelle Coudert	Creusot Hoire Industrie Research Center	T	Dec. 1995
U.K.			
Adviser.Ken Mills his party	Brunel University	T	May. 1995
Swutzerland			
Dr.Lukas Rohr	Swiss Federal Laboratory for Material Testing and Research	T	May. 1995
Singapore			
Dr.Kurnia Wira	Gintic Institute of Manufactaring Technology	T	May. 1995

❐ Brief Introduction of STA Fellowship Programme

The Science and Technology Agency(STA), an administrative organ of the Government of Japan, offers opportunities for promising young foreign researchers in the fields of science and technology to conduct research at Japan's national laboratories and public research corporations(excluding universities and university-affiliated institutes).

The program is managed by the Research Development Corporation of Japan (JRDC), a statutory organization under the supervision of STA in cooperation with the Japan International Science and Technology Exchange Center(JISTEC). Fellowship qualifications are as follows:

1.Possession of a doctor's degree in a scientific, technological, engineering or medical field.

2.Less than 35 years of age, in principle. (N.B.:Any age is acceptable for Short-Term Fellowships)

3.Sufficient good health for research work and life in Japan.

4.Sufficient language ability in Japanese or English.

The tenure is from 6 months to 2 years(Long-Term Fellowship), or 1～3 months(Short-Term Fellowship). JRDC provides Fellows with a round-trip airline ticket, a monthly living allowance, a family allowance, an initial international moving allowance, accommodations (Long-Term Fellowship), accommodations allowance (Short-Term Fellowship) and travel cost within Japan related to research activities. Research expenses will be paid to the host institute. This does not apply in the case of Short-Term Fellowships.

Further information can be obtained at:

Japan International Science and Technology Exchange Center(JISTEC)

2-20-5, Takezono, Tsukuba City, Ibaraki Pref. 305, Japan

Phone †81-298-53-8250

Fax †81-298-53-8260

Organization of NRIM

❐ Organization

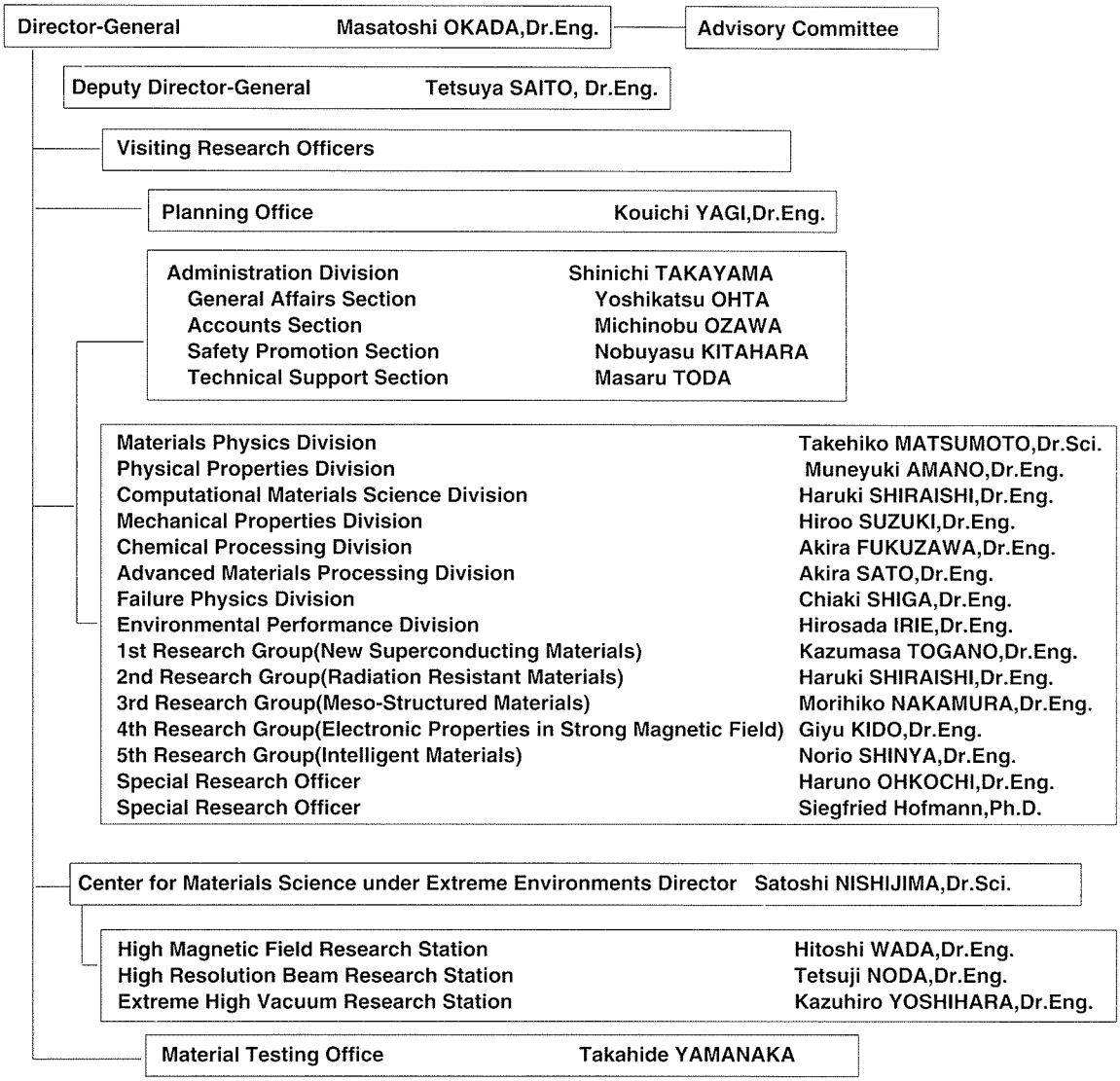

❐ Budget and Personnel in Fiscal Year of 1996

Budget	
Research and facilities	4,779
Personnel expenses	3,792
Total	8,571

unit: million yen

Personnel	
Administrative staffs	88 (8)
Researchers	329 (6)
Total	417 (14)

Number in parenthesis : Material Testing Office

How to get to NRIM

To NRIM Tsukuba Site
1-2-1 Sengen, Tsukuba-shi, Ibaraki 305
Phone +81-298-53-1000, Fax +81-298-53-1005

Narita Airport
↓ by JR Narita Express train approxmately 60 minutes
Tokyo Station
Yaesu-Minami Exit
↓ by Joban Highway Bus for Tsukuba Center approximately 70 minutes
Tsukuba Center
Bus Terminal
↓ by taxi approximately 5 minutes, or on foot approximately 15 minutes
NRIM

To NRIM Meguro Site
2-2-54 Nakameguro, Meguro-ku, Tokyo 153
Phone +81-3-3719-2271, Fax +81-3-3719-2177

Narita Airport
↓ by JR Narita Express train approxmately 60 minutes
Tokyo Station
↓ by JR Yamanote Line train approximately 25 minutes
Ebisu Station
↓ by taxi approximately 5 minutes, or on foot approximately 15 minutes
NRIM

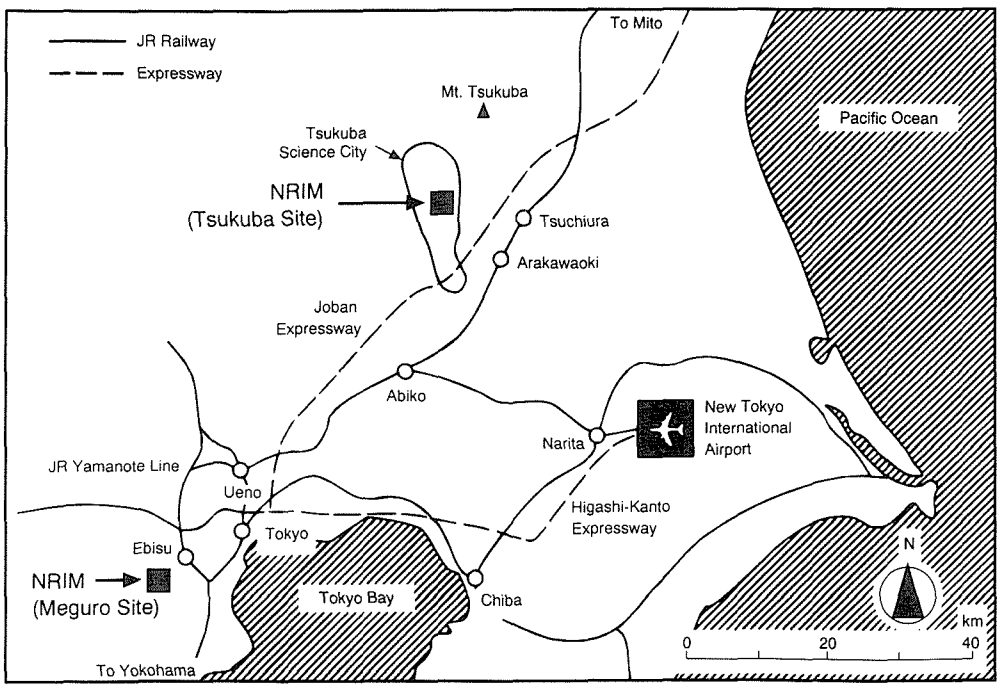

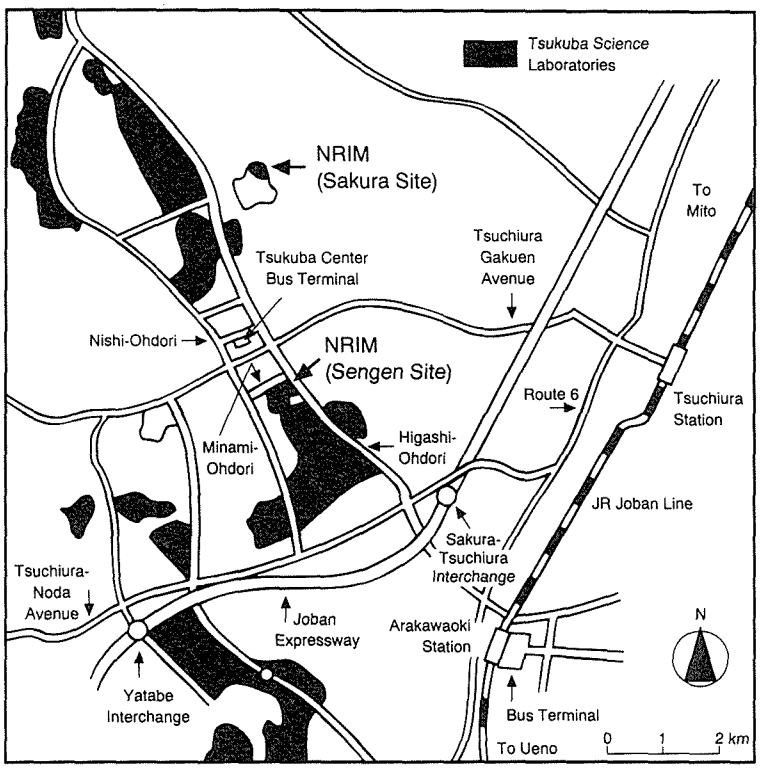

Tsukuba Site

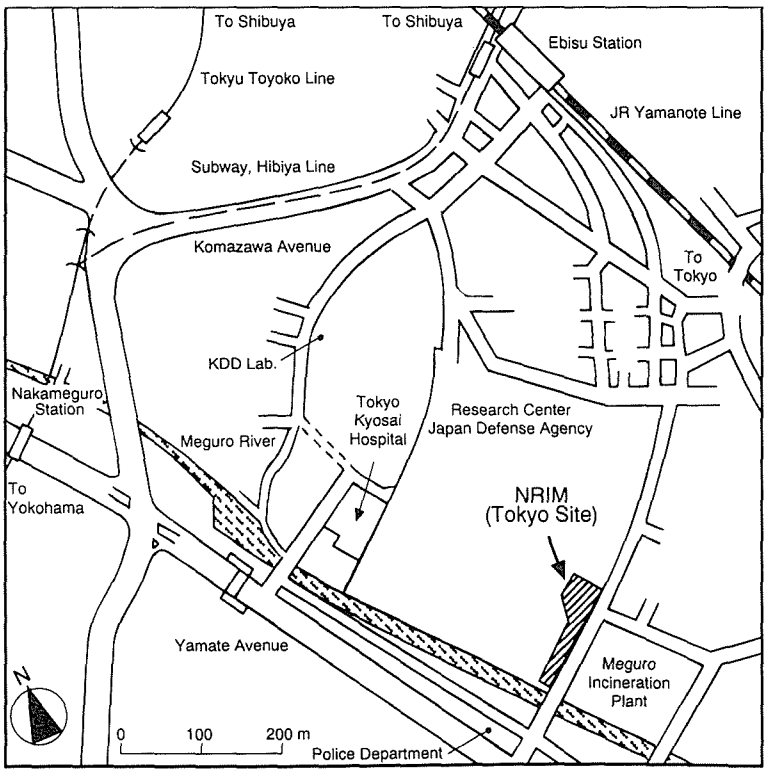

Tokyo Site

List of Keywords

D

E

F

G

H

I

S

T

U, V, W

X, Y, Z

NRIM Research Activities
1997
Date of Issue: 28 March, 1997

Publisher:
Eiichi MUTOU
Planning Office
National Research Institute for Metals
1-2-1, Sengen, Tsukuba-shi, Ibaraki 305-0047 Japan
Phone:+81-298-59-2045, Fax: +81-298-59-2049

Printed by Elite Printing Co., Ltd., Ibaraki

NRIM Research Activities

1996